BRUNO PAES DE MELO

TRANSCRIPTIONAL MODULATION AND CHARACTERIZATION OF PLANT-SPECIFIC TRANS-ACTING FACTORS IN ABIOTIC STRESS RESPONSES

Tese apresentada à Universidade Federal de Viçosa, como parte das exigências do Programa de Pós-Graduação em Bioquímica Aplicada, para obtenção do título de *Doctor Scientiae*.

Orientadora: Elizabeth Pacheco Batista Fontes

Coorientadores: Pedro Augusto Braga Reis
Maria Fátima Grossi-de-Sá
Janice de Almeida-Engler
Virgílio Adriano Pereira Loriato

VIÇOSA – MINAS GERAIS
2020

Ficha catalográfica elaborada pela Biblioteca Central da Universidade Federal de Viçosa - Campus Viçosa

T

M528t
2020

Melo, Bruno Paes de, 1992-
Transcriptional modulation and characterization of plant-specific trans-acting factors in abiotic stress responses / Bruno Paes de Melo. - Viçosa, MG, 2020.
192 f. : il. (algumas color.) ; 29 cm.

Inclui apêndice.
Orientador: Elizabeth Pacheco Batista Fontes.
Tese (doutorado) - Universidade Federal de Viçosa.
Inclui bibliografia.

1. Regulação da expressão gênica. 2. Plantas - Efeito do stress. 3. Stress (Fisiologia). 4. Soja - Genética. 5. Biologia molecular. I. Universidade Federal de Viçosa. Departamento de Bioquímica e Biologia Molecular. Programa de Pós-Graduação em Bioquímica Aplicada. II. Título.

CDD 22. ed. 572.865

BRUNO PAES DE MELO

TRANSCRIPTIONAL MODULATION AND CHARACTERIZATION OF PLANT-SPECIFIC TRANS-ACTING FACTORS IN ABIOTIC STRESS RESPONSES

Tese apresentada à Universidade Federal de Viçosa, como parte das exigências do Programa de Pós-Graduação em Bioquímica Aplicada, para obtenção do título de *Doctor Scientiae*.

APROVADA: 29 de outubro de 2020.

Assentimento:

Bruno Paes de Melo
Autor

Elizabeth Pacheco Batista Fontes
Orientadora

ACKNOWLEDGMENTS

A Deus, não só meu profundo agradecimento como à dedicação desse trabalho, por ser meu alento, minha força. Por me permitir caminhar essas longas jornadas cheio de esperança e fé. Por ser fonte de ânimo e de coragem, amor e perdão.

À minha família. Aos meus pais, Carmen e Duílio, que abriram mão de muitos de seus próprios sonhos para que eu pudesse realizar os meus. Fonte inesgotável de amor e de compreensão. À minha irmã, Mariana, com quem divido não somente o núcleo familiar, mas minhas vitórias, minhas alegrias e minha experiência.

Ao meu amor, Amanda. Que caminha comigo desde muito cedo. Que compreendeu minhas ausências, mas me deu força. Que entendeu meus anseios e me apoiou. Que muitas vezes foi a fonte da minha determinação, meu apoio emocional e financeiro. Sem ela meus passos teriam sido curtos e sem direção. Todo meu amor, carinho e gratidão.

À minha orientadora, a Professora Elizabeth Fontes, por todas as oportunidades enriquecedoras na pesquisa ao seu lado e por todos os ensinamentos. Exemplo de dedicação à ciência, de comprometimento e fonte de inspiração para que eu moldasse à sua semelhança o perfil profissional que eu desejo pra mim. Inenarrável gratidão.

As minhas coorientadoras, a Drª. Maria Fátima Grossi-de-Sá, que abriu as portas do seu laboratório na Embrapa da forma mais generosa que já vivenciei, que confiou em mim e não só me integrou à sua equipe, mas a todos os seus projetos. Impossível descrever tamanha gratidão; e a Drª. Janice de Almeida-Engler, que me recebeu no INRA-França e me permitiu expandir meus horizontes pela biologia celular e pelo mundo, me permitindo realizar um sonho de realizar o doutorado-sanduíche. Ao meu coorientador, Pedro, pela presença constante ao nosso lado na bancada, pelas dicas sempre úteis e construtivas.

Aos membros da banca de defesa. Aos Professores Humberto Ramos e Jurandir Magalhães, por aceitarem prontamente ao convite de contribuírem ativamente com a minha capacitação. A grande amiga e professora, Anésia Santos, pelos momentos

incríveis e divertidos dentro do laboratório, da sala de aula e fora deles. Por todos os ensinamentos.

As amizades agregadoras. De Viçosa e de Brasília para a vida. Meus agradecimentos a Drª. Paola de Avelar Carpinetti-Oliveira, antes parceira de trabalho e hoje grande amiga. A Drª. Isabela Tristan Lourenço-Tessutti, cuja parceria na bancada e fora dela são mantidas por laços de amor à ciência e a vida. Que compartilhou comigo as vitórias, mas repartiu o fardo das derrotas. Uma alma-irmã. A Drª. Carolina Morgante, cuja boa vontade e animação no trabalho são restauradoras. As palavras não são capazes de exprimir minha gratidão.

Aos grandes amigos dos laboratórios em que desenvolvi este trabalho. Em especial, aqueles que contribuíram diretamente comigo. No Laboratório de Biologia Molecular de Plantas (BIOAGRO-UFV), aos amigos Otto, Eduardo, Célio, Luiz, Larissa e Marco Aurélio, meus "deguinhas". Na Embrapa, as minhas alunas "sem salvação", Luanna e Camila e aos meus sempre "supremos" Helena, Reneida, Mayara e Firmas.

À toda equipe de apoio dos Laboratórios de Biologia Molecular de Plantas (UFV), Interação Molecular Planta-Praga (Embrapa Recursos Genéticos e Biotecnologia) e Interação Planta-Nematoide (INRA-França) por me apoiarem na execução dos meus experimentos. Em especial ao amigo Virgílio (UFV), às pesquisadoras Drª. Cristina Mattar e Maria Eugênia Lisei de Sá (Embrapa) e aos técnicos Ariane e Laurent (INRA).

À Universidade Federal de Viçosa, na figura do Programa de Pós-Graduação em Bioquímica Aplicada, pela oportunidade de cursar o doutorado numa instituição de excelência. Meus agradecimentos também aos secretários do PPGBA, Eduardo e Marco Aurélio, pelas infindáveis resoluções.

As agências de fomento à pesquisa. À CAPES, pela bolsa de doutorado e pelo suporte ao doutorado-sanduíche por meio do programa CAPES-COFECUB. À FAPEMIG e CNPq pelo suporte financeiro no desenvolvimento deste trabalho.

“É muito melhor lançar-se em busca de conquistas grandiosas, mesmo expondo-se ao fracasso, do que alinhar-se com os pobres de espírito, que nem gozam muito nem sofrem muito, porque vivem numa penumbra cinzenta, onde não conhecem nem vitória, nem derrota.”

Theodore Roosevelt

ABSTRACT

MELO, Bruno Paes de, D.Sc., Universidade Federal de Viçosa, October, 2020. **Transcriptional Modulation and Characterization of Plant-Specific Trans-acting Factors in Abiotic Stress Responses**. Adviser: Elizabeth Pacheco Batista Fontes. Co-advisers: Pedro Augusto Braga Reis, Maria Fátima Grossi-de-Sá, Janice de Almeida-Engler and Virgílio Adriano Pereira Loriato.

Transcription factors (TFs) are key regulators of gene expression in cells. Due to their functional plasticity and their role as pivotal players in controlling gene expression according to the environment, they may be considered hot spots to decipher the mechanisms of plant responses to multiple stresses and suitable targets for biotechnological intervention and development of adapted plants. Several plant TF families have been implicated in stress responses, including NAC, MYB, WRKY, and bZIP. The present work explores the functionality of Arabidopsis AREB-1, a well-characterized bZIP TF in drought stress response and physiological adaptation, and the soybean NAC superfamily and members associated with the control of multiple stress responses and senescence. In the first chapter, we introduced a new strategy of transcription modulation of AREB-1 by CRISPR/dCas9 in Arabidopsis for tolerance to drought. The following chapters deal with new insights toward GmNAC superfamily and functional studies of GmNAC065 and GmNAC085 based on genome- and transcriptome-wide analyses in soybean and a reverse genetics approach in Arabidopsis. Using the CRISPR activation (CRISPRa) technique, an inactive nuclease dCas9 was fused with a histone acetyl-transferase 1 (AtHAT1), optimizing gene expression via chromatin remodeling. The CRISPRa-mediated AREB1 overexpression promoted an improvement in the physiological performance of the transgenic plants under 30 days of water deprivation. The enhanced drought tolerance phenotype was associated with increased chlorophyll content, antioxidant enzyme activity, and soluble sugar content, with consequent lower reactive oxygen species (ROS) accumulation. Finally, we demonstrated that the up-regulation of AREB1 positively changed the transcription of downstream ABA-inducible genes involved in adaptive response and promoted a better plant performance under drought, validating CRISPRaas a biotechnological tool to improve specific plant traits.The NAC genes encode TFs involved in the control of plant morph-physiology and stress responses. The last soybean genome assembly (Wm82.a2.v1) raised the possibility of new NAC genes onthe soybean genome. In this

investigation, we identified 32 putative novel NAC genes, updating the superfamily to 180 gene members, clustered in15 phylogenetic subfamilies. We showed that 40% of the GmNACsare differentially regulated by developmental senescence. *GmNAC065* and *GmNAC085* display contrasting gene expression profiles in multiple stress responses and induce symptoms of leaf senescence to a different extent when transiently expressed in *N. benthamiana*, suggesting a divergent role of these genes. Subsequently, the soybean genome was interrogated for developmental and environmental senescence-associated genes (SAGs) belonging to the NAC superfamily. Using functionally characterized Arabidopsis SAGs as prototypes, we identified the putative NAC-SAGs in soybean, including *GmNAC065* and *GmNAC085*, whose functions in multiple stress responses and senescence were further investigated in soybean and Arabidopsis transgenic lines. The ectopic expression of GmNAC065 in Arabidopsis leads to a delayed-senescence phenotype, with enhanced oxidative performance under multiple stresses and lower stress-induced PCD. The *GmNAC085*-expressing lines displayed an opposite phenotype leading to the up-regulation of several downstream SAGs in Arabidopsis, further demonstrating their divergent roles in stress responses and PCD. Finally, if we are to use soybean as a model system for genetic studies and development of new cultivars, we need to develop an efficient protocol for soybean transformation and regeneration. The final chapter of this work proposes a new methodology for soybean genetic transformation combining biolistic and *Agrobacterium*-mediated DNA delivery. We developed a one-step protocol for transgenic soybean recovery in approximately 30 - 40 weeks more cost-effectively and straightforwardly exploring the high regenerative capacity of shoot-apex cells in the embryonic axis. The protocol allows the direct co-cultivation and plant regeneration, avoiding contamination generated by excessive tissue-manipulation, demanded in other protocols. Therefore, we are now better positioned to translate the fundamental studies developed in this investigation into biotechnological traits to get superior crops.

Keywords: Trans-acting factors. Modern crop breeding. Environmental stresses. Senescence. Plant genetic engineering

RESUMO

MELO, Bruno Paes de, D.Sc., Universidade Federal de Viçosa, outubro de 2020. **Modulação transcricional e caracterização de fatores de transcrição específicos de plantas em respostas a estresses abióticos**. Orientadora: Elizabeth Pacheco Batista Fontes. Coorientadores: Pedro Augusto Braga Reis, Maria Fátima Grossi-de-Sá, Janice de Almeida-Engler e Virgílio Adriano Pereira Loriato.

Fatores de transcrição (FTs) são reguladores centrais da expressão gênica nas células. Devido à sua plasticidade funcional e ao seu papel como protagonistas no controle da expressão gênica de acordo com o ambiente, podem ser considerados *hot spots* para decifrar os mecanismos de resposta das plantas a múltiplos estresses e alvos adequados para intervenção biotecnológica e desenvolvimento de plantas adaptadas. Diversas famílias de fatores de transcrição de plantas são relacionados as respostas ao estresse, incluindo NAC, MYB, WRKY e bZIP. O presente trabalho explora a funcionalidade de AREB-1, um FT da família bZIP em Arabidopsis, extensivamente caracterizado caracterizado nas adaptações fisiológicas em resposta ao estresse hídrico, além da superfamília NAC de soja e seus membros associados ao controle de respostas múltiplas ao estresse e senescência. No primeiro capítulo, apresentamos uma nova estratégia de modulação da transcrição de AREB-1 por CRISPR/dCas9 em Arabidopsis para tolerância à seca. Os capítulos a seguir lidam com novas idéias acerca da superfamília GmNAC e estudos funcionais de GmNAC065 e GmNAC085 com base em análises genômicas e transcritômicas, além de uma abordagem de genética reversa em Arabidopsis. Utilizando a técnica de ativação CRISPR (CRISPRa), uma nuclease inativa dCas9 foi fundida com uma histona acetil-transferase 1 (AtHAT1), otimizando a expressão gênica via remodelação da cromatina. A superexpressão de AREB1 mediada por CRISPRa promoveu uma melhora no desempenho fisiológico das plantas transgênicas em 30 dias de privação de água. O fenótipo de maior tolerância à seca foi associado ao aumento do conteúdo de clorofila, atividade de enzimas antioxidantes e conteúdo de açúcar solúvel, com consequente menor acúmulo de espécies reativas de oxigênio (EROS). Finalmente, demonstramos que a regulação positiva de AREB1 alterou positivamente a transcrição de genes induzíveis ABA *downstream* envolvidos na resposta adaptativa e promoveu um melhor desempenho da planta sob seca, validando o CRISPRa como uma ferramenta biotecnológica para melhorar características específicas desejáveis em plantas. Os genes NAC codificam TFs envolvidos no controle da

morfofisiologia da planta e respostas ao estresse. A última montagem do genoma da soja (Wm82.a2.v1) levantou a possibilidade de novos genes NAC no genoma da soja. Nesta investigação, identificamos 32 novos genes NAC putativos, atualizando a superfamília para 180 membros de genes, agrupados em 15 subfamílias filogenéticas. Mostramos que 40% dos GmNACs são regulados diferencialmente pela senescência do desenvolvimento. *GmNAC065* e *GmNAC085* apresentam perfis de expressão gênica contrastantes em múltiplas respostas de estresse e induzem sintomas de senescência foliar em diferentes extensões quando expressos transientemente em *N. benthamiana*, sugerindo um papel divergente para esses genes. Posteriormente, o genoma da soja foi interrogado para genes associados à senescência desencadeada por estresse e de desenvolvimento (SAGs) pertencentes à superfamília NAC. Usando SAGs de Arabidopsis funcionalmente caracterizados como protótipos, identificamos os NAC-SAGs putativos em soja, incluindo *GmNAC065* e *GmNAC085*, cujas funções em múltiplas respostas ao estresse e senescência foram investigadas em soja e linhagens transgênicas de Arabidopsis. A expressão ectópica de GmNAC065 em Arabidopsis leva a um fenótipo de senescência retardada, com desempenho oxidativo aprimorado sob estresse múltiplo e menor morte celular induzida por estresse. As linhas que expressam GmNAC085 exibiram um fenótipo oposto levando à regulação positiva de vários SAGs, reforçando ainda mais seus papéis divergentes nas respostas ao estresse e morte celular programada. Finalmente, se quisermos usar a soja como sistema modelo para estudos genéticos e desenvolvimento de novas cultivares, precisamos desenvolver um protocolo eficiente para a transformação e regeneração da soja. O capítulo final deste trabalho propõe uma nova metodologia para a transformação genética da soja combinando a biolística e a transformação mediada por *Agrobacterium*. Desenvolvemos um protocolo de uma etapa para a recuperação da soja transgênica em aproximadamente 30 a 40 semanas de maneira mais econômica e explorando de forma direta a alta capacidade regenerativa das células do meristema apical no eixo embrionário. O protocolo permite o co-cultivo direto e a regeneração da planta, evitando a contaminação gerada pela excessiva manipulação de tecidos, exigida em outros protocolos. Portanto, estamos agora mais bem preparados para transpor os estudos fundamentais desenvolvidos nesta investigação em produtos biotecnológicos na obtenção de cultivares superiores.

Palavras-chave: Fatores de transcrição. Melhoramento moderno de plantas. Estresses ambientais. Senescência. Engenharia genética de plantas

SUMMARY

GENERAL INTRODUCTION

Plants are sessile organisms confined to their environment and, to survive despite any imbalance in their surroundings, they have developed a sophisticated set of stress-responsive mechanisms that confer them physiological plasticity and ensure their growth, development, and reproduction (Reguera *et* al., 2012; Mickelbart *et al*., 2015; Khan *et al*., 2016). The major environmental issues limiting plant development are divided into two main classes: (i) abiotic stresses, characterized by the prejudicial effect of temperature, soil composition, and water availability over the plants, and (ii) biotic stresses caused by living organisms that parasitize and feed on plants. The most common examples of abiotic stresses include drought, heat, cold, and salinity, and biotic stresses are fungi, bacteria, viruses, nematodes and insects (Foyer *et al*., 2016; Cohen *et al*., 2019; Baillo *et al*., 2019). Approximately 50% of crops' yield losses are caused by abiotic stresses, while biotic stresses impose a ratio of 35% (Savary *et* al., 2012; Calanca *et al*., 2017), making urgent the demand for understanding the complex regulatory networks in plant multiple stress responses.

Stress-avoidance and tolerance mechanisms lead to plant acclimation and/or adaptation, with biochemical and molecular responses divided into four phases: (i) sensing- and responding-phase; (ii) restitution phase; (iii) end phase, and (iv) regeneration phase (Mittler *et al*., 2006; Khan *et al*. 2019). In the first phase, multiple stresses activate plant receptors and sensors, leading to an alert state that triggers the second phase, in which plant cells, throughout gene expression reprogramming, encompass adaptive morpho-physiological changes to re-establish the homeostasis. The plants remain in the restitution phase until the end phase, which can follow in different ways, according to the severity and stress duration. If plants overcome the stressful period, they trigger the regeneration phase following a normal growth and developmental program (Khan *et al*., 2019). However, if plants' stress-avoidance and tolerance mechanisms cannot cope with the stress, plants trigger environmental programmed cell death (Olvera-Carillo *et al*., 2015).

The strategies of plants to respond to multiple stresses are based on the global gene expression reprogramming. There is a broad range of stress-responsive genes, and several of them codify transcription factors (TFs). The TFs are clustered into the regulatory group of stress-responsive genes, besides the RLKs (receptor-like kinase),

ribosomal protein kinases, MAPKs (mitogen-activated protein kinase), proteinases, and hydrolases of signal transduction, such as lipases and esterases (Onaga and Wydra, 2016). These genes codify proteins involved in the first phase of the stress response, mainly in signal perception, transduction, and gene expression control. The effect of regulatory genes expression is the activation of the second set of genes, termed biosynthetic and structural genes, encompassing enzymes for ROS-detoxification (catalase, ascorbate peroxidase, superoxide dismutase, glutathione S-transferase), protectant proteins (LEA, chaperones, and chaperonins), and enzymes involved in osmolyte and osmoprotectant synthesis (Anjum *et al*., 2011; Onaga and Wydra, 2016; Khan *et al*., 2019).

The plant stress-sensing and signal transduction pathways are multilayered, and their regulators display overlapped functions in different types of stress. After sensing the primary signal of stress, such as the hyperosmotic effect of drought and salinity or ion toxicity, as well as the presence of molecules associated with pathogens, plant cells initiate the production of secondary signals: phytohormones, reactive oxygen species (ROS), calcium and potassium imbalances (Zhu *et al*., 2016).

The phytohormones are the primary regulators of stress-signaling cascades. In abiotic stresses, abscisic acid (ABA) display a pivotal role in stress responses and plant acclimation (Reguera*et al*., 2012;Gomez-Cadenas*et al*., 2015; Zhu *et al*., 2016; Khan *et al*., 2019). ABA regulates water content in plant cells and ROS-avoiding machinery, integrating a fine-tuned hormone signaling network essential in plant acclimation and senescence control (Yamagushi-Shinozaki and Shinozaki *et al*., 2006; Tujeta *et al*., 2007; Yoshida *et al*., 2014; Luoni *et al*., 2019). ABA can activate gene expression through the *cis*-acting element ABRE (ABA-responsive element) network, present in the promoter region of several stress-responsive genes. AREB/ABF (ABRE-binding protein/factor) TFs are activated by SnRK2-mediated phosphorylation and regulate the downstream targets actively involved in seed germination, stomatal opening/closure, osmotic stress response, and plant growth (Fujii and Zhu, 2009; Fujita *et al*., 2009). Despite the central role of ABA in abiotic stress responses, other hormones have shown to integrate biotic and abiotic stress signaling pathways, such as jasmonate (JA), ethylene (ET), and salicylic acid (SA) (Sanchez-Vallet *et al*., 2012. Khan *et al*., 2019).

Another notorious feature on stress sensing and signal transduction is the activation of MAPK cascades, culminating in fluctuations of the intracellular Ca^{2+}

levels (Golldack *et al*., 2014; Wilkings *et al*., 2016). In plants, most of the membrane-associated receptors, which sense the primary signals of stress, are Ca^{2+} channels, as OSCA1, GLRs, and COLD1 (Zhu *et al*., 2016). When active, they promote Ca^{2+} influx and activate SnRKs, an important kinase group that integrates ABA-signaling, NAC TFs, ROS-signaling, and ionic homeostasis (Halford *et al*., 2003; Diedhiou *et al*., 2008; Sirichandra *et al*., 2009; Kim *et al*., 2012). The SnRKs cascade activates ion antiporters in the plasma membrane and endoplasmic reticulum, leading to a hyper concentration of cytosolic Ca^{2+}, which culminates in the activation of other MAPKs cascades and ROS production, responsible for systemic signaling and PCD-triggering (Mittler, 2002; Zhu, 2016).

As a downstream step of the stress response, the active MAPKs, the ROS accumulation, and its effect over biomolecules' degradation activate TFs, central physiological adaption players. TFs can modulate gene expression by binding specific sequences on gene promoters under different biological contexts (Baillo *et al*., 2019). Structurally, they can recognize the *cis*-elements in the DNA and interact with other proteins in a transcriptional complex, modulating positively or negatively the target gene expression (Baillo *et al*., 2019). In plants, approximately 10% of the genome encodes TFs and they are clustered in superfamilies with more than a hundred members, such as WRKY, MYB, NAC, AP2/ERF, and bZIPs (Wang *et al*., 2016).

As transacting factor at the final step on stress-sensing, TFs are considered the effective player on plant adaption; thereby, they are hot spots for the modern genetic breeding towards the development of superior crops. These demands have arisen from the world's population growth, the emergent climate changes, and the searching for higher quality food and energy production. Therefore, the understanding of the basic mechanism of plant stress-responses comprises an elementary way to design new strategies to manipulate stress-responsive pathways and develop superior crops.

The present work explores the potential of *AREB*-1 (from *Arabidopsis thaliana*) TF as a viable target in biotechnological plant breeding throughout a CRISPR/dCas9 strategy. Additionally, it investigates the role of soybean NAC TFs in multiple stress responses and developmental- and environmental-triggered PCD. It further introduces a new methodology for soybean genetic transformation as a reproductive, cost-effective, and straightforward protocol for obtaining new soybean cultivars with desirable phenotypical characteristics.

In the first chapter, a previously designed sgRNA targeting the promoter region of *AREB-1* in Arabidopsis, which drives an inactive dCas9 nuclease fused to a histone acetyl-transferase, was used as a strategy to enhance drought tolerance by improving gene transcription. The results of this chapter were published as "*Transcriptional modulation of AREB-1 by CRISPRa improves plant physiological performance under severe water deficit*" (Melo *et al*., 2020 - Scientific Reports) and demonstrated that*AREB-1* overexpression promotes a better physiological performance of the transgenic plants subjected to 30 days of water deprivation.

The following chapters deal with a complete inventory of NAC superfamily in soybean and a functional analysis of the two uncharacterized GmNAC TFs, GmNAC065, and GmNAC085, involved in multiple stress responses and senescence. These studies were performed by analyzing the stress-induced expression profile of GmNAC065 and GmNAC085 in soybean and by overexpressing the GmNAC genes in Arabidopsis transgenic lines. Chapter 2 comprises the results of the published paper "*Revisiting the soybean GmNAC superfamily*" (Melo *et al*., 2018 – Frontiers in Plant Science, Abiotic Stress), which uncovered 32 new putative NAC TFs in the last soybean genome assembly (Wm82.a2.v1) and updated GmNAC superfamily to 180 members in soybean, clustered into 15 phylogenetic subfamilies with perfect correlation with Arabidopsis orthologous genes. Additionally, a transcription-wide analysis revealed a differential stress-responsiveness between NAC TFs and demonstrated that 40% of soybean NAC genes are differentially regulated by age-triggered leaf senescence. Furthermore, the ectopic expression of GmNAC065 and GmNAC085 promoted senescence symptoms in *Nicotiana benthamiana* leaves with a different extent, suggesting a contrasting role of these genes in PCD.

In chapter 3, *GmNAC065* and *GmNAC085* are investigated as senescence-associated genes (*Gm*NAC-SAGs) in soybean. Transcription-wide analysis associated these genes with different and contrasting roles in developmental and environmental programmed cell death. In addition, a functional analysis was performed in GmNAC065 and GmNAC085-overexpressing Arabidopsis transgenic lines. GmNAC065 overexpression delayed senescence, whereas GmNAC085 overexpression accelerated senescence, as a result of imbalances in the anti-oxidant plant systems and up-regulation of SAGs and their downstream targets.

Finally, chapter 4 describes a new methodology for soybean genetic transformation. The soybean is a recalcitrant species and the current protocols employing *Agrobacterium tumefaciens* or biolistic DNA-delivery display low efficiency and demand successive steps of *in vitro* plant cultivation and regeneration with extensive losses by contamination and tissue-browning, making them long and laborious. The soybean transformation protocol, published as "*Soybean embryonic axis transformation: combining biolistic and Agrobacterium-mediated protocols to overcome typical complications of in vitro plant regeneration*" (Melo *et al*., 2020 – Frontiers in Plant Science, Technical Advances in Plant Science), described a one-step protocol for *in vitro* plant regeneration. Particle acceleration promotes micro-wounding in shoot-apex cells from the embryonic axis enhancing *A. tumefaciens* infectiveness. Furthermore, the high regenerative capacity of the embryonic axis allows a one-step shoot elongation, root development and plant regeneration, making the methodology time- and cost-effective for the biotechnological development of superior cultivars.

REFERENCES

Anjum, S., Xie, X., Wang, L., Saleem, M., Man, C., and Lei, W. Morphological, physiological and biochemical responses of plants to drought stress.doi: 10.5897/AJAR10.027

BengoaLuoni, S., Astigueta, F. H., Nicosia, S., Moschen, S., Fernandez, P., and Heinz, R. (2019). Transcription Factors Associated with Leaf Senescence in Crops. *Plants* 8. doi:10.3390/plants8100411.

Calanca, P. P. (2017). "Effects of abiotic stress in crop production," in *Quantification of climate variability, adaptation and mitigation for agricultural sustainability*, eds. M. Ahmed and C. O. Stockle (Cham: Springer International Publishing), 165–180. doi:10.1007/978-3-319-32059-5_8.

Diédhiou, C. J., Popova, O. V., Dietz, K.-J., andGolldack, D. (2008). The SNF1-type serine-threonine protein kinase SAPK4 regulates stress-responsive gene expression in rice. *BMC Plant Biol.* 8, 49. doi:10.1186/1471-2229-8-49.

Fujii, H., and Zhu, J.-K. (2009). Arabidopsis mutant deficient in 3 abscisic acid-activated protein kinases reveals critical roles in growth, reproduction, and stress. *ProcNatlAcadSci USA* 106, 8380–8385. doi:10.1073/pnas.0903144106.

Fujita, Y., Nakashima, K., Yoshida, T., Katagiri, T., Kidokoro, S., Kanamori, N., Umezawa, T., Fujita, M., Maruyama, K., Ishiyama, K., et al. (2009). Three SnRK2 protein kinases are the main positive regulators of abscisic acid signaling in response to water stress in Arabidopsis. *Plant Cell Physiol.* 50, 2123–2132. doi:10.1093/pcp/pcp147.

Golldack, D., Li, C., Mohan, H., and Probst, N. (2014). Tolerance to drought and salt stress in plants: Unraveling the signaling networks. *Front. PlantSci.* 5, 151. doi:10.3389/fpls.2014.00151.

Gomez-Cadenas, A., Vives, V., Zandalinas, S. I., Manzi, M., Sanchez-Perez, A. M., Perez-Clemente, R. M., andArbona, V. (2015). Abscisic Acid: a versatile phytohormonein plant signaling and beyond. *Curr. Protein Pept. Sci.* 16, 413–434. doi:10.2174/1389203716666150330130102.

Halford, N. G., Hey, S., Jhurreea, D., Laurie, S., McKibbin, R. S., Paul, M., and Zhang, Y. (2003). Metabolic signalling and carbon partitioning: role of Snf1-related (SnRK1) protein kinase. *J. Exp. Bot.* 54, 467–475. doi:10.1093/jxb/erg038.

Khan, A., Khan, A. L., Muneer, S., Kim, Y.-H., Al-Rawahi, A., and Al-Harrasi, A. (2019). Silicon and Salinity: Crosstalk in Crop-Mediated Stress Tolerance Mechanisms. *Front. Plant Sci.* 10, 1429. doi:10.3389/fpls.2019.01429.

Kim, T.-W., Michniewicz, M., Bergmann, D. C., and Wang, Z.-Y. (2012). Brassinosteroid regulates stomatal development by GSK3-mediated inhibition of a MAPK pathway. *Nature* 482, 419–422. doi:10.1038/nature10794.

de Melo, B. P., Lourenço-Tessutti, I. T., Paixão, J. F. R., Noriega, D. D., Silva, M. C. M., de Almeida-Engler, J., Fontes, E. P. B., and Grossi-de-Sa, M. F. (2020). Transcriptional modulation of AREB-1 by CRISPRa improves plant physiological performance under severe water deficit. *Sci. Rep.* 10, 16231. doi:10.1038/s41598-020-72464-y.

Melo, B. P., Fraga, O. T., Silva, J. C. F., Ferreira, D. O., Brustolini, O. J. B., Carpinetti, P. A., Machado, J. P. B., Reis, P. A. B., and Fontes, E. P. B. (2018). Revisiting the soybean gmnac superfamily. *Front. Plant Sci.* 9, 1864. doi:10.3389/fpls.2018.01864.

Mittler, R. (2006). Abiotic stress, the field environment and stress combination. *Trends Plant Sci.* 11, 15–19. doi:10.1016/j.tplants.2005.11.002.

Olvera-Carrillo, Y., Van Bel, M., Van Hautegem, T., Fendrych, M., Huysmans, M., Simaskova, M., van Durme, M., Buscaill, P., Rivas, S., Coll, N. S., et al. (2015). A conserved core of programmed cell death indicator genes discriminates developmentally

and environmentally induced programmed cell death in plants. *Plant Physiol.* 169, 2684–2699. doi:10.1104/pp.15.00769.

Onaga, G., and Wydra, K. (2016). "Advances in plant tolerance to abiotic stresses," in *Plant Genomics*, ed. I. Y. Abdurakhmonov (InTech). doi:10.5772/64350.

Paes de Melo, B., Lourenço-Tessutti, I. T., Morgante, C. V., Santos, N. C., Pinheiro, L. B., de Jesus Lins, C. B., Silva, M. C. M., Macedo, L. L. P., Fontes, E. P. B., and Grossi-de-Sa, M. F. (2020). Soybean Embryonic Axis Transformation: Combining Biolistic and Agrobacterium-Mediated Protocols to Overcome Typical Complications of In Vitro Plant Regeneration. *Front. Plant Sci.* 11, 1228. doi:10.3389/fpls.2020.01228.

Sánchez-Vallet, A., López, G., Ramos, B., Delgado-Cerezo, M., Riviere, M.-P., Llorente, F., Fernández, P. V., Miedes, E., Estevez, J. M., Grant, M., et al. (2012). Disruption of abscisic acid signaling constitutively activates Arabidopsis resistance to the necrotrophic fungus Plectosphaerellacucumerina. *Plant Physiol.* 160, 2109–2124. doi:10.1104/pp.112.200154.

Savary, S., Nelson, A., Willocquet, L., Pangga, I., and Aunario, J. (2012). Modeling and mapping potential epidemics of rice diseases globally. *Crop Prot.* 34, 6–17. doi:10.1016/j.cropro.2011.11.009.

Sirichandra, C., Gu, D., Hu, H.-C., Davanture, M., Lee, S., Djaoui, M., Valot, B., Zivy, M., Leung, J., Merlot, S., et al. (2009). Phosphorylation of the Arabidopsis AtrbohF NADPH oxidase by OST1 protein kinase. *FEBS Lett.* 583, 2982–2986. doi:10.1016/j.febslet.2009.08.033.

Tuteja, N. (2007). Abscisic Acid and abiotic stress signaling. *Plant Signal. Behav.* 2, 135–138. doi:10.4161/psb.2.3.4156.

Wang, H., Wang, H., Shao, H., and Tang, X. (2016). Recent advances in utilizing transcription factors to improve plant abiotic stress tolerance by transgenic technology. *Front. Plant Sci.* 7, 67. doi:10.3389/fpls.2016.00067.

Wilkins, O., Hafemeister, C., Plessis, A., Holloway-Phillips, M.-M., Pham, G. M., Nicotra, A. B., Gregorio, G. B., Jagadish, S. V. K., Septiningsih, E. M., Bonneau, R., et al. (2016). Egrins (environmental gene regulatory influence networks) in rice that function in the response to water deficit, high temperature, and agricultural environments. *Plant Cell* 28, 2365–2384. doi:10.1105/tpc.16.00158.

Yamaguchi-Shinozaki, K., and Shinozaki, K. (2006). Transcriptional regulatory networks in cellular responses and tolerance to dehydration and cold stresses. *Annu. Rev. Plant Biol.* 57, 781–803. doi:10.1146/annurev.arplant.57.032905.105444.

Yoshida, T., Mogami, J., and Yamaguchi-Shinozaki, K. (2014). ABA-dependent and ABA-independent signaling in response to osmotic stress in plants. *Curr. Opin. Plant Biol.* 21, 133–139. doi:10.1016/j.pbi.2014.07.009.

CHAPTER I

TRANSCRIPTIONAL MODULATION OF AREB-1 BY CRISPRa IMPROVES PLANT PHYSIOLOGICAL PERFORMANCE UNDER SEVERE WATER DEFICIT

Published article

Bruno Paes de Melo, Isabela Tristan Lourenço-Tessutti, Joaquin Francisco Roca Paixão, Daniel David Noriega, Maria Cristina Mattar Silva, Janice de Almeida-Engler, Elizabeth Pacheco Batista Fontes and Maria Fatima Grossi-de-Sa. **Transcriptional modulation of AREB-1 by CRISPRa improves plant physiological performance under severe water deficit**. Scientific Reports 10, 16231 (2020). doi: 10.1038/s41598-020-72464-y.

Pages 22 to 31

RESUMO

As plantas são organismos sésseis, que são vulneráveis ao estresse ambiental. Como tal, as plantas desenvolveram múltiplos mecanismos moleculares, fisiológicos e celulares para lidar com os estresses ambientais. No entanto, essas adversidades ambientais, incluindo a seca, são fontes dos principais problemas do agronegócio, pois interferem no crescimento e na produtividade das plantas. Genes que pertencem a vias de resposta de plantas a estresses são alvos potenciais para a engenharia genética moderna, como o gene AREB1, que, particularmente, em condições de privação de água, codifica um fator de transcrição responsivo ao ácido abscísico, desempenha um papel importante na resposta ao estresse hídrico e na adaptação fisiológica. Em um estudo prévio, uma estratégia para modulação positiva de *AREB1* foi delineada utilizando o sistema *CRISPR-activation* (CRISPRa), em que uma histona acetil-transferase 1 (AtHAT1) fusionada à nuclease inativa dCas9 é direcionada ao promotor do gene alvo e promove a ativação da expressão gênica, alterando a cromatina local para um estado relaxado. Plantas transgênicas estáveis expressando dCas9-HAT demonstraram que o mecanismo CRISPRa dCas9-HAT aumentou a atividade do promotor controlando o gene repórter da β-glucuronidase (GUS) e o gene alvo em linhagens transgênicas homozigotas. No presente trabalho, fornecemos uma confirmação substancial para o papel de AREB1/ABF2 na sobrevivência de plantas sob déficit hídrico severo em plantas engenheiradas com a tecnologia CRISPRa visando aumentar a expressão do gene *AREB1*. A superexpressão de AREB1 promove uma melhora no desempenho fisiológico das plantas homozigotas transgênicas sob seca, que foi associada a um aumento no conteúdo de clorofila, atividade de enzimas antioxidantes e acúmulo de açúcar solúvel, levando ao menor acúmulo de espécies reativas de oxigênio. Finalmente, descobrimos que a regulação positiva mediada por CRISPR de AREB1 altera a abundância de vários genes *downstream* na via induzida por ABA, permitindo-nos relatar que CRISPRa dCas9-HAT é uma ferramenta biotecnológica valiosa para melhorar a tolerância ao estresse hídrico por meio da regulação positiva de AREB1.

SCIENTIFIC REPORTS
nature research

OPEN

Transcriptional modulation of *AREB-1* by CRISPRa improves plant physiological performance under severe water deficit

Bruno Paes de Melo[1,2,8], Isabela Tristan Lourenço-Tessutti[1,8], Joaquin Felipe Roca Paixão[1,3], Daniel David Noriega[1,4], Maria Cristina Mattar Silva[1], Janice de Almeida-Engler[5], Elizabeth Pacheco Batista Fontes[2,6] & Maria Fatima Grossi-de-Sa[1,4,7]✉

Plants are sessile organisms, which are vulnerable to environmental stresses. As such, plants have developed multiple molecular, physiological, and cellular mechanisms to cope with natural stressors. However, these environmental adversities, including drought, are sources of the main agribusiness problems since they interfere with plant growth and productivity. Particularly under water deprivation conditions, the abscisic acid-responsive element-binding protein AREB1/ABF2 plays an important role in drought stress response and physiological adaptation. In this investigation, we provide substantial confirmation for the role of AREB1/ABF2 in plant survival under severe water deficit using the CRISPR activation (CRISPRa) technique to enhance the *AREB1* gene expression. In our strategy, the inactive nuclease dCas9 was fused with an Arabidopsis histone acetyltransferase 1, which improves gene expression by remodeling chromatin. The *AREB1* overexpression promotes an improvement in the physiological performance of the transgenic homozygous plants under drought, which was associated with an increase in chlorophyll content, antioxidant enzyme activity, and soluble sugar accumulation, leading to lower reactive oxygen species accumulation. Finally, we found that the CRISPR-mediated up-regulation of *AREB1* changes the abundance of several downstream ABA-inducible genes, allowing us to report that CRISPRa dCas9-HAT is a valuable biotechnological tool to improve drought stress tolerance through the positive regulation of *AREB1*.

Plants are often exposed to stressful conditions, which trigger signaling networks leading to molecular, cellular and physiological modifications that culminate in stress tolerance. Water deprivation or high salinity induces abscisic acid (ABA) accumulation, which coordinates downstream signaling cascades involved in water-use optimization. A typical symptom of ABA accumulation is the stomatal closure, as the main consequence of an ionic imbalance in guard cells, activating pumps that promote ion efflux and consequent turgor losses[1]. Another typical feature of drought is the imbalance on photosynthetic apparatus that leads to reactive oxygen species (ROS) production and accumulation[2]. ROS can act as signaling molecules that regulates several stress-associated processes, encompassing other protective mechanisms, such as the production and accumulation of osmolytes, electron carriers and improvement of transcription, translation, and activity of antioxidant enzymes, among others[1–3]. Collectively, these mechanisms comprise a sophisticated and intricate hormone-responsive pathway, whose transcription factors appear as nodes on signal integration and gene expression remodeling. Desiccating

[1]Embrapa Genetic Resources and Biotechnology-EMBRAPA CENARGEN, Brasília, DF, Brazil. [2]Biochemistry and Molecular Biology, Universidade Federal de Viçosa (UFV), Viçosa, MG, Brazil. [3]Medical Biochemistry Institute, Universidade Federal Do Rio de Janeiro (UFRJ), Rio de Janeiro, RJ, Brazil. [4]Genomic Sciences and Biotechnology, Universidade Católica de Brasília (UCB), Brasília, DF, Brazil. [5]UMR Institut Sophia Agrobiotech INRA/CNRS/UNS, Sophia Antipolis, France. [6]National Institute of Science and Technology in Plant-Pest Interactions (INCTIPP)–BIOAGRO, Viçosa, MG, Brazil. [7]National Institute of Science and Technology–INCT PlantStress Biotech–EMBRAPA, Brasília, DF, Brazil. [8]These authors contributed equally to this work: Bruno Paes de Melo and Isabela Tristan Lourenço-Tessutti. ✉email: fatima.grossi@embrapa.br

regulatory gene networks and the role of transcription factors in global gene expression changes during the stress provide an effective and useful tool for biotechnological intervention and modern crop breeding programs.

Plants display a large set of transcription factor families involved in stress responses, such as NACs, bZIPs, and WRKYs[4–6]. In the ABA-dependent signaling pathway, one of the most important and well-characterized drought responses is assembled via the basic leucine zipper (bZIP) transcription factor AREB-1 (ABA-responsive element-binding protein 1), which emerges as a central regulator of drought-inducible adaptive pathways[5].

The AREB transcription factors can recognize a widely conserved sequence in promoters of different stress-responsive genes. These elements, named ABREs (ABA-responsive elements), are constituted by the PyACG TGG/TC sequence[7–9], and a monohybrid approach in Arabidopsis has identified nine AREB family members with possible overlapping functions[10–12]. In Arabidopsis, AREB-1, AREB-2, and AREB-3 cooperatively regulate the ABA-dependent signaling pathway. The triple mutant plants display an extremely low survival ratio when submitted to severe dehydration followed by rehydration and higher water and biomass losses than WT and single-mutant plants under drought stress[12,13]. In addition, the overexpression of *AREB-1* under the *CaMV 35S* constitutive promoter has been demonstrated to be a good strategy for drought tolerance improvement in different plant species, such as Arabidopsis, rice, and soybean[14–17].

Recently, our research group demonstrated that positive transcriptional modulation regulation of *AREB-1* using dCas9-HAT (histone acetyl-transferase) leads to constitutive expression of *AREB-1* and *RD29A*, other downstream genes of the AREB pathway[16], in transgenic *Arabidopsis thaliana* plants by CRISPRa. The CRISPRa approach constitutes a powerful biotechnological tool for stress tolerance improvement in plants. The gene overexpression approach using dCas9-HAT can be considered superior to the classical strategy using *CaMV 35S* because we can directly target specific cis-acting elements in gene promoters through the sgRNA use, avoiding the pleiotropic effects and post-transcriptional gene silencing despite the use of constitutive viral promoters.

The overexpression of *AREB* genes has been shown to provide significant improvements in osmotic stress tolerance, whereas the knock-down or knock-out mutants showed elevated sensitivity to osmotic stress. Nevertheless, in some cases, the overexpression of these genes leads to negative effects, which comprise reduced productivity, delay in development and growth. A considerable number of commodities have limited production due to water availability[13,14,16].

We previously provided a functional characterization of homozygous Arabidopsis lines, in which *AREB-1* is upregulated by the CRISPRa approach[16]. The AREB1-OX lines display a significant increase in *AREB*-1 expression, reaching at least twofold as compared to untransformed plants. Either during severe drought stress or mild-severe drought stress, the transgenic plants display enhanced physiological performance compared to that of the WT control. The chlorophyll loss ratio and stomatal opening in AREB1-OX plants were lower than those observed in WT plants, suggesting superior stress-associated physiological performance during drought. In addition, the survival ratio corroborates these data: after re-watering, AREB1-OX plants were almost totally recovered, whereas only 50% of WT plants did[16].

Hereafter, we provide a complete molecular, biochemical, and physiological characterization of a transgenic line of *A. thaliana* overexpressing *AREB-1* (AREB1-OE) simulating closed field drought conditions. Our analyses reinforce the applicability of genetic engineering in modern plant breeding programs to achieve agronomic relevant traits in different crops, according to the demands of each culture.

Results and discussion

CRISPRa plants overexpressing AREB-1 display classical phenotypes of drought tolerance. The transcriptional modulation of *AREB-1* expression by CRISPR was capable of upregulating many important genes related to drought adaptability through the ABA-dependent signaling pathway in plants. *AREB-1* expression improved their physiological performance under severe water deprivation (Fig. 1). To investigate whether AREB1-OX plants displayed enhanced physiological performance during drought, 5-week-old transgenic and WT plants were submitted to gradual desiccation by plant watering suspension for 30 days, followed by re-watering for 1 week (Fig. 2). During the stress, the AREB1-OX plants exhibited a high survival ratio, with a green and healthy phenotype even at 30 days of water suspension (Fig. 2A). After 10 days of stress, the differences between the WT and AREB1-OX plants were not significant. However, after 20 days, the effect of AREB-1 accumulation was notable, giving the transgenic plants more robustness than the WT plants, which displayed curly, dehydrated, and purple- and yellow-colored leaves (Fig. 2A). These symptoms indicated high levels of ROS and secondary metabolite production in response to drought. The enhanced performance of the AREB1-OX plants during stress allowed for complete recovery after re-watering.

We also investigated the drought tolerance of transgenic plants by analyzing the relative water content (RWC) and biomass loss under water scarcity conditions. The RWC observed in transgenic plants was superior to that in WT plants during drought (Fig. 2B). Even 10 days after water deprivation, when AREB1-OX and WT plants did not exhibit contrasting phenotypes, the RWC was at least two fold higher in the transgenic lineages than in the WT plants, demonstrating that the overexpression of *AREB-1* sustained the plants under drought conditions and enhanced adaptive physiological mechanisms during mild-severe stress. These responses could be associated with the most efficient water use ratio or morphological changes that allowed the plants to have enhanced water uptake and/or better evapotranspiration balance.

More importantly, drought-tolerant plants displayed low biomass losses. The biomass reduction rates of CRISPRa AREB-OX plants were significantly lower than the ratios observed in WT plants (Fig. 2C) at a similarly reduced soil moisture content. The biomass loss of AREB1-OX plants was almost the same after 10 and 20 days of stress. In contrast, the WT plants displayed a two fold increase in biomass loss during the same period. The RWC and biomass loss ratios are associated with water use efficiency and evapotranspiration balance in plants.

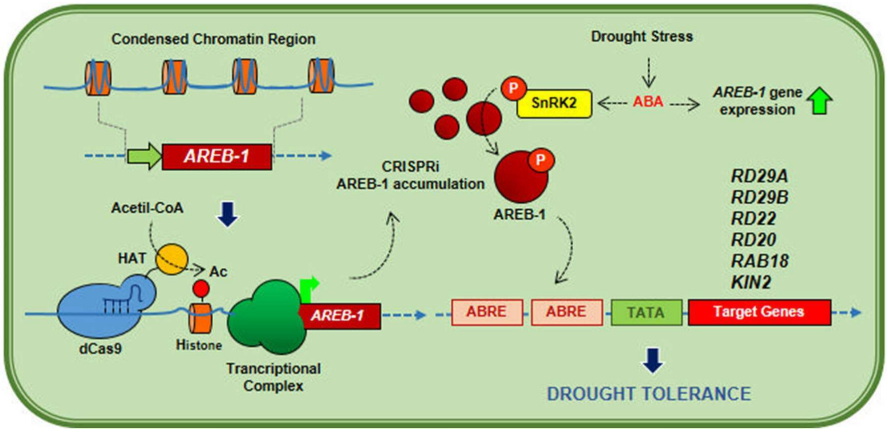

Figure 1. Schematic representation of the strategy of CRISPRa-mediated *AREB-1* overexpression in drought-tolerance improvement. A sgRNA targeting the *AREB-1* promoter region drives nuclease-inactive dCas9 fusion with *A. thaliana* histone acetyl-transferase. Histone acetylation causes structural changes in chromatin and facilitates the transcriptional machinery assembly, resulting in enhanced gene transcription and consequent protein accumulation. The accumulation of AREB-1 acts as a drought-preventive mechanism: during drought, plant cells release ABA, which activates the transcription of *AREB-1* and its transcriptional activity. Because of AREB-1 accumulation, ABA accumulation during the early stages of drought allows for its full activation, and triggers the transcriptional activation of several mechanisms of many genes involved in ABA-mediated drought tolerance, culminating in morpho-physiological changes, which enhances the CRISPRa plants' performance under severe water deprivation.

The overexpression of AREB-1 promotes a protective effect against drought-induced oxidative stress. As a result of water deprivation, plants under drought display imbalanced photosynthesis, and high levels of oxidative damage caused by ROS accumulation[18,19]. Since the transgenic plants showed a lower degree of leaf damage than the WT plants, we investigated whether CRISPRa AREB-OX plants also display lower ROS accumulation and consequent lower cell membrane damage.

Our results demonstrated that under 30 days of water deprivation conditions, the transgenic plants displayed higher levels of chlorophyll A than the WT plants (Fig. 3A). The levels of chlorophyll B were also significantly higher in transgenic lines than in WT plants (Fig. 3A). After recovery, the transgenic plants exhibited levels of chlorophyll close to those displayed by control plants, indicating an appreciable recovery capacity that was not displayed by the wild-type plants (Fig. 3A). Finally, the levels of total chlorophyll in AREB1-OX plants are higher than in WT as an adaptive preset mechanism, independently on the condition, which justifies the green and healthy phenotype previously observed as an effect of *AREB-1* up-regulation in transgenic plants.

We also compared the levels of H_2O_2 and TBA-reactive compounds, which are reliable biomarkers of drought-induced oxidative stress and lipid peroxidation, respectively. Under well-watered conditions, the content of TBA-reactive compound, which includes malonaldehyde (MDA), did not significantly differ between WT and AREB1-OX plants (Fig. 3B). During dehydration, imbalances in the photosystem lead to the formation of H_2O_2, whose damage can be observed in several varieties of biological molecules, such as membrane lipids[18,20,21]. Drought stress enhanced the accumulation of the TBA-reactive compound MDA in the WT and AREB1-OX plants, although to a different extent. The MDA levels were remarkably higher in WT plants than in transgenic plants. In the WT plants, the MDA levels increased 2.5- to 3.0-fold after 10 days and 8.0-fold after 20 days of treatment compared to those of the well-watered plants (Fig. 3B). In AREB1-OX plants the drought-mediated increases in TBA-reactive compounds were as low as 0.5- to 1.0-fold and 4.0- to 5.0-fold after 10 and 20 days of treatment, respectively, suggesting an enhanced antioxidant system in the transgenic plants.

As expected, the levels of H_2O_2 were also higher in WT plants than in transgenic plants submitted to a hyperosmotic environment. The accumulation of H_2O_2 was lower in transgenic plants, as indicated by the light-brown DAB-stained leaves (Fig. 3C). These results were closely linked to the lower MDA yield in transgenic plants and the phenotypical characterization results. The enhanced capacity to uptake water and the fine-tuned controlled evapotranspiration did not allow for electrons to escape in the photosystems, inhibiting the production of ROS and reducing the consequent chlorophyll losses and MDA production during drought. Associated with the higher RWC and chlorophyll content during severe or mild-severe stress as compared to the WT plants, these results confirm that the overexpression of *AREB-1* improves the mechanisms that preserve the cell water content, mitigating oxidative damage during drought.

To determine whether the decreased MDA and H_2O_2 levels in transgenic plants resulted from some mechanism of cell-water maintenance and increased antioxidant activity, we determined the content of soluble sugars and the activity of SOD, CAT, and APX antioxidant enzymes (Figs. 3D, 4). One of the mechanisms for avoiding

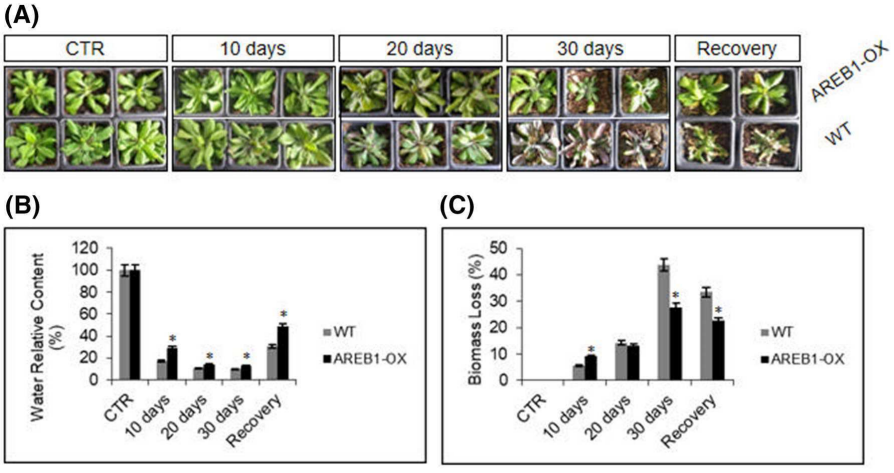

Figure 2. The overexpression of *AREB-1* leads to a classical drought-tolerance phenotype under severe water deprivation. To simulate a closed field drought, 5-week-old *A. thaliana* WT and homozygous lines overexpressing *AREB-1* were exposed to water deprivation for 30 days. (**A**) During drought, the transgenic lines display the classical phenotype of drought tolerance, exhibiting a low ratio of leaf yellowing and curliness, reinforced by the green, healthy phenotype of plants. The WT plants displayed, in addition to leaf yellowing, the production of defensive metabolites triggered by severe drought stress, indicated by purple-colored leaves. After recovery, AREB1-OX plants were almost fully recovered and only 45–50% of the WT plants recovered. (**B**) Relative water content (RWC) during drought. All pots were filled with 98 g of moist soil and *watered normally until drought* stress. During water deprivation, the pots were weighed, and the RWC was calculated according to the initial weight. The RWC values were normalized to the value at 100% RWC of the control groups. (**C**) Biomass loss ratio. The regularly watered plants were randomly distributed on trays and analyzed at intervals of 10 days under 30 days of water deprivation. After drought stress, plants were re-watered for 1 week to calculate the plant survival ratio. Control plants were normally watered during the stress period, and biomass loss was set as 0%. Values represent the increasing biomass loss as compared to 0% of the control group. All analyses were conducted with 3 biological and 2 technical replicates composed of a pool of 9 plants. The bars indicate 5% standard error, and asterisks indicate t-test statistical significance under 95% confidence.

water loss during drought is the enhancement of osmolyte synthesis. The accumulation of simple sugars, such as fructose and glucose, or amino acids, such as proline, reestablishes the osmotic balance, maintaining cell homeostasis[5]. The WT and transgenic lineages accumulated, stably, soluble sugars during stress, exhibiting small ratio variance over time. The transgenic lineages displayed higher sugar content even in well-watered conditions, as observed for the chlorophyll content. These results may suggest that the overexpression of *AREB-1* could affect the regulation of osmotic control mechanisms in plant cells (Fig. 3D).

Under normal water availability, SOD, but not CAT and APX, displayed significantly higher activity in the AREB1-OX plants, which may be a result of CRISPRa-mediated up-regulation of *AREB-1* (Fig. 4A) In contrast, the activities of all three examined enzymes were higher in both transgenic and WT plants under drought, although to a greater extent in AREB1-OX plants (Fig. 4A). Consistent with this result, the expression levels of SOD, CAT and APX genes were higher in AREB1-OX than in WT plants under drought (Fig. 4B).

In well-watered control plants, the levels of TBA-reactive compounds and antioxidative enzyme activities (except for SOD) were not correspondingly different between the WT and transgenic plants (Figs. 3B, 4A). AREB-1 transcription and protein accumulation on their own cannot promote notable improvements in plant physiology because ABA, which is required to activate AREB-1 fully, is produced mainly under drought. Collectively, these mechanisms indicate that the constitutive expression of AREB-1 may act as a preset mechanism of drought response and that previous accumulation of AREB-1 allows for efficient and quick activation in the presence of ABA. AREB-1 positively regulates the mechanisms involved in the antioxidative protection, providing CRISPRa *AREB-1*-enhanced plants with an improved antioxidant system, which mainly contributes to protection against oxidative damage and consequent cell death triggered by drought stress.

Downstream genes in the ABA-mediated drought-responsive stress pathway are upregulated in transgenic plants overexpressing AREB-1. ABA-responsive genes display multiple ABREs or a combination of them with other complementary elements that enhance the transcription of these genes under drought or ABA accumulation[13,22–24]. Given that overexpression of *AREB-1* in Arabidopsis led to notably enhanced drought tolerance, we investigated whether the phenotypic and physiological changes in transgenic

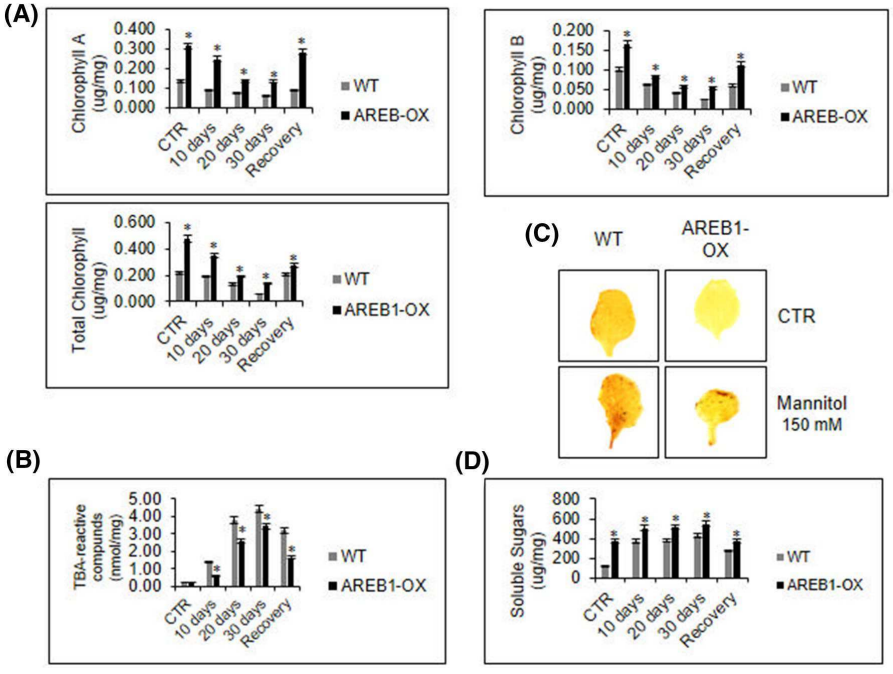

Figure 3. Biochemical characterization of AREB1-OX plants under drought. (**A**) Chlorophyll levels. The levels of chlorophyll A, B, and total chlorophyll were determined in ethanolic extracts during water deprivation by spectrophotometry at 645 nm and 663 nm. Total chlorophyll was expressed as µg/mg of tissue. (**B**) TBA-reactive compounds. In several stresses, plant cells produce ROS. During drought, the collapse of the photosynthetic apparatus enhances the effects of tissue oxidation, culminating in higher levels of malondialdehyde, a TBA-reactive compound produced during lipid peroxidation. (**C**) DAB-mediated hydrogen peroxide detection in leaves. Stressed leaves were stained with DAB and distained in an ethanol bath for H_2O_2 detection. (**D**) Soluble sugar quantification. The soluble sugars were spectrophotometrically quantified in ethanolic extracts by the DNS method using a glucose-based standard curve. Biochemical analyses were conducted with 3 biological and 2 technical replicates. The bars indicate 5% standard error, and asterisks indicate t-test statistical significance under 95% confidence.

plants were correlated with the changes in the expression of downstream genes in the ABA-mediated pathway. These genes included *RD29A*, *RD29B*, *RD22* and *RD20*, *RAB18,* and *KIN2* (Fig. 5).

AREB-1 controls the expression of two classes of drought-responsible genes: (a) LEA genes, which encompass a large group of encoded proteins that display LEA or LEA-like hydrophilic proteins and accumulate during embryogenesis and dehydration and (b) regulatory genes involved in ABA signal transduction and gene expression regulation[14].

Among our analyzed stress markers, RAB 18 is a classical dehydrin of the group 2 LEA proteins, and RD29B and KIN2 are LEA-like proteins, as they do not display canonical consensus motifs but have relatively high amino acid similarity with group 1 and group 2[14]. In addition, the promoter of *RD29B* displays two ABRE sequences, and its expression is strongly related to drought responses mediated by ABA induction[25].

As expected, the overexpression of *AREB-1* upregulated the genes carrying ABRE sequences. During drought, the expression levels of the marker genes demonstrated variable kinetics, but these levels were always higher in the transgenic plants than in the wild type plants (Fig. 5). This variable pattern is already described for other stress- responsive transcription factors, such as NAC transcription factors under multiple stresses in plants[4]. During the stress, the transcription factors that belong to hormone-controlled stress-responsive pathways have their expression modulated by a multilayered network of signal transducers according to the environmental and the intracellular signals. The expression of upstream genes in ABA-responsive pathways, such as *KIN2*, decreases along time after activating downstream cascades. Multiple physiological features lead to a variable expression of *RD29A, RD29B, RD22, RD20* and *RAB18* while plants try to cope with longstanding adverse conditions upon activation of programmed cell death pathways in severe stresses[5–7,12]. In well-watered plants, except for *AREB-1* expression, the levels of the marker genes were not different probably because AREB-1 was not fully activated in the absence of ABA.

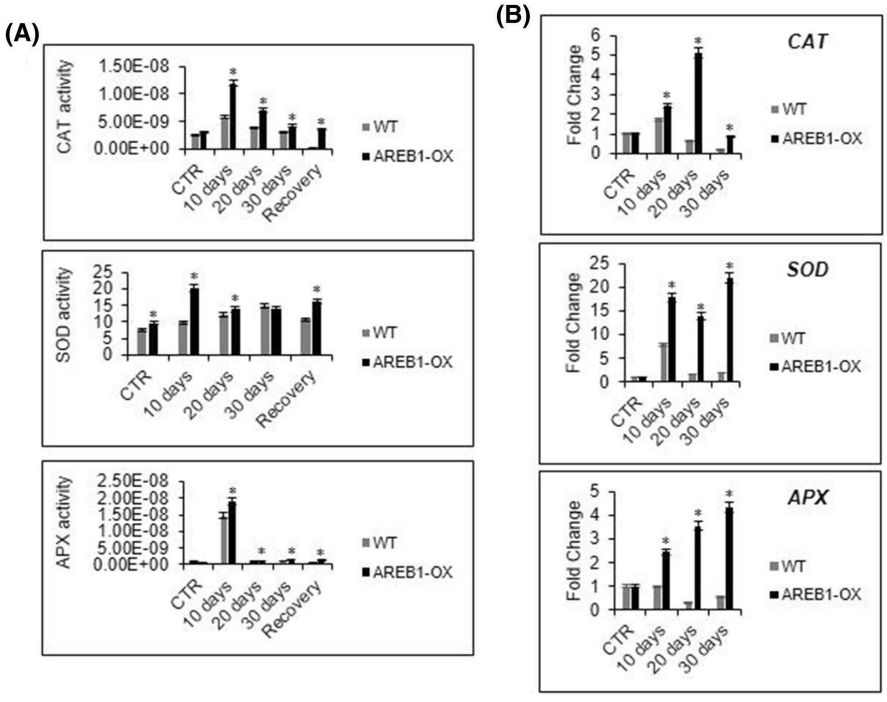

Figure 4. Antioxidant enzymatic activity. (**A**) Enzymatic activity of superoxide dismutase (SOD), catalase (CAT) and ascorbate peroxidase (APX) during drought. The enzymatic activity was spectrophotometrically determined in the whole protein extract, and total protein was determined by the Bradford method. SOD specific activity was expressed as U/total protein, and CAT and APX specific activities were expressed as μmol H_2O_2/min/mg protein and μmol ascorbate/min/mg protein, respectively. All analyses were conducted with 3 biological and 3 technical replicates. The bars indicate 5% standard error, and asterisks indicate *t* test statistical significance under 95% confidence. (**B**) Antioxidant enzyme transcript accumulation. The transcript accumulation of the enzyme genes was quantified by qRT-PCR. Fold change (FC) was calculated by the $2^{-\Delta\Delta Ct}$ method, and the results are expressed in a CTR-normalized manner. Gene expression analysis was conducted with 3 biological and 2 technical replicates. The bars indicate 5% standard error, and asterisks indicate *t* test statistical significance under 95% confidence.

Conclusion

In conclusion, our study shows that overexpression of *AREB-1* mediated by the CRISPRa strategy results in highly improved drought stress responses, encompassing a powerful biotechnology tool for genetic engineering. We provide a complete physiological and biochemical characterization of the AREB-1 function in drought tolerance, reinforcing the relevant role of ABA-related transcription factors in the activation of several molecular mechanisms of stress coping. Collectively, the data demonstrate remarkable transcriptional activation of genes involved in drought stress tolerance, culminating in the improvement of morphological and molecular characteristics related to enhanced plant performance under water deprivation regimes (Fig. 5). The transcriptional activation of *AREB-1* leads to lower biomass loss and higher relative water content during 30 days under water deprivation conditions than those of the WT plants. The water deficit tolerant phenotype may be associated with higher antioxidant enzyme activity, and higher levels of soluble sugars, which regulated the efficiency of water use and consequent ROS accumulation, chlorophyll maintenance, and plant survival.

Methods

Plant growth and stress treatment. The transgenic homozygous Arabidopsis seeds of AREB1-OX and WT ecotype Columbia (Col 0) were germinated on soil under controlled growth-chamber conditions: 22 °C, a 12 h/12 h photoperiod and 70% humidity. After 2 weeks, the seedlings were transferred to individual pots filled with 98 g of moist soil homogenized with glufosinate-ammonium (100 mg/L). The pots were randomly distributed in trays, exposed to the same light intensity and regularly watered with 500 mL of water two times/week. The controlled conditions in the growth chamber and experimental design should be precisely followed to guarantee similar reducing rate in the soil moisture to all lines during the drought assay. After acclimation,

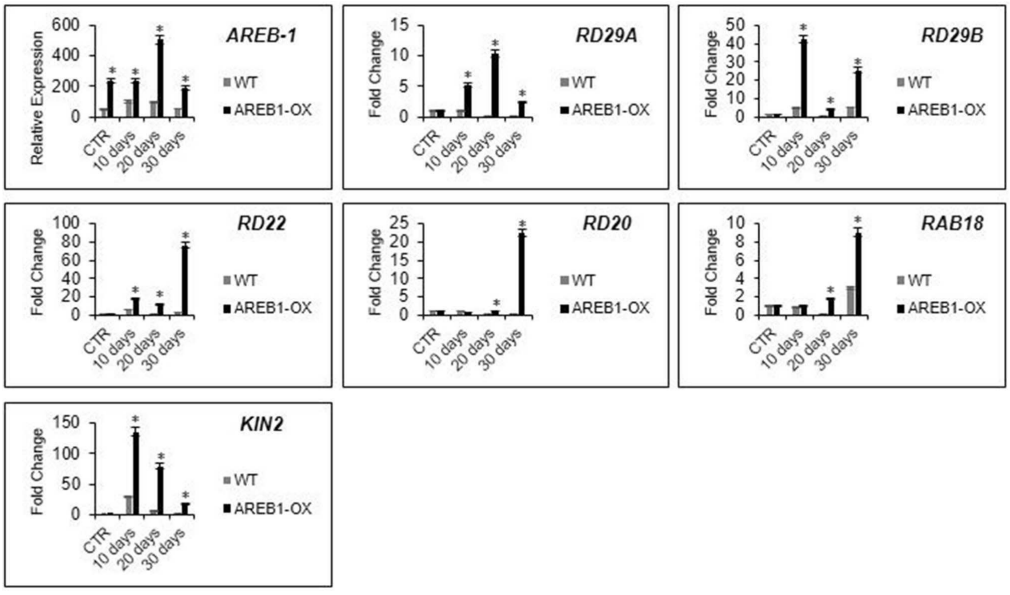

Figure 5. The effect of *AREB-1* overexpression on transcriptional regulation of ABA-responsive downstream genes. The water deprivation increases ABA content in plant cells, which triggers an adaptive osmotic stress response via morpho-physiological changes. High levels of ABA up-regulate the expression of AREB-1, which is fully activated by SnRK2-mediated phosphorylation, which isalso positively regulated by ABA. Once active, AREB-1 can bind ABRE *cis*-elements on ABA-responsive promoters, eliciting a drought-responsive pathway that confers tolerance. The level of expression of *AREB-1* was determined at each predetermined time point during water deprivation. As expected, the relative expression was markedly higher in the CRISPRa lines than in the WT plants. The relative expression was calculated using the $2^{-\Delta Ct}$ method and expressed as a relation between endogenous and target-gene transcript levels. The expression of the *AREB-1* downstream genes (*RD29A*, *RD29B*, *RD22*, *RD20*, *RAB18,* and *KIN2*) was determined by the $2^{-\Delta\Delta Ct}$ method, and FC was expressed in a CTR-normalized manner. Gene expression analysis was conducted with 3 biological and 2 technical replicates. The bars indicate 5% standard error, and asterisks indicate *t* test statistical significance under 95% confidence.

all pots were weighed, and the watering was suspended for 30 days to generate osmotic stress. The control group (unstressed plants) consisted of plants under regular and controlled watering. The samples for physiological assays were collected every 10 days after water deprivation and immediately frozen in liquid nitrogen. The pots were weighed during each sample collection. After 30 days under continuous drought, the plants were irrigated daily with 200 mL of water for 1 week. All analyses were conducted with 3 biological and 2 technical replicates composed of a pool of 9 plants.

RNA extraction and cDNA synthesis. Total RNA was extracted from 100 to 150 mg of leaves using TRIzol (Invitrogen, Carlsbad, CA-USA) according to the manufacturer's recommendations. The RNA was quantified spectrophotometrically using a NanoDrop instrument (Thermo Fisher, Waltham, Massachusetts, USA), and its quality and integrity were evaluated by electrophoresis on a 1% (w/v) agarose gel. A total of 1 µg of RNA was used to perform cDNA synthesis according to the MMLV reverse transcriptase (Invitrogen, Carlsbad, CA-USA) protocol.

qPCR and gene expression analysis. The expression profile of ABA-related and antioxidant enzyme genes was performed with a QuantStudio3 qPCR System (Thermo Fisher, Waltham, Massachusetts-USA) using SYBR Green (Invitrogen, Carlsbad, CA-USA) reagent according to the manufacturer's recommendations. All genes were analyzed with 3 biological samples and 2 technical replicates using gene-specific primers (Supplementary Table 1). The reaction was performed as follows: 2 min at 50 °C, 10 min at 95 °C, and 40 cycles of 94 °C for 15 s and 60 °C for 1 min. *GAPDH* and *EFL1A* were chosen as endogenous control genes (normalizer), and relative gene expression was calculated by the $2^{-\Delta\Delta Ct}$ comparative method.

Relative water content and biomass loss. During the stress treatment, the pots were filled with the same amount of soil moisture and watered with the same volume of water. After the seedling transfer, the pots

were well-watered for 1 week, and their initial weights were recorded. During water deprivation, the pots were weighed every day for 10 days. To calculate the relative water content (RWC), the weight of each pot was compared with the weight of the well-watered pot, and the difference between them was expressed as RWC (%) according to the following equation: $[RWC = (100 \times W_n)/W_0]$, in which W_n represents the weight at the time of analysis (expressed in days under water deprivation; n = 10, 20 or 30). W_0 represents the weight of the well-watered pot. For recovered plants, the same equation was used replacing W_n by W_r, in which W_r = weight of re-watered pot.

To calculate biomass loss (BL), the initial weight of each plant was considered to be 1, and the biomass loss was expressed as a percentage throughout the water deprivation period, comparing the weight of the plant at the time of analysis and that of the well-watered plant at the beginning of the stress period. The equation used in this analysis was $[BL = ((W_0 - W_n) \times 100)/W_0]$, in which W_n represents the plant weight at the time of analysis and W_0 represents the weight of the well-watered plant.

Chlorophyll content. Total chlorophyll was determined spectrophotometrically, according to described by Melo et al.[4]. Approximately 100 mg of leaves were weighed, and total chlorophyll was extracted with 1 mL of absolute ethanol in a dark tube. The ethanolic extract was centrifuged at 12,000*g* and 4 °C for 15 min, and the supernatant was quantified in a spectrophotometer at 645 nm and 663 nm. Total chlorophyll was expressed in µg/mg of tissue.

Sugar content. The reducing sugar content was determined in the ethanolic extract by the 3,5-dinitrosalycilic acid (DNS) method. DNS (0.1% w/v) was prepared in sodium and potassium tartrate (30% w/v) and sodium hydroxide (0.4 M). An aliquot of 100 µL of leaf extract was added to 900 µL of water and 500 µL of DNA, and the reaction was performed in a boiling water bath for 5 min. After the reaction, the samples were immersed on ice, and their absorbance was acquired with a spectrophotometer at 540 nm. The sugar content was determined using a glucose-based standard curve (0–1.2 µg/µL).

Oxygen species analysis. Reactive oxygen species accumulation was analyzed by quantification of TBA-reactive compounds and in situ H_2O_2 staining. Lipid peroxidation is a process with a final product of malondialdehyde (MDA), which reacts with thiobarbituric acid (TBA). TBA-reactive compounds were quantified as described by Melo et al.[4]. Approximately 200 mg of leaves were homogenized in 2 mL of 0.1% (v/v) trichloroacetic acid (TCA) and then centrifuged at 12,000*g* for 15 min. An aliquot of 500 µL of the clarified supernatant was added to 1.5 mL of 0.5% (w/v) thiobarbituric acid (TBA) in 20% (v/v) TCA, and the samples were incubated at 90 °C for 20 min. The reaction was stopped by incubation on ice, followed by centrifugation for 4 min. The absorbance of the supernatant was measured at 532 nm, and the concentration of TBA-reactive compounds was calculated considering the MDA molar extinction coefficient of 155 mM cm^{-1}.

For hydrogen peroxide staining, the plants were submerged in a mannitol (150 mM) solution for 24 h, and the leaves were carefully removed and immediately incubated with 3,3-diaminobenzamidine (DAB) solution (1 mg/mL, pH 3.8) for 8 h under continuous agitation. After staining, the leaves were distained in 100% ethanol until total chlorophyll was lost. The leaves were rehydrated in water and glycerol (10% v/v) and photographed stereoscopically.

Antioxidant enzyme activity. The enzymatic activities of superoxide dismutase (SOD), catalase (CAT) and ascorbate peroxidase (APX) were determined in the whole protein extract. The proteins from 150 to 200 mg of leaves were extracted in 1 mL of 100 mM phosphate buffer pH (7.8) and added to DTT (0.5 g/L), EDTA (10 µM) and PVPP (0,3 mg/mL). Then, all samples were centrifuged at 12,000*g* and 4 °C for 15 min. An aliquot of 500 µL of the clarified supernatant was transferred to 500 µL of extraction buffer and kept on ice until enzymatic activity determination. All enzymatic activities were determined in 3 biological samples and 2 technical replicates, and total protein was determined by the Bradford method.

For SOD activity, a reaction mix was prepared with 100 µL of phosphate buffer, 40 µL of methionine solution (12 g/L), 2 µL of EDTA (3.5 g/L), 15 µL of NBT (0.35 g/L), 2 µL of riboflavin (0.008 g/L), 31 µL of milli-Q water, and 10 µL of protein extract for each reaction. An aliquot of 200 µL of the reaction mix was separated to be used as the "absolute blank", and another aliquot was separated to be used as the "light blank" during NBT light-mediated reduction. The assay was performed in chilled 96-well microplates avoiding exposure of the samples to light. NBT reduction was performed under intense white light exposure for 40 min, and the absorbance was immediately measured in a spectrophotometer at 560 nm. SOD activity was expressed in relation to the percentage of inhibition of light-mediated NBT reduction. To calculate SOD activity, the inhibition percentage was calculated by the expression $IN\ (\%) = \frac{LB - SA - AB}{LB}$, in which LB = light blank, SA = sample absorbance, and AB = absolute blank. Once the IN (%) was calculated, it was used to calculate the units of SOD (U), considering that 1 SOD unit is necessary to inhibit 50% of light-mediated NBT reduction. Finally, the specific SOD activity was calculated by the expression $SOD = \frac{IN\ (\%).10}{U \cdot TP}$, in which IN (%) = the percentage of inhibition, U = SOD units, and TP = total protein (µg/g). The SOD specific activity was expressed in U/total protein.

The CAT activity was determined using a reaction mixture composed of 144 µL of phosphate buffer, 30 µL of water and 16 µL of hydrogen peroxide solution (50 mM). To determine CAT activity, the reaction mixture was added to 10 µL of protein extract, and the absorbance reading was performed for 10 min at intervals of 30 s at 240 nm using a chilled optical 96-well plate. To calculate CAT activity, the absorbance of samples was subtracted from the blank absorbance by the expression $CAT = \frac{dA\ .0{,}0067}{T\ .39{,}4.\ W}$, in which dA = (initial absorbance–final absorbance), T = time of reaction, 39.4 mol cm^{-1} represents the molar extinction coefficient of hydrogen peroxide, and W = sample weight. The CAT specific activity is expressed in µmol H_2O_2/min/mg protein.

The APX activity was determined as described for CAT, and the reaction mixture was added to 10% (v/v) ascorbic acid solution (18 g/L). The molar extinction coefficient of ascorbic acid is 2.8 mol cm^{-1}, and the absorbance was measured at 290 nm. As for CAT activity, APX activity is expressed in µmol ascorbate/min/mg protein.

Received: 7 May 2020; Accepted: 2 September 2020
Published online: 01 October 2020

References

1. Baxter, A., Mittler, R. & Suzuki, N. ROS as key players in plant stress signaling. *J. Exp. Bot.* **65**, 1229–1240 (2013).
2. Bota, J., Medrano, H. & Flexas, J. Is photosynthesis limited by decreased Rubisco activity and RuBP content under progressive water stress?. *New Phytol.* **162**, 671–681 (2004).
3. Zhu, J.-K. Abiotic stress signaling and responses in plants. *Cell* **167**, 313–324 (2016).
4. Melo, B. P. *et al.* Revisiting the soybean GmNAC superfamily. *Front. Plant Sci.* **9**, 1864 (2018).
5. Nakashima, K., Yamaguchi-Shinozaki, K. & Shinozaki, K. The transcriptional regulatory network in the drought response and its crosstalk in abiotic stress responses including drought, cold, and heat. *Front. Plant Sci.* **5**, 170 (2014).
6. Singh, K., Foley, R. & Oñate-Sánchez, L. Transcription factors in plant defense and stress responses. *Curr. Opin. Plant Biol.* **5**, 430–436 (2002).
7. Busk, P. K. & Pagès, M. Regulation of abscisic acid-induced transcription. *Plant Mol. Biol.* **37**, 425–435 (1998).
8. Guiltinan, M., Marcotte, W. Jr. & Quatrano, R. A plant leucine zipper protein that recognizes abscisic acid response element. *Science* **250**, 267–271 (1990).
9. Mundy, J. & Yamaguchi-Shinozaki, K. Nuclear proteins bind conserved elements in the abscisic acid-responsive promoter of a rice rab gene. *Proc. Natl. Acad. Sci. U. S. A.* **87**, 1406–1410 (1990).
10. Choi, H. I., Hong, J. H., Ha, J. O., Kang, J.-Y. & Kim, S. Y. ABFs, a family of ABA-responsive element binding factors. *J. Biol. Chem.* **275**, 1723–1730 (2000).
11. Uno, Y. *et al.* Arabidopsis basic leucine zipper transcription factors involved in an abscisic acid-dependent signal transduction pathway under drought and high-salinity conditions. *Proc. Natl. Acad. Sci.* **97**, 11632–11637 (2000).
12. Yoshida, T., Mogami, J. & Yamaguchi-Shinozaki, K. ABA-dependent and ABA-independent signaling in response to osmotic stress in plants. *Curr. Opin. Plant Biol.* **21**, 133–139 (2014).
13. Yoshida, T. *et al.* AREB1, AREB2, and ABF3 are master transcription factors that cooperatively regulate ABRE-dependent ABA signaling involved in drought stress tolerance and require ABA for full activation. *Plant J.* **61**, 672–685 (2010).
14. Fujita, Y. *et al.* AREB1 is a transcription activator of novel ABRE-dependent ABA signaling that enhances drought stress tolerance in Arabidopsis. *Plant Cell* **17**, 3470–3488 (2005).
15. Oh, S.-J. *et al.* Arabidopsis CBF3/DREB1A and ABF3 in transgenic rice increased tolerance to abiotic stress without stunting growth. *Plant Physiol.* **138**, 341–351 (2005).
16. Roca Paixão, J. F. *et al.* Improved drought stress tolerance in arabidopsis by CRISPR/dCas9 fusion with a Histone AcetylTransferase. *Sci. Rep.* **9**, 8080 (2019).
17. Todaka, D., Shinozaki, K. & Yamaguchi-Shinozaki, K. Recent advances in the dissection of drought-stress regulatory networks and strategies for development of drought-tolerant transgenic rice plants. *Front. Plant Sci.* **6**, 84 (2015).
18. Petrov, V., Hille, J., Mueller-Roeber, B. & Gechev, T. S. ROS-mediated abiotic stress-induced programmed cell death in plants. *Front. Plant Sci.* **6**, 69–69 (2015).
19. Choudhury, F. K., Rivero, R. M., Blumwald, E. & Mittler, R. Reactive oxygen species, abiotic stress and stress combination. *Plant J.* **90**, 856–867 (2017).
20. Petrov, V. D. & Van Breusegem, F. Hydrogen peroxide-a central hub for information flow in plant cells. *AoB PLANTS* **2012**, pls014–pls014 (2012).
21. Gill, S. S. & Tuteja, N. Reactive oxygen species and antioxidant machinery in abiotic stress tolerance in crop plants. *Plant Physiol. Biochem. PPB* **48**, 909–930 (2010).
22. Marcotte, W. R. Jr., Russell, S. H. & Quatrano, R. S. Abscisic acid-responsive sequences from the em gene of wheat. *Plant Cell* **1**, 969–976 (1989).
23. Shen, Q., Zhang, P. & Ho, T. H. Modular nature of abscisic acid (ABA) response complexes: composite promoter units that are necessary and sufficient for ABA induction of gene expression in barley. *Plant Cell* **8**, 1107–1119 (1996).
24. Narusaka, Y. *et al.* Interaction between two cis-acting elements, ABRE and DRE, in ABA-dependent expression of Arabidopsis rd29A gene in response to dehydration and high-salinity stresses. *Plant J.* **34**, 137–148 (2003).
25. Yamaguchi-Shinozaki, K. & Shinozaki, K. A novel cis-acting element in an Arabidopsis gene is involved in responsiveness to drought, low-temperature, or high-salt stress. *Plant Cell* **6**, 251–264 (1994).

Acknowledgements

This work was supported by fellowships from INCT PlantStress Biotech, EMBRAPA, UCB, CNPq, CAPES, and FAPDF. The authors declare no conflict of interest.

Author contributions

M.F.G.S. was the leading researcher for all the work and provided intellectual input and financial support. B.P.M. and I.T.L.T. performed all the molecular experiments, biochemical assays, phenotypical and physiological observations. J.R.P. performed plant transformation and D.D.N. performed RNA extraction and cDNA synthesis. M.F.G.S., E.P.B.F., J.A.E., and M.C.M. provided intellectual input. B.P.M. and I.T.L.T. wrote the first draft of the manuscript. E.P.B.F. critically read and corrected the manuscript. All authors read and approved the final version.

Competing interests

The authors declare no competing interests.

Additional information

Supplementary information is available for this paper at https://doi.org/10.1038/s41598-020-72464-y.

Correspondence and requests for materials should be addressed to M.F.G.-d.

Reprints and permissions information is available at www.nature.com/reprints.

CHAPTER II

REVISITING THE SOYBEAN GmNAC SUPERFAMILY

Published article

Bruno P. Melo, Otto T. Fraga, José Cleydson F. Silva, Dalton O. Ferreira, Otávio J. B. Brustolini, Paola A. Carpinetti, Joao Paulo B. Machado, Pedro A. B. Reis and Elizabeth P. B. Fontes. **Revisiting the soybean GmNAC superfamily**. Frontiers in Plant Sciences 9, 1864 (2018). doi: 10.3389/fpls.2018.01864

Pages 35 to 56

RESUMO

Os genes *NAC* (NAM, ATAF e CUC) codificam fatores de transcrição envolvidos no controle da morfofisiologia de plantas e respostas ao estresse. A liberação da última montagem do genoma da soja (*Glycine max* - Wm82.a2.v1) levantou a possibilidade de que novos genes NAC estariam poderiam estar presentes em seu genoma. Aqui, interrogamos a última versão do genoma da soja contra a estrutura conservada do domínio NAC. Nossa análise identificou 32 novos genes *NAC* putativos, atualizando a superfamília para 180 membros. Também organizamos os genes em 15 subfamílias filogenéticas, que demostraram uma correlação perfeita entre a conservação de sequência, perfil de expressão e função dos genes ortólogos de *Arabidopsis thaliana* e soja. Para validar nossas análises *in silico*, monitoramos os perfis de expressão gênica mediada por estresse de oito novos genes NAC por qRT-PCR e os genes *GmNAC* associados à senescência natural por RNA-seq. Entre estresse no ER, estresse osmótico e tratamento com ácido salicílico simulando estresse biótico, todos os novos genes *GmNAC* testados responderam a pelo menos um tipo de estresse, exibindo um perfil de expressão complexo sob diferentes cinéticas e extensão da resposta. Além disso, mostramos que 40% dos *GmNACs* foram regulados diferencialmente pela senescência natural da folha, incluindo oito (8) *GmNACs* recém-identificados. Os perfis de expressão de desenvolvimento dos novos genes *NAC* se ajustaram perfeitamente à sua subfamília filogenética. Finalmente, examinamos duas proteínas associadas à senescência não caracterizadas, GmNAC065 e GmNAC085, e uma nova proteína NAC, previamente não identificada, GmNAC177, e mostramos que são localizadas no núcleo e, exceto para GmNAC065, exibem atividade de transativação em leveduras. Consistente com um papel na senescência foliar, a expressão transitória de GmNAC065 e GmNAC085 induz o aparecimento de marcas de senescência foliar, incluindo perda de clorofila, amarelecimento da folha, peroxidação lipídica e acúmulo de H_2O_2, porém, com perfis constrastantes. GmNAC177 foi agrupado em uma subfamília não caracterizada, mas em estreita proximidade com a subfamília TIP. Consequentemente, foi rapidamente induzido por estresse ER e por ácido salicílico sob resposta cinética tardia e promoveu a morte celular in planta. Coletivamente, nossos dados fundamentaram ainda mais a noção de que os genes *GmNAC* exibem perfis funcionais e

de expressão consistentes com sua relação filogenética e estabeleceram uma estrutura completa da superfamília NAC de soja como base para análises futuras.

frontiers in Plant Science

ORIGINAL RESEARCH
published: 18 December 2018
doi: 10.3389/fpls.2018.01864

Revisiting the Soybean GmNAC Superfamily

*Bruno P. Melo[1,2], Otto T. Fraga[1,2], José Cleydson F. Silva[1], Dalton O. Ferreira[1], Otávio J. B. Brustolini[1], Paola A. Carpinetti[2], Joao Paulo B. Machado[3], Pedro A. B. Reis[1,2] and Elizabeth P. B. Fontes[1,2]**

[1] National Institute of Science and Technology in Plant-Pest Interactions, Bioagro, Universidade Federal de Viçosa, Viçosa, Brazil, [2] Departamento de Bioquímica e Biologia Molecular/BIOAGRO, Universidade Federal de Viçosa, Viçosa, Brazil, [3] Agronomy Institute, Universidade Federal de Viçosa, Florestal, Brazil

The *NAC* (NAM, ATAF, and CUC) genes encode transcription factors involved with the control of plant morph-physiology and stress responses. The release of the last soybean *(Glycine max)* genome assembly (Wm82.a2.v1) raised the possibility that new NAC genes would be present in the soybean genome. Here, we interrogated the last version of the soybean genome against a conserved NAC domain structure. Our analysis identified 32 putative novel NAC genes, updating the superfamily to 180 gene members. We also organized the genes in 15 phylogenetic subfamilies, which showed a perfect correlation among sequence conservation, expression profile, and function of orthologous *Arabidopsis thaliana* genes and NAC soybean genes. To validate our *in silico* analyses, we monitored the stress-mediated gene expression profiles of eight new NAC-genes by qRT-PCR and monitored the GmNAC senescence-associated genes by RNA-seq. Among ER stress, osmotic stress and salicylic acid treatment, all the novel tested GmNAC genes responded to at least one type of stress, displaying a complex expression profile under different kinetics and extension of the response. Furthermore, we showed that 40% of the GmNACs were differentially regulated by natural leaf senescence, including eight (8) newly identified GmNACs. The developmental and stress-responsive expression profiles of the novel NAC genes fitted perfectly with their phylogenetic subfamily. Finally, we examined two uncharacterized senescence-associated proteins, GmNAC065 and GmNAC085, and a novel, previously unidentified, NAC protein, GmNAC177, and showed that they are nuclear localized, and except for GmNAC065, they display transactivation activity in yeast. Consistent with a role in leaf senescence, transient expression of GmNAC065 and GmNAC085 induces the appearance of hallmarks of leaf senescence, including chlorophyll loss, leaf yellowing, lipid peroxidation and accumulation of H_2O_2. GmNAC177 was clustered to an uncharacterized subfamily but in close proximity to the TIP subfamily. Accordingly, it was rapidly induced by ER stress and by salicylic acid under late kinetic response and promoted cell death *in planta*. Collectively, our data further substantiated the notion that the GmNAC genes display functional and expression profiles consistent with their phylogenetic relatedness and established a complete framework of the soybean NAC superfamily as a foundation for future analyses.

Keywords: NAC, soybean, phylogenetic analysis, senescence-associated genes, genome-wide expression profiling, GmNAC superfamily, transcriptional factors

OPEN ACCESS

Edited by:
Alejandra A. Covarrubias, National Autonomous University of Mexico, Mexico

Reviewed by:
Oswaldo Valdes-Lopez, National Autonomous University of Mexico, Mexico
Marina E. Battaglia, CONICET Instituto de Investigaciones en Biodiversidad y Biotecnología (INBIOTEC), Argentina

***Correspondence:**
Elizabeth P. B. Fontes
bbfontes@ufv.br

Specialty section:
This article was submitted to Plant Abiotic Stress, a section of the journal Frontiers in Plant Science

Received: *29 June 2018*
Accepted: *04 December 2018*
Published: *18 December 2018*

Citation:
Melo BP, Fraga OT, Silva JCF, Ferreira DO, Brustolini OJB, Carpinetti PA, Machado JPB, Reis PAB and Fontes EPB (2018) Revisiting the Soybean GmNAC Superfamily. Front. Plant Sci. 9:1864. doi: 10.3389/fpls.2018.01864

INTRODUCTION

As sessile organisms, plants are exposed to various environmental adverse conditions including drought, salinity, pest, and pathogen attacks. To cope with these stress conditions, plants have evolved a sophisticated mechanism for the perception of stimuli and transduction of signals, which leads to the reprogramming of gene expression for adaptation. The knowledge about the molecular mechanisms by which plants avoid the stresses conditions and adapt themselves to maintain yield may allow the identification of molecular targets for genetic engineering of stress tolerance. In these cascades of signals, the transcription factors (TF) are among the most promising molecular targets to promote adaptive plant physiology changes.

Among the TF families, the plant-specific NAC (an acronym for NAC, ATAF and CUC) superfamily comprises one of the largest family of TFs (Shao et al., 2015). NAC TFs display a conserved amino-terminus, encompassing the DNA binding domain, and a rather variable carboxyl-terminus, which harbors a transcriptional regulatory domain with either repressing or activating functions (Aida et al., 1997; Olsen et al., 2005; Nakashima et al., 2011). A subset of NAC proteins may also exhibit protein binding activity and an additional transmembrane domain present in the membrane-tethered NAC proteins (Tran et al., 2009; Seo et al., 2010). The DNA binding domain, the NAC domain, which has been used as a template for the identification of NAC genes in different plant species, contains 150–200 conserved amino acids split into two exons that are further divided into five conserved subdomains, designated A-E.

The NAC genes were first identified as major players in plant development. Several NAC members have been functionally characterized in floral development (Sablowski and Meyerowitz, 1998), apical meristem formation (Hegedus et al., 2003; Hibara et al., 2003), lateral root development (Xie et al., 2000; Hao et al., 2011; Quach et al., 2014), growth hormone signaling (Xie et al., 2000; Fujita et al., 2004), cell-cycle control (Kim et al., 2006), secondary cell wall thickening and biogenesis (Mitsuda et al., 2005, 2007; Zhong et al., 2006; Mitsuda and Ohme-Takagi, 2008; Dong et al., 2013), and senescence (Guo and Gan, 2006; Kim et al., 2016). High-resolution temporal expression profiles revealed that a large fraction of NAC TFs is differentially expressed during several stages of natural leaf senescence in Arabidopsis (Breeze et al., 2011), suggesting that they play a crucial role in the regulation of senescence. Although functional information in developmental programmed leaf senescence is available for family members of different plant species (Guo and Gan, 2006; Kim et al., 2009; Balazadeh et al., 2010, 2011; Yang et al., 2011; Lee et al., 2012; Wu et al., 2012; Li et al., 2016b; Pimenta et al., 2016), demonstrating the biotechnological potential of the senescence NAC genes for seed yield (Liang et al., 2014), the repertoire of differential expressed senescence-associated NAC genes in the genome of relevant crops, including soybean, maize, and rice, remains to be determined.

From the pioneering studies of NAC TFs in developmental programs, the NAC TF function has expanded to include key regulators of plant defenses against environmental stresses; thereby, emerging as potential targets for engineering stress tolerance in crops (Nakashima et al., 2011; Puranik et al., 2012; Shao et al., 2015). The NAC TFs have also been shown to play relevant roles in the control of plant defenses against pathogens (Puranik et al., 2012), programmed cell death (Faria et al., 2011; Mendes et al., 2013; Mao et al., 2018) and endoplasmic reticulum stress (Yang et al., 2014a,b; Reis et al., 2016).

Concerning abiotic stress responses, the NAC genes have been primarily studied for drought tolerance. The functions of NAC TFs in the improvement of drought tolerance was firstly demonstrated in Arabidopsis by the overexpression of the *ANAC019*, *ANAC055,* and *ANAC072* genes (Tran et al., 2004, 2007). Abiotic stress-related functions of NAC TFs in various plant species, including important crops such as rice and wheat, have also been reported (Nakashima et al., 2007, 2011; Puranik et al., 2012), even in field trials (Hu et al., 2006; Redillas et al., 2012). Likewise, in soybean, GmNAC020 has been demonstrated to promote abiotic stress tolerance and lateral root formation in transgenic plants (Hao et al., 2011). Furthermore, by examining contrasting soybean genotypes for drought tolerance, a positive correlation between the expression of a subset of GmNACs and drought tolerance has been reported (Kim et al., 2006), further supporting the notion that GmNACs may be selected as a target for improving drought tolerance. The drought-sensitive (B217 and H228) and the drought-tolerant (Jindou 74 and 78) soybean cultivars have also been used to select GmNACs highly expressed in the drought-resistant soybean varieties (Hussain et al., 2017). The potential of NAC genes for tolerance to high salinity and cold has also been investigated in several plant species (Hu et al., 2006, 2008; Nakashima et al., 2007; Zheng et al., 2009; Takasaki et al., 2010; Hao et al., 2011; Song et al., 2011; Cao et al., 2017). However, most NAC transcription factors have not yet been functionally characterized, and the extension and complexity of the NAC family in the plant kingdom have not been thoroughly examined.

In soybean, the first study of NAC genes included the molecular cloning of six NAC genes designated as GmNAC1-6 (Meng et al., 2007). Subsequently, the expression of these genes in response to various stress conditions and hormone treatments was analyzed and the identification of 111 NAC genes in the soybean genome was reported (Pinheiro et al., 2009). These studies were expanded to cover the expression of 31 GmNAC genes at the seedling stage and under different stress conditions (Tran et al., 2009). A more complete genome-wide survey identified 152 full-length GmNAC TFs, including 11 membrane-bound members, and 31 drought-responsive GmNACs with some degree of tissue-specificity (Le et al., 2011). However, the dynamic of drought-responsiveness of GmNACs was found to be complex and integrated with tissue-specific and/or developmental stage-dependent expression profiles of these genes (Le et al., 2012). More recently, the number of membrane-bound NAC transcription factor (NTL) genes was expanded from 11 to 15 genes, from which seven duplicated genes were identified (Le et al., 2011; Li et al., 2016b). An evolutionary and functional analysis of the soybean membrane-bound NAC transcription factor genes indicated that their

membrane release is essential for function and the duplicate genes diverge functionally, which contributes as an evolutionary driving force for the retention of these GmNTL duplicate genes (Li et al., 2016b). These recent studies together with the release of the last version of the soybean genome (version V11) indicate that the complete repertoire of the NAC genes in the soybean genome remains to be described.

The size of the NAC family has also been examined in Arabidopsis (111 genes), rice (151), maize (152), and other plant species (Shao et al., 2015). The family has been divided into subgroups based on phylogenetic relatedness, showing a clear relationship between structure and expression for representatives of each subgroup (Pinheiro et al., 2009). A common theme that has emerged from these genome-wide analyses and expression-profiling studies is that the plant NAC family is structurally and functionally conserved with a high degree of ascertaining for functional predictions of putative orthologs from different species. Accordingly, the full determination of the NAC superfamily among plant species is expected to accelerate the functional characterization of this extensive family of plant-specific TFs in relevant crops to which molecular tools are limited and hence functional studies are more difficult to pursue. In this study, we revisited the GmNAC family by using the most recent assembly of the soybean genome, which allowed us to perform a phylogenetic reconstruction of the family. Through this analysis, we identified 32 additional members of the soybean NAC family, which were clusters in the previously characterized subgroups of GmNACs based on phylogeny and expression analysis. We also confirmed the size of the membrane-tethered GmNACs, identified the GmNAC-associated senescence genes by genome-wide expression analyses and performed functional assays of cell death-associated gene representatives.

MATERIALS AND METHODS

Phylogenetic Reconstruction of the Soybean NAC Superfamily

A revised soybean genome assembly (version Wm82.a2.v1-v11.0) released in 2015 in the Pthytozome database (www.phytozome.jgi.doe.gov) led us to investigate the existence of new NAC genes (complete ORFs) in the soybean genome. We used the Pfam (29.0-http://pfam.xfam.org/) NAC domain as the prototype sequence for searching against all deduced protein sequences from the last soybean genome assembly Wm82.a2.v1-v11.0 in the FASTA format. The sequences comparison was performed in InterProScan 5 (http://www.ebi.ac.uk/Tools/pfa/iprscan5/) software, and newly identified proteins, not described by Le et al. (2011), were grouped by ID number (Glyma v11.0 pattern), size (amino acid number), NAC domain position (the first and the least amino acids that characterize NAC domain), *E*-value (statistical significance), and transmembrane-domain probability (**Supplementary Table 1**). Only the sequences that contained a full-length NAC domain were used for the multiple alignments and phylogenetic analysis.

For the phylogenetic reconstruction of the soybean NAC superfamily, the *Arabidopsis thaliana* deduced NAC protein (available in Phytozome) sequences were used in a global alignment with all soybean full-length NAC sequences. The alignment was conducted using Muscle algorithm (http://www.ebi.ac.uk/Tools/msa/muscle/) and allowed not only a sequence-based comparison but also a function-based comparison, as *A. thaliana* NAC transcription factors have been well-characterized. To refine the phylogenetic reconstruction, *A. thaliana* ortholog proteins from EggNOG database (http://eggnogdb.embl.de/#/app/home) were individually compared with soybean proteins. The sequences were used to reconstruct the NAC soybean and Arabidopsis phylogenetic tree by the maximum likelihood statistical method with 10.000 bootstraps. The tree was edited using the FigTree (http://tree.bio.ed.ac.uk/software/figtree/) software.

Distribution of the New NAC Genes in the Soybean Chromosomes

To determine the distribution of the NAC genes along 20 soybean chromosomes, the NAC domain sequence available on InterProScan database (code: IPR003441) was used as a guide and the analysis was performed using PLAZA 3.0 (Plant Comparative Genome-http://bioinformatics.psb.ugent.be/plaza/versions/plaza_v3_dicots/genome_mapping/index), which provides a schematic diagram of soybean chromosomes and the position of the guide-related genes. PLAZA's diagram and Phytozome ID NAC numbers were used to organize the superfamily in a schematic chromosome map.

Synteny Analysis

The duplicated GmNAC CDS sequences were aligned with Clustal Omega (https://www.ebi.ac.uk/Tools/msa/clustalo) to predict the duplications/ paralogous pairs. The R package seqinr (http://seqinr.r-forge.r-project.org) was used to calculate the non-synonymous (Ka) and synonymous (Ks) rate ratio of the paralog genes. We used the same formula applied by Zhang et al. (2018) to calculate the divergence time [$T = \mathrm{Ks}/(2 \times 6.1 \times 10^{-9}) \times 10^{-6}$ Mya].

Plant Growth Conditions and Stress Treatments

Soybean (*Glycine max*-Conquista) seeds were germinated and grown under greenhouse conditions (12 h of light, 15–30°C, 70% relative humidity). At the V2/V3 developmental stage, the roots were immersed in Hoagland Hydroponic Solution supplemented with 10% (w/v) PEG (molecular weight 8,000), 5 μg/mL tunicamycin (TUN) or 5 mM salicylic acid (SA) to induce osmotic, endoplasmic reticulum and biotic stress conditions, respectively. Dimethyl sulfoxide (DMSO) was used as a control for TUN treatment. Leaf disks from stressed and control leaves were collected at 0.5, 2, and 12 h post-treatment (for PEG treatment, a 24 h harvest time was included), immediately frozen in liquid nitrogen, and stored at −80°C until processing. For the analysis of gene expression of putative genes in different soybean vegetative tissues, samples of leaf disks (1 cm diameter), pivotal and lateral roots, stem's segments (1 cm), entire flowers and pods segments were collected and frozen in liquid nitrogen from R2/R3 developmental stage plants.

RNA Extraction and cDNA Synthesis

For gene expression profile of putative new NAC genes under stress conditions, total RNA was extracted from the leaf disks using Trizol (ThermoFisher). For expression analysis, we used four biological replicates of a pool of 3 plants for each stress treatment. cDNA synthesis was performed with 4 μg of total RNA, 10 μM oligoDT (18T), 10 mM dNTPs, and 200U of MMLV reverse transcriptase, according to the manufacturer's instructions (ThermoFischer). The expression profile of NAC genes was also determined in different soybean tissues. For this analysis, three biological replicates of a pool of 5 plants for each vegetative collected tissue were used and 2 μg of RNA were used for cDNA synthesis. For the analysis of differential expression during senescence, cDNAs were prepared from leaves of plants 20 days after germination (DAG) and 80 DAG. In this case, 3 biological samples and 3 technical replicates for each treatment were used. cDNAs from RNA of stressed leaf disks were used for the isolation of ORFs from the drought-repressed GmNAC065, drought-induced GmNAC085 (Carvalho et al., 2014a) genes and the newly identified GmNAC177 (this work).

Construction of Plasmids

All recombinant plasmids were obtained through the GATEWAY system (ThermoFisher). GmNAC065, GmNAC085, GmNAC177 coding regions were amplified by PCR from cDNA of stressed leaves using gene-specific primers harboring appropriate extensions and introduced by recombination into the entry vectors pDONR201 and pDONR207 and then transferred to pDEST22, pDEST32, and pEARLEY103/104. The PCR amplicons were purified from ethidium bromide-staining agarose gel by QIAquick Gel extraction kit (QIAGEN). After spectrophotometric quantification, 50 fmol of empty vector and PCR product were incubated at 25°C—with 1 μL of BpClonase (ThermoFisher) for 8 h. The same conditions were used to transfer the insert from pDONR201 or pDONR2007 to pDEST22, pDEST32 or pEARLEY103/104 using LrClonase enzyme (ThermoScientific). Recombination plasmids were transformed into *E. coli* DH5α and selected on LB-agar medium supplemented with 10 μM gentamicin (for pDONR207 or pDEST32), 100 μM kanamycin (for pDONR201 or pEARLEY103/104) or 100 μM ampicillin (for pDEST22). The resulting clones were confirmed by sequencing. Primers used and generated clones are described in **Supplementary Tables 2**, **3**, respectively.

Transient Expression and Subcellular Localization of Fused Proteins in *Nicotiana benthamiana*

To confirm the nuclear subcellular localization of NAC065, NAC085, and NAC177, the DNA constructions 35S:NAC065-GFP, 35S:NAC117-GFP or 35S:YFP-NAC085 were used to transfect *Nicothiana benthamiana* leaves by agroinfiltration. *Agrobacterium tumefaciens* GV3101 strain was transformed with pUFV2830, pUFV3007, or pUFV3008 (**Supplementary Table 3**) the bacterial suspension at $O.D_{600} = 0.5$ was mechanically inoculated in leaf abaxial surface. All three constructions were co-infiltrated with AtWWP1-mCherry (pUFV 2224), an *A. thaliana* nuclear marker gene (Silva et al., 2015; Calil et al., 2018). Three days after inoculation, 1 cm^2 infiltrated leaf sections were analyzed under Zeiss LSM510 META Laser Confocal Microscopy. YFP and GFP were excited by argon/helium-neon laser system in 488 nm wavelength, and emission was collected in 500–530 nm band-pass filter, while mCherry was excited in 543 nm wavelength and emission collected in 596–638 nm band-pass filter. Images were captured and treated in LSM Image Browser 4 (Carl-Zeiss) software.

Transactivation Assay in Yeast and Yeast-Two-Hybrid Assay

For transactivation assay in yeast cells, the NAC coding regions were fused to the GAL4 binding domain and transactivation of reporter genes were assayed in *Saccharomyces cerevisiae*, strain AH109 (MATa, Trp1-901, leu2-3, 112, ura3-52, his3-200, gal4Δ, LYS2::GAL1UAS-GAL1TATA-HIS3, MEL1 GAL2UAS-GALTATA::MELUAS- MEL1TATA-lacZ). AH109 competent cells were transformed with pBD-NAC065, pBD- NAC085, and pBD-NAC117 (**Supplementary Table 3**) or pBD (control), along with 100 μg of salmon sperm carrier DNA (ssDNA), using the lithium acetate/polyethylene glycol (PEG) method. Transactivation activity was monitored by placing different optical dilutions ($O.D_{600} = 1.0, 0.1$, and 0.01) of the transformant suspension on synthetic dropped (SD) medium lacking leucine and histidine but supplemented with 10 mM 3-amino-1,2,4-triazole (AT) *HIS3* gene-product competitive inhibitor and cultured for 3 days at 28°C. For the yeast two-hybrid assay, AH109 was cotransformed with pAD-NAC fusions and pBD-NAC fusions (**Supplementary Table 3**) and interactions were monitored by the ability of the reporter strain to grow on SD/-leu/-tryp/-his selective medium supplemented with 3-amino-1,2,4-triazole (10 mM).

Quantitative RT-PCR

Real-time RT-PCR assays were performed with an ABI 7500 instrument (ThermoFisher) using SYBR Green PCR Master Mix (Life Technologies), gene-specific primers (**Supplementary Table 4**) and cDNA from stressed seedlings and R2/R3 plants under normal growth conditions. Three biological replicates (three unstressed or stressed seedlings) were used to obtain two independent mRNAs pools for the quantitative RT-PCR data with two technical replicates. Relative gene expression was quantified using the comparative $2^{-\Delta\Delta Ct}$ or $^{2-\Delta Ct}$ method for the analysis of stressed and control plants, respectively. *UKN-2* was chosen as the normalizer, endogenous control gene (Libault et al., 2008). Analysis of expression of *SMP* (seed maturation protein), a drought-induced gene, *CNX* (calnexin) and *PDI* (protein disulfide isomerase), ER stress-responsive genes, and *PR-4* (pathogenesis-related 4), an SA-induced gene, were used as control genes for the respective stress treatments. The amplification reactions were performed as follows: 2 min at 50°C, 10 min at 95°C, and 40 cycles of 94°C for 15 s and 60°C for 1 min. The relative gene expression quantification was converted into a heat map using MORPHEUS (https://software.

broadinstitute.org/morpheus/) software. Ct data and standard deviation were organized in **Supplementary Tables 5**, **6**).

RNA Sequencing Experiment

Fresh tissue (six 0.9 cm diameter disks) from the middle leaflet of third trifoliate and seventh trifoliate leaf of soybean plants was collected and stored at −80°C. Leaves were collected in two plant stages, vegetative stage three (V3) and reproductive stage seven (R7). For RNA-sequencing, wild-type plants (BR16) were used in biological triplicates. Total RNA was extracted using the Trizol reagent (ThermoFischer), as recommended by the manufacturer, followed by precipitation with isopropanol. The integrity and quality of the extracted RNA were monitored using the Agilent RNA 6000 assay on the Agilent Bioanalyzer 2100 system. The quantification of total RNA was obtained by Quant-iTRiboGreen RNA Assay Kit (ThermoFisher). The sequencing libraries were prepared with TruSeq® Stranded Total RNA Sample Preparation Kit (Illumina) using the LowSample (LS) Protocol, according to the manufacturer's recommendations. Additionally, ribosomal RNA was depleted through Ribo-Zero Deplete beads. One microgram total RNA per sample was used as input material for the RNA sample preparation, after treatment with DNase I Amplification Grade (ThermoFisher). The products were purified using AMPure XP system (Beckman Coulter, Beverly, MA) and quantified using the Agilent High Sensitivity DNA assay on the Agilent Bioanalyzer 2100 system.

The clustering of the index-coded samples was performed using the cBot Cluster Generation System with TruSeq PE Cluster Kit v3-cBot for 101 cycle paired-end reads (Illumina), according to the manufacturer's recommendations. The samples were sequenced on Illumina Hiseq 2500 platform (Illumina), and 100 bp paired-end reads were generated. The run was performed using the High Output mode.

For differential gene expression (DGE) analysis, it was applied the R/Bioconductor package DESeq2 for the normalization and statistical test (Love et al., 2014). The p-value was corrected by False Discovery Rate (FDR) and significance was considered with $p < 0.05$. To minimize false positive DE genes, the output of DESeq2 was applied to the Bioconductor package IHW that was used to do an independent hypothesis weighting (IHW). For the downstream analysis, the data were converted to SQL tables stored in PostgreSQL version 10.1 database. The Gene Ontology (GO) analysis was performed by the R/Bioconductor package GOstats (Falcon and Gentleman, 2007). For gene enrichment of GO terms, we used hypergeometric tests. The significant p-value for enrichment was $P < 0.01$. Pathway analyses were performed by the R/Bioconductor package path view (Luo and Brouwer, 2013). The orthology table was used by comparing *Glycine max* to the matched gene at *A. thaliana* database. Hence, the maps referred to Arabidopsis organism was applied using KEGG graphics. RNA-sequencing data have been deposited in the Gene Expression Omnibus under accession number GSE122915 (https://www.ncbi.nlm.nih.gov/geo/query/acc.cgi?acc=GSE122915).

Transient Expression of GmNAC065, GmNAC085, and GmNAC177 in *Nicotiana benthamiana* and Cell Death Progression Analyses

Agrobacterium-mediated transient expression of NAC fusion in *N. Benthamiana* leaf epidermal cells was performed as described (Silva et al., 2015). GmNAC081 and NRP-B were used as positive control for the induction of cell death (Costa et al., 2008; Faria et al., 2011). Three days after infiltration, leaf disks were collected and used to quantify total chlorophyll and TBA-reactive compounds and for western-blotting of NAC proteins from total protein extracts. The leaves were used to observe the development of typical symptoms of cell death and to monitor hydrogen peroxide production by DAB staining.

Total chlorophyll content was determined spectrophotometrically after quantitative extraction from leaves (Wellburn, 1994). Briefly, leaf disks were weighted, and total chlorophyll was extracted with absolute ethanol, transferred to a dark tube, centrifuged at 12,000 g and quantified from the supernatant by spectrophotometry. Absorption values were collected at 645 nm and 663 nm and total chlorophyll expressed as μg/g.

TBA-reactive compounds were quantified as described by Cakmak and Horst (1991). Approximately 200 mg of leaves were homogenized in 2 ml of 0.1% (v/v) trichloroacetic acid (TCA) and then centrifuged at 12,000 g for 15 min. All steps were performed at 4°C. A 500 μL-aliquot of the supernatant was added to 1.5 ml of 0.5% (v/v) thiobarbituric acid (TBA) in 20% (v/v) TCA, and the samples were incubated at 90°C for 20 min. The reaction was stopped by incubation on ice followed by centrifugation for 4 min. The absorbance of the supernatant was measured at 532 nm, and the concentration of TBA-reactive compounds was calculated using the molar absorption coefficient of 155 mM^{-1} cm^{-1}, according to Heath and Packer (1968).

For hydrogen peroxide staining, the infiltrated leaves were incubated during 8 h in a 3,3-diaminobenzamidine (DAB) solution (1 mg/mL-pH 3.8) under continuous agitation. After staining, the leaves were immersed in a 100% hot ethanol bath, rehydrated at 80% ethanol bath, followed by 70% ethanol, 50% ethanol and, finally, water.

Statistical Analyses

All statistical analyses (ANOVA and T-test) were performed using the online software ANOVA calculator and T-test calculator (http://www.socscistatistics.com).

RESULTS

Phylogenetic Reconstruction of the GmNAC Superfamily: Identification of New Members in the Soybean Genome

Due to the relevance of the NAC gene family in developmental programs and stress response, this large family of plant-specific TFs has been extensively studied in different plant species. The most complete description of the soybean superfamily was provided by Le et al. (2011), which described 152 members

(with complete ORFs), from which 58 members were associated with dehydration response. Here, we used the NAC domain for searching against all deduced protein sequences from the last version of the soybean genome Wm82.a2.v1-v11.0. Our current wide-genome analysis revealed 32 new NAC candidate genes, not previously described (Le et al., 2011). A complete inventory of the GmNAC superfamily is presented in **Supplementary Table 1**, in which new, previously unidentified, members are highlighted in yellow. The nomenclature Glyma was provided by Phytozome and identifies the gene locus position among 20 soybean chromosomes. For standardization in scientific communication, in the previous nomenclature from Le et al. (2011), the NAC genes received an increasing number after the GmNAC prefix taking into consideration the order of the chromosome and locus position. To maintain the nomenclature of the 152 previously described NAC genes, the new NAC genes were numbered successively after GmNAC152 using the same system as in Le et al. (2011) (**Table 1**, **Figure 1**).

Among the 32 new genes identified, the genome analysis revealed 5 truncated NAC proteins (GmNAC158, GmNAC160, GmNAC167, GmNAC168, and GmNAC173), which harbor a complete NAC domain with the conserved sub-domains A–E (Olsen et al., 2005), but lack the C-terminus transactivation domain (**Supplementary Table 1**-orange highlights). The presence of a full-length NAC domain in all new members was confirmed by multiple sequence alignment with the previously characterized GmNAC030 as a prototype (**Supplementary Figure 1**; Mendes et al., 2013). Most likely, these truncated GmNAC proteins represent either pseudogenes or transcriptional repressors, which retain the capacity to bind to promoters but are incapable of activating transcription. The previously described Gm*NAC089, GmNAC096, GmNAC108,* and *GmNAC119* genes were not found in the last version of the soybean genome (**Supplementary Table 1**-green highlights). According to the Phytozome's information (available in https://phytozome.jgi.doe.gov/pz/portal.html#!info?alias=Org_Gmax) the gene maintenance in a novel genome assembly requires that the coding nucleotide sequence (CDS) and deduced amino acid sequence share more than 90% sequence identity with the previous annotation. As a result, the NAC soybean superfamily was updated to 180 members, 148 already described and 32 novel members from this work.

The inventory of the soybean NAC superfamily from Le et al. (2011) demonstrated the presence of 11 transmembrane domain-containing transcription factors, which was later updated by Li et al. (2016b) to 15 putative membrane-tethered GmNAC proteins (NTL), including 3 novel identified ones and the GmNAC079, designated by Li et al. (2016b) as NTL8. Except for NTL5 whose pair (Glyma.16G016400) does not have a transmembrane (TM) segment, all the other 14 membrane-bound NACs are phylogenetically clustered in pairs and both duplicated genes have TM segments. This observation was reproduced in our phylogenetic analysis, which included the NAC genes from Arabidopsis (**Figure 2**).

The current phylogenetic analysis clustered the soybean NAC proteins into 15 subgroups with a high bootstrap score (>80%). This level of internal stability supported the classification of the soybean NAC superfamily into 15 subfamilies. The only exception was the ANAC063 subfamily that replicated with a low bootstrap score (0.14). Among them, 12 subfamilies were named according to previously characterized NAC clusters from Arabidopsis and rice and three subfamilies were unnamed because no reference of function or expression from these GmNACs was available (Ooka et al., 2003). The largest subfamily, NAM, comprises 23% of the NAC genes, followed by SNAC-B/NAP (12.8%) and VND-NAC (11.7%). The two least subfamilies were TIP (2.2%) and OsNAC8 (1.1%).

The 32 newly discovered GmNAC genes were distributed phylogenetically among the soybean NAC subfamilies and the soybean chromosomes (**Figure 1**, in red and **Figure 2**, in red and orange). The new mapped genes did not change the density of GmNACs among the 20 soybean chromosomes (chromosome 12 kept the highest number of GmNACs, 9.4%; **Supplementary Figure 2**) with an increment of three possible tandem duplications (in chromosomes X, XII, and XVI; **Figure 1**), which were not confirmed by the phylogenetic and synteny analyses (see *GmNAC174*, Glyma.12G186900, OsNAC8 subfamily and *GmNAC177*, Glyma.16G016400, unnamed subfamily; **Figures 2**, **3** and **Table 2**). For the new genes, the only possible tandem duplication confirmed by the synteny analysis refers to the pair *GmNAC167* (Glyma.10G077000) and *GmNAC168* (Glyma.10G077400) in chromosome X, SNAC-B(NAP) subfamily (**Figure 3B**). However, the inclusion of the new NAC proteins in our phylogenetic analysis showed that 21 of 32 new NAC genes were clustered in pairs, consistent with duplication events. The synteny-based analysis focused on the distribution of the new 32 genes on the genome (**Figure 3A**) and in the 21 duplicated pairs containing new NAC genes (**Figure 3B** and **Table 2**). The significant number of new NAC genes duplications had spread among the chromosome. A few syntenic groups have found at the chromosome X and XX as well as XII and XIII (**Figure 3A**). A striking feature of the soybean genome is the retention of extended blocks of duplicated genes with a low frequency for reversion to singletons (Schlueter et al., 2008). Concerning the membrane-tethered GmNAC (NTL) transcriptional factors, 14 of 15 GmNTLs are clustered as paralogs (Li et al., 2016b). An evolutionary and functional analysis of the soybean NTL genes, previously described, indicated that the duplicated genes diverge functionally, which contributes as an evolutionary driving force for the retention of these GmNTL duplicate genes (Li et al., 2016b). This precedent in the literature raised the possibility that other GmNAC pairs may exhibit partially overlapping but distinct functions.

The soybean genome has undergone two duplication events, which occurred approximately 59 and 13 million years ago (Schmutz et al., 2010). As for the 21 duplicated gene pairs containing new NAC genes, except for 3 NAC gene pairs with a divergence period higher than 13 Mya, the remaining 18 duplicated gene pairs were formed by the second event of whole genome duplication of *Glycine max* (**Table 2**). The molecular evolution of the new NAC duplicated pairs were investigated by calculating the ratio of non-synonymous to synonymous substitutions (Ka/Ks). Only the duplicated gene pair Glyma.10G077000 (*GmNAC167*) / Glyma.10G077400

TABLE 1 | New, previously unidentified, putative NAC genes.

Glyma v11.0	Name	Length	NAC-domain	*E*-value	TM***	Chromos	Subfamily
Glyma.02G050100.1.p	GmNAC153	362	6–135	6.8E-53		II	VND-NAC
Glyma.02G284300.1.p	GmNAC154	320	22–149	1.0E-47		II	ONAC022
Glyma.03G164200.1.p	GmNAC155	296	10–138	6.7E-48		III	NAM
Glyma.03G179600.1.p	GmNAC156	287	11–138	9.4E-48		III	SNAC-B
Glyma.04G014900.1.p	GmNAC157	350	22–149	1.4E-49		IV	NAM
Glyma.04G175800.1.p*	GmNAC158	78	02–78	1.3E-21		IV	Senu5
Glyma.04G199000.1.p	GmNAC159	169	28–73	4.0E-11		IV	Senu5
Glyma.05G086000.1.p	GmNAC160	177	11–140	1.5E-48		V	SNAC-B
Glyma.05G108700.1.p	GmNAC161	212	18–98	6.4E-9		V	ANAC001
Glyma.06G014900.1.p	GmNAC162	374	22–149	1.6E-49		VI	NAM
Glyma.06G288500.1.p	GmNAC163	285	49–189	3.5E-30		VI	ANAC001
Glyma.07G04790.1.p**	GmNAC164	497	12–141	2.1E-44	470–492	VII	unnamed
Glyma.07G192900.1.p	GmNAC165	362	15–142	3.8E-51		VII	SNAC-B
Glyma.08G163100.1.p	GmNAC166	348	6–133	1.8E-54		VIII	SNAC-B
Glyma.10G077000.1.p	GmNAC167	128	11–128	1.3E-38		X	SNAC-B
Glyma.10G077400.1.p	GmNAC168	136	11–136	1.7E-43		X	SNAC-B
Glyma.10G197600.1.p	GmNAC169	448	5–97	2.1E-29	424–446	X	NAM
Glyma.10G204700.1.p	GmNAC170	422	56–195	1.5E-28		X	ANAC063
Glyma.12G003200.1.p	GmNAC171	356	9–138	3.2E-51		XII	VND-NAC
Glyma.12G145100.1.p	GmNAC172	180	11–138	1.6E-46		XII	SNAC-B
Glyma.12G160100.1.p	GmNAC173	133	2–115	5.2E-35		XII	Senu5
Glyma.12G186900.1.p	GmNAC174	493	17–143	8.8E-47	303–325	XII	OsNAC8
Glyma.13G294000.1.p	GmNAC175	279	48–188	6.1E-30		XIII	ANAC001
Glyma.14G140100.1.p	GmNAC176	373	27–154	4.8E-53		XIV	NAM
Glyma.16G016400.1.p	GmNAC177	267	11–140	1.0E-44		XVI	unnamed
Glyma.16G069300.1.p	GmNAC178	399	56–198	4.8E-27		XVI	ANAC063
Glyma.18G301500.1.p	GmNAC179	229	14–138	1.3E-49		XVIII	Senu5
Glyma.19G002900.1.p	GmNAC180	389	56–197	1.9E-28		XIX	ANAC063
Glyma.19G108800.1.p	GmNAC181	336	8–138	5.8E-51		XIX	SNAC-B
Glyma.19G165600.1.p	GmNAC182	294	10–138	4.1E-48		XIX	NAM
Glyma.19G195800.1.p	GmNAC183	254	4–134	7.5E-43		XIX	TERN
Glyma.20G175500.1.p	GmNAC184	341	19–147	1.6E-51		XX	VND-NAC

*Orange indicates truncated NAC proteins harboring just a full-length NAC domain.
**Purple denotes NAC proteins with a transmembrane segment.
***Transmembrane segment.

(*GmNAC168*) with a significant ratio Ka/Ks > 1 may have undergone a positive selection in soybean. The other 20 duplicated gene pairs had been under purifying selection in soybean, as suggested by their Ka/Ks ratio <1.

Organ- and Tissue-Specific Expression Profile of the 32 New NAC Genes

The NAC genes are involved in developmental programs and stress-response. To gain insights into potential developmental roles of the new NAC genes and to validate these new genes in the soybean genome, we analyzed the expression profile of these genes in different developmental stages and tissues based on publically accessed transcriptomes obtained from phytozome (**Figure 4**). These data were confirmed by qRT-PCR of a sub-set of NAC genes (**Figure 5**, **Supplementary Figure 3** and **Supplementary Table 5**). All the newly identified NAG genes are expressed in some, but not all, tissues. A group of new NAC genes is highly expressed in most tissues, including *GmNAC158*, *GmNAC169*, *GmNAC174*, *GmNAC177*, *GmNAC179*, and *GmNAC181*, which was confirmed by qRT-PCR for *GmNAC169*, *GmNAC174*, and *GmNAC177* (**Figure 5**). There is also a group of newly identified GmNACs, which displays low transcript accumulation in all tissues analyzed (see the dark blue cluster of genes). Some genes displayed a distinct tissue-specific expression, suggesting different functions in development. While *GmNAC153* and *GmNAC166* are most expressed in roots, a sub-set of genes (*GmNAC155*, *GmNAC165*, and *GmNAC182*) is highly expressed in flowers, for example. Quantitative RT-PCR confirmed that the GmNAC165 transcript accumulates to high levels in flower (**Figure 5** and **Supplementary Figure 3**).

Among the 32 new NAC genes, we observed 3 duplicated gene pairs containing only new NAC genes (**Table 2**). Except for the *GmNAC167*/*GmNAC168* pair which had undergone positive selection (**Table 2**), the other two pairs *GmNAC162*/*GmNAC175*

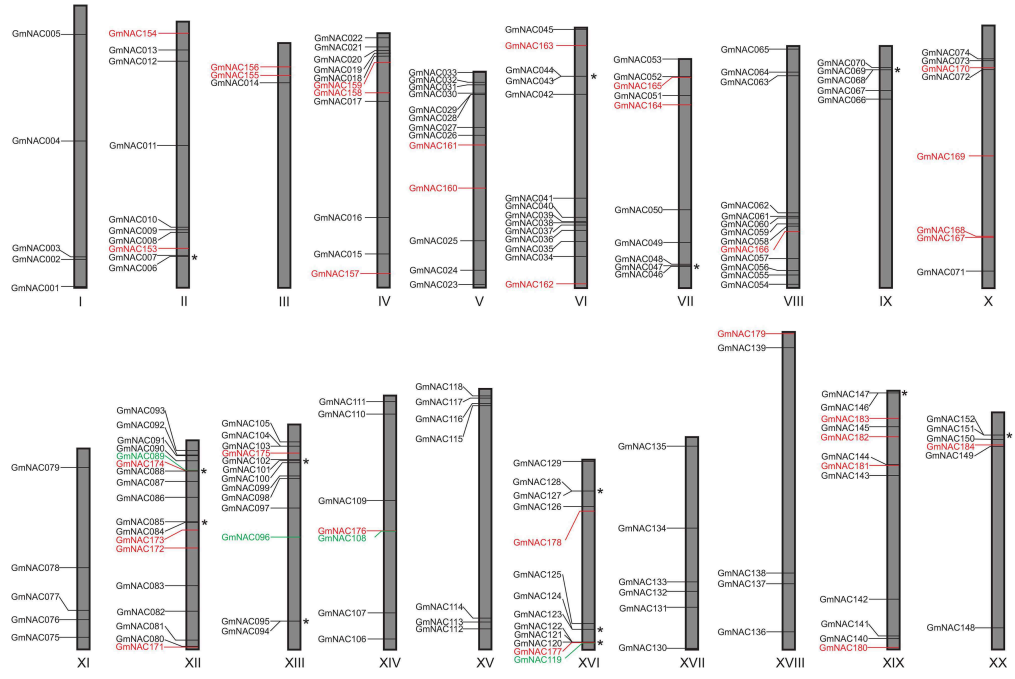

FIGURE 1 | Graphical representation of the location for the GmNACs on the soybean chromosomes. Previously described genes are indicated in black, and the newly identified genes are in red. GmNACs in green represent the previously identified ones, which were no longer found in the soybean genome reassembly. The asterisks indicate tandem duplicated genes.

and *GmNAC173*/*GmNAC158*, which had experienced purifying selection, exhibited distinct expression patterns in different tissues. This profile may suggest diversification in expression level, which may be associated with a certain degree of sub-functionalization as the mechanism for the retention of these duplicated GmNAC genes.

Stress Regulation of a Representative Sample of the Newly Identified GmNAC Genes

Comparing Arabidopsis and soybean, several GmNAC subfamilies have undergone expansion after their speciation. The domestication process of soybean could account at least in part for this variation because some GmNACs have been linked to traits targeted by artificial selection such as drought tolerance and morphological adaptation (Dong et al., 2013; Thao et al., 2013; Thu et al., 2014; Hussain et al., 2017). These data suggest that the expansion of soybean NAC genes may reflect amplification or lineage-specific responses to various biotic and abiotic stress responses under the influence of artificial selection. In view of this observation, we next examined the stress-induced expression profile for a representative sample (eight genes) of the new NAC genes (**Figure 6A**). This quantitative expression analysis also allowed us to validate further these new genes in the soybean genome. Three-week-old soybean seedlings were treated with the osmotic-stress inducer PEG, the ER-stress inducer TUN, and the defense inducer SA. Three-period intervals after the treatment were chosen (0.5, 2, 12, and 24 h to PEG) to include a time range of early responses, intermediate responses, and late responses. We also examined the expression of the osmotic stress-induced control gene *SMP,* ER stress-induced control genes, *CNX* and *PDI*, and the SA-induced control *PR1* to monitor the effectiveness of the respective stress treatment (**Supplementary Figure 4**). All examined GmNACs were regulated by at least one of the stress treatments, confirming they are expressed in response to some stimulus (**Figure 6B**).

GmNAC154, GmNAC163, *GmNAC169,* and *GmNAC065* were up-regulated by PEG, TUN and SA, although to different extents and kinetics of induction (**Figure 6**, **Supplementary Figure 5** and **Supplementary Table 6**). In contrast, *GmNAC157* was down-regulated by all stress treatments. The four up-regulated genes belong to subfamilies with stress-responsive members (**Figure 6A**), whereas *GmNAC157* is most related to AT1G76420

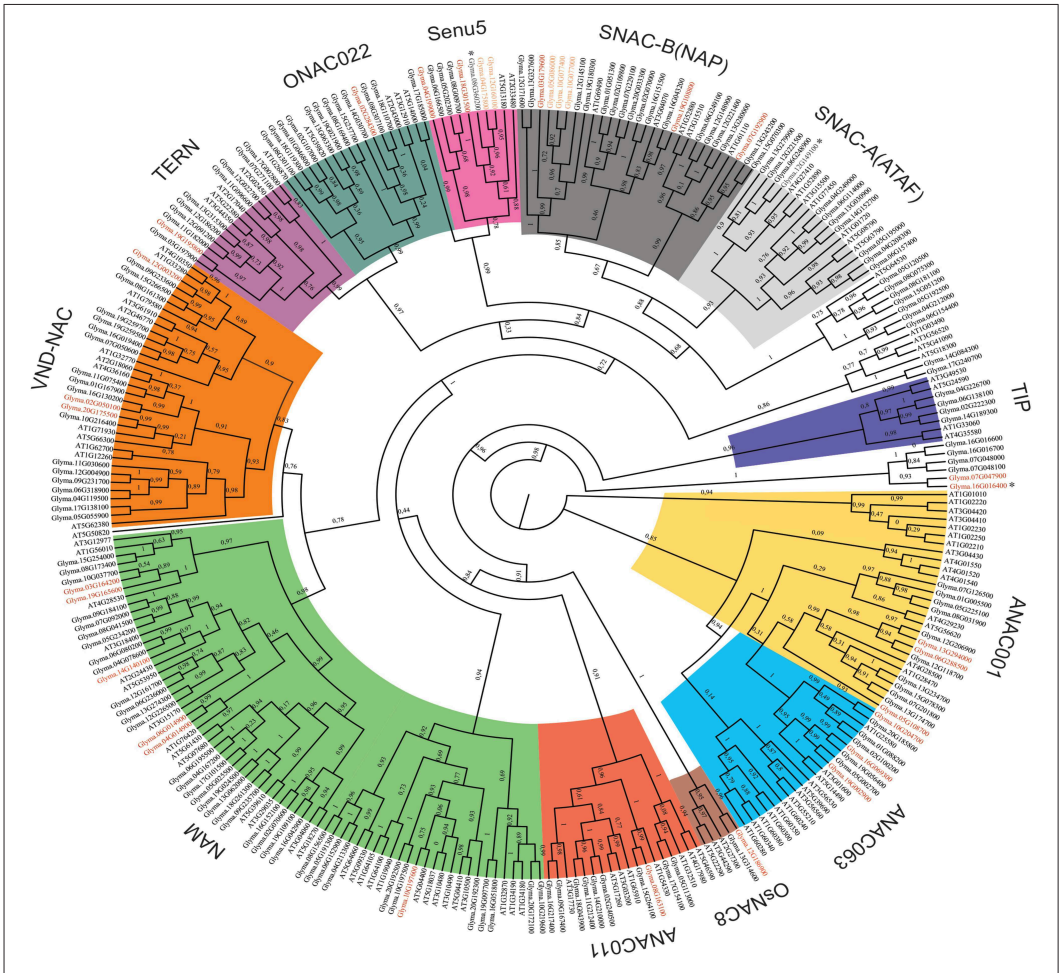

FIGURE 2 | Phylogenetic reconstruction of the soybean and *Arabidopsis thaliana* NAC superfamily. All NAC deduced amino acid sequences from the soybean genome and the *Arabidopsis thaliana* genome were used to perform the phylogenetic analysis. Phylogenetic tree reconstruction was performed using the maximum likelihood statistical method with 10.000 bootstraps. NAC genes were grouped into 15 subgroups, including SNAC-A (ATAF—light gray), SNAC-B (NAP—dark gray), Senu5 (pink), ONAC022 (dark green), TERN (purple), VND-NAC (*vascular related NAC*-domain - orange), NAM (*no apical meristem* - light green), ANAC011 (red), OsNAC8 (brown), ANAC063 (light blue), ANAC001 (yellow), TIP *(turnip crinkle virus interaction protein* - dark blue) and unnamed groups (white). New putative NAC genes are shown in red. Asterisks indicate genes that were further characterized. Some possible pseudo-genes are shown in orange. The bootstrap score to each phylogenetic relation is shown at nodes.

(*ANAC031*), also designated CUP-SHAPED COTYLEDON3 (*CUC3*), which has not been implicated in stress responses. It functions partially redundant with *CUC1* and *CUC2* in the establishment of the cotyledon boundary specification and the shoot meristem (Hibara et al., 2003; Vroemen et al., 2003).

The expression profile of *GmNAC174* and *GmNAC177* was similar, down-regulated by PEG, but up-regulated by TUN and SA, which was in marked contrast with *GmNAC085*. While *GmNAC085* belongs to SNAC-A (ATAF) subfamily, which harbors stress-responsive members, *GmNAC174* is closely related to the ER stress-induced *ANAC089* (AT2G22290) and *GmNAC177* clusters closely to the TIP subfamily with members involved in biotic interactions and immune response control. Therefore, they display a

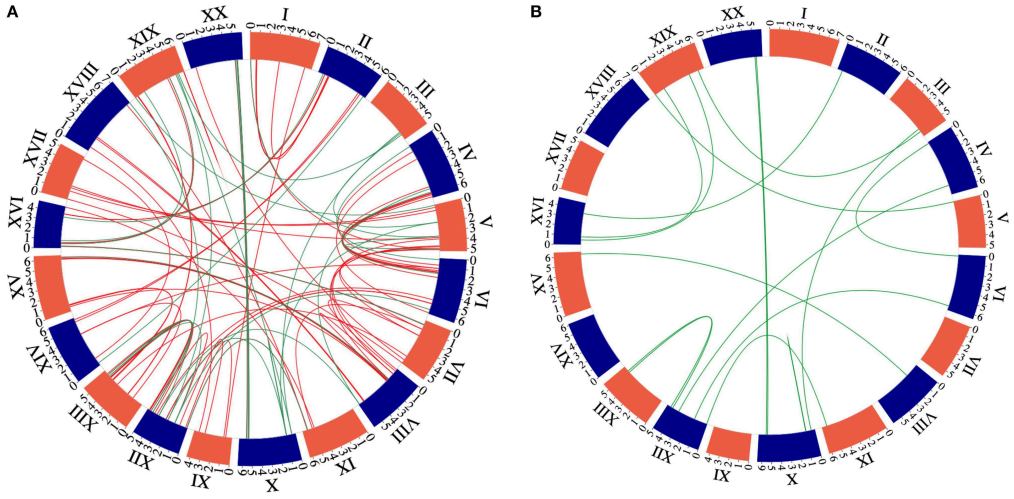

FIGURE 3 | Circle plot of the soybean chromosomes and the GmNAC family. A. Circle plot of the soybean chromosomes showing the location of the new 32 NACs genes compared with the former NAC group. The green color represents 21 new NAC genes presented at the pairs of paralogous comparing with all NAC genes. We used the criterion of 80% identity to recover the paralogous pairs. B. Circle plot of soybean chromosomes and the 21 newly identified NAC genes displayed as duplicated gene pairs based on the phylogenetic analysis.

stress-responsive expression profile consistent with their subfamily classification.

GmNAC165 was repressed by prolonged ER stress and SA treatment, which is consistent with its classification as a SNAC-B (NAP) member. GmNAC183, which is a member of the TERN subfamily, was rapidly (0.5 h) induced by PEG and TUN but repressed if the stress persisted. The members of the TERN subfamily GmNAC081 and ANAC36 has been shown to be induced by PEG and TUN (Reis et al., 2011, 2016; Mendes et al., 2013). Therefore, the stress-responsive expression profile of the novel GmNACs is consistent with their phylogenetic relatedness as they share similar expression profile with homologous genes of the soybean or other plant species that belong to the same subfamily.

Genome-Wide Expression Analysis Uncovers an Extended List of Senescence-Associated GmNACs

High-resolution temporal expression profiles associate approximately one-third of Arabidopsis NAC genes with senescence (Breeze et al., 2011) and functional studies of a few members have been conducted confirming their crucial role in developmentally programmed senescence (Hickman et al., 2013; Kim et al., 2018). In addition to identifying new NAC genes in the soybean genome, we performed a transcriptomic analysis to examine the differential expression of GmNACs during natural leaf senescence. Remarkably, 44% of the GmNAC genes were differentially expressed (DE) at the onset of senescence [BR17_80d(R7)-BR16_20d(V3)], including eight (8) newly identified GmNACs (**Figure 7**, **Supplementary Table 7**). In this set of senescence DE GmNAC genes, the up-regulated changes predominated over the down-regulated changes (**Figure 7A**). Among the up-regulated genes, GmNAC030 (SNAC-A/ATAF subfamily) and GmNAC081 (TERN subfamily) have already been demonstrated to be induced by leaf senescence (Carvalho et al., 2014b) and GmNAC081 functions as a positive regulator of developmentally programmed leaf senescence (Pimenta et al., 2016). The results of RNA-seq were further confirmed by qRT-PCR targeting a representative sample of senescence-induced and senescence-repressed genes (**Figure 7B**, **Supplementary Table 9**). During senescence, *GmNAC065*, *GMNAC154* and *GmNAC183* were induced, whereas *GmNAC163*, and *GmNAC169* were down-regulated as demonstrated by RNA-seq.

The most represented subfamily of senescence-associated genes was the SNAC-A (ATAF) family (90%) followed by TERN (80%) and TIP (75%). No senescence-associated NAC gene was detected in subfamilies OsNAC8 and ANAC011 (**Supplementary Table 8**). All the senescence DE genes from subfamilies SNAC-B (NAP), TERN, TIP, and Senu5 were up-regulated during senescence. Accordingly, the representative type of the SNAC-B(NAP) subfamily, AtNAP, has been shown to function as a positive regulator of leaf senescence (Guo and Gan, 2006) and representatives of the TERN subfamily, like GmNAC081, have also been shown to control leaf senescence (Pimenta et al., 2016).

TABLE 2 | Divergence between NAC gene pairs in soybean.

Gene Name*	Gene Name	Ka	SD	Ks	*SD*	Ka/Ks	Duplication Date (Mya)**	Selection	*p*-value (FDR)***
Glyma.07G047900 (GmNAC164)	Glyma.16G016400 (GmNAC177)	0.05994566	0.0144061	0.1303571	0.0363278	0.459857269	10.69	Purifying	0.03557996
Glyma.12G206900 (GmNAC090)	Glyma.13G294000 (GmNAC175)	0.01789244	0.00727299	0.1173597	0.0337963	0.152458127	9.62	Purifying	0.05012003
Glyma.06G288500 (GmNAC163)	Glyma.12G118700 (GmNAC083)	0.01752367	0.00879841	0.2001884	0.0489479	0.087535891	16.41	Purifying	0.08495689
Glyma.10G204700 (GmNAC170)	Glyma.20G185800 (GmNAC150)	0.02990029	0.00760776	0.06833386	0.01774	0.437561847	5.60	Purifying	0.02610727
Glyma.16G069300 (GmNAC178)	Glyma.19G056400 (GmNAC142)	0.04890274	0.0105635	0.0998735	0.0245792	0.489646803	8.19	Purifying	0.02745994
Glyma.05G002700 (GmNAC025)	Glyma.19G002900 (GmNAC180)	0.05709798	0.0122494	0.08683529	0.0248523	0.657543494	7.12	Purifying	0.02610727
Glyma.12G186900 (GmNAC174)	Glyma.13G314600 (GmNAC103)	0.07831763	0.014255385	0.191407	0.040780976	0.409168056	15.69	Purifying	0.0429662
Glyma.08G163100 (GmNAC166)	Glyma.15G264100 (GmNAC117)	0.02198773	0.0070702	0.08570832	0.0238959	0.256541372	7.03	Purifying	0.03736929
Glyma.06G014900 (GmNAC162)	Glyma.04G014900 (GmNAC157)	0.05260988	0.011301031	0.07860409	0.024974149	0.669302068	6.44	Purifying	0.02610727
Glyma.03G164200 (GmNAC155)	Glyma.10G037700 (GmNAC071)	0.1584804	0.025821503	0.7327278	0.153642442	0.216288231	60.06	Purifying	0.20150153
Glyma.10G216400 (GmNAC073)	Glyma.20G175500 (GmNAC184)	0.02807372	0.00854546	0.1685033	0.0449916	0.166606351	13.81	Purifying	0.0644157
Glyma.02G050100 (GmNAC153)	Glyma.16G130200 (GmNAC126)	0.03756366	0.00954128	0.07316453	0.0223967	0.513413535	6.00	Purifying	0.02610727
Glyma.09G233600 (GmNAC069)	Glyma.12G003200 (GmNAC171)	0.007916301	0.0046751	0.06380496	0.0233777	0.124070307	5.23	Purifying	0.03736929
Glyma.03G197900 (GmNAC014)	Glyma.19G195800 (GmNAC183)	0.06498027	0.0164195	0.1111914	0.0379041	0.584400142	9.11	Purifying	0.02610727
Glyma.12G160100 (GmNAC173)	Glyma.04G175800 (GmNAC158)	0.00671151	0.0067342	0.02543455	0.01863	0.263873747	2.08	Purifying	0.02610727
Glyma.10G077000 (GmNAC167)	Glyma.10G077400 (GmNAC168)	0.0410012	0.0166212	0.02319112	0.0136607	1.767969809	1.90	Positive	0.02610727
Glyma.16G043200 (GmNAC124)	Glyma.19G108800 (GmNAC181)	0.0346605	0.0101229	0.1196774	0.0345572	0.289616085	9.81	Purifying	0.04214007

**The 21 duplicated genes retrieved from the gourp of the 32 new NACs are shown in red.*

***Based on a rate of 6.1 × 10^{-9} substitutions per site per year, it was calculated the divergenece time (T) as T = Ks/(2 × 6.1 × 10^{-9}) x 10^{6} Mya (Zhang et al., 2018).*

****H0: Ka=Ks; The P-value corrected by false discover rate (FDR) was calculated based on multiple chi-square test.*

Biological and Biochemical Properties of Previously Uncharacterized GmNAC Genes

Based on expression profiles and phylogenetic relatedness between already characterized *A. thaliana* NACs and the homologous soybean genes, one can formulate a hypothesis about their precise functions. We examined next the biochemical and biological properties of two uncharacterized NAC genes, *GmNAC065* (Glyma.08G360200; Senu5) and *GmNAC085* [Glyma.12G149100; SNAC-A (ATAF)], in addition to *GmNAC177* (Glyma.16G016400; unnamed subfamily) as a representative of the novel NAC genes. We showed first that all three NAC genes are nuclear localized, as the fluorescence of transiently expressed GFP-fused NAC genes (GmNAC065-GFP, GmNAC085-GFP, and GmNAC177-GFP) concentrated in the nucleus and co-localized with a nuclear marker gene, which was fused to mCherry (**Figure 8**; Calil et al., 2018). The fluorescence from the expression of GFP alone displayed a different pattern and concentrated in the cytosol and nucleus (**Supplementary Figure 6**).

To investigate whether GmNAC065, GmNAC085, and GmnAC177 harbor a functional transcriptional activator domain, we used a yeast transactivation assay, in which the coding region of each *GmNAC* gene was fused to the DNA binding domain of GAL4 (BD) and *S. cerevisiae* AH109, harboring a *HIS3* reporter gene under the control of GAL4 promoter, was transformed with the BD-NAC fusions (**Figure 9**). The expression of the BD-NAC fused genes in yeast was monitored by RT-PCR (**Figure 9B**). Then, we monitored the capacity of the fusion proteins (BD-GmNACs) to activate transcription of *HIS3* reporter gene and hence to display His prototrophy (**Figure 9A**). The yeast transforming lines expressing BD-GmNAC085 and BD-GmNAC177 fusions

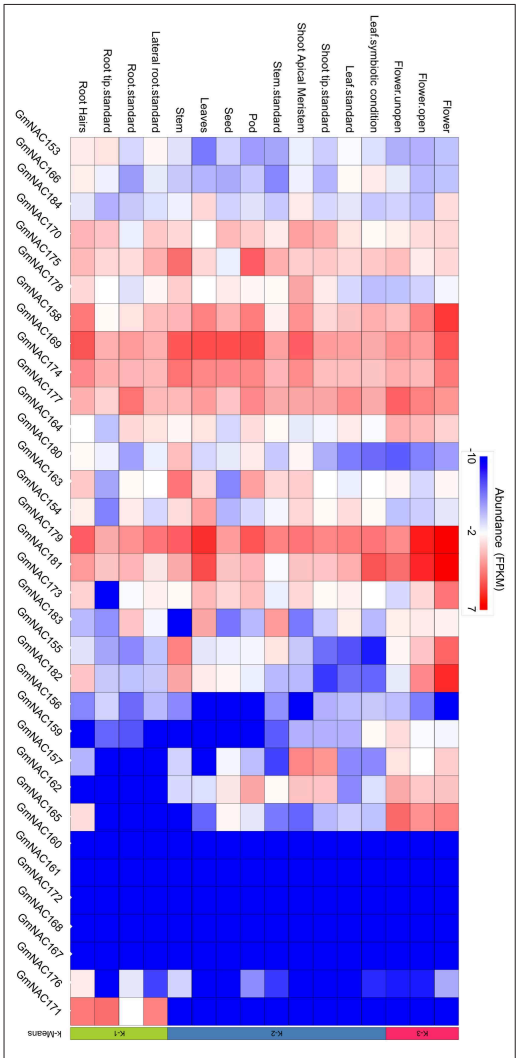

FIGURE 4 | Organ and tissue-specific expression of the new NAC genes. The heat map plot was created by the PhytoMine tool (https://phytozome.jgi.doe.gov/phytomine/begin.do) presented at the Phytozome v12 website (https://phytozome.jgi.doe.gov). The heat map was built using all gene expression data at the database regarding tissue- and organ-specific expression.

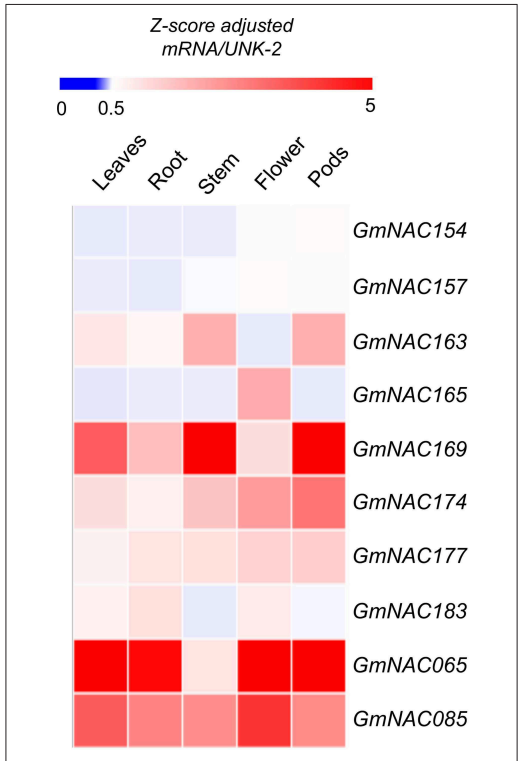

FIGURE 5 | GmNAC gene expression profile in different soybean tissues. Heat map of 8 putative NAC genes in addition to GmNAC065 and GmNAC85. The expression levels of a randomly selected representative sample of new GmNAC genes were measured in R2/R3 plants under normal growth conditions by qRT-PCR. The *UNK-2* gene was used as endogenous control. The data displayed in the figure comprise the qRT-PCR from **Supplementary Figure 3** and **Supplementary Table 5**.

displayed the most pronounced growth in the selective medium SD-Leu-His, supplemented with 10 mM 3-AT. The BD-NAC065 lines displayed a slow growth rate in histidine depleted medium, but growth was prevented in medium supplemented with 10 mM 3-AT. These results demonstrated that GmNAC085 and GmNAC177 display transactivation activity in yeast, which was in contrast with GmNAC065 that may act as a transcriptional repressor. Several precedents in the literature have evoked a repressive transcriptional function of NAC proteins from different species (Delessert et al., 2005; Lu et al., 2007). Alternatively, GmNAC065 may depend on specific interactions with other transfactors to activate their target genes as heterodimers. The lack of transactivation activity in yeast has also been observed for GmNAC081, which belongs to the subfamily TERN, and interacts with GmNAC030 from the SNAC-A (ATAF) subfamily to activate the expression of *VPE* (vacuolar processing enzyme) that promotes cell death (Pinheiro et al., 2009).

We then asked whether GmNAC065 (Senu5 subfamily) would form a homodimer and/or interact with GmNAC085 (SNAC-A/ATAF subfamily) or GmNAC0177 (unnamed subfamily)

A

Glyma v11.0	Gene Name	Subfamily
Glyma.08G360200	NAC065	Senu5
Glyma.12G149100	NAC085	SNAC-A (ATAF)
Glyma.02G284300	NAC154	ONAC022
Glyma.04G014900	NAC157	NAM
Glyma.06G288500	NAC163	ANAC001
Glyma.07G192900	NAC165	SNAC-B (NAP)
Glyma.08G163100	NAC169	NAM
Glyma.12G186900	NAC174	OsNAC8
Glyma.16G016400	NAC183	TERN
Glyma.19G195800	NAC177	unnamed

B

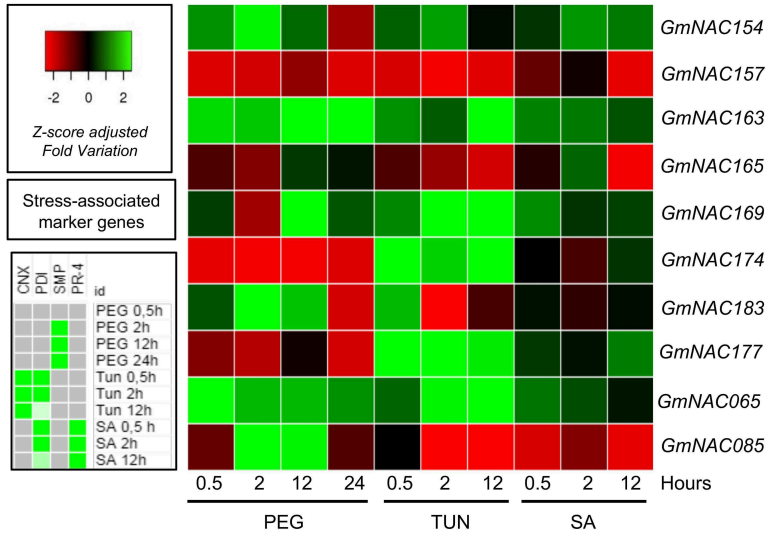

FIGURE 6 | Expression patterns of new GmNACs during multiple stress. **(A)** The identity of the selected GmNAC genes. **(B)** Heatmap of the stress-induced expression of 8 new putative GmNAC genes, GmNAC065 and GmNAC85. For the expression analysis of randomly selected GmNACs, soybean seedlings were stressed with PEG (10%), tunicamycin (5 μg/mL) and salicylic acid (5 mM) for 0.5, 4 and 12 h (24 h, exclusively for PEG treatment) and the transcript accumulation was monitored by qRT-PCR. The *UNK-2* gene was used as endogenous control, and gene-associated stress markers were used to monitor the effectiveness of treatment (on the left). The data presented in the figure comprise the qRT-PCR from **Supplementary Figures 4**, **5** and **Supplementary Table 6**.

through yeast two-hybrid assays. While GmNAC065 was fused to the GFAL4-BD, GmNAC085, and GmNAC177 were fused to the GAL4-AD (**Figure 9C**). The coexpression of the BD-GmNAC065 and AD-GmNAC085 fusion proteins promoted the growth of yeast in the selective medium, which was more pronounced than that of the positive control (BD-WWP1+AD-NIG), whereas the coexpression of BD-GmNAC065 with either AD-GmNAC065, AD-GmNAC177, or pAD did not promote his prototrophy. These results confirmed the specific interaction of GmNAC065 with GmNAC085 and raised the possibility that GmNAC065 may function as heterodimers in cell death events, as *GmNAC065* is a member of Senu5 subfamily induced by leaf senescence (**Figure 7**) and *GmNAC085* is a member of the SNAC-A (ATAF) subfamily that harbors cell death-induced members (**Figure 2**). However, these putative partners are not coordinately expressed in response to stress and developmental programs. While *GmNAC065* is induced by developmentally programmed leaf senescence (**Figure 7**), PEG, TUN, and SA (**Figure 6**) and repressed by drought (Carvalho et al., 2014a), the expression of *GmNAC085* is repressed by senescence, TUN, SA

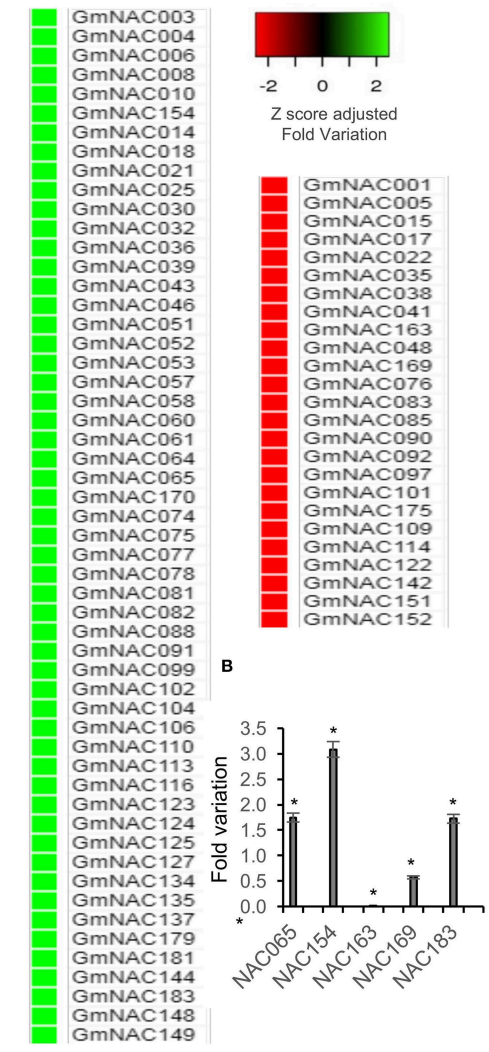

FIGURE 7 | Expression profile of NAC genes during natural leaf senescence in soybean. **(A)** Heatmap of senescence-associated GmNAC genes. The data presented in the figure comprise an RNA-seq analysis showing the differential expression of NAC genes in BR16_80d (R7)-BR16_20d(V3). **(B)** Senescence-induced variation of expression for representative senescence-associated NAC genes. Total RNA was isolated from 20 DAG to 80 DAG soybean leaves and the transcript accumulation of the indicated genes was measured by qRT-PCR. *UKN-2* was used as the normalizer, endogenous control gene. Relative gene expression was quantified using the comparative $2^{-\Delta\Delta Ct}$ method. The bars indicate standard-error and the asterisks indicate statistical significance by the *t*-test, ($P < 0.05$, $n = 3$).

and induced by PEG (**Figures 6**, **7**) and drought (Carvalho et al., 2014a). Therefore, the only overlap in the expression profile of *GmNAC065* and *GmNAC085* is the up-regulation by PEG, which may indicate heterodimerization under this stress condition.

The Involvement of GmNAC065, GmNAC085, and GmNAC177 With Cell Death Progression

To address the possibility that *GmNAC065, GmNAC085, and GmNAC177* are involved in cell death events, the transient expression of NAC genes was induced by agroinfiltration into *N. benthamiana* leaves and the resulting phenotypes were compared with those displayed by previously characterized senescence-associated genes, including *GmNAC081* and *NRP-B* (Faria et al., 2011; Reis et al., 2011; **Figure 8A**). GmNACs and controls accumulated stably in the agroinoculated leaf sectors (**Figure 10B**). After three days, the leaf sectors that were agroinoculated with the DNA constructs expressing *GmNAC065, GmNAC085, and GmNAC177* and the positive controls *NRP-B* and *GmNAC081* (**Figure 10B**) displayed a chlorotic phenotype characteristic of leaf senescence that was associated with decreased chlorophyll content and consequent yellowing of the leaf sector (**Figures 10A,C**). We further examined the GmNACs-induced senescence by measuring the accumulation of thiobarbituric acid (TBA)-reactive compounds such as malondialdehyde (MDA). These compounds are products of senescence-associated lipid peroxidation, a process resulting in the generation of reactive oxygen species. A significantly higher concentration of TBA-reactive compounds was observed in the *GmNAC065*-, *GmNAC085*-, *GmNAC177*-expressing leaf sectors and in the *NRP-B*- and *GmNAC081* control sectors than in the *GFP*-expressing leaf sectors (**Figure 10D**). Likewise, the accumulation of H_2O_2 was enhanced in GmNACs and *NRP-B* agroinoculated leaves in comparison with *GFP*-expressing leaves (**Figure 10E**). Collectively, our results indicate that transient expression of *GmNAC065*, *GmNAC085,* and *GmNAC177* in *N. benthamiana* leaves induces senescence and cell death. Because *GmNAC065* and *GmNAC085* are differentially expressed during leaf senescence they may be involved in developmentally programmed leaf senescence in soybean. In contrast, the newly identified *GmNAC177* was not differentially regulated during natural leaf senescence, but it may be involved in cell death events induced by biotic stress, as it clusters in an unnamed subfamily that is closely related to the TIP subfamily of GmNACs implicated in pathogen-host interactions.

DISCUSSION

Phylogenetic Reconstruction of the GmNAC Superfamily Enlarges This Family to 180 Members Distributed Into 15 Structurally and Functionally Conserved Subfamilies

Despite the extensive literature regarding the plant-specific TFs of the NAC family, functional studies have been restricted

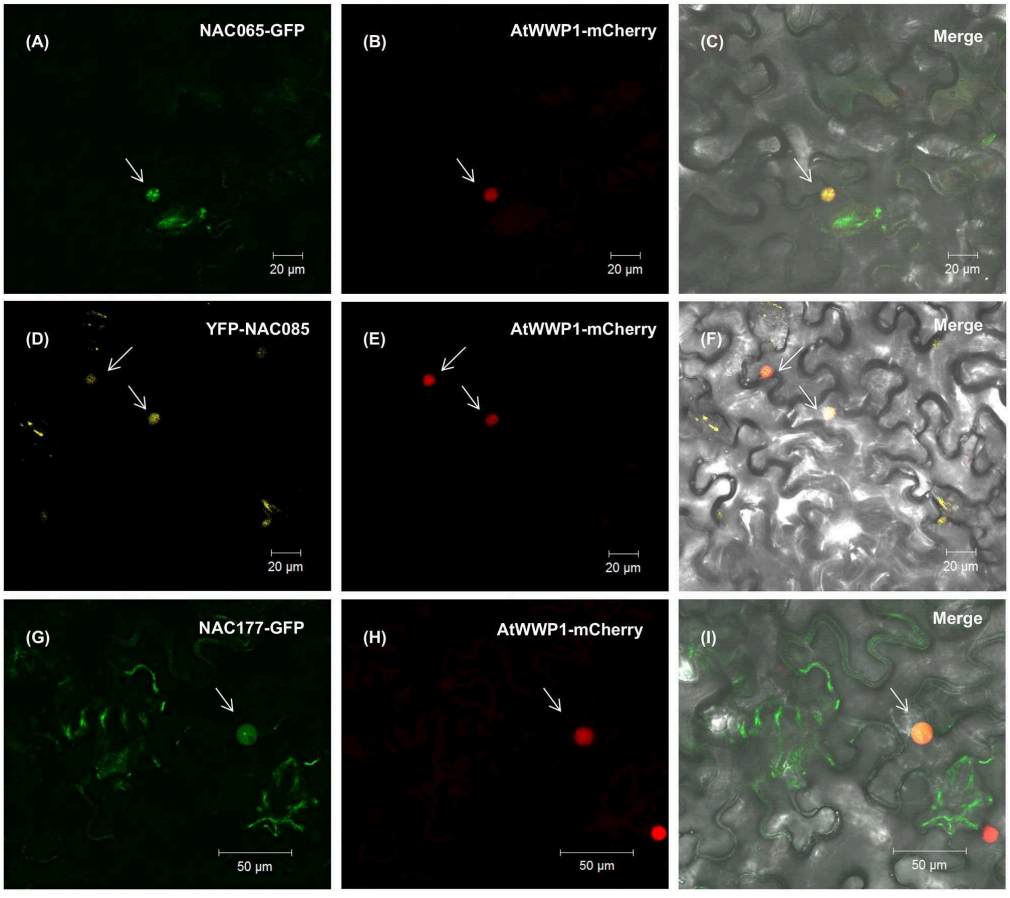

FIGURE 8 | NAC065, NAC085, and NAC177 subcellular localization. Leaves of *Nicothiana benthamiana* were infiltrated with *Agrobacterium tumefaciens* GV3101 carrying the GFP-NAC or YFP-NAC constructs, and the localization of the fused protein was monitored by confocal microscopy. In the left column, **(A,D,G)** show the expression of NAC065-GFP, YFP-NAC085 and NAC177-GFP (top to bottom) in the nuclei, indicated by white arrows. In the middle column, **(B,E,H)** show the expression of the nuclear marker AtWWP1-mCerry in the corresponding nuclei field of the first column. **(C,F,I)** merged images of NAC fusions and AtWWP1 marker in the bright-field.

to few members of the family as they have been conducted primarily with orthologs of different species, multiplying the number of GmNACs analyzed but with similar function. Because the extension and complexity of the NAC family in the plant kingdom have not been thoroughly examined, orthologous genes from different species cannot be fully predicted. Here we performed an in-depth examination of the NAC superfamily from soybean, interrogating the last version of the soybean genome, version Wm82.a2.v1-v11.0. The phylogenetic reconstruction of the GmNAC superfamily uncovered 32 new members in the soybean genome, raising the size of this family to 180 members. As compared to the Arabidopsis NAC superfamily, the soybean GmNAC subfamilies showed an extensive expansion in the number of their NAC members, which may be a result of artificial selection associated with relevant agronomic traits, including yield, drought tolerance, pathogen resistance, etc. As an important economic crop, soybean has been exposed to intense breeding programs, which may have contributed to the establishment of the current NAC superfamily profile in this species.

This comprehensive analysis comparing the complete repertory of Arabidopsis and soybean NACs provided a

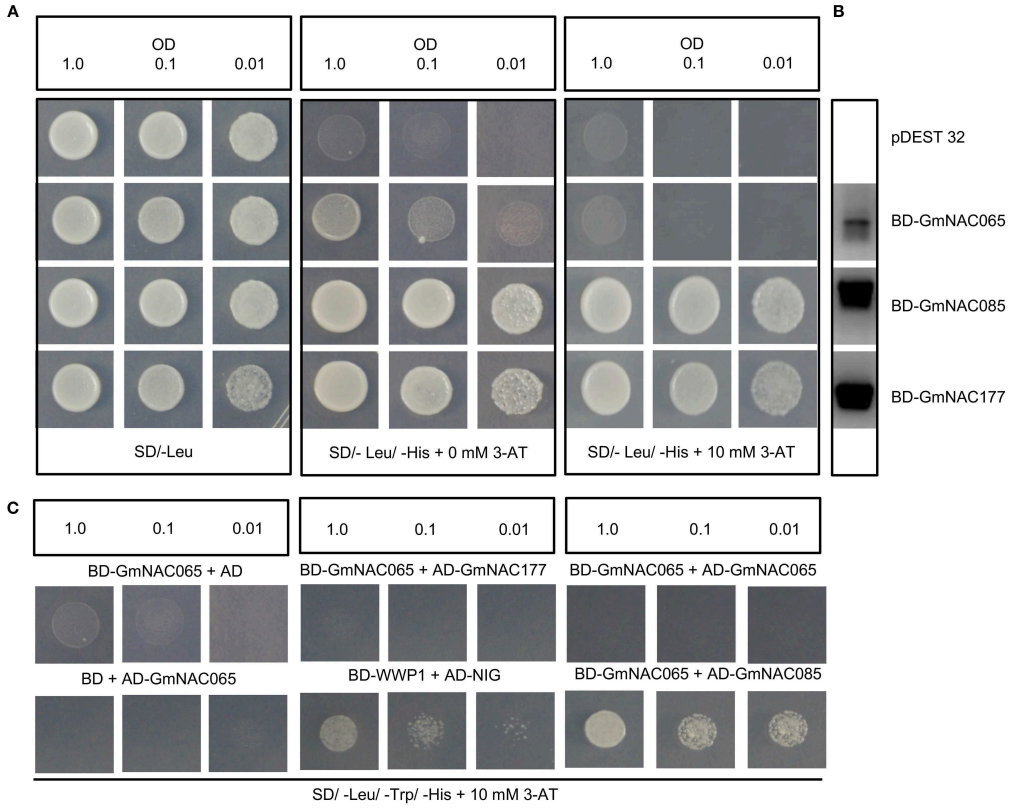

FIGURE 9 | NAC065, NAC085 and NAC177 transactivation capacity and protein-protein interaction. **(A)** Transactivation activity of GmNAC proteins. The fusions BD-NAC065, BD-NAC085 and BD-NAC177, and the empty vector were transformed separately into yeast strains AH109 and activity was determined by monitoring His prototrophy on selective medium. The transformants were incubated for 3 days at 28°C in SD media lacking leucine and histidine but supplemented with 10 mM 3-aminotriazol (3AT). **(B)** Expression analysis of BD-NAC065, BD-NAC085 and BD-NAC177 fusions in yeast. Total RNA was extracted from yeast cells transformed with the indicated DNA constructs, and gene expression was monitored by RT-PCR. **(C)** Interactions of GmNAC065 with GmNAC085 in yeast. GmNAC065 was expressed in yeast as GAL4 binding domain (BD) fusion, and GmNAC085 and GmNAC177 were expressed in yeast as GAL4 activation domain (AD) fusions. Interactions between the tested proteins were examined by monitoring His prototrophy in the presence of 10 mM 3-AT. In the control experiments, the GmNAC065 fusions was expressed with the reciprocal empty vector (pBD or pAD).

framework to rationalize future functional studies of the members of this family. In fact, in addition to sequence conservation, the previously characterized soybean NACs were correctly placed in the corresponding subfamily based on expression profile and function. Accordingly, GmNAC030 (Glyma.05G195000), which has been characterized as a component of the stress-induced NRP/DCD-mediated cell death signaling (Mendes et al., 2013), was clustered with members of the SNAC-A subfamily of stress-induced NAC proteins, which encompasses highly conserved and functionally characterized proteins from Arabidopsis, displaying partially overlapping function, such as ATAF1 (AT1G01720) and ATAF2 (AT5G08790). *ATAF1* has been shown to be induced by both biotic and abiotic stress, to regulate negatively drought stress-responsive genes and positively ABA biosynthesis (Lu et al., 2007; Wu et al., 2009; Jensen et al., 2013). *ATAF1* also serves as a positive regulator of senescence by coupling stress-induced response with photosynthesis- and senescence-related transcriptional cascade in addition to acting as a negative regulator of defense responses against both necrotrophic fungal and bacterial pathogens (Wang et al., 2009; Garapati et al., 2015). ATAF2 functions as a central regulator of plant defense, ABA-mediated leaf senescence, hormone metabolism and light-mediated seedling development (Delessert et al., 2005;

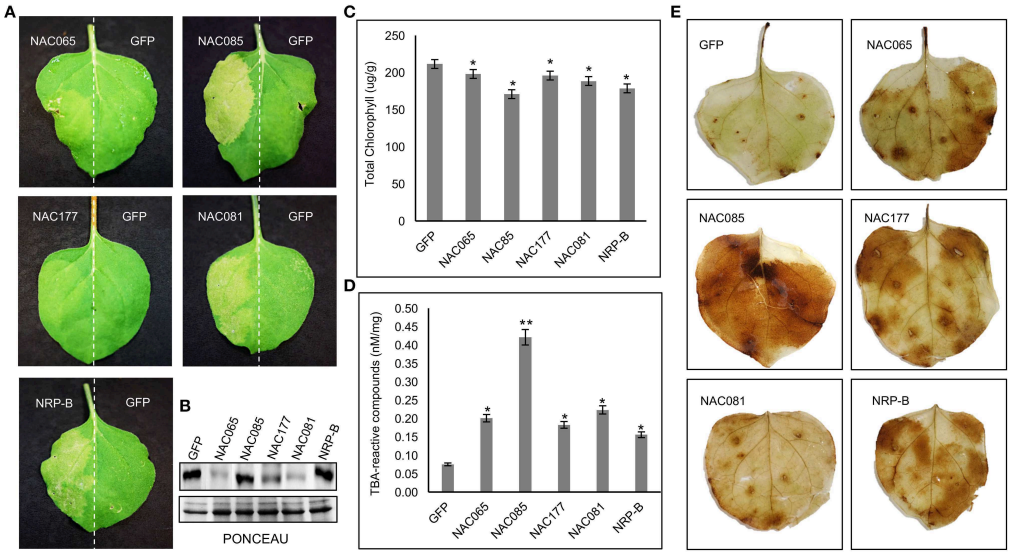

FIGURE 10 | Transient expression of NAC065, NAC085, and NAC177 induces cell death *in planta*. **(A)** *Nicotiana benthamiana* leaves were agroinfiltrated with GmNAC065-GFP, GmNAC085-GFP or GmNAC177-GFP on one side and the other half of the leaves was agroinfiltrated with GFP (as a negative control). GmNAC081 and NRP-B were used as positive controls. **(B)** Accumulation of NAC proteins in agroinfiltrated leaf sectors. Total proteins were extracted from agroinfiltrated leaf sectors and immunoblotted with an anti-GFP antibody **(C)** Total chlorophyll content 3 days after agroinfiltration. **(D)** TBA-reactive compounds accumulation after NAC expression. **(E)** DAB leaf-staining 3 days after agroinfiltration. The bars indicate standard-error and the asterisks indicate statistical significance by the *t*-test: *($P < 0.05$, $n = 3$); **($P < 0.01$, $n = 3$).

Wang et al., 2009; Huh et al., 2012; Wang and Culver, 2012; Peng et al., 2015). All seven SNAC genes from Arabidopsis are induced by long-term treatment with ABA and/or during age-dependent senescence (Takasaki et al., 2015). *GmNAC030* shares several biological properties with *ATAF1* and *ATAF2*. It is induced by abiotic stress, biotic stress, hormone signaling and it is also involved in stress-induced and developmentally programmed leaf senescence (Mendes et al., 2013; Carvalho et al., 2014b; Pimenta et al., 2016). The SNAC-A member AT5G22380 (ANAC090) is also involved in senescence as part of a senescence-regulating NAC tripartite module (Kim et al., 2018). Likewise, GmNAC011 (Glyma.13G030900, firstly described as GmNAC020) belongs to the SNAC-A subfamily and has been described as a stress-responsive protein, which confers salt and freezing tolerance and is involved in lateral root formation (Hao et al., 2011). Other members of the SNAC-A subfamily, including GmNAC035 (Glyma.06G1140000), GmNAC011 (Glyma.13G030900), GmNAC109 (Glyma.14G152700), and GmNAC039 (Glyma.06G157400), have shown to display a stress-induced expression profile consistent with their clustering into this family (Tran et al., 2009).

Another component of the stress-induced NRP/DCD-mediated signaling, GmNAC081 (Glyma.12G022700; Faria et al., 2011), was clustered in the TERN (Tobacco elicitor-responsive gene encoding NAC-domain protein) subfamily, which encompasses functionally similar NAC proteins that are involved in resistance to biotic and abiotic stresses. Examples from this subfamily include (i) *Gossypium barbadense* (Gb)NAC1, which is involved in the positive regulation of resistance to Verticillium and in abiotic stress response in cotton (Wang et al., 2016), (ii) the chitin-responsive gene *AT3G44350 (ANAC061)* and (iii) *AT2G17040* (*ANAC036),* an orthologous gene of *GmNAC081* (Libault et al., 2007; Reis et al., 2016). GmNAC081 has been shown to regulate stress-induced and developmentally programmed leaf senescence (Mendes et al., 2013; Pimenta et al., 2016).

GmNAC124 (Glyma.16G043200, firstly described as GmNAC11) belongs to the SNAC-B (NAP). Accordingly, it is induced by stress and confers salt tolerance (Hao et al., 2011). The founding member of the SNAC-B (NAP) subfamily, the NAC-like activated by AP3/PI (AtNAP, AT1G69490), is a crucial regulator of leaf senescence and couples ABA biosynthesis with chlorophyll loss (Yang et al., 2014c). *GmNAC006* (Glyma.02G070000), which also clusters with members of this family, has been shown to be salt- and dehydration-induced (Tran et al., 2009). GmNAC representatives of the vascular-related NAC domain (VND-NAC) subfamily include GmNAC048 (Glyma.07G05060) and GmNAC122 (Glyma.16G019400), functionally characterized as orthologs of the Arabidopsis NAC secondary wall thickening promoting factor 1, NST1 (AT2G46770), NST2 (AT3G61910),

and NST3 (AT1G32770) (Mitsuda et al., 2005, 2007; Mitsuda and Ohme-Takagi, 2008; Dong et al., 2013). In Arabidopsis, members of this family are very well characterized NAC proteins, involved in the control of vascular differentiation, including also the vascular-related NAC domain 6 (VND6) and VND7 (Yamaguchi et al., 2010, 2011). These examples of characterized members of the soybean NAC family substantiate the notion that NACs of the same subfamily from different species conserve similar function, expression, and sequence.

Stress- and Senescence-Associated Expression Analyses Confirm the Phylogenetic Classification of the New GmNAC Genes

We also showed that a fraction of the novel NAC genes responds to at least one of the stimuli tested, including ER stress (TUN treatment), osmotic stress (PEG treatment), SA treatment, or developmentally programmed leaf senescence. Although not functionally characterized, these new, previously unidentified, GmNACs displayed expression profiles consistent with their subfamily classification, which may extend to accommodate similar function. Accordingly, GmNAC154 (Glyma.02G284300), a member of the ONAC022 subfamily, shares a high degree of conservation with ANA042 (JUB1; AT2G4300000), which has been described as a negative regulator of important growth repressors and key genes involved in gibberellin (GA), brassinosteroid (BR) biosynthesis and senescence (Wu et al., 2012; Shahnejat-Bushehri et al., 2016). Besides its developmental function, JUB1 displays other functions in promoting tolerance to drought, heat and salinity (Wu et al., 2012; Shahnejat-Bushehri et al., 2016; Ebrahimian-Motlagh et al., 2017). *JUB1* is up-regulated by H_2O_2 -mediated oxidative stress, which may explain its dual involvement with development and stress response. In fact, JUB1 has been implicated as a central regulator of a finely tuned control system that modulates the cellular H_2O_2 level and primes the plants for upcoming stress through a gene regulatory network that involves DREB2A (Wu et al., 2012). Accordingly, the tomato *JUB1* ortholog has also been shown to be induced by H_2O_2, NaCl, osmotic stress and leaf dehydration and to enhance drought tolerance in transgenic tomato lines (Thirumalaikumar et al., 2017). In addition to sharing similar expression profiles, the abiotic stress-related gene regulatory networks controlled by tomato and Arabidopsis JUB1 have been demonstrated to be highly conserved. The expression profile of GmNAC154 indicated that this soybean NAC might be a JUB1 ortholog as it is controlled by biotic and abiotic stresses, which are triggered by H_2O_2 accumulation as the common denominator.

GmNAC163 (Glyma.06G288500), which was shown to be strongly up-regulated by PEG, TUN and SA, belongs to the ANAC001 subfamily and is closely related to ANAC073/SND2 (AT4G28500) that regulates genes involved in secondary cell wall development. ANAC073 controls the expression of cellulose and hemicellulose biosynthetic genes in addition to those involved in lignin polymerization and signaling (Hussey et al., 2011).

GmNAC174 (Glyma.12G186900) and *GmNAC177* (Glyma.16G0164000), which belong to different phylogenetic subfamilies, were rapidly induced by TUN and SA. GmNAC174 (subfamily OsNAC8) is closely related to ANAC089 (AT5G22290) a membrane-tethered transcription factor that negatively regulates floral initiation. ANAC089 also controls ER-stress-induced programmed cell death and is induced by TUN, like the predicted transmembrane soybean ortholog GmNAC174 (Yang et al., 2014b). Under severe ER stress conditions, the membrane-associated transcription factor ANAC089 relocates from the ER membrane to the nucleus to induce programmed cell death. *GmNAC177*, also induced by TUN and SA, belongs to an unnamed monophyletic group of soybean NAC genes, that cluster very closely to the TIP subfamily. Proteins from the TIP subfamily are involved in senescence progression and immune response control (Pinheiro et al., 2009; Wang et al., 2009; Block et al., 2014). Specifically, AT4G35580 has been demonstrated to interact with the *Pseudomonas syringae* type III effector HopD1 in the endoplasmic reticulum to suppress effector-triggered immunity (Block et al., 2014). Hence, it is not surprising that *GmNAC177*, a soybean close relative of AT4G35580, is regulated by ER stress and SA. As a representative of the novel GmNACs, GmNAC177 was further characterized and showed that displays transcriptional activity in yeast, is nuclear localized and induces cell death *in planta*, which is consistent with its close relatedness with the TIP subfamily.

The *GmNAC065* (Glyma.08G307100) orthologous gene from Arabidopsis, *ANAC083* (*AT5G13180*), also designated VND-interacting 2 (*VNI2*), interacts with VND7 and negatively regulates xylem vessel formation in Arabidopsis (Yamaguchi et al., 2010). In addition, VNI2 has been shown to integrate ABA-mediated abiotic stress signals into leaf aging by regulating a subset of COLD-REGULATED (COR) and RESPONSIVE TO DEHYDRATION (RD) genes (Yang et al., 2011). The *VNI2* gene is induced by high salinity in an ABA-dependent manner and displays spatial and temporal expression patterns correlated with leaf aging and senescence. VNI2 may also be involved in biotic stress responses as it has been shown to interact with the geminiviral replication initiator protein (Rep) from *Mungbean yellow mosaic India virus* (Suyal et al., 2014). We showed here that *GmNAC065* share developmental and stress response similarly to its orthologous gene VNI2 and may play a similar function related to cell death events.

GmNAC085 (Glyma.12G149100) belongs to the SNAC-A (ATAF) subfamily, which contains seven homologous genes from Arabidopsis. All seven SNAC-A genes from Arabidopsis, *ANAC055* (AT3G15500), *ANAC019* (AT1G52890), *ANAC072/RD26* (AT4G27410), *ANAC002/ATAF1* (AT1G01720), *ANAC081/ATAF2* (AT5G08790), *ANAC102* (AT5G63790), and *ANAC032* (AT1G77450), are induced during age-dependent senescence; thereby, up-regulating ABA- and senescence-inducible genes and play crucial roles in ABA-induced leaf senescence signaling (Takasaki et al., 2015). Likewise, 90% of the orthologous SNAC-A (ATAF) genes from soybean were differentially expressed during natural leaf senescence (**Supplementary Table 6**). The most closely related protein of GmNAC085, ANAC072 (AT4G27410), also designated RD26, RESPONSIVE TO DESICCATION 26, acts as a transcriptional activator in ABA-mediated dehydration response. ANAC072

positively regulates both age- and dark-induced leaf senescence through activating the transcription of NYE1, a key regulatory gene in chlorophyll degradation (Li et al., 2016a). Except for PEG treatment, *GmNAC085* did not respond to TUN and SA treatments, and in contrast to the SNAC-A genes from Arabidopsis, which are induced during leaf senescence, *GmNAC085* was repressed by developmentally programmed leaf senescence. Among the SNAC-A proteins, GmNAC085 forms a more divergent and separate clade along with other three GmNACs, which may explain a different expression profile and functional divergence from characterizing SNAC-As.

In summary, our results represent an update of the NAC inventory in the soybean genome. Furthermore, our results demonstrated that a representative sample of the novel, previously unidentified transcription factors of the GmNAC superfamily is expressed in response to stress conditions or a senescence signal, and their regulation may be necessary for elicitation of diverse response pathways triggered by different stimuli. The expression profiles of newly identified NAC genes and functional characterization of previously uncharacterized ones validate the genome annotation and reinforce the plasticity of biological functions played by GmNACs. The soybean GmNACs were separated into 15 subfamilies based on phylogeny relatedness, showing a clear relationship between structure, expression, and function for representatives of each subfamily. The large number of proteins encoded by this family and their great diversity allow plants to elaborate complex responses, with gradual levels of hormonal, temporal and spatial regulation with the high plasticity of responses, which, nevertheless, may be anticipated with a high degree of ascertaining by phylogenetic relatedness of the GmNAC proteins.

AUTHOR CONTRIBUTIONS

BM conducted all experiments, analyzed data and wrote the first draft of the manuscript. OF performed qRT-PCR. JS and OB performed the bioinformatics and RNA-seq analyses. DF, PC, and JM carried out RNA-seq. PR designed experiments. EF designed experiments, analyzed data and wrote the manuscript. All authors contributed to the discussion and approved the final manuscript.

ACKNOWLEDGMENTS

The authors are grateful to Amanda dos Santos Silva for the figure edition of NAC chromosome distribution and NAC phylogenetic tree. The authors also acknowledge the financial support of the National Institute of Science and Technology in Plant-Pest Interactions (Grant 573600/2008-2 to EPBF) and from the Brazilian institutions CAPES, CNPq and FAPEMIG.

SUPPLEMENTARY MATERIAL

The Supplementary Material for this article can be found online at: https://www.frontiersin.org/articles/10.3389/fpls.2018.01864/full#supplementary-material

REFERENCES

Aida, M., Ishida, T., Fukaki, H., Fujisawa, H., and Tasaka, M. (1997). Genes involved in organ separation in Arabidopsis: an analysis of the cup-shaped cotyledon mutant. *Plant Cell* 9, 841–857. doi: 10.1105/tpc.9.6.841

Balazadeh, S., Kwasniewski, M., Caldana, C., Mehrnia, M., Zanor, M. I., Xue, G. P., et al. (2011). ORS1, an H2O2-responsive NAC transcription factor, controls senescence in *Arabidopsis thaliana*. *Mol. Plant*. 4, 346–360. doi: 10.1093/mp/ssq080

Balazadeh, S., Siddiqui, H., Allu, A. D., Matallana-Ramirez, L. P., Caldana, C., Mehrnia, M., et al. (2010). A gene regulatory network controlled by the NAC transcription factor ANAC092/AtNAC2/ORE1 during salt-promoted senescence. *Plant J.* 62, 250–264. doi: 10.1111/j.1365-313X.2010.04151.x

Block, A., Toruño, T. Y., Elowsky, C. G., Zhang, C., Steinbrenner, J., Beynon, J., et al. (2014). The *Pseudomonas syringae* type III effector HopD1 suppresses effector-triggered immunity, localizes to the endoplasmic reticulum, and targets the Arabidopsis transcription factor NTL9. *New Phytol.* 201, 1358–1370. doi: 10.1111/nph.12626

Breeze, E., Harrison, E., McHattie, S., Hughes, L., Hickman, R., Hill, C., et al. (2011). High-resolution temporal profiling of transcripts during Arabidopsis leaf senescence reveals a distinct chronology of processes and regulation. *Plant Cell* 23, 873–894. doi: 10.1105/tpc.111.083345

Cakmak, I., and Horst, J. H. (1991). Effects of aluminum on lipid peroxidation, superoxide dismutase, catalase, and peroxidase activities in root tips of soybean (*Glycine max*). *Physiol. Plantarum* 83, 463–468. doi: 10.1111/j.1399-3054.1991.tb00121.x

Calil, I. P., Quadros, I. P. S., Araújo, T. C., Duarte, C. E. M., Gouveia-Mageste, B. C., Silva, J. C. F., et al. (2018). A WW domain-containing protein forms immune nuclear bodies against begomoviruses. *Mol. Plant* 11, 1449–1465. doi: 10.1016/j.molp.2018.09.009

Cao, L., Yu, Y., Ding, X., Zhu, D., Yang, F., Liu, B., et al. (2017). The Glycine soja NAC transcription factor GsNAC019 mediates the regulation of plant alkaline tolerance and ABA sensitivity. *Plant. Mol. Biol.* 95, 253–268. doi: 10.1007/s11103-017-0643-3

Carvalho, H. H., Brustolini, O. J., Pimenta, M. R., Mendes, G. C., Gouveia, B. C., Silva, P. A., et al. (2014a). The molecular chaperone binding protein BiP prevents leaf dehydration-induced cellular homeostasis disruption. *PLoS ONE* 9:e86661. doi: 10.1371/journal.pone.0086661

Carvalho, H. H., Silva, P. A., Mendes, G. C., Brustolini, O. J., Pimenta, M. R., Gouveia, B. C., et al. (2014b). The endoplasmic reticulum binding protein BiP displays dual function in modulating cell death events. *Plant Physiol.* 164, 654–670. doi: 10.1104/pp.113.231928

Costa, M. D. L., Reis, P. A. B., Valente, M. A. S., Irsigler, A. S. T., Carvalho, C. M., Loureiro, M. E., et al. (2008). A new branch of endoplasmic reticulum stress signaling and the osmotic signal converge on plant-specific asparagine-rich proteins to promote cell death. *J. Biol. Chem.* 283, 20209–20219. doi: 10.1074/jbc.M802654200

Delessert, C., Kazan, K., Wilson, I. W., Van Der Straeten, D., Manners, J., Dennis, E. S., et al. (2005). The transcriptionfactor ATAF2 represses the expression of pathogenesis-related genes in Arabidopsis. *Plant J.* 43, 745–757. doi: 10.1111/j.1365-313X.2005.02488.x

Dong, Y., Wang, B. H., and Wang, Y. Z. (2013). Functional characterization of the orthologs of AtNST1/2 in *Glycine soja* (*Fabaceae*) and the evolutionary implications. *J. System. Evol.* 51 , 693–703. doi: 10.1111/jse.12025

Ebrahimian-Motlagh, S., Ribone, P. A., Thirumalaikumar, V. P., Allu, A. D., Chan, R. L., Mueller-Roeber, B., et al. (2017). JUNGBRUNNEN1 confers drought tolerance downstream of the HD-Zip I transcription factor AtHB13. *Front. Plant Sci.* 8:2118. doi: 10.3389/fpls.2017.02118

Falcon, S., and Gentleman, R. (2007). Using GOstats to test gene lists for GO term association. *Bioinformatics* 23, 257–258. doi: 10.1093/bioinformatics/btl567

Faria, J. A., Reis, P. A., Reis, M. T., Rosado, G. L., Pinheiro, G. L., Mendes, G. C., et al. (2011). The NAC domain-containing protein, GmNAC6, is a downstream component of the ER stress and osmotic stress-induced NRP-mediated cell-death signaling pathway. *BMC Plant Biol.* 11:129. doi: 10.1186/1471-2229-11-129

Fujita, M., Fujita, Y., Maruyama, K., Seki, M., Hiratsu, K., Ohme-Takagi, M., et al. (2004). A dehydration-induced NAC protein, RD26, is involved in a novel ABA-dependent stress-signaling pathway. *Plant J.* 39, 863–876. doi: 10.1111/j.1365-313X.2004.02171.x

Garapati, P., Xue, G. P., Munné-Bosch, S., and Balazadeh, S. (2015). Transcription factor ATAF1 in Arabidopsis promotes senescence by direct regulation of key chloroplast maintenance and senescence transcriptional cascades. *Plant Physiol.* 168, 1122–1139. doi: 10.1104/pp.15.00567

Guo, Y., and Gan, S. (2006). AtNAP, a NAC family transcription factor, has an important role in leaf senescence. *Plant J.* 46, 601–612. doi: 10.1111/j.1365-313X.2006.02723.x

Hao, Y. J., Wei, W., Song, Q. X., Chen, H. W., Zhang, Y. Q., Wang, F., et al. (2011). Soybean NAC transcription factors promote abiotic stress tolerance and lateral root formation in transgenic plants. *Plant J.* 68, 302–313. doi: 10.1111/j.1365-313X.2011.04687.x

Heath, R. L., and Packer, L. (1968). Photoperoxidation in isolate chloroplasts: I. kinetics and stoichiometry of fatty acid peroxidation. *Arch. Biochem. Biophys.* 125, 189–198. doi: 10.1016/0003-9861(68)90654-1

Hegedus, D. M., Yu, D., Baldwin, M., Gruber, A., Sharpe, I., Parkin, S., et al. (2003). Molecular characterization of *Brassica napus* NAC domain transcriptional activators induced in response to biotic and abiotic stress. *Plant Mol. Biol.* 53, 383–397. doi: 10.1023/B:PLAN.0000006944.61384.11

Hibara, K., Takada, S., and Tasaka, M. (2003). CUC1 gene activates the expression of SAM-related genes to induce adventitious shoot formation. *Plant J.* 36, 687–696. doi: 10.1046/j.1365-313X.2003.01911.x

Hickman, R., Hill, C., Penfold, C. A., Breeze, E., Bowden, L., Moore, J. D., et al. (2013). A local regulatory network around three NAC transcription factors in stress responses and senescence in Arabidopsis leaves. *Plant J.* 75, 26–39. doi: 10.1111/tpj.12194

Hu, H., Dai, M., Yao, J., Xiao, B., Li, X., Zhang, Q., et al. (2006). Overexpressing a NAM, ATAF, and CUC (NAC) transcription factor enhances drought resistance and salt tolerance in rice. *Proc. Natl. Acad. Sci. U.S.A.* 103, 12987–12992. doi: 10.1073/pnas.0604882103

Hu, H., You, J., Fang, Y., Zhu, X., Qi, Z., and Xiong, L. (2008). Characterization of transcription factor gene SNAC2 conferring cold and salt tolerance in rice. *Plant Mol. Biol.* 67, 169–181. doi: 10.1007/s11103-008-9309-5

Huh, S. U., Lee, S. B., Kim, H. H., and Paek, K. H. (2012). ATAF2, a NAC transcription factor, binds to the promoter and regulates NIT2 gene expression involved in auxin biosynthesis. *Mol. Cells* 34, 305–313. doi: 10.1007/s10059-012-0122-2

Hussain, R. M., Ali, M., Feng, X., and Li, X. (2017). The essence of NAC gene family to the cultivation of drought-resistant soybean (*Glycine max* L. Merr.) cultivars. *BMC Plant Biol.* 17:55. doi: 10.1186/s12870-017-1001-y

Hussey, S. G., Mizrachi, E., Spokevicius, A. V., Bossinger, G., Berger, D. K., and Myburg, A. A. (2011). SND2, a NAC transcription factor gene, regulates genes involved in secondary cell wall development in Arabidopsis fibres and increases fibre cell area in Eucalyptus. *BMC Plant Biol.* 1:173. doi: 10.1186/1471-2229-11-173

Jensen, M. K., Lindemose, S., de Mais, F., Reimer, J. J., Nielsen, M., Perera, V., et al. (2013). ATAF1 transcription factor directly regulates abscisic acid biosynthetic gene NCED3 in *Arabidopsis thaliana*. *FEBS Open Bio.* 3, 321–327. doi: 10.1016/j.fob.2013.07.006

Kim, J. H., Nam, H. G., and Lim, P. O. (2016). Regulatory network of NAC transcription factors in leaf senescence. *Curr. Opin. Plant Biol.* 33, 48–56. doi: 10.1016/j.pbi.2016.06.002

Kim, J. H., Woo, H. R., Kim, J., Lim, P. O., Lee, I. C., Choi, S. H., et al. (2009). Trifurcate feed-forward regulation of age-dependent cell death involving miR164 in Arabidopsis. *Science* 323, 1053–1057. doi: 10.1126/science.1166386

Kim, J. K., Park, J. H., Kim, J., Kim, J. K., Hong, S., Kim, J., et al. (2018). Time-evolving genetic networks reveal a NAC troika that negatively regulates leaf senescence in Arabidopsis. *Proc. Natl. Acad. Sci. U.S.A.* 115, 4930–4939. doi: 10.1073/pnas.1721523115

Kim, Y. S., Kim, S. G., Park, J. E., Park, H. Y., Lim, M. H., Chua, N. H., et al. (2006). A membrane-bound NAC transcription factor regulates cell division in Arabidopsis. *Plant Cell* 18, 3132–3144. doi: 10.1105/tpc.106.043018

Le, D. T., Nishiyama, R., Watanabe, Y., Mochida, K., Yamaguchi-Shinozaki, K., Shinozaki, K., et al. (2011). Genome wide survey and expression analysis of the plant-specific NAC transcription factor family in soybean during development and dehydration stress. *DNA Res.* 18, 263–276. doi: 10.1093/dnares/dsr015

Le, D. T., Nishiyama, R., Watanabe, Y., Tanaka, M., Seki, M., et al. (2012). Differential gene expression in soybean leaf tissues at late developmental stages under drought stress revealed by genome-wide transcriptome analysis. *PLoS ONE* 7:e49522. doi: 10.1371/journal.pone.0049522

Lee, S., Seo, P. J., Lee, H. J., and Park, C. M. (2012). A NAC transcription factor NTL4 promotes reactive oxygen species production during drought-induced leaf senescence in Arabidopsis. *Plant J.* 70, 831–844. doi: 10.1111/j.1365-313X.2012.04932.x

Li, S., Gao, J., Yao, L., Ren, G., Zhu, X., Gao, S., et al. (2016a). The role of ANAC072 in the regulation of chlorophyll degradation during age- and dark-induced leaf senescence. *Plant Cell Rep.* 35, 1729–1741. doi: 10.1007/s00299-016-1991-1

Li, S., Wang, N., Ji, D., Xue, Z., Yu, Y., Jiang, Y., et al. (2016b). Evolutionary and functional analysis of membrane-bound NAC transcription factor genes in soybean. *Plant Physiol.* 172, 1804–1820. doi: 10.1104/pp.16.01132

Liang, C., Wang, Y., Zhu, Y., Tang, J., Hu, B., Liu, L., et al. (2014). OsNAP connects abscisic acid and leaf senescence by fine-tuning abscisic acid biosynthesis and directly targeting senescence-associated genes in rice. *Proc. Natl. Acad. Sci. U.S.A.* 111, 10013–10018. doi: 10.1073/pnas.1321568111

Libault, M., Thibivilliers, S., Bilgin, D., Radwan, O., Benitez, M., et al. (2008). Identification of four soybean reference genes for gene expression normalization. *Plant Genome* 1, 44–54. doi: 10.3835/plantgenome2008.02.0091

Libault, M., Wan, J., Czechowski, T., Udvardi, M., and Stacey, G. (2007). Identification of 118 Arabidopsis transcription factor and 30 ubiquitin-ligase genes responding to chitin, a plant-defense elicitor. *Mol. Plant Microbe Interact.* 20, 900–911. doi: 10.1094/MPMI-20-8-0900

Love, M. I., Huber, W., and Anders, S. (2014). Moderated estimation of fold change and dispersion for RNA-seq data with DESeq2. *Genome Biol.* 15:550. doi: 10.1186/s13059-014-0550-8

Lu, P. L., Chen, N. Z., An, R., Su, Z., Qi, B. S., Ren, F., et al. (2007). A novel drought-inducible gene, ATAF1, encodes a NAC family protein that negatively regulates the expression of stress-responsive genes in Arabidopsis. *Plant Mol. Biol.* 63, 289–305 doi: 10.1007/s11103-006-9089-8

Luo, W., and Brouwer, C. (2013). Pathview: an R/Bioconductor package for pathway-based data integration and visualization. *Bioinformatics* 29, 1830–1831. doi: 10.1093/bioinformatics/btt285

Mao, C., Ding, J., Zhang, B., Xi, D., and Ming, F. (2018). OsNAC2 positively affects salt-induced cell death and binds to the OsAP37 and OsCOX11 promoters. *Plant J.* 94, 454–468. doi: 10.1111/tpj.13867

Mendes, G. C., Reis, P. A. B., Calil, I. P., Carvalho, H. H., Aragão, F. J. L., and Fontes, E. P. B. (2013). GmNAC30 and GmNAC81 integrate the endoplasmic reticulum stress and osmotic stress-induced cell death responses through a vacuolar processing enzyme. *Proc. Natl. Acad. Sci. U.S.A.* 110, 19627–19632. doi: 10.1073/pnas.1311729110

Meng, Q., Zhang, C., Gai, J., and Yu, D. (2007). Molecular cloning, sequence characterization and tissue-specific expression of six NAC-like genes in soybean (*Glycine max* (L.) Merr.). *J. Plant Physiol.* 164, 1002–1012. doi: 10.1016/j.jplph.2006.05.019

Mitsuda, N., Iwase, A., Yamamoto, H., Yoshida, M., Seki, M., Shinozaki, K., et al. (2007). NAC transcription factors, NST1 and NST3, are key regulators of the formation of secondary walls in woody tissues of Arabidopsis. *Plant Cell* 19, 270–280. doi: 10.1105/tpc.106.047043

Mitsuda, N., and Ohme-Takagi, M. (2008). NAC transcription factors NST1 and NST3 regulate pod shattering in a partially redundant manner by promoting secondary wall formation after the establishment of tissue identity. *Plant J.* 56, 768–778. doi: 10.1111/j.1365-313X.2008.03633.x

Mitsuda, N., Seki, M., Shinozaki, K., and Ohme-Takagi, M. (2005). The NAC transcription factors NST1 and NST2 of Arabidopsis regulate secondary wall thickenings and are required for anther dehiscence. *Plant Cell* 17, 2993–3006. doi: 10.1105/tpc.105.036004

Nakashima, K., Takasaki, H., Mizoi, J., Shinozaki, K., and Yamaguchi-Shinozaki, K. (2011). NAC transcription factors in plant abiotic stress responses. *Biochim. Biophys. Acta*. 1819, 97–103. doi: 10.1016/j.bbagrm.2011.10.005

Nakashima, K., Tran, L. S., Van Nguyen, D., Fujita, M., Maruyama, K., and Todaka, D. (2007). Functional analysis of a NAC- type transcription factor OsNAC6 involved in abiotic and biotic stress- responsive gene expression in rice. *Plant J.* 51, 617–630. doi: 10.1111/j.1365-313X.2007.03168.x

Olsen, A. N., Ernst, H. A., Leggio, L. L., and Skriver, K. (2005). NAC transcription factors: structurally distinct, functionally diverse. *Trends Plant Sci.* 10, 79–87. doi: 10.1016/j.tplants.2004.12.010

Ooka, H., Satoh, K., Doi, K., Nagata, T., Otomo, Y., Murakami, K., et al. (2003). Comprehensive analysis of NAC family genes in *Oryza sativa* and *Arabidopsis thaliana*. *DNA Res.* 10, 239–247. doi: 10.1093/dnares/10.6.239

Peng, H., Zhao, J., and Neff, M. M. (2015). ATAF2 integrates *Arabidopsis* brassinosteroid inactivation and seedling photomorphogenesis. *Development* 142, 4129–4138. doi: 10.1242/dev.124347

Pimenta, M. R., Silva, P. A., Mendes, G. C., Alves, J. R., Caetano, H. D. N., Machado, J. P. B., et al. (2016). The stress-induced soybean NAC transcription factor GmNAC81 plays a positive role in developmentally programmed leaf senescence. *Plant Cell Physiol.* 57, 1098–1114. doi: 10.1093/pcp/pcw059

Pinheiro, G. L., Marques, C. S., Costa, M. D., Reis, P. A. B., Alves, M. S., Carvalho, C. M., et al. (2009). Complete inventory of soybean NAC transcription factors: sequence conservation and expression analysis uncover their distinct roles in stress response. *Gene* 444, 10–23. doi: 10.1016/j.gene.2009.05.012

Puranik, S., Sahu, P. P., Srivastava, P. S., and Prasad, M. (2012). NAC proteins: regulation and role in stress tolerance. *Trends Plant Sci.* 17, 369–381. doi: 10.1016/j.tplants.2012.02.004

Quach, T. N., Tran, L. S. P., Valliyodan, B., Nguyen, H. T., Kumar, R., Neelakandan, A. K., et al. (2014). Functional analysis of water stress-responsive soybean GmNAC003 and GmNAC004 transcription factors in lateral root development in Arabidopsis. *PLoS ONE* 9:e84886. doi: 10.1371/journal.pone.0084886

Redillas, M. C., Jeong, J. S., Kim, Y. S., Jung, H., Bang, S. W., et al. (2012). The overexpression of OsNAC9 alters the root architecture of rice plants enhancing drought resistance and grain yield under field conditions. *Plant Biotechnol. J.* 10, 792–805. doi: 10.1111/j.1467-7652.2012.00697.x

Reis, P. A., Carpinetti, P. A., Freitas, P. P., Santos, E. G., Camargos, L. F., Oliveira, I. H., et al. (2016). Functional and regulatory conservation of the soybean ER stress-induced DCD/NRP mediated cell death signaling in plants. *BMC Plant Biol.* 16:156. doi: 10.1186/s12870-016-0843-z

Reis, P. A. B., Rosado, G. L., Silva, L. A., Oliveira, L. C., Oliveira, L. B., Costa, M. D., et al. (2011). The binding protein BiP attenuates stress induced cell death in soybean via modulation of the N-rich protein-mediated signaling pathway. *Plant Physiol.* 157, 1853–1865. doi: 10.1104/pp.111.179697

Sablowski, R. W., and Meyerowitz, E. M. (1998). A homolog of NO APICAL MERISTEM is an immediate target of the floral homeotic genes APETALA3/PISTILLATA. *Cell* 92, 93–103. doi: 10.1016/S0092-8674(00)80902-2

Schlueter, J. A., Scheffler, B. E., Jackson, S., and Shoemaker, R. C. (2008). Fractionation of synteny in a genomic region containing tandemly duplicated genes across *Glycine max*, *Medicago truncatula*, and *Arabidopsis thaliana*. *J. Hered.* 99, 390–395. doi: 10.1093/jhered/esn010

Schmutz, J., Cannon, S. B., Schlueter, J., Ma, J., Mitros, T., Nelson, W., et al. (2010). Genome sequence of the palaeopolyploid soybean. *Nature* 463, 178–183 doi: 10.1038/nature08670

Seo, P. J., Kim, M. J., Park, J. Y., Kim, S. Y., Jeon, J., Lee, Y. H., et al. (2010). Cold activation of a plasma membrane-tethered NAC transcription fator induces a pathogen resistance response in Arabidopsis. *Plant J.* 61, 661–671. doi: 10.1111/j.1365-313X.2009.04091.x

Shahnejat-Bushehri, S., Tarkowska, D., Sakuraba, Y., and Balazadeh, S. (2016). Arabidopsis NAC transcription factor JUB1 regulates GA/BR metabolism and signalling. *Nat. Plants* 2:16013 doi: 10.1038/nplants.2016.13

Shao, H., Wang, H., and Tang, X. (2015). NAC transcription factors in plant multiple abiotic stress responses: progress and prospects. *Front. Plant. Sci.* 6:902. doi: 10.3389/fpls.2015.00902

Silva, P. A., Silva, J. C., Caetano, H. D., Machado, J. P., Mendes, G. C., Reis, P. A., et al. (2015). Comprehensive analysis of the endoplasmic reticulum stress response in the soybean genome: conserved and plant-specific features. *BMC Genomics* 16:783. doi: 10.1186/s12864-015-1952-z

Song, S. Y., Chen, Y., Chen, J., Dai, X. Y., and Zhang, W. H. (2011). Physiological mechanisms under- lying OsNAC5-dependent tolerance of rice plants to abiotic stress. *Planta* 234, 331–345. doi: 10.1007/s00425-011-1403-2

Suyal, G., Rana, V. S., Mukherjee, S. K., Wajid, S., and Choudhury, N. R. (2014). *Arabidopsis thaliana* NAC083 protein interacts with Mungbean yellow mosaic India virus (MYMIV) Rep protein. *Virus Genes* 48, 486–493. doi: 10.1007/s11262-013-1028-6

Takasaki, H., Maruyama, K., Kidoro, S., Ito, Y., Fujita, Y., Shinozaki, K., et al. (2010). The abiotic stress-responsive NAC-type transcription factor OsNAC5 regulates stress-inducible genes and stress tolerance in rice. *Mol. Genet. Genomics* 284, 173–183. doi: 10.1007/s00438-010-0557-0

Takasaki, H., Maruyama, K., Takahashi, F., Fujita, M., Yoshida, T., Nakashima, K., et al. (2015). SNAC-As, stress-responsive NAC transcription factors, mediate ABA-inducible leaf senescence. *Plant J.* 84, 1114–1123. doi: 10.1111/tpj.13067

Thao, N. P., Nguyen Thu, B. A., Hoang, X. L. T., Ha, C. V., Tran, L. S. P., et al. (2013). Differential expression analysis of a subset of drought-responsive GmNAC genes in two soybean cultivars differing in drought tolerance. *Int. J. Mol. Sci.* 14, 23828–23841. doi: 10.3390/ijms141223828

Thirumalaikumar, V. P., Devkar, V., Mehterov, N., Ali, S., Ozgur, R., Turkan, I., et al. (2017). NAC transcription factor JUNGBRUNNEN1 enhances drought tolerance in tomato. *Plant Biotechnol. J.* 16, 354–366. doi: 10.1111/pbi.12776

Thu, N. B., Hoang, X. L., Doan, H., Nguyen, T. H., Bui, D., Thao, N. P., et al. (2014). Differential expression analysis of a subset of *GmNAC* genes in shoots of two contrasting drought-responsive soybean cultivars DT51 and MTD720 under normal and drought conditions. *Mol. Biol. Rep.* 41, 5563–5569. doi: 10.1007/s11033-014-3507-9

Tran, L. S., Nakashima, K., Sakuma, Y., Osakabe, Y., Qin, F., Simpson, S. D., et al. (2007). Co- expression of the stress-inducible zinc finger homeodomain ZFHD1 and NAC transcription factors enhances expression of the ERD1 gene in Arabidopsis. *Plant J.* 49, 46–63. doi: 10.1111/j.1365-313X.2006.02932.x

Tran, L. S., Nakashima, K., Sakuma, Y., Simpson, S. D., Fujita, Y., Maruyama, K., et al. (2004). Isolation and functional analysis of Arabidopsis stress-inducible NAC transcription factors that bind to a drought-responsive cis-element in the early responsive to dehydration stress 1 promoter. *Plant Cell* 16, 2481–2498. doi: 10.1105/tpc.104.022699

Tran, L. S., Quach, T. N., Guttikonda, S. K., Aldrich, D. L., Kumar, R., Neelakandan, A., et al. (2009). Molecular characterization of stress-inducible GmNAC genes in soybean. *Mol. Genet. Genomics* 281, 647–664. doi: 10.1007/s00438-009-0436-8

Vroemen, C. W., Mordhorst, A. P., Albrecht, C., Kwaaitaal, M. A. C. J., and de Vries, S. C. (2003). The CUP-SHAPED COTYLEDON3 gene is required for boundary and shoot meristem formation in Arabidopsis. *Plant Cell* 15, 1563–1577. doi: 10.1105/tpc.012203

Wang, W., Yuan, Y., Yang, C., Geng, S., Sun, Q., Cai, C., et al. (2016). Characterization, expression and analysis of a novel NAC gene associates with resistance to Verticilium wilt and abiotic stress in cotton. *G3 (Bethesda)* 6, 3951–3961. doi: 10.1534/g3.116.034512

Wang, X., Basnayake, B. M., Zhang, H., Li, G., Li, W., Virk, N. et al. (2009). The Arabidopsis ATAF1, a NAC transcription factor, is a negative regulator of defense responses against necrotrophic fungal and and bacterial pathogens. *Mol. Plant Microbe Interact.* 22, 1227–1238. doi: 10.1094/MPMI-22-10-1227

Wang, X., and Culver, J. N. (2012). DNA binding specificity of ATAF2, a NAC domain transcription factor targeted for degradation by Tobacco mosaic virus. *BMC Plant Biol.* 12:157. doi: 10.1186/1471-2229-12-157

Wellburn, A. R. (1994). The spectral determination of chlorophylls a and b, as well as total carotenoids, using various solvents with spectrophotometers of different resolution. *J. Plant Physiol.* 144, 307–313. doi: 10.1016/S0176-1617(11)81192-2

Wu, A., Allu, A. D., Garapati, P., Siddiqui, H., Dortay, H., Zanor, M. I., et al. (2012). JUNGBRUNNEN1, a reactive oxygen species-responsive NAC transcription factor, regulates longevity in Arabidopsis. *Plant Cell* 24, 482–506. doi: 10.1105/tpc.111.090894

Wu, Y., Deng, Z., Lai, J., Zhang, Y., Yang, C., Yin, B., et al. (2009). Dual function of Arabidopsis ATAF1in abiotic stress and biotic stress responses. *Cell Res.* 19, 1279–1290. doi: 10.1038/cr.2009.108

Xie, Q., Frugis, G., Colgan, D., and Chua, N. H. (2000). Arabidopsis NAC1 transduces auxin signal downstream of TIR1 to promote lateral root development. *Genes Dev.* 14, 3024–3036. doi: 10.1101/gad.852200

Yamaguchi, M., Mitsuda, N., Ohtani, M., Ohme-Takagi, M., Kato, K., and Demura, T. (2011). VASCULAR-RELATED NAC-DOMAIN7 directly regulates the expression of a broad range of genes for xylem vessel formation. *Plant J.* 66, 579–590. doi: 10.1111/j.1365-313X.2011.04514.x

Yamaguchi, M., Ohtani, M., Mitsuda, N., Kubo, M., Ohme-Takagi, M., Fukuda, H., et al. (2010). VND-INTERACTING2, a NAC domain transcription factor, negatively regulates xylem vessel formation in Arabidopsis. *Plant Cell* 22, 249–263. doi: 10.1105/tpc.108.064048

Yang, J., Worley, E., and Udvardi, M. (2014c). A NAP-AAO3 Module promotes chlorophyll degradation via ABA biosynthesis in Arabidopsis leaves. *Plant Cell* 26, 4862–4874. doi: 10.1105/tpc.114.133769

Yang, S. D., Seo, P. J., Yoon, H. K., and Park, C. M. (2011). The Arabidopsis NAC transcription factor VNI2 integrates abscisic acid signals into leaf senescence via the COR/RD genes. *Plant Cell* 23, 2155–2168. doi: 10.1105/tpc.111.084913

Yang, Z. T., Lu, S. J., Wang, M. J., Bi, D. L., Sun, L., Zhou, S. F., et al. (2014a). A plasma membrane-tethered transcription factor, NAC062/ANAC062/NTL6, mediates the unfolded protein response in Arabidopsis. *Plant J.* 79, 1033–1043. doi: 10.1111/tpj.12604

Yang, Z. T., Wang, M. J., Sun, L., Lu, S. J., Bi, D. L., and Sun, L. (2014b). The membrane-associated transcription factor NAC089 controls ER-stress-induced programmed cell death in plants. *PLoS Genet.* 10:e1004243. doi: 10.1371/journal.pgen.1004243

Zhang, Z., Zhao, Y., Feng, X., Luo, Z., Kong, S., Zhang, C., et al. (2018). Genomic, molecular evolution, and expression analysis of NOX genes in soybean (*Glycine max*). Genomics. doi: 10.1016/j.ygeno.2018.03.018. [Epub ahead of print].

Zheng, X., Chen, B., Lu, G., and Han, B. (2009). Overexpression of a NAC transcription factor enhances rice drought and salt tolerance. *Biochem. Biophys. Res. Commun.* 379, 985–989. doi: 10.1016/j.bbrc.2008.12.163

Zhong, R. Q., Demura, T., and Ye, Z. H. (2006). SND1, a NAC domain transcription factor, is a key regulator of secondary wall synthesis in fibers of Arabidopsis. *Plant Cell* 18, 3158–3170. doi: 10.1105/tpc.106.047399

Conflict of Interest Statement: The authors declare that the research was conducted in the absence of any commercial or financial relationships that could be construed as a potential conflict of interest.

Table S1. Complete Inventory of soybean NAC superfamily

Glyma v11.0	Name	Lenth	NAC-domain	E-value	Transmemb. domain
Glyma.01G005500.1.p	GmNAC001	451	47 - 189	1.4E-33	
Glyma.01G046800.1.p	GmNAC002	438	16 - 143	4.2E-50	
Glyma.01G051300.1.p	GmNAC003	279	9 - 134	5.3E-52	
Glyma.01G088200.1.p	GmNAC004	451	58 - 197	1.2E-29	
Glyma.01G167900.1.p	GmNAC005	344	9 - 137	9.6E-53	
Glyma.02G050100.1.p	GmNAC153	362	6 - 135	6.8E-53	
Glyma.02G070000.1.p	GmNAC006	354	9 - 140	2.1E-50	
Glyma.02G070600.1.p	GmNAC007	410	23 - 149	1.8E-53	
Glyma.02G100200.1.p	GmNAC008	436	58 - 197	4.0E-30	
Glyma.02G107000.1.p	GmNAC009	442	18 - 145	4.3E-50	
Glyma.02G109800.1.p	GmNAC010	279	9 134	4.7E-52	
Glyma.13G030900.1.p	GmNAC011	268	9 - 133	7.1E-50	
Glyma.02G222300.1.p	GmNAC012	589	21 - 147	7.9E-50	565 - 587
Glyma.02G240500.1.p	GmNAC013	643	5 - 132	4.9E-54	567 - 586 e 620 - 637
Glyma.02G284300.1.p	GmNAC154	320	22 - 149	1.0E-47	
Glyma.03G164200.1.p	GmNAC155	296	10 - 138	6.7E-48	
Glyma.03G179600.1.p	GmNAC156	287	11 - 138	9.4E-48	
Glyma.03G197900.1.p	GmNAC014	257	4 - 134	1.1E-42	
Glyma.04G014900.1.p	GmNAC157	350	22 - 149	1.4E-49	
Glyma.04G078600.1.p	GmNAC015	357	28 - 155	2.1E-52	
Glyma.04G119500.1.p	GmNAC016	341	7 - 136	1.6E-53	
Glyma.04G167200.1.p	GmNAC017	357	18 - 143	2.4E-54	
Glyma.04G175800.1.p	GmNAC158	78	02 -- 78	1.3E-21	
Glyma.04G199000.1.p	GmNAC159	169	28 - 73	4.0E-11	
Glyma.04G208300.1.p	GmNAC018	291	7 - 131	3.4E-50	
Glyma.04G212000.1.p	GmNAC019	201	8 - 125	6.4E-30	
Glyma.04G213300.1.p	GmNAC020	483	6 - 132	2.9E-46	
Glyma.04G226700.1.p	GmNAC021	603	22 - 148	7.9E-50	579 - 601
Glyma.04G249000.1.p	GmNAC022	300	7 - 131	2.8E-49	
Glyma.05G025500.1.p	GmNAC023	350	16 - 142	3.3E-53	
Glyma.05G055900.1.p	GmNAC024	364	7 - 136	3.4E-53	
Glyma.05G002700.1.p	GmNAC025	390	56 - 197	9.3E-28	
Glyma.05G086000.1.p	GmNAC160	177	11 - 140	1.5E-48	
Glyma.05G108700.1.p	GmNAC161	212	18 - 98	6.4E-9	
Glyma.05G113000.1.p	GmNAC026	345	6 - 135	2.0E-50	
Glyma.05G120500.1.p	GmNAC027	189	8 - 127	1.1E-33	
Glyma.05G191300.1.p	GmNAC028	317	5 - 123	1.1E-31	
Glyma.05G192500.1.p	GmNAC029	206	9 - 125	1.7E-30	
Glyma.05G195000.1.p	GmNAC030	298	7 - 131	1.3E-49	
Glyma.05G234200.1.p	GmNAC031	321	5 - 131	9.8E-51	

Glyma.05G225100.1.p	GmNAC032	448	47 - 189	9.6E-33	
Glyma.05G202300.1.p	GmNAC033	241	14 - 141	6.2E-44	
Glyma.06G014900.1.p	GmNAC162	374	22 -149	1.6E-49	
Glyma.06G080200.1.p	GmNAC034	355	28 - 155	1.8E-52	
Glyma.06G114000.1.p	GmNAC035	299	7 - 131	2.0E-49	
Glyma.06G138100.1.p	GmNAC036	598	22 - 148	6.1E-50	574 - 593
Glyma.06G152900.1.p	GmNAC037	503	6 - 132	7.0E-46	
Glyma.06G154400.1.p	GmNAC038	204	8 - 127	2.3E-31	
Glyma.06G157400.1.p	GmNAC039	295	7 - 131	2.7E-50	
Glyma.06G166500.1.p	GmNAC040	248	14 - 140	4.5E-45	
Glyma.06G195500.1.p	GmNAC041	357	18 - 143	2.0E-54	
Glyma.06G236000.1.p	GmNAC042	375	23 - 151	1.1E-52	
Glyma.06G248900.1.p	GmNAC043	337	14 - 139	2.6E-49	
Glyma.06G249100.1.p	GmNAC044	368	18 - 143	3.8E-51	
Glyma.06G288500.1.p	GmNAC163	285	49 - 189	3.5E-30	
Glyma.06G318900.1.p	GmNAC045	363	27 - 156	2.5E-53	
Glyma.07G047900.1.p	GmNAC164	497	12 -141	2.1E-44	470 - 492
Glyma.07G048000.1.p	GmNAC046	405	6 - 138	3.1E-35	
Glyma.07G048100.1.p	GmNAC047	308	6 - 138	7.0E-37	
Glyma.07G050600.1.p	GmNAC048	400	15 - 143	4.5E-50	
Glyma.07G092000.1.p	GmNAC049	324	5 - 131	4.5E-53	
Glyma.07G126500.1.p	GmNAC050	447	48 - 190	1.1E-32	
Glyma.07G192900.1.p	GmNAC165	362	15 - 142	3.8E-51	
Glyma.07G201800.1.p	GmNAC051	326	68 - 208	9.7E-31	
Glyma.07G229100.1.p	GmNAC052	233	10 - 135	6.5E-53	
Glyma.07G271100.1.p	GmNAC053	400	43 - 168	2.2E-47	
Glyma.08G009700.1.p	GmNAC054	241	14 - 140	3.7E-44	
Glyma.08G031900.1.p	GmNAC055	452	47 - 189	1.5E-33	
Glyma.08G041500.1.p	GmNAC056	313	5 - 130	1.2E-50	
Glyma.08G075300.1.p	GmNAC057	190	8 - 127	1.3E-33	
Glyma.08G156500.1.p	GmNAC058	323	5 - 130	5.1E-42	
Glyma.08G161300.1.p	GmNAC059	328	10 - 139	6.0E-52	
Glyma.08G163100.1.p	GmNAC166	348	6 - 133	1.8E-54	
Glyma.08G169400.1.p	GmNAC060	80	27 - 72	1.2E-16	
Glyma.08G173400.1.p	GmNAC061	302	11 - 134	1.1E-49	
Glyma.08G181100.1.p	GmNAC062	190	8 - 128	1.6E-34	
Glyma.08G301100.1.p	GmNAC063	413	15 - 142	3.1E-50	
Glyma.08G307100.1.p	GmNAC064	304	19 - 146	6.8E-48	
Glyma.08G360200.1.p	GmNAC065	224	14 - 139	7.1E-48	
Glyma.09G167400.1.p	GmNAC066	265	34 - 161	3.6E-52	
Glyma.09G184100.1.p	GmNAC067	331	5 - 131	3.4E-52	
Glyma.09G231700.1.p	GmNAC068	354	7 - 136	8.7E-54	
Glyma.09G233600.1.p	GmNAC069	359	9 - 138	3.1E-51	

Glyma.09G235700.1.p	GmNAC070	363	19 - 145	1.9E-52	
Glyma.10G037700.1.p	GmNAC071	296	10 - 138	9.3E-48	
Glyma.10G077000.1.p	GmNAC167	128	11 - 128	1.3E-38	
Glyma.10G077400.1.p	GmNAC168	136	11 - 136	1.7E-43	
Glyma.10G197500.1.p	GmNAC072	465	33 - 160	8.5E-51	
Glyma.10G197600.1.p	GmNAC169	448	5 -- 97	2.1E-29	424 - 446
Glyma.10G204700.1.p	GmNAC170	422	56 - 195	1.5E-28	
Glyma.10G216400.1.p	GmNAC073	346	19 - 147	4.2E-51	
Glyma.10G219600.1.p	GmNAC074	560	20 - 146	4.3E-51	529 -551
Glyma.11G030600.1.p	GmNAC075	360	7 - 138	4.2E-53	
Glyma.11G075400.1.p	GmNAC076	380	40 - 169	9.4E-53	
Glyma.11G096600.1.p	GmNAC077	302	19 - 146	4.5E-45	
Glyma.11G182000.1.p	GmNAC078	246	5 - 137	2.3E-40	
Glyma.11G212400.1.p	GmNAC079	672	8 - 135	1.3E-53	
Glyma.12G003200.1.p	GmNAC171	356	9 - 138	3.2E-51	
Glyma.12G004900.1.p	GmNAC080	347	7 - 136	1.4E-53	
Glyma.12G022700.1.p	GmNAC081	297	16 - 143	4.3E-45	
Glyma.12G091200.1.p	GmNAC082	248	6 - 140	1.6E-40	
Glyma.12G118700.1.p	GmNAC083	284	49 - 189	6.7E-31	
Glyma.12G145100.1.p	GmNAC172	180	11 - 138	1.6E-46	
Glyma.12G148900.1.p	GmNAC084	360	14 - 142	2.3E-51	
Glyma.12G149100.1.p	GmNAC085	340	14 - 139	1.7E-49	
Glyma.12G160100.1.p	GmNAC173	133	2 - 115	5.2E-35	
Glyma.12G161700.1.p	GmNAC086	366	21 - 149	1.1E-52	
Glyma.12G171600.1.p	GmNAC087	349	13 - 139	4.6E-49	
Glyma.12G186200.1.p	GmNAC088	244	4 - 134	2.1E-45	
not found - NAC89					
Glyma.12G186900.1.p	GmNAC174	493	17 - 143	8.8E-47	303 - 325
Glyma.12G206900.1.p	GmNAC090	279	48 - 188	6.1E-30	
Glyma.12G221400.1.p	GmNAC091	375	15 - 142	5.8E-51	
Glyma.12G221500.1.p	GmNAC092	345	14 - 139	4.3E-49	
Glyma.12G226500.1.p	GmNAC093	343	8 - 136	6.7E-53	
Glyma.13G063300.1.p	GmNAC094	380	13 - 138	1.6E-51	
Glyma.13G062000.1.p	GmNAC095	358	20 - 146	6.4E-53	
not found - NAC096					
Glyma.13G174700.1.p	GmNAC097	329	69 - 209	1.7E-30	
Glyma.13G234700.1.p	GmNAC098	332	73 - 214	1.0E-30	
Glyma.13G243200.1.p	GmNAC099	363	19 - 147	4.1E-51	
Glyma.13G274300.1.p	GmNAC100	352	16 - 144	7.1E-53	
Glyma.13G279900.1.p	GmNAC101	343	14 - 139	4.2E-49	
Glyma.13G280000.1.p	GmNAC102	375	15 - 142	4.5E-51	
Glyma.13G294000.1.p	GmNAC175	279	48 - 188	6.1E-30	
Glyma.13G314600.1.p	GmNAC103	371	18 - 144	5.1E-47	331 - 353

Glyma.13G315300.1.p	GmNAC104	253	4 - 134	4.2E-45	
Glyma.13G327600.1.p	GmNAC105	349	13 - 139	4.4E-49	
Glyma.14G030700.1.p	GmNAC106	326	36 - 163	7.7E-48	
Glyma.14G084300.1.p	GmNAC107	278	9 - 142	9.0E-24	
not found - NAC108					
Glyma.14G140100.1.p	GmNAC176	373	27 - 154	4.8E-53	
Glyma.14G152700.1.p	GmNAC109	280	9 - 133	1.1E-49	
Glyma.14G189300.1.p	GmNAC110	590	21 - 147	2.0E-50	566 - 588
Glyma.14G210000.1.p	GmNAC111	644	5 - 132	1.8E-54	568 - 587
Glyma.15G051200.1.p	GmNAC112	191	8 - 128	1.7E-34	
Glyma.15G070300.1.p	GmNAC113	354	16 - 144	1.4E-50	
Glyma.15G078300.1.p	GmNAC114	322	61 - 203	7.9E-31	
Glyma.15G254000.1.p	GmNAC115	303	11 - 134	2.4E-49	
Glyma.15G257700.1.p	GmNAC116	318	27 - 155	4.9E-47	
Glyma.15G264100.1.p	GmNAC117	347	6 - 133	1.6E-54	
Glyma.15G266500.1.p	GmNAC118	326	10 - 139	1.1E-51	
not found - GmNAC119					
Glyma.16G016400.1.p	GmNAC177	267	11 - 140	1.0E-44	
Glyma.16G016600.1.p	GmNAC120	431	5 - 135	7.6E-40	
Glyma.16G016700.1.p	GmNAC121	400	6 - 138	1.1E-36	
Glyma.16G019400.1.p	GmNAC122	443	15 - 143	5.5E-50	
Glyma.16G042900.1.p	GmNAC123	407	16 - 143	2.8E-54	
Glyma.16G043200.1.p	GmNAC124	353	8 - 138	2.7E-51	
Glyma.16G051800.1.p	GmNAC125	216	14 - 140	5.3E-26	
Glyma.16G069300.1.p	GmNAC178	399	56 - 198	4.8E-27	
Glyma.16G130200.1.p	GmNAC126	362	7 - 135	2.7E-53	
Glyma.16G151500.1.p	GmNAC127	363	9 - 139	1.6E-50	
Glyma.16G152100.1.p	GmNAC128	410	23 - 149	7.1E-54	
Glyma.16G217400.1.p	GmNAC129	264	33 - 160	1.8E-52	
Glyma.17G002800.1.p	GmNAC130	403	47 - 172	2.2E-47	
Glyma.17G101500.1.p	GmNAC131	350	16 - 142	3.3E-53	
Glyma.17G138100.1.p	GmNAC132	366	7 - 136	3.4E-53	
Glyma.17G154100.1.p	GmNAC133	342	6 - 135	3.8E-50	
Glyma.17G185000.1.p	GmNAC134	217	15 - 132	2.0E-31	
Glyma.17G240700.1.p	GmNAC135	285	9 - 143	2.6E-25	
Glyma.18G043900.1.p	GmNAC136	678	8 - 135	1.1E-53	580 - 599
Glyma.18G110700.1.p	GmNAC137	304	19 - 146	6.9E-48	
Glyma.18G119300.1.p	GmNAC138	401	15 - 142	4.2E-50	
Glyma.18G261300.1.p	GmNAC139	388	43 - 169	5.3E-51	
Glyma.18G301500.1.p	GmNAC179	229	14 - 138	1.3E-49	
Glyma.19G002900.1.p	GmNAC180	389	56 - 197	1.9E-28	
Glyma.19G021900.1.p	GmNAC140	367	14 - 139	1.5E-51	
Glyma.19G024500.1.p	GmNAC141	362	21 - 147	3.0E-53	

Glyma.19G056400.1.p	GmNAC142	398	56 - 198	1.5E-27	
Glyma.19G097700.1.p	GmNAC143	215	14 - 140	6.8E-25	
Glyma.19G108800.1.p	GmNAC181	336	8 - 138	5.8E-51	
Glyma.19G109100.1.p	GmNAC144	405	16 - 143	2.8E-55	
Glyma.19G165600.1.p	GmNAC182	294	10 - 138	4.1E-48	
Glyma.19G180300.1.p	GmNAC145	337	13 - 140	1.4E-49	
Glyma.19G195800.1.p	GmNAC183	254	4 - 134	7.5E-43	
Glyma.19G259500.1.p	GmNAC146	265	16 - 144	7.8E-48	
Glyma.19G259700.1.p	GmNAC147	265	16 - 144	4.8E-48	
Glyma.20G033300.1.p	GmNAC148	280	10 - 135	1.4E-52	
Glyma.20G172100.1.p	GmNAC149	549	20 - 143	2.8E-51	518 - 540
Glyma.20G175500.1.p	GmNAC184	341	19 - 147	1.6E-51	
Glyma.20G185800.1.p	GmNAC150	442	76 - 215	1.2E-29	
Glyma.20G192300.1.p	GmNAC151	604	5 - 131	1.2E-48	579 - 601
Glyma.20G192500.1.p	GmNAC152	465	34 - 161	8.5E-51	

Table S2. PCR-primers used for cloning the NAC genes

Primers	Sequence(5' - 3')	Gene identity
GlymaNAC85 fwd	AAAAAGCAGGCTTCACAATGG GAAGTTCAGAGAGAGA	Glyma.12G149100
GlymaNAC85 rvs	AGAAAGCTGGGTCTCAGTCCC CTAAACCCGAACTC	Glyma.12G149100
GlymaNAC65 fwd	AAAAAGCAGGCTTCACAATGG AGAAGGTGAAATTTTGTG	Glyma.08G360200
GlymaNAC65 rvs	AGAAAGCTGGGTCTTCTAATA GTATAAGGGAAGG	Glyma.08G360200
NAC177fwd	AAAAGCAGGCTTCACAATGGA GAACATAATTTCCATATGT GGATC	Glyma.16G016400
NAC177rvs	AGAAAGCTGGGTCGGGTATGA ACTCATCTTCGTCATCCGT AACT	Glyma.16G016400
attB1	GGGGACAAGTTTG TACAAAAAAGCAGGCT	-
attB2	GGGGACCACTTTGTA CAAGAAAGCTGGGT	-

Table S3. Recombinant plasmids.

Clone Name	Description*
pUFV2589	GmNAC065 ORFwas isolated from 48h-tunicamycin-stressed leaf cDNA and cloned into pDONR201.
pUFV2770	GmNAC065 was transferred from pUFV2589 to pDEST32 through LR clonase recombination.In the resulting clone,GmNAC065 was fused to the GAL4 binding domain (BD NAC065).
pUFV2780	GmNAC065 was transferred from UFV2589 to pDEST22 through recombination.In the resulting clone GmNAC065 was fused to the GAL4 activating domain (AD-NAC0065)
pUFV2826	GmNAC177ORF was isolated from a pool of cDNA from tunicamycin-, PEG- and salicylic acid-stressed leaves and cloned into pDONR201.
pUFV2827	GmNAC085 ORF was isolated from a pool of cDNA from tunicamycin-, PEG- and salicylic acid-stressed leaves and cloned into pDONR207.
pUFV2828	GmNAC177was transferred from pUFV2826 to pDEST32 by recombination (BD-NAC117)
pUFV2829	GmNAC085 was transferred from pUFV2827to pDEST32 through LR clonase recombination reaction using the clone 2827 (BD-NAC85).
pUFV2830	GmNAC177was transferredfrom pUFV2826to pEARLEY103 through LR clonaserecombination. The resulting clone expressesNAC177-GFP fusion, under the control of 35S promoter.
pUFV3007	GmNAC065 was transferred from pUFV3013 topEARLEY103 through recombination. The resulting clone expresses NAC065-GFP protein fusion, under the control of 35S promoter.
pUFV3008	GmNAC085 was transferred from pUFV2827 topERALEY104 by recombination. The resulting clone expresses YFP-NAC85 protein fusion, under the control of the 35S promoter.
pUFV3009	GmNAC085 ORF wasamplified from pUFV2827andcloned into pDONR201 byrecombination.
pUFV3010	GmNAC085 ORF was transferred from pUFV3009 topDEST22 by recombination, generating AD-NAC085 fusion.
pUFV3011	GmNAC177ORF was amplifiedfrom pUFV2826 and cloned into pDONR 207 by recombination.
pUFV3012	GmNAC177ORF was transferred from pUFV2826 topDEST22 through recombination, generating AD-NAC117 fusion.
pUFV3013	GmNAC065 ORF was amplified from pUFV2589and cloned into pDONR 207 byrecombination.

*All recombinant plasmids were obtained through the GATEWAY system.

TabeS4. Primers for qRT-PCR.

Primer	Sequence (5’ - 3’)	Gene Identity
CNXfwd	TGATGGGGAGGAGAAGAAAAAGGC	Glyma.05G199200
CNXrvs	CGGTGTAGACATGGGAAAGC	Glyma.05G199200
PDIfwd	TTGGTTGAAGGCGGTACAAGGATGG	Glyma.10G217600
PDIrvs	ACTCCAGCAGAACTATCTTCCCAG	Glyma.10G217600
PR-4fwd	TGCGGGTGACAAATACAGGA	Glyma.19G245400
PR-4rvs	TGCTGCACTGATCTACGATTCTC	Glyma.19G245400
qRTNAC177fwd	AAATCCGGCAAGAGCAGAAG	Glyma.16G016400
qRTNAC177rvs	CCACTGCCCGAAGATTTCA	Glyma.16G016400
qRTNAC154fwd	GTAGCTCAGGCTCCAACATCC	Glyma.02G284300
qRTNAC154rvs	ACCACAGACGTGAGATCATCC	Glyma.02G284300
qRTNAC157fwd	GGACATTCAGATGCTTCTTCGTC	Glyma.04G014900
qRTNAC157rvs	AAAGATGAGGGTGAG AGAGGC	Glyma.04G014900
qRTNAC163fwd	GGTCAAAGTGTGCATGTTGAGG	Glyma.06G288500
qRTNAC163rvs	TTGAGCATTTTGCCCTCCTT	Glyma.06G288500
qRTNAC165fwd	TCC CTG CTA AGC CAG TTT CC	Glyma.07G192900
qRTNAC165rvs	ATG AAA TTG TTG CCT CGG CG	Glyma.07G192900
qRTNAC169fwd	CTGGATGCCAACGAGAATC	Glyma.10G197600
qRTNAC169rvs	TATCCCCATTCCCATTGCA	Glyma.10G197600
qRTNAC174fwd	GGGAGAGGACCGAATGGATTA	Glyma.12G186900
qRTNAC174rvs	CTTGAGGCGACAAATGACCAA	Glyma.12G186900
qRTNAC183fwd	AGC AGA GAG CTC TTC CTC CG	Glyma.19G195800
qRTNAC183rvs	CCA AGA ACA TAT CCA CTT TCT CC	Glyma.19G195800
qRTNAC65fwd	TGGGATTTGCCAGGTGATTT	Glyma.08G360200
qRTNAC65rvs	GAGCGATTTCCGTTGGGATA	Glyma.08G360200
qRTNAC85fwd	CAGCAGCAGGACGAGAAATTC	Glyma.12G149100
qRTNAC85rvs	TCAAGATCCGTCGGGTTGAC	Glyma.12G149100
SMPfwd	GCCGAACTGAGGAAAAGACGAACC	Glyma.20G147500
SMPrvs	CTTGGGCTGTTTGTTGGTCTTC	Glyma.20G147500
UNK-2fwd	GCCTCTGGATACCTGCTCAAG	Glyma.06G041800
UNK-2rvs	ACCTCCTCCTCAAACTCCTCTG	Glyma.06G041800

* The primers were designed by PrimerExpress 3.0 software to minimize performance-penalties

Supp. Table 5. Expression profile of new putative GmNAC genes in soybean tissue

GmNAC154				
Tissue	Ct	dCT	FC	SD
Leaves	17.714	8.184	0.003	0.0707
Root	17.501	7.412	0.006	0.6341
Stem	18.365	7.518	0.005	0.2712
Flower	18.022	4.433	0.046	0.3548
Pods	18.573	3.768	0.073	0.4587

GmNAC174				
Tissue	Ct	dCT	FC	SD
Leaves	18.393	0.679	0.625	0.355
Root	19.247	1.746	0.298	0.140
Stem	18.140	-0.225	1.169	0.005
Flower	17.073	-0.950	1.931	0.608
Pods	17.117	-1.457	2.745	0.217

GmNAC157				
Tissue	Ct	dCT	FC	SD
Leaves	25.593	7.879	0.004	0.2560
Root	26.787	9.286	0.002	0.1343
Stem	23.982	5.617	0.020	0.4393
Flower	21.452	3.430	0.093	0.2211
Pods	22.855	4.281	0.051	0.1103

GmNAC177				
Tissue	Ct	dCT	FC	SD
Leaves	19.541	1.827	0.282	0.283
Root	18.289	0.788	0.579	0.049
Stem	19.061	0.696	0.617	0.138
Flower	18.171	0.149	0.902	0.062
Pods	18.637	0.064	0.957	0.213

GmNAC163				
Tissue	Ct	dCT	FC	SD
Leaves	18.907	1.194	0.437	0.063
Root	19.913	2.412	0.188	0.463
Stem	17.769	-0.596	1.511	0.244
Flower	27.535	9.513	0.001	0.296
Pods	17.924	-0.650	1.569	0.512

GmNAC183				
Tissue	Ct	dCT	FC	SD
Leaves	19.807	2.093	0.23433	0.273
Root	18.205	0.704	0.61393	0.001
Stem	30.612	12.246	0.00021	0.757
Flower	19.261	1.239	0.42380	0.099
Pods	24.237	5.663	0.01973	0.554

GmNAC165				
Tissue	Ct	dCT	FC	SD
Leaves	35.395	17.681	0.000005	0.226
Root	25.425	7.924	0.004117	0.450
Stem	25.573	7.208	0.006762	0.417
Flower	17.317	-0.705	1.629800	0.014
Pods	27.460	8.886	0.002113	0.761

GmNAC065				
Tissue	Ct	dCT	FC	SD
Leaves	15.153	-2.561	5.901	0.073
Root	15.207	-2.294	4.905	0.057
Stem	19.152	0.787	0.580	0.036
Flower	15.426	-2.596	6.045	0.213
Pods	16.143	-2.430	5.390	0.029

GmNAC169				
Tissue	Ct	dCT	FC	SD
Leaves	16.041	-1.673	3.189	0.170
Root	17.167	-0.335	1.261	0.555
Stem	15.429	-2.936	7.656	0.244
Flower	18.669	0.647	0.639	0.328
Pods	15.407	-3.167	8.980	0.214

GmNAC085				
Tissue	Ct	dCT	FC	SD
Leaves	16.033	-1.681	3.206	0.007
Root	16.232	-1.269	2.410	0.042
Stem	17.221	-1.144	2.210	0.020
Flower	16.022	-2.000	4.001	0.045
Pods	17.368	-1.206	2.307	0.147

Supp. Table 6. Fold-change and statistical data for the gene expression profile of new putative GmNAC genes

GmNAC154			
	FC	SD	p
PEG 0.5h	2.75585777	0.29483796	0.0005
PEG 2h	3.9186959	1.01545271	0.00761
PEG 12h	1.84042306	0.48093045	0.0388
PEG 24h	0.49704739	0.31225376	0.04953
Tun 0.5h	1.61120042	0.03395775	0.0001
Tun 2h	2.06677789	0.42259311	0.01197
Tun 12h	1.06548869	0.0725278	0.19164
SA 0.5h	1.19453986	0.16774405	0.11459
SA 2h	2.02451156	0.20518823	0.00098
SA 12h	2.44441442	0.17053006	0.00013
GmNAC157			
	FC	SD	p
PEG 0.5h	0.31386797	0.05059124	0.00002
PEG 2h	0.33868946	0.1133695	0.00055
PEG 12h	0.53846045	0.08699785	0.00071
PEG 24h	0.30814861	0.16994683	0.00214
Tun 0.5h	0.3228719	0.08920941	0.0002
Tun 2h	0.24172237	0.17349473	0.00163
Tun 12h	0.27775457	0.05463028	2.1E-05
SA 0.5h	0.67914138	0.60015652	0.40651
SA 2h	0.33553515	0.23957401	0.0086
SA 12h	0.26165632	0.08318414	0.00011
GmNAC163			
	FC	SD	p
PEG 0.5h	3.59247838	0.84892139	0.00612
PEG 2h	3.39198348	1.19420286	0.02561
PEG 12h	6.17679913	1.17753319	0.0016
PEG 24h	5.61255341	2.85369451	0.04882
Tun 0.5h	2.70441695	0.41312572	0.02022
Tun 2h	1.59707283	0.27064804	0.01876
Tun 12h	4.62822263	1.34669073	0.00954
SA 0.5h	1.94339405	0.11886034	0.00016
SA 2h	2.8181112	0.57942372	0.00556
SA 12h	1.93952163	0.43275162	0.01978
GmNAC165			
	FC	SD	p
PEG 0.5h	0.82253296	0.92246987	0.7557
PEG 2h	0.64511603	0.29875495	0.10845
PEG 12h	1.31321304	0.58032274	0.4025
PEG 24h	1.1760225	0.63707899	0.6566

Tun 0.5h	0.82424491	0.0788844	ns
Tun 2h	0.56534179	0.03098952	1.7E-05
Tun 12h	0.34900795	0.304443	0.02083
SA 0.5h	0.98184337	0.69773179	0.96649
SA 2h	1.55830879	0.2908942	0.02923
SA 12h	0.24146507	0.09527294	0.00016
GmNAC169			
	FC	SD	p
PEG 0.5h	1.723732	0.13153822	0.00077
PEG 2h	0.57062926	0.10961346	0.00246
PEG 12h	5.0455612	1.30217674	0.00576
PEG 24h	2.44912449	0.40109053	0.00333
Tun 0.5h	2.61064568	0.25214438	0.00038
Tun 2h	4.19839401	0.42827448	0.00021
Tun 12h	4.39458657	0.40706435	0.00001
SA 0.5h	2.37948891	0.33225377	0.00198
SA 2h	1.60710878	0.35670339	0.04199
SA 12h	1.77769331	0.34506751	0.01751
GmNAC174			
	FC	SD	p
PEG 0.5h	0.08446194	0.0260692	0.00001
PEG 2h	0.04067113	0.01308952	0.00001
PEG 12h	0.04958393	0.02901487	0.00001
PEG 24h	0.13735685	0.07604004	0.00004
Tun 0.5h	4.32787259	0.41995398	0.00016
Tun 2h	3.50822131	0.61239407	0.00209
Tun 12h	5.66649362	1.05294906	0.00155
SA 0.5h	1.03326945	0.26504843	0.83996
SA 2h	0.72475253	0.41221992	0.31207
SA 12h	1.61012315	0.26255856	0.01577
GmNAC183			
	FC	SD	p
PEG 0.5h	1.76324102	0.19535504	0.00241
PEG 2h	4.16261002	1.5581699	0.02455
PEG 12h	3.33565977	1.28247329	0.03436
PEG 24h	0.41400475	0.15426507	0.00277
Tun 0.5h	3.20629889	0.69385716	0.00531
Tun 2h	0.18546875	0.12666475	0.00037
Tun 12h	0.79987073	0.77166089	0.67672
SA 0.5h	1.19958718	0.51120024	0.53605
SA 2h	0.86212925	0.93158036	0.81062
SA 12h	1.09044741	0.45751093	0.74945
GmNAC177			
	FC	SD	p
PEG 0.5h	0.66837162	0.33850599	0.16731
PEG 2h	0.4859039	0.11681559	0.00155

PEG 12h	1.09892572	0.58667725	0.78211
PEG 24h	0.36532387	0.185752	0.00432
Tun 0.5h	9.72359544	1.34722406	0.00036
Tun 2h	7.70951903	1.39685769	0.00114
Tun 12h	4.75357514	0.44086856	0.00012
SA 0.5h	2.36633281	0.53100071	0.0112
SA 2h	1.45398679	0.41118443	0.12659
SA 12h	3.11323939	0.60833858	0.00392
GmNAC065			
	FC	SD	p
PEG 0.5h	6.61169514	3.00778311	0.03193
PEG 2h	3.91517561	0.63497106	0.00135
PEG 12h	2.63562232	0.56781897	0.00755
PEG 24h	3.27658342	0.88891527	0.01139
Tun 0.5h	2.60538816	0.59341903	0.00942
Tun 2h	4.8373158	1.06962576	0.00341
Tun 12h	7.52361198	1.14743088	0.0006
SA 0.5h	3.17766408	1.00311824	0.01976
SA 2h	2.20857013	0.71482015	0.04288
SA 12h	1.37517204	0.38126277	0.16327
GmNAC085			
	FC	SD	p
PEG 0.5h	0.67894821	0.42426443	0.26046
PEG 2h	23.3176155	1.62956017	1.9E-05
PEG 12h	4.84097978	0.65621041	0.00053
PEG 24h	0.73947191	0.59096136	0.48537
Tun 0.5h	0.98678272	0.34902422	0.95039
Tun 2h	0.13894054	0.01428081	0.00001
Tun 12h	0.2063542	0.10706035	0.00021
SA 0.5h	0.31813608	0.15541389	0.00161
SA 2h	0.5863298	0.56428874	0.27285
SA 12h	0.27478064	0.12668218	0.00058

Table S7 - Differential expression of NAC genes in BR16_80d (R7)-BR16_20d(V3)

UP regulated				
ID	**Name**	**log2FoldChange**	**Ajusted p-value**	**Family**
Glyma.01G051300	GmNAC003	1.382654532	7.35E-05	SNAC-B (NAP)
Glyma.01G088200	GmNAC004	1.131662346	2.46E-09	ANAC063
Glyma.02G070000	GmNAC006	3.115867323	7.32E-11	SNAC-B (NAP)
Glyma.02G100200	GmNAC008	1.032141513	4.98E-10	ANAC063
Glyma.02G109800	GmNAC010	1.466347399	0.000166553	SNAC-B (NAP)
Glyma.02G284300	GmNAC154	2.440101106	2.42E-08	ONAC022
Glyma.03G197900	GmNAC014	3.37983317	1.20E-06	TERN
Glyma.04G208300	GmNAC018	1.937361453	7.01E-06	SNAC-A(ATAF)
Glyma.04G226700	GmNAC021	1.130027064	3.70E-08	TIP
Glyma.05G002700	GmNAC025	1.320824163	0.038556283	ANAC063
Glyma.05G195000	GmNAC030	4.439857474	1.65E-17	SNAC-A(ATAF)
Glyma.05G225100	GmNAC032	1.285811241	0.001074849	ANAC001
Glyma.06G138100	GmNAC036	1.739162278	1.50E-19	TIP
Glyma.06G157400	GmNAC039	3.764708169	3.04E-20	SNAC-A(ATAF)
Glyma.06G248900	GmNAC043	1.057209749	0.036167212	SNAC-A(ATAF)
Glyma.07G048000	GmNAC046	0.771593813	0.006310306	Unnamed
Glyma.07G201800	GmNAC051	0.84552683	0.000177465	ANAC001
Glyma.07G229100	GmNAC052	1.143614091	0.000317698	SNAC-B (NAP)
Glyma.07G271100	GmNAC053	0.76558352	0.000717815	TERN
Glyma.08G075300	GmNAC057	2.996023861	0.000141835	Unnamed
Glyma.08G156500	GmNAC058	0.659125714	0.000211128	NAM
Glyma.08G169400	GmNAC060	2.954399718	3.06E-05	ONAC022
Glyma.08G173400	GmNAC061	2.32670595	3.54E-12	NAM
Glyma.08G307100	GmNAC064	2.254137943	1.96E-09	ONAC022
Glyma.08G360200	GmNAC065	0.487237671	0.010019431	Senu5
Glyma.10G204700	GmNAC170	1.89552705	1.21E-05	ANAC063
Glyma.10G219600	GmNAC074	1.625654721	2.53E-14	NAM
Glyma.11G030600	GmNAC075	1.826176994	0.006194579	VND-NAC
Glyma.11G096600	GmNAC077	2.141891325	1.90E-05	TERN
Glyma.11G182000	GmNAC078	2.919917495	8.28E-07	TERN
Glyma.12G022700	GmNAC081	2.605231816	8.59E-08	TERN
Glyma.12G091200	GmNAC082	4.376078482	1.32E-12	TERN
Glyma.12G186200	GmNAC088	3.622193859	7.29E-05	TERN
Glyma.12G221400	GmNAC091	2.915120253	1.32E-17	SNAC-B (NAP)
Glyma.13G243200	GmNAC099	2.016972868	4.70E-05	SNAC-B (NAP)
Glyma.13G280000	GmNAC102	0.836793624	0.003494575	SNAC-B (NAP)
Glyma.13G315300	GmNAC104	1.529953989	0.000542514	TERN
Glyma.14G030700	GmNAC106	3.30122907	1.57E-09	ONAC022

Glyma.14G189300	GmNAC110	0.83100608	0.006200161	TIP
Glyma.15G070300	GmNAC113	4.861618506	3.43E-24	SNAC-B (NAP)
Glyma.15G257700	GmNAC116	1.712650457	0.005801893	ONAC022
Glyma.16G042900	GmNAC123	2.352025351	1.01E-07	NAM
Glyma.16G043200	GmNAC124	3.623008315	2.74E-35	SNAC-B (NAP)
Glyma.16G051800	GmNAC125	1.279558786	0.000174639	NAM
Glyma.16G151500	GmNAC127	2.75917519	1.76E-08	SNAC-B (NAP)
Glyma.17G185000	GmNAC134	1.888228263	1.31E-06	ONAC022
Glyma.17G240700	GmNAC135	0.588614106	0.000876776	Unnamed
Glyma.18G110700	GmNAC137	2.78271019	2.07E-08	ONAC022
Glyma.18G301500	GmNAC179	2.340873355	2.96E-31	Senu5
Glyma.19G108800	GmNAC181	2.743077701	7.00E-22	SNAC-B (NAP)
Glyma.19G109100	GmNAC144	1.642506844	0.004129614	NAM
Glyma.19G195800	GmNAC183	3.837697505	3.05E-06	NAM
Glyma.20G033300	GmNAC148	5.396838452	1.03E-13	SNAC-B (NAP)
Glyma.20G172100	GmNAC149	1.603646859	5.39E-15	NAM
DOWN regulated				
ID	**Name**	**log2FoldChange**	**Ajusted p-value**	**Family**
Glyma.01G005500	GmNAC001	-1.267279604	0.003496759	ANAC001
Glyma.01G167900	GmNAC005	-3.150570901	5.14E-07	VND-NAC
Glyma.04G078600	GmNAC015	-2.900324157	5.10E-06	NAM
Glyma.04G167200	GmNAC017	-1.778480522	0.008732018	NAM
Glyma.04G249000	GmNAC022	-1.643178902	2.43E-22	SNAC-A(ATAF)
Glyma.06G114000	GmNAC035	-1.049770773	0.000454655	SNAC-A(ATAF)
Glyma.06G154400	GmNAC038	-7.318745496	2.97E-20	Unnamed
Glyma.06G195500	GmNAC041	-2.049857512	0.001892939	NAM
Glyma.06G288500	GmNAC163	-5.568561397	2.39E-12	ANAC001
Glyma.07G050600	GmNAC048	-6.705809453	8.86E-19	VND-NAC
Glyma.10G197600	GmNAC169	-0.514370431	4.57E-05	NAM
Glyma.11G075400	GmNAC076	-0.912646368	0.007717037	VND-NAC
Glyma.12G118700	GmNAC083	-5.462431519	5.45E-12	ANAC001
Glyma.12G149100	GmNAC085	-2.634062537	5.42E-05	SNAC-A(ATAF)
Glyma.12G206900	GmNAC090	-4.872392154	7.79E-10	ANAC001
Glyma.12G221500	GmNAC092	-4.302370996	1.15E-10	SNAC-A(ATAF)
Glyma.13G174700	GmNAC097	-1.215909141	0.002021262	ANAC001
Glyma.13G279900	GmNAC101	-2.868510712	4.61E-06	SNAC-A(ATAF)
Glyma.13G294000	GmNAC175	-3.747501546	6.79E-06	ANAC001
Glyma.14G152700	GmNAC109	-1.062885692	2.64E-11	SNAC-A(ATAF)
Glyma.15G078300	GmNAC114	-1.041465625	0.020560516	ANAC001
Glyma.16G019400	GmNAC122	-4.749748216	1.96E-11	VND-NAC
Glyma.19G056400	GmNAC142	-3.310952289	2.30E-41	ANAC063
Glyma.20G192300	GmNAC151	-0.502225949	0.001572343	NAM
Glyma.20G192500	GmNAC152	-0.877968006	6.38E-08	NAM

Table S8 - Number of differentially expressed NAC genes/sub-family in BR16_80d (R7)-BR16_20d(V3)

	Total	UP	Down	
SNAC-A	10	4	6	
SNAC-B	12	12		
TERN	8	8		
ANAC063	5	4	1	
ONAC022	7	7		
TIP	3	3		
ANAC0001	9	2	7	
NAM	14	8	6	
Senu5	2	2		
VND-NAC	5	1	4	
unnamed	4	3	1	
	79	54	25	

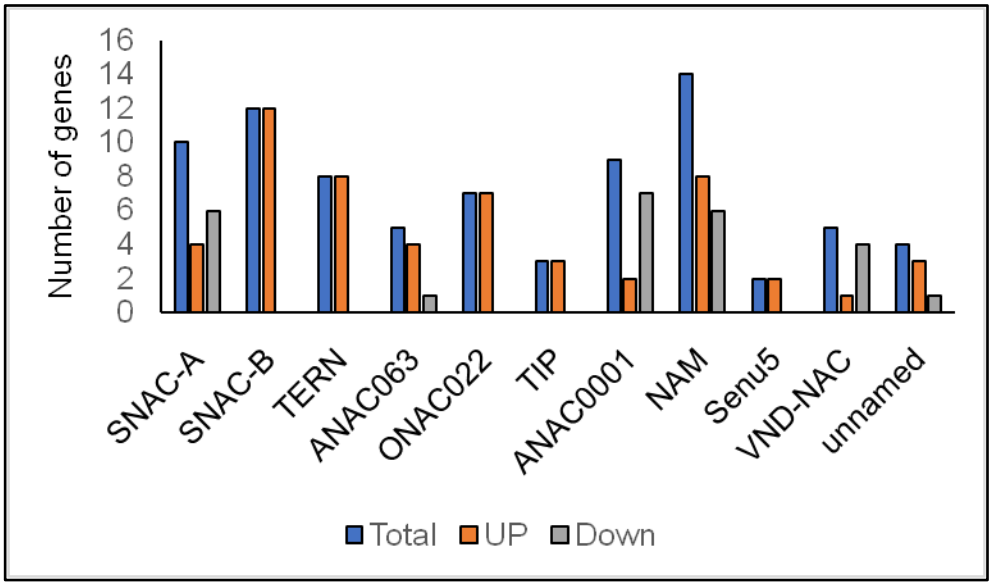

Supp. Table 9. Fold change data for the gene expression profile of new putative GmNAC genes during natural leaf senescence in soybean.

GmNAC065					
	Ct	dCT	ddCT	FC	SD
BR16_20d	20.084	-4.388	-0.804	1.747	0.031
BR16_80d	19.179	-5.365			
GmNAC163					
	Ct	dCT	ddCT	FC	SD
BR16_20d	22.517	-1.976	9.475	0.001	0.000
BR16_80d	31.777	7.499			
GmNAC183					
	Ct	dCT	ddCT	FC	SD
BR16_20d	26.827	2.477	-0.727	1.723	0.677
BR16_80d	26.005	1.750			

GmNAC154					
	Ct	dCT	ddCT	FC	SD
BR16_20d	23.978	-0.733	-1.620	3.085	0.386
BR16_80d	22.673	-2.352			
GmNAC169					
	Ct	dCT	ddCT	FC	SD
BR16_20d	22.272	-2.200	0.820	0.571	0.099
BR16_80d	22.958	-1.320			

Data were obtained from average of 3 biological samples and 3 technical replicates for each treatment.

Supplementary Figures

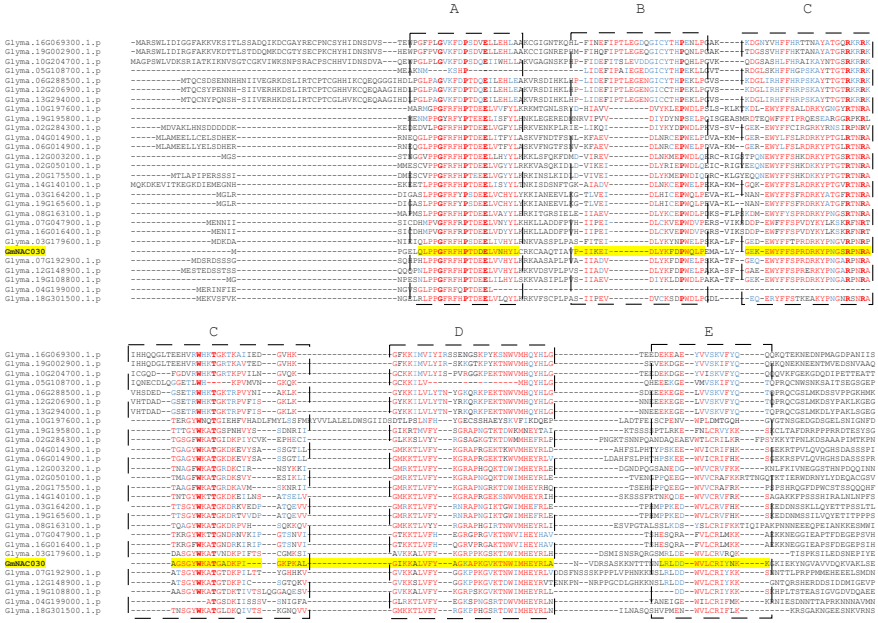

Supplementary Figure 1. Structural organization of the NAC domain of newly identified GmNACs. The multiple sequence alignment of the N-terminal of 27 new GmNACs shows the NAC domain, which is sub-divided into the five motifs (A to E) delimited by the dashboards. The most frequent amino acids are shown in red and the second most frequents in blue. Conserved amino acids are shown in bold. GmNAC030 (yellow) was used as a guide for the multiple sequence alignment.

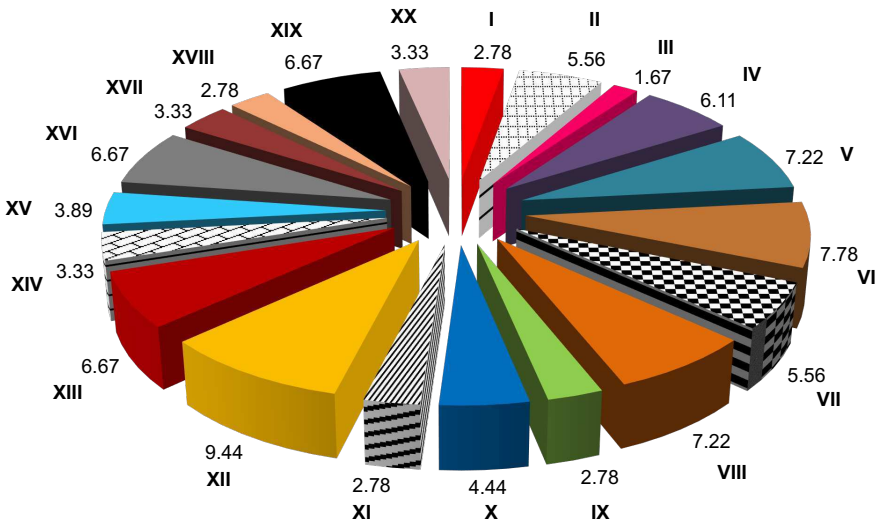

Supplementary Figure 2. Percentage of NAC genes located in each soybean chromosome. The sectorial graphic presents the proportion (%) of the distribution of NAC genes in all 20 soybean chromosomes.

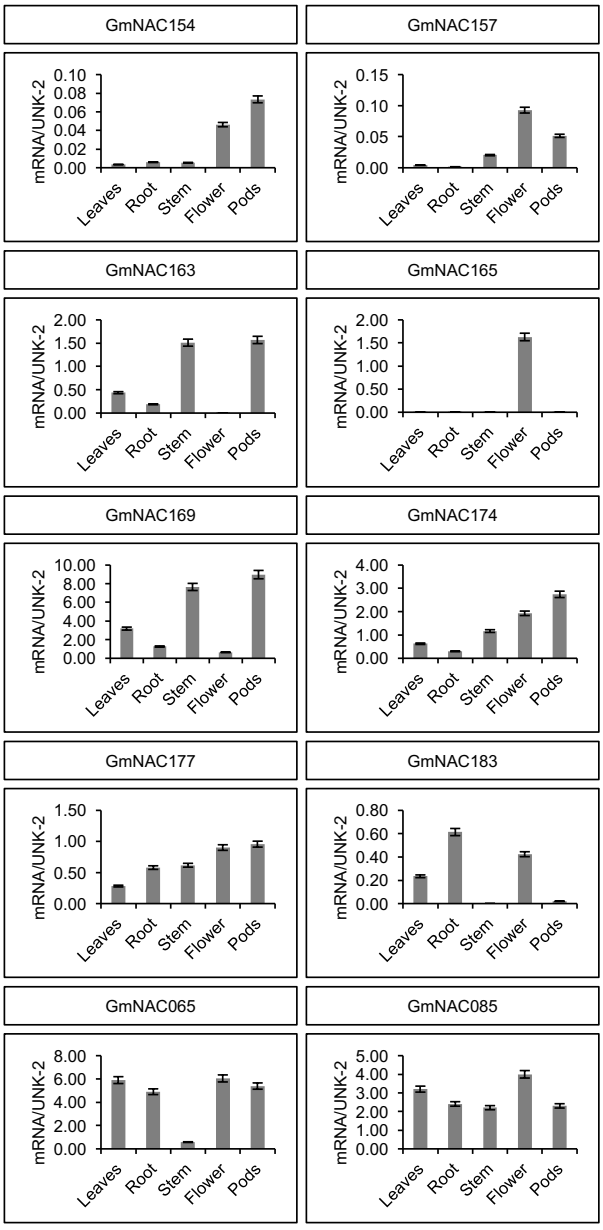

Supplementary Figure 3. The organ-specific profile of for a representative sample of the new NAC genes, GmNAC065 and GmNAC085. At the R2/R3 developmental stage, 200 mg of fresh tissue from different soybean vegetative organs/tissues, including leaf disks (1 cm diameter), pivotal and lateral roots, stem's segments (1 cm), entire flowers and pods segments were collected and frozen in liquid nitrogen. Total RNA was isolated from the indicated organs, and the transcript accumulation of the indicated genes was measured by qRT-PCR. U*KN-2* was chosen as the normalizer, endogenous control gene. Gene expression was quantified using the e $2^{-\Delta Ct}$ method. Data were obtained from the average of 3 biological samples (pools of 5 plants) and 2 technical replicates for each treatment. The bars indicate standard error.

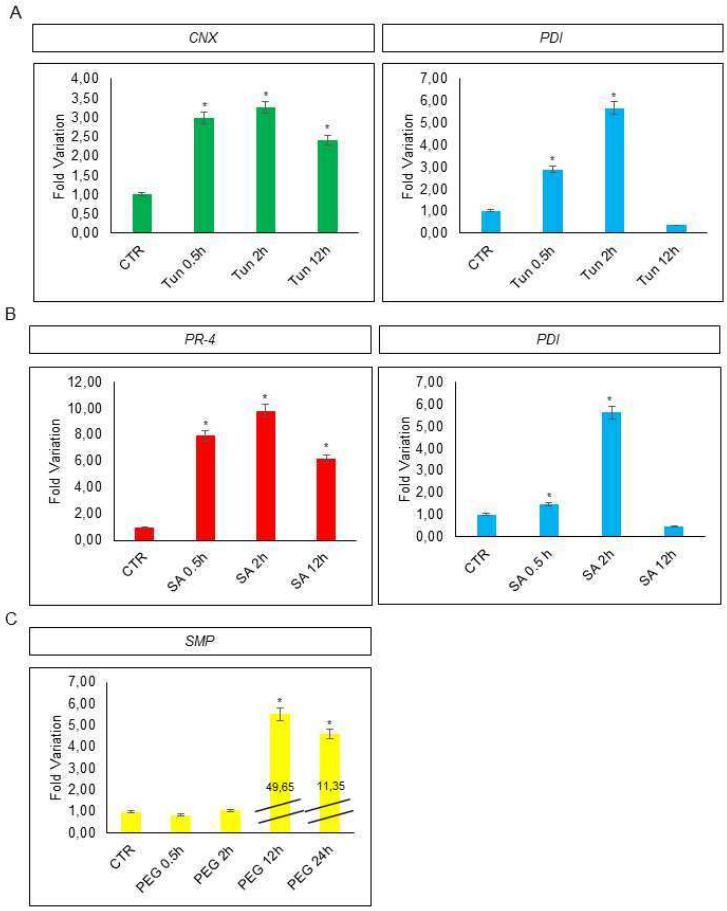

Supplementary Figure 4. Expression of stress-associated marker genes in soybean seedlings. (A) Calnexin (*CNX*) and Protein–dissulfide isomerase (*PDI)* gene expression during tunicamicyn treatment. **(B)** Pathogenesis-related gene 4 (*PR-4*) and *PDI* gene expression during SA treatment. **(C)** Seed maturation protein (*SMP*) expression during PEG treatment. Dimethyl sulfoxide (DMSO) was used as a control for tunicamycin treatment. Leaf disks from stressed and control leaves were collected at 0.5, 2 and 12 h post-treatment (for PEG treatment, 24-h harvest time was included). *UKN-2* was chosen as the normalizer, endogenous control gene. Relative gene expression was quantified using the comparative $2^{-\Delta\Delta Ct}$ method. The bars indicate standard-error and the asterisks indicate statistical significance by the t-test, ($P < 0.05$, $n = 3$).

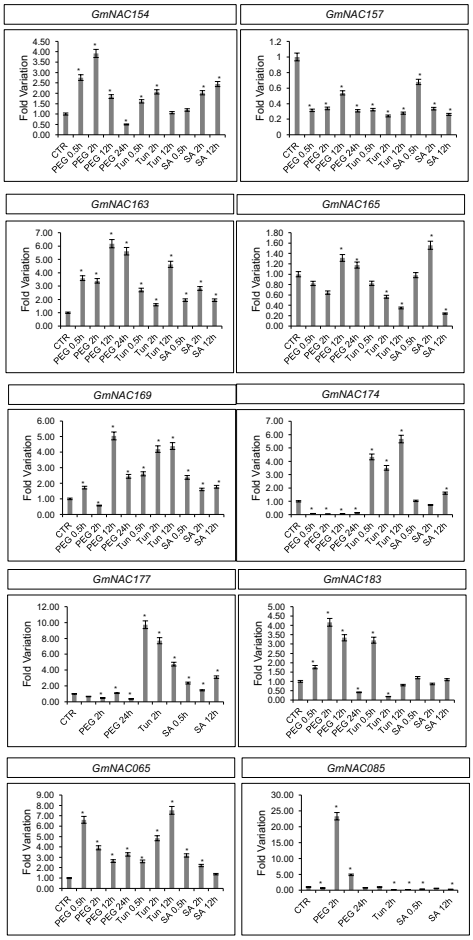

Supplementary Figure 5. The stress-induced expression profile for a representative sample of the new NAC genes, *GmNAC065 and GmNAC085*. Expression profile of 8 new putative NAC genes: GmNAC154 (ONAC022), GmNAC157 (NAM), GmNAC163 (ANAC001), GmNAC165 (SNAC-B - NAP), GmNAC169 (NAM), GmNAC174 (OsNAC8), GmNAC177 (unnamed), GmNAC 183 (TERN), GmNAC065 (Senu5) and GmNAC085 (SNAC-A – ATAF) during multiple stress. At the V2/V3 developmental stage, the roots were immersed in Hoagland Hydroponic solution supplemented with 10% (w/v) PEG (MW 8,000), 5 µg/mL tunicamycin or 5 mM salicylic acid (SA) to induce osmotic, endoplasmic reticulum and biotic stress conditions, respectively. Dimethyl sulfoxide (DMSO) was used as a control for tunicamycin treatment. Leaf disks from stressed and control leaves were collected at 0.5, 2 and 12 h post-treatment (for PEG treatment, 24-h harvest time was included). *UKN-2* was chosen as the normalizer, endogenous control gene. Relative gene expression was quantified using the comparative $2^{-\Delta\Delta Ct}$ method. The bars indicate standard-error and the asterisks indicate statistical significance by the t-test, ($P < 0.05$, $n = 3$).

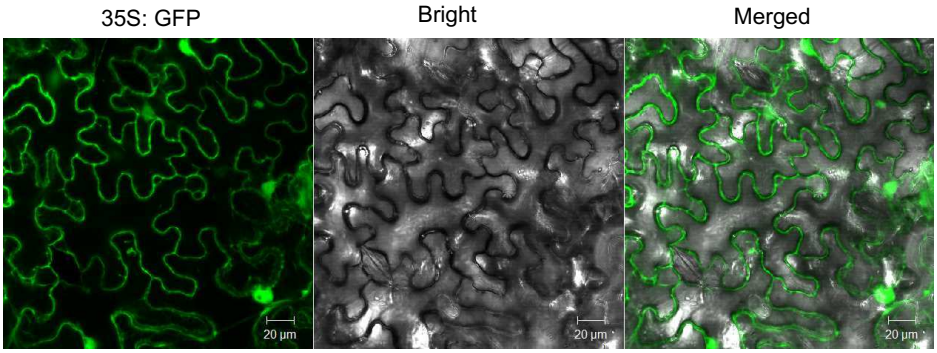

Supplementary Figure 6. Confocal fluorescence image of transiently expressed GFP in epidermal cells of *N. benthamiana* leaves. The conditions of GFP expression and imaging was as described in Figure 8. Scale bars, 20 mm.

CHAPTER III

CONTRASTING ROLES OF SENESCENCE-ASSOCIATED *GmNAC* GENES IN PLANT DEVELOPMENT, MULTIPLE STRESS AND CELL DEATH RESPONSES

Manuscript draft

Bruno Paes de Melo, Isabela Tristan Lourenço-Tessutti, Otto Teixeira Fraga, Luanna Bezerra Pinheiro, Camila Barrozo de Jesus Lins, Carolina Vianna Morgante, Janice de Almeida-Engler, Pedro Augusto Braga Reis, Maria Fátima Grossi-de-Sá and Elizabeth Pacheco Batista Fontes

Pages 79 to 169

RESUMO

Os fatores de transcrição NAC compreendem uma superfamília de proteínas envolvida no controle do desenvolvimento de plantas, respostas ao estresse e senescência. Como genes associados à senescência (SAGs), os NACs integram as vias elicitadas por idade e vias de resposta a estresses múltiplos que convergem para a morte celular programada (PCD) em plantas. Em Arabidopsis, NAC-SAGs pertencem a redes regulatórias bem caracterizadas, que são, por sua vez, mal compreendidas em soja. Neste trabalho, nós interrogamos o genoma da soja e fornecemos uma análise abrangente de NACs associados à senescência natural e induzida por estresse. Para examinar funcionalmente o GmNAC-SACs, selecionamos GmNAC065 e GmNAC085, ortólogos putativos dos genes de Arabidopsis ANAC083/VNI2 e ANAC072, respectivamente. A análise de expressão de GmNAC065 e GmNAC085 em soja demonstrou que (i) esses GmNAC-SAGs exibem mudanças de expressão contrastantes durante a senescência induzida por idade e estresse; (ii) são co-expressos com conjuntos de genes funcionalmente diferentes envolvidos em respostas ao estresse e progressão de PCD, e (iii) são diferencialmente expressos por indutores de morte celular. Além disso, demonstramos que a expressão ectópica de GmNAC065 retarda a senescência em Arabidopsis, um fenótipo associado ao desempenho oxidativo aprimorado das plantas transgênicas sob diferentes estresses, maior teor de clorofila, carotenóides e açúcares, além de uma extensão menor dos sintomas de PCD induzida por estresse. Em contraste, plantas expressando GmNAC085 sofreram uma aceleração do envelhecimento induzido pelo estresse, associado a uma maior perda de clorofila, aumento do acúmulo de EROS e morte celular, com notória diminuição da expressão e da atividade de enzimas do sistema antioxidante. Finalmente, GmNAC065 e GmNAC085 pertencem a conjuntos gênicos funcionalmente diferentes e regulam diferencialmente genes associados à progressão da morte celular induzida por estresse, indicando ainda que, como reguladores desse processo, funcionam inversamente em PCD de desenvolvimento e ambiental.

Abstract

NAC (*NAM, ATAF,* and *CUC*) transcription factors comprise a protein superfamily involved in the control of plant morph-physiology, stress responses, and senescence. As SAGs (senescence-associated genes), NAC genes integrate age- and stress-dependent pathways that converge to programmed cell death. In Arabidopsis, NAC-SAGs have been extensively studied and belong to well-characterized regulatory networks, but the soybean NAC-SAGs are relatively poorly understood. We have previously demonstrated that *Glycine max (Gm)NAC065* and *GmNAC085*, putative orthologous of the two SAGs *ANAC083/VNI2* and *ANAC072* from Arabidopsis, display contrasting expression profiles under multiple stresses and differentially promote classic symptoms of senescence when ectopically expressed in *N. benthamiana*. Here, we interrogated the soybean genome for developmental and environmental senescence-derived SAGs belonging to the NAC superfamily. This work identified the putative NAC-SAGs in soybean and provided a comprehensive analysis of *GmNAC065* and *GmNAC085* functions in multiple stress responses and senescence in soybean and Arabidopsis transgenic lines. We demonstrated that these soybean NAC-SAGs are multiple stress-responsive genes that display extensive-expression changes during age-induced senescence. Furthermore, they showed different expression levels in bleomycin-treated soybean seedlings and were co-expressed with different sets of genes involved in stress responses and PCD progression. Finally, we demonstrated that GmNAC065 ectopically expressed in Arabidopsis leads to a delayed senescence phenotype, with enhanced oxidative performance under multiple stresses, higher chlorophyll, carotenoids and soluble sugars content, and lower extension of stress-induced PCD compared to wild-type. Not surprisingly, the *GmNAC085*-expressing lines displayed an opposite phenotype leading to the up-regulation of several downstream SAG genes in Arabidopsis.

Keywords

Soybean NAC genes, SAGs, soybean stress-responsive genes, drought, biotic stress, ER stress, cell death, senescence, *GmNAC065*, *GmNAC085*

Introduction

Senescence is a naturally- and genetically-programmed biological process characterized by cell-, tissue- and organ-disassembly and degeneration, culminating in death (Kim *et al*., 2016;Luoni*et al*., 2019). At the cellular level, senescence is synonymous with Programmed Cell Death (PCD), and all signaling and biochemical events are related to the control of cell suicide, which starts at one single-cell or a discrete group of cells into specific tissue. PCD is a part of the typical developmental program of all organisms. In advanced stages of development or under stressful conditions, plant cells trigger an extensive genome reprogramming in order to initiate PCD (Buchanan-Wollaston *et al*., 2003; Lim *et al*., 2007; Olvera-Carrillo *et al*., 2015; Kim *et al*., 2016; Woo, *et al*., 2019). Recently, different sets of genes have been associated with age-triggered PCD, called developmental PCD (dPCD) and environmental-triggered PCD (ePCD), despite their common biochemical-bases and phenotypes (Lam *et al*., 2004; Olvera-Carrillo *et al*., 2015).

In plants, senescence is well understood in leaves, which display notorious phenotypes' changes with a consequent reduction in functionality until the abscission (Woo *et al*., 2019; Luoni *et al*., 2019). During the leaf lifecycle, the leaves can accumulate nutrients throughout carbon fixation by robustness and efficiency of the photosynthetic apparatus, the leading site of energy harvesting and storage (Woo *et al*., 2019; Kim *et al*., 2016). In the senescence onset, leaves promote a dramatic metabolism reduction process and nutrient mobilization to other organs, such as seeds or tubers, as part of reproductive and survival investment (Kim *et al*., 2016). The chloroplast is the first cell-component to suffer disassembly, causing leaf yellowing. Changes in leaves color and morpho-physiology occur mainly by water loss and subsequent degradation of chlorophyll and other pigments, besides stomatal- and other cell-proteins, making senescing leaves possible sources of nitrogen for nutrient redistribution (Park *et al*., 2007; Martinéz *et al*., 2008; Thomas *et al*., 2009; Carrión *et al*., 2013; Luoni *et al*., 2019).

Other catabolic pathways are also activated during senescence. Typical symptoms as lipid peroxidation, high accumulation of reactive oxygen species (ROS), and high mobilization of soluble sugars are detected in stress- and age-induced senescence (Thompson and Lake, 1987; Leshem, 1988; Petrov *et al*., 2015). These events are precisely controlled by phytohormones, which integrate endogenous and exogenous

signals throughout the activity of several senescence-promoting genes that control the onset, progression, and final of PCD (Oh *et al*., 1997; Woo *et al*., 2001; Lim *et al*., 2007; Woo *et al*., 2013; Kim *et al*., 2016; Luoni *et al*., 2019).

Several plant hormones related to stress responses also act as senescence promoting messengers, depending on synergistic factors contributing to plant adaption or ePCD. If the severity of the stress overcomes the efficiency of stress-avoiding mechanisms, these signals, collectively, trigger premature senescence. Phytohormones such as ethylene, abscisic acid (ABA), jasmonates (JA), auxins, and salicylic acid (SA) regulate normal morpho-physiology, but also promote senescence. They control the expression of senescence-associated genes (SAGs) as a part of a multilayered regulatory genetic-programming, integrated by signaling transducers, chromatin-modifiers and, mainly, stress-responsive transcription factors (TFs - Buchanan-Wollatson *et al*., 2003, 2005; Woo *et al*., 2013; Podzimska-Sroka *et al*., 2015; Kim *et al*., 2016; Luoni *et al*., 2019).

The hormones signal transduction results in a global gene expression remodeling. Genome-wide analysis reveals that the expression pattern of several TFs is modified along with plant development and under stress. These changes are compatible with the changes in expression of SAGs, suggesting some functional overlapping in dPCD and ePCD (Buchanan-Wollaston *et al*., 2003; Guo *et al*., 2004; Balazadeh *et al*., 2010; Breeze *et al*., 2011; Hickman *et al*., 2013; Pruneda-Paz *et al*., 2014; Kim *et al*., 2016). The crosstalk among phytohormones, TFs, and other combinatorial factors imposes complexity in understanding stresses-related pathways and molecular mechanisms governing plant senescence (Kim *et al*., 2016; Luoni *et al*., 2019).

NAC and WRKY constitute the most expressive families of TFs in senescence, with several members reported as SAGs (Woo *et al*., 2013; Kim *et al*., 2016; Luoni *et al*., 2019). In *Arabidopsis thaliana*, more than 30 NAC genes display enhanced expression during dPCP (Breeze *et al*., 2011), and many of them are significantly up-regulated by at least one type of abiotic stress (Buchanan-Wollaston *et al*., 2005; Breeze *et al*., 2011; Puranik *et al*., 2012 and Nakashima *et al*., 2012). These analyses indicate that NACs can be critical regulatory TFs, which integrate developmental signals, stress responses, and PCD (Kim *et al*., 2016).

Regulatory networks involving NAC TFs have established connections between stress responses and senescence in Arabidopsis. ANAC092/ORE1 is an example of environmental- and developmental-signals crosstalk. ANAC092/ORE1 is activated by ATAF1, which is responsive to ABA and H_2O_2 accumulation, produced at late developmental stages and environmental stress. This regulatory circuit is implicated in chloroplast collapse and leaf senescence (Rauf *et al*., 2013)..*ANAC019*,*ANAC055*, and *ANAC072* have also been reported as positive regulators of senescence in Arabidopsis. These genes display high sequence similarity, even in their promoter regions, reinforcing their overlapped function in senescence and stress-responses (Hickman *et al*., 2013; Lindemose *et al*., 2014). ANAC072 activates the transcription of CV (CHLOROPLAST VESICULATION), a protein involved in chloroplast-protein degradation. It also controls the expression of the sugar transporter SWEET 15, activated during nutrient redistribution in senescence (Kamranfar *et al*., 2018). ANAC019 is also involved in biotic stress responses, whereas it acts as a repressor of genes involved in SA metabolism (Zheng *et al*., 2012). In contrast, the NAC TFs ANAC083/VNI2 and JUB1 are associated with a senescence delay. Accordingly, *vin2* and *jub1* mutants display accelerated senescence phenotype (Yang *et al*., 2011; Wu *et al*., 2012). *VNI2* is up-regulated by high salinity, and ABA-treatment and *JUB1* is induced by ROS accumulation. They are attractive gene-targets for drought- and oxidative-tolerance enhancement, respectively.

The involvement of NAC TFs in senescence has also been reported in crops. In rice, *OsNAP* (Os03g21060) was associated with the onset of dPCD, drought, and biotic stress responses. Overexpression of *OsNAP* causes precocious senescence and up-regulation of chlorophyll degradation- and JA metabolism-related genes (Zhou *et al*., 2013; Chen *et al*., 2014; Liang *et al*., 2014). Moreover, six rice NAC genes (*OsNAC005*, *OsNAC006*, *OsNAC009*, *OsNAC010*, *OsNAC011*, and *ONAC106*) are involved in both abiotic stress response and senescence (Ricachenevsky *et al*., 2013; Sakuraba *et al*., 2016; El Mannai *et al*., 2017; Chung *et al*., 2018). In barley, the gene *HvNAC026* was up-regulated during the senescence and barely expressed in other plant life-stages. In addition, four barley genes (*HvNAC023*, *Hvnac027*, *HvNAC029*, and *HvNAC030*) were also up-regulated at the latest stage of senescence, whereas *HvNAC005* was implicated in early-senescence regulation (Christiansen *et al.*, 2011, 2014, 2016).

In soybean, GmNAC030 and GmNAC081 are involved in both dPCD and ePCD and are induced by ER stress and osmotic stress (Irsgler *et al*., 2007; Mendes *et al*., 2013). These NAC TFs are induced via a developmental cell death (DCD) domain-containing N-rich protein (DCD/NRP)-mediated cascade activated by either stresses and/or leaf senescence (Reis *et al*., 2011: Pimenta *et al*., 2016). Therefore, *GmNAC030* and *GmNAC081* integrate stress-induced and developmental signals, culminating in VPE (vacuolar processing enzyme) enhanced expression (Irsigler *et al*., 2007; Costa *et al*., 2008; Faria *et al*., 2011; Reis *et al*., 2011). VPE is a caspase-like 1 protein that executes a plant-specific PCD throughout the vacuole collapse (Hara-Nishimura *et al*., 2005; Mendes *et al*., 2013; Reis *et al*., 2016). The DCD/NRP – NAC – VPE regulatory circuit also operates in Arabidopsis, suggesting a conserved PCD regulatory network in *planta* (Reis *et al*., 2016). Global gene expression analysis of senescing soybean-leaves demonstrated that 40% of NAC genes, including GmNAC030 and GmNAC081, are differentially expressed *during leaf senescence* (Pimenta *et al*., 2016; Melo *et al*., 2018). Other uncharacterized NAC genes displayed a strong relationship with multiple stress responses and cell death progression. *GmNAC065* and *GmNAC085*, which are putative orthologous of the SAGs *ANAC083/VIN2* and *ANAC072*, respectively, display contrasting patterns of expression under different stresses in soybean. When transiently expressed in *Nicotiana benthamiana* leaves, they trigger typical symptoms of senescence, including leaf yellowing, chlorophyll loss, ROS production, and lipid peroxidation (Melo *et al*., 2018).

Despite the involvement of NAC TFs in multiple stress responses, dPCD, and ePCD in crops, several regulatory mechanisms of PCD in plants are still unclear. The soybean genome encompasses more than 180 NAC members (Melo *et al*., 2018), which have been often associated with multilayered signaling events in stressful conditions, making them functionally complicated, poorly understood, and frequently unfeasible as a target for biotechnological intervention. Here, we identified putative NAC SAGs in soybean and validated their association with PCD by wide-gene expression analyses in different environmental conditions. Furthermore, we functionally characterized two GmNAC SAGs, *GmNAC065* and *GmNAC085*, in plant development, multiple stress responses, and cell death progression.

Our data demonstrate that *GmNAC065* and *GmNAC085* are induced by different stress conditions, with different kinetics and extensions of responses, playing contrasting roles in PCD through mechanisms coordinated by ABA- and SA-signaling. They displayed a divergent expression profile from other SAGs and downstream target genes implicated in the antioxidative system and photosynthetic apparatus. Collectively, our data provided new insights into the soybean NAC-mediated PCD and reinforced the importance of these TFs as targets for understanding PCD regulatory gene networks and biotechnological plant breeding.

Material and Methods

Identification and phylogenetic analysis of NAC-SAGs in soybean

The identification and the phylogenetic analysis of NAC-SAGs in soybean were performed using *Arabidopsis thaliana* (At)SAGs as templates. The deduced amino acid sequences of previously described AtNAC-SAGs (Luoni *et* al., 2019) were accessed from TAIR database (https://phytozome.jgi.doe.gov/pz/portal.html#!info?alias=Org_Athaliana) and used as query sequences against the soybean genome. For a global alignment analysis, we used Phytozome's BLASTp algorithm (https://phytozome.jgi.doe.gov/pz/portal.html#!search?show=BLAST&method=Org_Gmax). The putative-recovered GmSAGs were confirmed by the best score of sequence-similarity (e-vallue < 10^{-10}) and alignment cover-ratio (coverture > 90%). Using the Soybase dataset (https://soybase.org/), we identified the putative GmNAC-SAGs paralogous-genes and, finally, AtNAC-SAGs and GmNAC-SAGs were phylogenetically analyzed. The phylogenetic analysis and tree rendering were conducted in the MABL online phylogeny-platform (http://www.phylogeny.fr/simple_phylogeny.cgi?workflow_id=e72d406522a15231c99e208ac9396b27&tab_index=6&go_next=1#anchor) supported by MUSCLE alignment algorithm and neighbor-joining statistical method with 10,000 bootstraps. We also used the GmNAC081 and GmNAC030 (Mendes *et al*., 2013; Pimenta *et* al., 2016) as non-related AtNAC-SAGs but previously described as age- and stress-senescence promoter genes in soybean.

Transcriptome-wide analysis of soybean NAC-SAGs in response to multiple stresses

The expression levels of the putative GmNAC-SAGs were monitored from eight soybean differentially expressed gene (DEG)-datasets available in public transcriptome raw-data from GEO – Gene Expression Omnibus/NCBI (https://www.ncbi.nlm.nih.gov/geo/), comprising different types of abiotic and biotic stresses, age- and hormone-induced senescence. DEGs were determined using the edgeR package for gene expression analysis, and differential gene expression was supported by F and t-tests. Target genes were only searched against annotated DEGs after FDR (false discovery rate) correction and considered differentially expressed with $1 < FC < -1$ and p-value <0.05. All stress conditions, soybean treatments, access numbers, and references used in the transcriptome-wide analysis are organized in **Supplementary Table 1**.

For *GmNAC065* and *GmNAC085*, we performed a co-expression analysis of soybean plants submitted to different abiotic and biotic stresses using the EXPath 2.0 platform. We used Pearson's correlation-method with a cut-off of 0.8 (positive/negative) to determine the positive and negative correlated genes. The correlated genes were organized by biological function and process according to the internal GO enrichment analysis.

GmNAC065 and GmNAC085 promoter analysis

To analyze the incidence of *cis*-acting elements involved in multiple stress responses, we considered as the up-stream regulatory region of *GmNAC065* (Glyma.08G360200) and *GmNAC085* (Glyma.12G149100) the 1500 bp upstream to the putative transcription starting site (TSS) of the genes, comprising 2,045 bp for *GmNAC065* and 1722 bp for *GmNAC085*. The promoter sequences were recovered from Phytozome (https://phytozome.jgi.doe.gov/pz/portal.html#!info?alias=Org_Gmax) and analyzed by PlantPAN 3.0 (http://plantpan.itps.ncku.edu.tw/index.html) and NewPLACE (https://www.dna.affrc.go.jp/PLACE/?action=newplace) plant-specific *cis*-elements databases. The relevant *cis*-elements ($p \leq 0.01$) were grouped according to the transcription factors binding sites.

Soybean growth and multiple stress assay

Soybean (*Glycine max* – Williams82) seeds were soil-germinated and grown under greenhouse conditions (12 hours of light, 15 ^{o}C – 30 ^{o}C, 70% relative humidity). At the

V2/V3 developmental stage, the roots were acclimated in Hoagland Hydroponic Solution (HHS) for 24 hours prior to multiple stress simulations. The stress assay was performed in a hydroponic system, with HHS supplemented with 10% (w/v) PEG (MW 8,000) to induce osmotic stress, 5 µg/mL tunicamycin (Tun) to induce ER-stress, the phytohormones ABA (150 mM) and salicylic acid (SA - 75 µM), to trigger droughtand biotic stress-responses, respectively. For the air-dry treatment, the plants were removed from the HHS and placed on cotton-filled pots. Leaf discs of stressed and control (0h - untreated plants) seedlings were collected after 2h, 4h, and 12h of stress-treatment, immediately frozen in liquid nitrogen and stored at -80°C. All treatments were performed with biological triplicates, consisting of three pools of three plants. For induced PCD assay, the soybean seedlings in the same growth conditions were subjected to bleomycin treatment (420 mM) in HSS. The sample's collection and storage were conducted as described previously (Melo *et al*., 2018).

Soybean RNA-extraction, cDNA synthesis, and gene expression analysis

Total RNA of soybean leaf disks was extracted from approximately 150 mg of tissue, according to the Trizol® (Invitrogen) manufacturer's recommendations and previously described by Melo *et al*. (2018). The RNA quality was assessed by agarose 1% (w/v) electrophoresis and quantified using a NanoDrop™ Spectrophotometer ND-1000 (Thermo Scientific). A total of 1 µg of RNA, 10 uMoligoDT (18T), 10 mM dNTPs, and 200 U of MMLV were used for cDNA synthesis, performed according to the manufacturer's protocol (ThermoFischer).

The genes' expression profilewas determined by qRT-PCR. The analysis was performed in QuantStudio 3 instrument (ThermoFischer), with GoTaq qPCR master mix (Promega) and the specific primers **(Supplementary Table 2)**. For experiment accuracy, three independent cDNA pools for each treatment were used. The reactions were performed as follows: 2 min at 50 °C, 10 min at 95 °C, and 40 cycles of 94 °C for 15 sec and 60 °C for 1 min. *ELF1A* soybean gene was used as the endogenous control, with stability determined by Freitas *et al*. (2018). Relative gene expression was determined by the $2^{-\Delta\Delta Ct}$or $2^{-\Delta Ct}$ method and gene expression results converted into a heatmap using MORPHEUS software (https://software.broadinstitute.org/morpheus/).

Arabidopsis GmNAC-overexpressing lines

Arabidopsis thaliana (ecotype Columbia) transgenic lines ectopically expressing the genes *GmNAC065* and *GmNAC085*(designated GmNAC065-OX and GmNAC085-OX, respectively) were generated by the floral dip method (Clough and Bent, 1998). The complementary DNA sequences (CDS) of the genes were cloned into pEARLEY 103 and pEARLEY 104, respectively, under CaMV 35S promoter control using the Gateway cloning-technology (Thermo Scientific). The clones were confirmed by sequencing. The recombinant plasmids were transformed into *Agrobacterium tumefaciens* (GV3101 strain), and one single-colony for each construction was selected on LB-agar medium supplemented with 50 µg/mL of gentamycin, 100 µg/mL of kanamycin, and 50 µg/mL of rifampicin. The isolated colony was growth in LB medium until OD_{600} = 0.8.The culture was centrifuged at 5.000 g for 5 min, and the pellet was resuspended in 200 mL of dip-solution (5% w/v of sucrose and 0.02 % v/v of Silwet L-77) and used to inflorescence dip for 20 sec. The transformation process was performed three times, with an interval of 10 days between the rounds. Transgenic plants with a T-DNA insertion were selected in $T_0$by ammonium-glufosinate pulverization (120 mg/L) of sowed-seedlings and confirmed by PCR. Three T_2 homozygous independent lines were obtained for each construction, and the gene expression level was monitored by qRT-PCR.

GmNAC065-OX and GmNAC085-OX phenotypic characterization

For the phenotypic characterization, the seeds of three independent lines of GmNAC065-OX, GmNAC085-OX, and Col 0 previously refrigerated at dark for dormancy-broken were soil-sowed and germinated under a controlled growth chamber (12 h of photoperiod, 21 °C and 70% of relative humidity). After germination, two-week-old seedlings were carefully transferred to individual pots, randomly distributed in trays, and cultivated up to 70 days (10 weeks). During the developmental cycle, we analyzed: i. Rosette diameter; ii. The number of leaves; iii. Shoot length; iv. Duration of the vegetative stage; v. Duration of the reproductive stage; vi. Senescence onset. These parameters were monitored according to natural plant life-stages' progression in intervals of 7 days between measurements.

Arabidopsis stress treatment, RNA extraction, and cDNA synthesis

Four-week-old seedlings were organized in three pools of three plants for each treatment. Plant germination and growth were performed according to the phenotypic

and morphological analyses section. For the stress assay, the seedlings were carefully removed from the soil and transferred to MS medium (2.3 g/L of MS basal medium) for 24h for plant acclimation. After the acclimation, the plants were transferred to PEG, Tun, or SA solutions and collected after 24h. Total RNA extraction and cDNA synthesis were performed as described in *the soybean growth and multiple stress assay* section.

Biochemical and cellular analysis of plant antioxidative system

The plant antioxidative system was evaluated by different approaches, including H_2O_2-DAB leaf-staining, TBA-reactive compounds quantification, enzymatic activity analysis of superoxide dismutase (SOD), catalase (CAT), and ascorbate peroxidase (APX). For H_2O_2 detection, the plants were soaked in 3,3-diaminobenzamidine (DAB) solution (1 mg/mL, pH 3.8) for 8 h under continuous agitation. After staining, the leaves were submitted to 100% (v/v) ethanol bath until total chlorophyll removal. The leaves were rehydrated in water and glycerol (10% v/v) and photographed in a stereoscope.

TBA-reactive compounds were quantified as described by Cakmak and Horst (1991) and optimized by Melo *et al*. (2018). Approximately 150 mg of leaves werehomogenized in 2 mL of 0.1% (v/v) trichloroacetic acid (TCA) and centrifuged at 12,000 gfor 15 min. An aliquot of 500 µL of the supernatant was added to 1.5 mL of 0.5% (w/v) thiobarbituric acid (TBA) in 20% (v/v) TCA, and the samples were incubated at 90 °C for 20 min. The reaction was finished in an ice-bath, followed by centrifugation for 4 min. The absorbance of the supernatant was measured at 532 nm, and the concentration of TBA-reactive compounds was calculated considering the MDA molar extinction coefficient of 155 $mM.cm^{-1}$.

The enzymatic activities were determined in the total protein extract, as described by Melo *et* al. (2020). The proteins from approximately 150 mg of leaves were extracted in 1 mL of phosphate buffer (100 mM - pH 7.8) and added to DTT (0.5 g/L), EDTA (10 µM) and PVPP (0,3 mg/mL). The samples were subsequently centrifuged (12,000 x g - 4 °C) for 15 minutes. All enzymatic activities were determined using pools of 3 plants, and three biological and two technical replicates, respectively. Total protein quantification was performed by Bradford's method.

For SOD activity, a reaction mix was prepared with 100 µL of phosphate buffer, 40 µL of methionine solution (12 g/L), 2 µL of EDTA (3.5 g/L), 15 µL of NBT (0.35 g/L), 2 µL of riboflavin (8.0mg/L), 31 µL of milli-Q water, and 10 µL of protein extract for each reaction. An aliquot of 200 µL of the reaction mix was used as an absolute blank, and NBT reduction was performed under intense white-light exposure for 40 minutes. After the reaction, absorbance was measured in a spectrophotometer at 560 nm. SOD activity was expressed as the percentage of inhibition of light-mediated NBT reduction, calculated by the expression IN (%) = $\frac{\mathrm{LB}-\mathrm{SA}-\mathrm{AB}}{\mathrm{LB}}$, in which LB = light blank, SA = sample absorbance, and AB = absolute blank. Finally, the specific SOD activity was calculated by the expression SOD = $\frac{\mathrm{IN}\ (\%)\ .\ 10}{\mathrm{U}\ .\ \mathrm{TP}}$, in which U = SOD units, and TP = total protein (µg/g). The SOD specific activity was expressed as U/total protein.

The CAT activity was determined using a reaction mixture of 144 µL of phosphate buffer, 30 µL of water, and 16 µL of hydrogen peroxide solution (50 mM). The reaction mix was supplemented with 10 µL of protein extract, and the absorbance-reading was performed for 10 minutes, in intervals of 30 seconds, at 240 nm. The CAT activity was determined by the expression CAT = $\frac{\mathrm{dA}\ .\ 0{,}0067}{\mathrm{T}\ .\ 39{,}4\ .\ \mathrm{W}}$, in which dA = (initial absorbance–final absorbance), T = time of reaction, 39.4 $\mathrm{mol.cm^{-1}}$represents the molar extinction coefficient of hydrogen peroxide, and W = sample weight. All absorbance values were blank-corrected. The CAT specific activity was expressed as µmol H_2O_2/min/mg protein.

The APX activity was determined as previously described. The reaction mix was added to a 10% (v/v) ascorbic acid solution (18 g/L). The molar extinction coefficient of ascorbic acid is 2.8 $\mathrm{mol.cm^{-1}}$, and the absorbance was measured at 290 nm. The APX activity was expressed as µmol ascorbate/min/mg protein.

From data of total protein quantification, we determined the rate of protein degradation. To predict protein decay, the following expression was applied: (%) of protein degradation = $\frac{100\ .\ (P0-Pn)}{P0}$, P_0 = total protein of unstressed plants and P_n = total protein at specific stress-time.

Cellular analysis of cell death progression

Cell death progression was monitored in leaves and roots by Evans blue and propidium iodide (PI) staining. The Evans blue leaf-staining was performed in Evans dye aqueous solution (0.5 % w/v). Stressed (24h) and non-stressed leaves were immersed into the staining-solution for 8h under agitation. After staining, the leaves were distained in absolute ethanol and preserved in glycerol (50% v/v) until observation under a stereoscope.

For the PI root-staining, 24 h-stressed plants were dipped into propidium iodide solution (0.6 µg/mL) for 24 hours. After staining, the plants were rinsed in distilled water and roots arranged at slides under a water drop. The slides were covered and submitted to confocal microscopy scanning (Zeiss LSM510 META) under argon/helium-neon laser with a maximum excitation wavelength of 488 nm. Fluorescence was collected in a 596-638 bandpass filter. Images were recovered and treated in ZEN BLACK EDITION 3.0 (Carl-Zeiss) software.

Secondary metabolites quantification

Metabolite content was monitored in ethanolic plant-extracts. The levels of chlorophyll, carotenoids, soluble sugars, and anthocyanins were monitored using the same leaf extract. The frozen samples were weighted, powdered in liquid nitrogen, and metabolites extracted in ethanol for 24 hours under refrigeration and sheltered from the light.

Chlorophyll, carotenoids, and anthocyanin levels were determined spectrophotometrically. An aliquot of 1 mL from the ethanolic extract was transferred to a dark tube and centrifuged at 12,000 g and 4 °C for 5 min. The supernatant was quantified in a spectrophotometer at 480 nm, 645 nm, and 663 nm. Chlorophyll a, b, and total chlorophyll were calculated by the expression $Clf_a = \frac{(12.7.\ A663)-(2.69\ .\ A645)}{m}$; $Clf_b = \frac{(22.9\ .\ A645)-(4.68\ .\ A663)}{m}$; $Clf_{(a+b)} = \frac{(20.2\ .\ A645)+(8.02\ .\ A663)}{m}$, respectively, and expressed as µg/mg of tissue. To calculate the concentration of carotenoids, we used the equation $Car = \frac{[10.\ A480]}{\varepsilon.\ m}$, considering ε = 2592 $mM.cm^{-1}$ for standard carotenoids in ethanol. Carotenoid data were expressed as µg/mg of tissue. Finally, anthocyanin content was determined according to the method described by Murray and Hackett

(1991) and adapted by Sims and Gamon (2002). The samples were spectrophotometrically analyzed at 529 nm and 650 nm, considering the interference peak of chlorophyll over anthocyanins' absorption peak. The final concentration of anthocyanins was calculated by the expression $Cyan = \frac{A529 - 0.288.A650}{\varepsilon . m}$, in which m = tissue weight (mg) and ε = 98,2 $mM.cm^{-1}$ (molar extinction coefficient determined for a mixture of standard-anthocyanins in acidic solution according to described by Lees and Frances (1972) and the results expressed as mmol/mg of tissue.

For reducing-sugar quantification, we performed a DNS-based (3,5-dinitrosalycilic acid) reaction. DNS (0,1% w/v) was prepared in sodium and potassium tartrate (30% w/v) and sodium hydroxide (0,4 M). An aliquot of 100 µL of the extract was added to 900 µL of water and 500 µL of DNS and incubated in a boiling water bath for 5 minutes. The reactions were stopped by immersion on ice, and absorbance was determined at 540 nm. The sugar content was predicted using a glucose-based standard curve (0–1,2 µg/µL).

Quantitative RT-PCR

The expression of SAGs and downstream targets in Arabidopsis was determined by real-time RT-PCR using the GoTaq qPCR master mix (Promega), gene-specific primers **(Supplementary Table 3)**, and cDNA from stressed-plants under normal development. Three stressed-plants were used to obtain independent mRNAs pools for the quantitative RT-PCR, with three biological and two technical replicates. Relative gene expression was quantified using the comparative $2^{-\Delta\Delta Ct}$ or $2^{-\Delta Ct}$ method. *ACT2* was selected as the normalizer control gene. The expression of the drought-responsive genes *RD29A, RD29B,* and *RD20*; ER stress-induced *ANAC036, CNX*, and *AtNRP1* genes and biotic stress-associated marker genes *WRKY70, AtNRP1*, and *RAB18* were monitored by RT-qPCR. The amplification reactions were performed as follows: 2 min at 50 °C, 10 min at 95 °C, and 40 cycles of 94 °C for 15 sec and 60 °C for 1 min.

Results

Genome- and transcriptome-wide analysis identified soybean NAC genes associated with developmental- and environmental-senescence

Transcription factors (TFs) act as essential players of the multilayered mechanisms integrating age- and stress-induced senescence signals, which results in adaptive responses. Thus, they are considered converging nodes on regulatory mechanisms involving gene and physiological reprogramming (Guo *et al*., 2004; Woo *et al*., 2013; Kim *et al*., 2016; Luoni *et al*., 2019).

In Arabidopsis, several studies of temporal gene expression profiling along developmental and environmental programmed cell death (dPCD and ePCD, respectively) have associated NAC TFs with the control of the onset, progression, and final events in PCD (Olvera-Carrillo *et al*., 2015; Kim *et al*., 2016; Luoni *et al*., 2019). In order to identify the soybean NAC TFs associated with the control of PCD in developmental programs and multiple stresses responses, we performed a genome and transcriptome-wide analysis of soybean under different stresses. Kim *et al*. (2016) and Luoni *et al.* (2019) provided a complete inventory of senescence-associated NAC genes (NAC-SAGs) in *Arabidopsis thaliana*. Here, we used these functionally characterized SAG-NAC genes from Arabidospis as templates, and we identified 16 putative GmNAC-SAGs in the soybean genome **(Table 1)**.

Table 1. Senescence-associated genes in *Arabidopsis thaliana* and soybean (*Glycine max*)

Group	NAC-SAG (*Arabidopsis thaliana*)	NAC subgroup *	Soybean-putative NAC-SAG	Locus	Soybean paralogous-gene	Locus
1	*ANAC016*	NAM	*GmNAC074*	Glyma.10G219600	*GmNAC149*	Glyma.20G172100
2	*ANAC059/ORS1*	NAM	*GmNAC023*	Glyma.05G025500	**	-
	ANAC092/ORE1	NAM	*GmNAC131*	Glyma.17G101500	**	-
3	*ANAC042/JUB1*	ONAC022	*GmNAC106*	Glyma.14G030700	*GmNAC154*	Glyma.02G284300
4	*ANAC083/VNI2*	Senu5	*GmNAC065*	Glyma.08G360200	*GmNAC179*	Glyma.18G301500
5	*AtNAP*	SNAC-B	*GmNAC010*	Glyma.02G109800	*GmNAC003*	Glyma.01G051300
6	*ATAF1*	SNAC-A	*GmNAC109*	Glyma.14G152700	*GmNAC011*	Glyma.13G030900
7	*ANAC072*	SNAC-A	*GmNAC085*	Glyma.12G149100	*GmNAC043*	Glyma.06G248900
	ANAC019	SNAC-A	*GmNAC101*	Glyma.13G279900	***	-
	ANAC055	SNAC-A	*GmNAC092*	Glyma.12G221500	***	-

(*) According to Melo *et al*. (2018)

(**) GmNAC023 and GmNAC131 are putative soybean paralogous genes.

(***) GmNAC092 and GmNAC101 are putative soybean paralogous genes.

The last phylogenetic analysis of the soybean NAC superfamily updated the family to 180 members, divided into 15 subfamilies, according to sequence and functional relationship (Melo *et al.*, 2018). The phylogenetic analysis of GmNAC-SAGs clustered the putative genes in 7 phylogenetic groups, whose members belong to 5 different NAC subfamilies **(Figure 1)**. The most representative senescence-associated NAC subfamily is SNAC-A, followed by SNAC-B subfamilies. SNAC-A and SNAC-B subfamilies contain 50% of GmNAC-SAGs, divided into three close-related groups (5, 6, and 7 – **Figure 1**). *GmNAC010* and *GmNAC003* belong to the SNAC-B subfamily, whereas *GmNAC109*, *GmNAC011*, *GmNAC085*, *GmNAC043*, *GmNAC101*, and *GmNAC092* are SNAC-A subfamily members. These clusters also harbor the Arabidopsis genes *AtNAP* (group 5), *ATAF1* (group 6) and *ANAC072*, *ANAC019*, and *ANAC055* (group 7), functionally associated with senescence progression and multiple stress responses (Tran *et al*., 2004; Wu *et al*., 2009; Garapati *et al*., 2015; Li *et al*., 2016).

In addition to the SNAC subfamilies, the NAM subfamily holds 25% of NAC-SAGs divided into groups 1 and 2 **(Figure 1)**. The NAM subfamily encompasses the genes *GmNAC074*, *GmNAC023*, *GmNAC131*, and *GmNAC149*, besides their orthologous in Arabidopsis *ANAC016*, *ANAC059/ORS1* and *ANAC092/ORE1*, respectively. Finally, groups 3 and 4 belong to two different NAC subfamilies. *GmNAC106* and *GmNAC154* (group 3 – **Figure 1**) are phylogenetically related to ONAC022 subfamily, and *GmNAC065* and *GmNAC179* (group 4 – **Figure 1**) belong to the Senu5 subfamily.

The analysis of putative GmNAC-SAGs in soybean genome did not target *GmNAC030* and *GmNAC081*, the final regulators of the NAC-VPE circuit into environmental and developmental cell death programs (Irsigler *et al*., 2007; Costa *et al*., 2008; Faria *et al*., 2011; Reis *et al*., 2011, 2016). *GmNAC081* belongs to the TERN subfamily and is clustered with a most divergent branch of the phylogenetic tree **(**group 1**- Figure 1)**. However, *GmNAC030* belongs to the SNAC-A subfamily, covered by the members of the groups 6 and 7, but it displays some structural divergence that promotes a branch collapse and places it in a new phylogenetic branch.

To identify NAC TFs associated with the regulatory mechanisms of dPCD and ePCD in soybean, we analyzed the expression profile of the putative GmNAC-SAGs on a publically accessed soybean-transcriptome dataset from the GEO (NCBI) database **(Supp. Table 1, Figure 2)**. Their expression profiles were assessed in response to different stress conditions and natural senescence (dPCD), such as hormone-induced senescence, abiotic stresses (moderate and severe drought conditions, oxidative stress), biotic stresses (fungi and insect attacks). In addition, their expression levels were also examined in soybean seedlings treated with bleomycin, a genotoxic PCD-inducer.

Our transcriptome analysis demonstrated that GmNAC-SAGs are differentially expressed at least in one type of abiotic and/or biotic stresses, and most of them are differentially expressed during age-induced senescence **(Figure 2A)**.We also monitored the expression of *GmNAC081* and *GmNAC030* as marker genes of stress- and leaf senescence-induced genes (Carvalho *et al*., 2014). *GmNAC074*, *GmNAC149*, *GmNAC010*, and *GmNAC003*, which share a similar expression profile as *GmNAC030*, display similar expression patterns in response to multiple stresses and during leaf senescence **(Figure 2A)**. In general, GmNAC-SAGs were up-regulated by the stress and demonstrated a pattern of expression consistent with their subfamily. The SNAC-A genes within groups 6 and 7 were up-regulated during drought and oxidative stresses. Specifically, *GmNAC085*, *GmNAC043*, *GmNAC101*, and *GmNAC092* also displayed a similar expression pattern during biotic stresses (*Fusarium oxysporum* and *Lamprosema indicata* infection, **Figure 2A**). In contrast, these genes were down-regulated during age-induced senescence. An opposite trend was observed for *GmNAC065*, *GmNAC179*, *GmNAC081*, and *GmNAC077* (groups 1 and 4, respectively, Senu5 and TERN). These genes were down-regulated in multiple-stress responses and up-regulated during age-induced senescence **(Figure 2A)**.

To corroborate our hypothesis of the involvement of GmNAC-SAGs with PCD, we analyzed their expression levels in soybean leaves treated with bleomycin for 24 hours **(Figure 2B)**. All GmNAC-SAGs were highly induced by bleomycin treatment. The only exception was *GmNAC106*, which was negatively regulated by the treatment. Some genes, including *GmNAC023* (group 2 – NAM) and *GmNAC109* (group 6 – SNAC-A), were strongly induced (more than 1.000 fold variation), indicating involvement of these genes with the process of stress-induced PCD. *GmNAC003* (group

5 – SNAC-B), *GmNAC085*, and *GmNAC092* (group 7 - SNAC-A) were also induced by bleomycin treatment, as expected for the members of S-NAC subfamily already described as positive regulators of PCD, such as *ANAC016*, *ORE1*, *ORS1*, and *ATAF1* (Wu *et al*., 2009; Garapatti *et al*., 2015; Podzimska-Sroka *et al.*, 2015; Luoni *et al*., 2019). In contrast, the genes *GmNAC106* and *GmNAC154*, which clustered together with the Arabidopsis negative regulator of senescence JUB1 (ONAC022 – Wu *et al*., 2012), displayed low induction compared with the other GNAC-SAGs genes. Likewise, *GmNAC065* and *GmNAC179* (group 4 – Senu5) clustered with another negative regulator of senescence in Arabidopsis (*ANAC083/VNI2* - Yang e*t al*., 2011).

The promoter regions of GmNAC065 and GmNAC085 harbor multi-responsive regulatory elements consistent with their gene expression profile in soybean

Previous analysis of *GmNAC065* and *GmNAC085* expression during the onset of leaf senescence and multiple stresses in soybean have associated these genes to different roles in stress responses and senescence control (Melo *et al*., 2018). *GmNAC065* was up-regulated during the onset of leaf senescence and in response to several treatments simulating drought, ER-stress, and biotic stress. In contrast, *GmNAC085* was down-regulated during natural senescence and up-regulated only in the intermediary-to-late stages of PEG treatment (Melo *et al*., 2018). These contrasting expression patterns were also reported in soybean leaves submitted to 25 days of dehydration (Carvalho *et al*., 2104). In prolonged drought stress, *GmNAC085* was strongly induced while *GmNAC065* was repressed. These data suggest that these genes do not play an overlapped function in age-induced senescence but may play complementary functions in specific time-points during drought stress-responses.

To understand how *GmNAC065* and *GmNAC085* respond to different stress, the presence of different *cis*-acting elements at their promoter regions was investigated **(Supplementary Table 4, Supp. Fig. 1)**. The up-stream regulatory regions of *GmNAC065* and *GmNAC085* hold canonical motifs of the prominent stress-responsive TFs families. In the G*mNAC065* promoter, the most abundant *cis*-acting elements are the consensus of MREs (MYB responsive elements – ANCNNCC): EBOXBNNAPA/MYCCONSENSUSAT and MYB1AT display the highest frequency, with 7-clustered regulatory regions each. They are followed by WBOX element, with a

frequency of 6 regulatory-blocks in *pGmNAC065*. These elements are recognized by MYB and WRKY TFs, respectively, and have been frequently associated with ABA-signaling, multiple-stress responses, and senescence (Basu *et al*., 2014; Llorca *et al*., 2014; Sheshadri *et al*., 2016). MREs are the canonical DNA-binding site for MYB TFs, one of the largest TFs families in plants, divided into four subfamilies, according to their number and distribution protein-domains (Streckle *et al*., 2007; Sheshadri *et al*., 2016). The biological roles of MYB TFs are diverse and regulate developmental processes, such as cell wall formation, pollen structure, cell fate, and differentiation. In addition, they also regulate environmental processes like drought and biotic stress responses, control the biosynthesis of lignin, anthocyanins, and other phenylpropanoids (Lu *et al*., 2002; Du *et al*., 2012; Cao *et al*., 2013; He *et al*., 2016; Gates *et al*., 2016; Sheshadri *et al*., 2016; Freitas *et al*., 2019). WRKY TFs can recognize the WBOX *cis*-elements, a 6-bp region (C/TTGACC/T) widely spread in genes of primary and specialized metabolism, involved in developmental processes, biotic and abiotic stress responses, and senescence (Basu *et al*., 2014; Llorca *et al*., 2014). The promoter region of *GmNAC085* also encompasses MYB and WBOX *cis*-acting elements, although in low frequency. The most abundant regulatory elements in this promoter are WBOX, distributed 11 times along *pGmNAC085*, and ABA-responsive element (ABRE), covering ten regulatory regions.

The 5' flanking regions of *GmNAC065* and *pGmNAC085* harbor other responsive elements, including AP2/ERF, ERD, NAC, and bZIPs DNA-binding sites. AP2/ERF TFs control several hormone-signaled biological processes in plant cells, including ABA-dependent and –independent dehydration responses, jasmonic- and salicylic-acid pathways under biotic stresses, ethylene-, auxin- and cytokinin-coordinated developmental programs (Guo and Ecker, 2004; Cheng *et al*., 2013; Guo *et al*., 2016; Sheshadra*et al*., 2016). These functions are partially overlapped by bZIPs, which recognize ACEs core (-ACTG-), found in GBOX, CBOX, EBOX, and ABRE *cis*-regulatory elements. These TFs are universally associated with gene expression reprogramming during biotic and abiotic stresses, hormone-signaling, sugar-, nitrogen- and carbon-signaling and metabolism, besides light responsiveness, cell elongation, cell division, and senescence (Wei *et* al., 2012; Llorca *et al*., 2014; Zhao *et al*., 2016; Sheshadra *et al*., 2016).

GmNAC065 and GmNAC085 are differentially expressed in soybean tissues during normal growth conditions and stressful conditions.

To gain new insights toward the function of these genes in developmental processes, stress-responses, and PCD, we investigated the expression profile of G*mNAC065* and *GmNAC085* in different tissues of the Williams82 soybean-variety under normal and stressful conditions **(Figure 3, Supp. Fig. 2A)**. *GmNAC065* is expressed in all tissues during the vegetative and reproductive stages **(Figure 3A)**. The only exception is the stem, in which its expression is barely detected. In the vegetative stage, the expression of *GmNAC065* is higher in leaves than in roots. However, in the reproductive stage, the expression of *GmNAC065* is stable amongst all tissues, displaying a discrete variation. In contrast, *GmNAC085* displays a very low expression in leaves and roots during the vegetative stage, but a significantly enhanced expression in all tissues during the reproductive stage **(Figure 3A)**. Like *GmNAC065*, the expression of *GmNAC085* is higher in leaves than in roots in the reproductive stage, indicating involvement with the senescence process, which appears to be more extensive in leaf tissue.

We also determined the expression levels of *GmNAC065* and *GmNAC085* in soybean seedlings exposed to PEG, air-dry, and ABA-treatments, simulating drought. ER-stress was induced by tunicamycin-treatment, and biotic stresses were simulated by salicylic acid treatment. Our analyses were performed in four time-points (0.5h, 2h, 4h, and 12h) to determine whether these genes are early, intermediate or late stress-responsive.

GmNAC065 and GmNAC085 are regulated by at least one type of stress treatment and respond with different levels and kinetics of induction in leaves and roots **(Figure 3B, Supp. Fig. 2B)**. Both genes are most expressed in leaves than in roots, as observed under normal growth conditions. In leaves, *GmNAC065* was weakly up-regulated by PEG, Tun, and air-dry treatments. GmNAC065 displays an expressive induction during the early-to-intermediate ABA treatment stages but decays at a late stage post-treatment. During the PEG treatment, *GmNAC065* responded with early-to-intermediate induction kinetics, displaying the highest expressions between 2h and 4h, similarly to air-dried and ABA-treated plants. Differently, in ER-stress, *GmNAC065* was only induced in late stages of stress, after 12h of treatment. In contrast, *GmNAC085* was strongly induced by PEG, ABA, and dry air treatments, but not by Tun and SA in leaves. The temporal

expression pattern was also different; GmNAC085 displays anintermediate-to-late response, with higher expression levels between 4h and 12h, when *GmNAC065* expression decays **(Figure 3B)**. In roots, these NAC genes are weakly expressed. Nonetheless, *GmNAC085* responds to SA treatment at late stages and displays a stable expression during ABA-treatment.

Despite the similar incidence of *cis*-acting elements in the promoter region of *GmNAC065* and *GmNAC085*, the expression profiles of these NAC genes differ under stress conditions. Therefore, we next examined whether they participate in different cascades of stress-responses. To support our investigation, we performed a co-expression analysis in publically accessed RNA-seq and Microarray data of soybean under biotic and abiotic stresses.Differentially expressed genes (DEGs) were subjected to Pearson's correlation method, and positively and negatively correlated genes were grouped according to their biological function and process by GO enrichment analysis**(Table 3)**.

Table 3. *GmNAC065* and *GmNAC085* co-expressed genes in soybean under biotic and abiotic stresses

GO ID	GO Term	Gene	Functional Annotation	P-value*
GmNAC065 – positive correlation (PCC ≥ 0.8)				
0004871	Signal Transducer	Glyma.15G074900	Protein kinase superfamily	$5.93E^{-3}$
		Glyma.12G187600	LEA Hydroxy-proline rich glycoprotein	
0055114	Oxidative/reductive process	Glyma.16G179100	β-carotene-hydroxylase 1	0.05
		Glyma.01G025500	2-oxoglutarate and Fe(II)-dependent oxygenase	
		Glyma.04G123800	Ubiquinol oxidase	
		Glyma.06G285400	Acyl-CoA oxidase 3	
GmNAC065 – negative correlation (PCC ≤ -0.08)				
0046423	Oxidative/reductive process	Glyma.01G086900	Allene-oxide cyclase 3	$1.18E^{-5}$
0009740	GA-mediated signaling	Glyma.10G241100	Gibberillin-oxidase 2 (A44)	$2.96E^{-4}$

	pathway	Glyma.13G371400	GA_3-recquiring oxidase	
GmNAC085 – positive correlation (PCC ≥ 0.8)				
0009808	Lignin metabolic process	Glyma.02G236500	Trans-cinnamate 4-monooxygenase	$2.13E^{-4}$
0009073	Aromatic amino acid biosynthesis	Glyma.11G189100	Prephenate dehydratase	$4.48E^{-4}$
		Glyma.14G176600	3-deoxy-7-phosphoheptulonate synthase	
		Glyma.05G183700	Shikimatekinase	
0009737	ABA-responsive genes	Glyma.03G056000	EM-likeprotein GEA6	$1.66E^{-3}$
		Glyma.04G009900	Dehydrin	
		Glyma.18G203500	EM-likeprotein GEA1	
000502	Proteasome Complex	Glyma.06G171200	20S proteasomesubunit beta 5	$1.88E^{-3}$
		Glyma.11G227700	26S proteasome regulatory subunit N8	
		Glyma.01G124900	20S proteasomesubunit alpha 3	
		Glyma.06G078500	20S proteasomesubunit beta 1	
		Glyma.17G252100	20S proteasomesubunit alpha 6	
0004175	Endopeptidase activity	Glyma.12G072600	Sentrin-specific protease 8	$1.99E^{-3}$
0042744	Hydrogen peroxide catabolic process	Glyma.U021900	L-ascorbate peroxidase	$2.62E^{-3}$
		Glyma.06G275900	Peroxidase	
0005741	External mitochondrial membrane	Glyma.19G020100	Voltage-dependent anion-selective channel	$3.56E^{-3}$
		Glyma.05G241100	Mitochondrialimport receptor subunit TOM40	
0043248	Proteasome Assembly	Glyma.16G126300	26S proteasome regulatory subunit N10	0.02
		Glyma.09G210000	26S proteasome regulatory subunit N9	
0051603	Proteolysis involved in cellular protein catabolic process	Glyma.04G155900	Serine-carboxypeptidase-like 29	0.08
		Glyma10G207300	Serine-carboxypeptidase-like 47	
GmNAC085 – negative correlation (PCC ≤ -0.08)				
0016117	Carotenoid biosynthetic process	Glyma.03G128900	Lycopene β-cyclase	$2.60E^{-4}$
		Glyma.02G188200	Prolycopene isomerase	
0009507	Chloroplast	Glyma.11G195900	Chaperonin 60 subunit alpha 1	$2.14E^{-3}$
		Glyma.06G159400	GTP-binding protein LEPA	

		Glyma.06G039700	Photosystem I light-harvesting complex 5	

(*) P-value of statistical analysis of FDR (false discovery rate) for GO-enrichment

GmNAC065 is positively correlated with genes related to primary cell signaling pathways, such as kinase proteins, and genes associated with cell survival in multiple stresses tolerance. The analysis indicates its co-expression with LEA proteins, β-carotene hydroxylase, acyl-CoA oxidase, and ubiquinol oxidase. These proteins and enzymes are frequently associated with ROS-avoiding mechanisms, photosynthetic apparatus preservation, jasmonate-mediated tolerance to biotic stresses, and drought-tolerance (Davison *et al*., 2002; Saha *et al*., 2016; Magwanga *et al*., 2018). *GmNAC065* negatively correlates with one gene of jasmonic acid biosynthesis (allene-oxide 3-cyclase – Stenzel *et al*., 2003) and several genes from gibberellin biosynthesis pathways (Yamaguchi, 2008). In contrast, *GmNAC085* is co-expressed with ABA-responsive genes, genes involved in aromatic amino acids metabolism, and, mainly, genes involved in protein catabolism and degradation, such as components of proteasome and endopeptidases, besides peroxidases. Interestingly, *GmNAC085* displays negative co-relation with genes controlling pigment biosynthesis and the photosynthetic apparatus assembly, including lycopene-β-cyclase, prolycopene isomerase, and the complex V of the light-harvesting system on photosystem 1, indicating that these genes are expressed in divergent situations compared to *GmNAC085*.

Ectopic expressions of *GmNAC065* and *GmNAC085* promote contrasting phenotypic and physiological changes in Arabidopsis.

To uncover the functions of *GmNAC065* and *GmNAC085* in developmental and stress-responsive programs in plants, we generated three independent homozygous transgenic lines of *Arabidopsis thaliana* expressing the soybean genes under the C*aMV*35S promoter control. The selected lines (L1, L2, and L3) of GmNAC065-OX and GmNAC085-OX demonstrated similar transgene expression, monitored by RT-qPCR **(Supp. Fig. 3A)**. The ectopic expression of GmNAC065 and GmNAC085 in the Columbia background caused phenotypic alterations **(Figure 4, Supp. Fig. 3)**. The transgenic plants displayed stunted growth compared to wild-type plants during the vegetative stage **(Figure 4A)**. From 14 days after germination (DAG) up to 49 DAG,

considered as the transition point to the reproductive stage, hallmarked by shoot elongation in plants, the leaf number and rosette diameter of both GmNAC065-OX and GmNAC085-OX were lower compared to Col 0 **(Figure 4A, Supp. Fig. 3B, C)**. GmNAC065-OX plants reached an average of maximum rosette diameter of 9.88 (± 0.47) cm, against 9.80 (± 0.11) cm of GmNAC085-OX and 10.89 (± 0.94 cm) of Col 0.

During the reproductive stage, the transgenic lines also displayed lower inflorescence length than wild type plants **(Figure 4B, Supp. Fig. 3D)**, and the phenotypic alterations were more pronounced between the different transgenic lines. The development of GmNAC065-OX lines was delayed compared to Col 0 and GmNAC085-OX plants. At 49 DAG, Col 0 and GmNAC085-OX emerged their shoot-inflorescence, reaching 2 – 3 cm of inflorescence length, while only one of five GmNAC065-OX L1 plants displayed shoot elongation **(Figure 4A, Supp. Fig. 3D)**. At the same time point, GmNAC085-OX L1 flowered, indicating an accelerated development compared to the other plants **(Figure 4A)**. These phenotypic variations persisted during the late reproductive stages. At 56 and 63 DAG, Col 0 and GmNAC085-OX lines presented elongated shoots with flowers, although the inflorescence length was shorter in GmNAC085-OX than in Col 0 **(Figure 4B, Supp. Fig 3D)**. The reduced number of leaves, rosette diameter, and shoot length displayed by GmNAC065-OX lines indicate a longer lifecycle and a stay-green phenotype. At 70 DAG, after flower abscission and silique maturation, GmNAC065-OX plants kept the green phenotype, with discrete senescence marks, whereas GmNAC085 OX plants displayed more intense necrotic lesions as compared to Col-0. Collectively, these phenotypic alterations indicate that the overexpression of *GmNAC065* delays the developmental cycle of transgenic plants, whereas *GmNAC085* overexpression accelerates leaf senescence, which is consistent with the GmNAC065 and GmNAC085 expression patterns in soybean under normal growth conditions and in response to multiple stresses.

GmNAC065 and GmNAC085 promote changes in the antioxidant plant system and secondary metabolite content.

A common feature of the plant responses to multiple stresses is the production and accumulation of reactive oxygen species (ROS - Jaspers and Kangasjarvi, 2010; Petrov *et al*., 2015). With the different extent of damages, they are potent oxidizers and lead to

deleterious effects, triggering ePCD (Gechev and Hille, 2005; Petrov *et al*., 2015). The ectopic expression of *GmNAC065* and *GmNAC085* in *N. benthamiana* leaves has already been shown to differentially accumulate H_2O_2 and thiobarbituric acid (TBA)-reactive compounds, such as malonaldehyde (MDA – a product of lipid peroxidation), consequently reducing the chlorophyll content after 72 hours (Melo *et al*., 2018). Hereafter, we investigated the effect of ROS accumulation on activity of antioxidative enzymes and osmo- and oxidative-protectant content in Arabidopsis transgenic lines constitutively expressing these genes **(Figures 5 - 7)**.

In untreated control (CTR) plants, the levels of H_2O_2 were very similar, indicating that additional stress was not generated during the plant acclimation **(Figure 5A)**. In PEG-treated plants, GmNAC065-OX lines show a discretely lower accumulation of ROS compared to Col-0, but significantly lower ROS content compared to GmNAC085-OX plants, as demonstrated by the MDA content **(Figure 5)**. Tun- and SA-treated plants display a similar pattern of TBA-reactive compounds, although the differences between GmNAC065-OX lines and GmNAC085-OX lines are accentuated. These treatments drastically impose an oxidative burst but the H_2O_2 and MDA contents of GmNAC065-OX plants remain lower than those of GmNAC085-OX lines, which show similar levels of these compounds as in wild type plants **(Figure 5B)**.

ROS accumulation emerges from imbalances in the photosynthetic apparatus and an impaired antioxidant system. In the transgenic plants, the gene induction of antioxidative enzymes catalase (CAT), superoxide-dismutase (SOD), and ascorbate-peroxidase (APX) was monitored **(Figure 6A).** GmNAC065-OX lines exhibit higher induction of anti-oxidative enzymes in multiple stresses than Col-0 and GmNAC085-OX plants. The activity of antioxidative enzymes correlated with the expression levels detected in wild type and transgenic plants. GmNAC065-OX lines displayed higher enzymatic activity even in untreated plants because of the enhanced transcript accumulation of the encoded genes **(Figure 6B)**. Under multiple stresses, the activity of the anti-oxidative enzymes remains significantly higher in GmNAC065 lines, followed by Col-0 and GmNAC085-OX.

A typical symptom of ROS accumulation is the breakdown of chlorophyll and other pigments (Torres *et al*., 2006; Petrov and Van Breusegem, 2012; Petrov *et al*., 2015).

The total chlorophyll content of *GmNAC065*-overexpressing transgenic leaves was higher than that of Col-0 and GmNAC085-OX leaves **(Figure 7A)**. After 24h of stresses, the chlorophyll content decreases, but GmNAC065-OX plants maintain the chlorophyll content higher than wild type and GmNAC085-OX plants. In contrast, GmNAC085-OX lines display a lower chlorophyll content in untreated plants, displaying a further decrease under multiple stresses, similarly to wild type plants.

ROS accumulation also leads to protein and DNA degradation. The protein decay in response to stress conditions in GmNAC085-OX lines was extensively higher than in GmNAC065-OX and Col-0 plants **(Figure 7B)**. In response to PEG and Tun treatments, the protein content decay reached almost 40% in GmNAC085-OX lines, against 15 - 20% (PEG) and 25 – 30% (Tun) observed in GmNAC065-OX and Col 0 plants, suggesting a robust biomolecules' breakdown system by high ROS accumulation in these plants. In SA-treated plants, the protein decay differences between the lines were attenuated, probably due to the oxidative burst caused by SA. However, GmNAC065-OX plants remained with the best performance.

The stress responses in plants involve multilayered stress-avoidance mechanisms that, along with tolerance mechanisms, confer the resistant phenotype. The co-expression analysis of genes in soybean revealed that *GmNAC065* positively correlates to genes involved in redox reactions, specifically those belonging to pigments biosynthesis. Thus, other antioxidant system branches were monitored, including the carotenoids, anthocyanins and soluble sugars contents in transgenic plants **(Figure 7C - E)**.

The carotenoid content displayed the same chlorophyll pattern in the transgenic lines, as *GmNAC065*-overexpressing plants exhibited higher levels of carotenoids than wild type and GmNAC085-OX plants **(Figure 7C)**. Curiously, anthocyanins content may not participate efficiently in the mechanisms involved in oxidative stress tolerance in GmNAC065-OX plants. Untreated GmNAC065-OX plants displayed lower anthocyanin content compared to untreated Col-0 and GmNAC085-OX plants. Under stress conditions, the anthocyanin content of GmNAC065-OX lines decreased to a similar level to Col-0, but it remained lower compared to GmNAC085-OX plants, except in response to Tun treatment. In this latter case, the GmNAC065-OX plants

displayed an anthocyanin content punctually higher than GmNAC085-OX plants **(Figure 7D)**.

Finally, the soluble sugars content was also analyzed. Untreated Col-0 and GmNAC065-OX lines displayed similar levels of soluble sugars in contrast to GmNAC085-OX lines, which displayed the lowest levels of these metabolites **(Figure 7E)**. After PEG treatment, GmNAC065-OX plants demonstrated higher sugar levels, indicating an osmoprotectant effect caused by sugar accumulation **(**Puniran-Hartley *et al*., 2014). The sugar content also increased in Col 0 and GmNAC085-OX lines, but in a lower ratio. In other treatments, the sugar content decayed after 24h of stress because of the extensive mobilization during ePCD triggering programs (Shi *et al*., 2016) and remained higher in plants overexpressing *GmNAC065*.

***GmNAC065* and *GmNAC085* differently regulates stress-triggered programmed cell death.**

Our genome- and transcriptome-wide analyses, supported by the biochemical characterization of the Arabidopsis transgenic lines, have associated *GmNAC065* and *GmNAC085* with different roles in ePCD. The extent of *GmNAC065*- and *GmNC085*-mediated ePCD was monitored by Evans blue leaf-staining **(Figure 8A)** and propidium iodide (PI) root-staining **(Figure 8B)** after 24h-treatment of transgenic lines with PEG, Tun and SA as well as by the transcriptional modulation of several SAGs regulated by different stimuli in Arabidopsis **(Figures 9 and 10)**.

Evans blue is a vital dye and only penetrates dead cells, indicating the extension of cell death in leaves. Likewise, PI is a fluorescent base-intercalating dye and stains the nucleus of dead cells in roots. The biochemical analyses showed that Tun and SA treatments induced ePCD, with extensive ROS accumulation and biomolecules breakdown **(Figures 5 and 7)**. Consequently, the extent of Tun- and SA-induced PCD was more remarkable compared to PEG-induced cell death **(Figure 8)**.

GmNAC065-OX lines displayed an attenuated ePCD phenotype compared to Col-0 and GmNAC085-OX, which displayed the most extensive cell death, as demonstrated by intense blue-staining in leaves and higher nuclei-staining and disrupted cells in

roots**(Figure 8)**. These results are consistent with thephenotypic and molecular analyses of GmNAC065-OX and GmNAC085-OX lines, which converge to an accentuated ePCD-phenotype observed in GmNAC085-OX lines in contrast to the GmNAC065-OX lines.

The basis for the intensity of a senescence phenotype is the extensive gene expression reprogramming and signaling in plants (Luoni *et al*., 2019). In Arabidopsis, gene regulatory networks (GRNs) involved in environmental and developmental signal integration triggering PCD are well characterized, and several NAC TFs function as regulators of these pathways (Balazadeh *et al*., 2011; Kim *et al*., 2014; Jensen *et al*., 2014; Podzimska-Sroka *et al*., 2015). In order to clarify how *GmNAC065* and *GmNAC085* affect ePCD in Arabidopsis, the expression levels of several AtSAGs and downstream targets that promote classic PCD phenotypes were accessed in a pool of transgenic lines exposed to different stresses. We also investigated the expression of drought-associated gene-markers (*RD29A*, *RD29B*, and *RD20*), as well as ER-stress-(*ANAC036*, *CNX*, and *AtNRP1*) and SA-associated markers (*WRKY70*, *RAB18*, and *AtNRP1*).

All stress marker genes were correctly up-regulated in Col-0, GmNAC065-OX, and GmNAC085-OX plants, indicating that the stress treatments were effective **(Figure 9)**. The expression levels of the putative *GmNAC065* and *GmNAC085* orthologs from Arabidopsis, the *ANAC083/VNI2* and *ANAC072 genes*, respectively, were also monitored. The induction of *ANAC083* and *ANAC072* in different stresses is not affected by the ectopic expression of the soybean orthologous genes **(Figure 9A)**. Nevertheless, under PEG, Tun, and SA treatments, their expression is remarkably higher in wild type plants than in transgenic lines. Interestingly, *ANAC083* in response to multiple stresses displays lower induction than *ANAC072*, supporting the phylogenetic analysis and the contrasting roles of these genes in ePCD, as suggested for their soybean orthologs.

In all treatments, several SAGs were up-regulated because of the severity of stress **(Figure 9B)**. In addition, many of them participate in integrative responses among environmental, hormone signaling, and adaptive responses (Luoni *et al*., 2019). In

general, GmNAC085-OX lines display expressive induction of SAGs in all analyzed treatments, opposing GmNAC065-OX lines **(Figure 9B)**.

Under PEG treatment, among the downstream SAGs targets, only the DNA-degrading promoter *BFN1*, the SA-catabolic gene *BMST1*, and the chlorophyll catabolic gene (CCG) *NYC1* were repressed in GmNAC085-OX lines. As expected, the chloroplast-maintenance gene *GLK1* was also repressed. In contrast, all SAGs and ePCD effectors were up-regulated with significantly higher levels than observed in GmNAC065-OX and Col-0 **(Figure 9B)**. In GmNAC065-OX lines, AtNAC-SAGs (*AtNAP*, *ATAF1*, *ORE1*, *ANAC016*, *ANAC019* and *ANAC055*) were weakly induced, and their downstream targets *NYC1* (NONYELLOW COLORING 1), *SINA1* (SEVEN IN ABSENTIA), *BFN1* (BIFUNCTIONA NUCLEASE1), *BSMT1* (S-ADENOSYLMETHIONINE-DEPENDENT METHYL-TRANSFERASE), *GLK1* (GOLDEN2-LIKE 1), and *SAG113* were down-regulated, and *CHL1* (CHS1-LIKE 1) was up-regulated, supporting our results of chlorophyll maintenance, lower protein decay and attenuated cell death symptoms.

A very similar pattern is observed in response to Tun treatment, and other SAGs not related to ER-stress responsive pathways were repressed or weakly induced in transgenic lines. Only the sugar-transporter *Sweet15* was down-regulated in GmNAC065-OX lines. All AtSAGs were up-regulated during SA treatment, in both GmNAC085-OX and GmNAC065-OX lines, although to a much higher extent in GmNAC085-lines. Pivotal AtSAGs controlling downstream genes involved in chlorophyll degradation/chloroplast maintenance (including *ATAF1*, *ORE1*, *SAG113*, *AtNAP*, and *PaO*), DNA and protein degradation (*SINA1* and *BFN1*), and hormone- and ROS-mediated signaling (*ATAF1*, *NCED3*) were massively up-regulated in GmNAC085 by at least one tested stress.

Discussion

Genome and transcriptome analysis of *Gm*NAC-SAGs uncover multiple stress-responsive genes that share sequence and functional conservation with *At*NAC-SAGs.

TFs act as converging nodes that integrate stress signals and programmed cell death responses. NAC TFs have been frequently associated with stress and cell death responses in several plants, such tobacco, oat, rice, maize, sunflower, and soybean (Even-Chen *et al*., 2015; Gepstein *et al*., 1980; Philosoph-Hadas *et al*., 1993; Quirino *et al*., 2000; Olsen *et al*., 2005; He *et al*., 2005; Lim *et al*., 2007; Podzimska-Sroka *et al*., 2015; Camargos *et al*., 2018). In Arabidopsis, the NAC TFs that respond to stress- and age-induced PCD are designated SAGs (senescence-associated genes), which have been shown to integrate GRN, but in crops, they are poorly studied, and their mechanisms of actions are still unclear. The comprehensive analysis of SAGs in crops offers a new insight over the cellular mechanisms of stress adaption and PCD, raising new possibilities for biotechnological intervention and development of modern agribusiness.

Herein, we performed a wide-genome analysis of NAC superfamily in soybean, and we identified 16 putative *Gm*NAC-SAGs, according to their phylogenetic relationship with *At*NAC-SAGs. Our analysis clustered the *At*NAC- and *Gm*NAC-SAGs in 7 groups, whose members were distributed into 5 different NAC subfamilies, as described by Melo *et al*. (2018). Eight genes, corresponding to 50% of putative *Gm*NAC-SAGs, belonged to the SNAC-A and SNAC-B subfamilies (Melo *et al*., 2018). These groups harbor functionally characterized Arabidopsis NAC-SAGs that have been implicated as positive regulators of leaf senescence, including *AtNAP* (group 5), *ATAF1* (group 6), *ANAC072*, *ANAC019*, and *ANAC055* (group 7 – Guo *et al*., 2006; Rauf *et al*., 2013; Hickman *et al*., 2013; Garapati *et al*., 2015). AtNAP targets directly SAG113, which enhances water losses, inhibiting the stomatal-closure (Zhang *et al*., 2012). In addition, the low levels of ABA along with the repression of ABA-responsive genes involved in chlorophyll catabolism, such as *NYC1* (non-yellow coloring 1) and *PaO* (pheide-a oxygenase), in *nap* mutants suggest that AtNAP controls chlorophyll content in an ABA-dependent manner (Yang *et al*., 2014). A similar mechanism is observed for ATAF1, which controls both the ABA and H_2O_2 signaling. In anti-ROS defective mutants, the expression of ATAF1 is higher than in the wild type, and it controls the expression of *NCED3* and *ABCG40*, genes involved in ABA biosynthesis and transport (Garapati *et al*., 2015). Furthermore, ATAF1 is supposed to be an essential player of ROS-mediated expression of *ORE1* and *GLK1*, up-regulating the expression of *ORE1* and down-regulating the expression of *GLK1*, a senescence-inducer and a gene involved

in chloroplast maintenance, respectively (Kim *et al*., 2009; Balazadeh *et al*., 2010; Garapati *et al*., 2015).

ANAC019, ANAC055, and ANAC072 are ATAF1 are close-related proteins (SNAC-A subgroup – Melo *et al*., 2018). They are induced by multiple stresses and display the same expression pattern under ABA treatment (Tran *et al*., 2004; Balazadeh *et al*., 2008; Jensen *et al*., 2010) and during age-induced senescence (Breeze *et al*., 2011). Microarray analysis in *anac019* and *anac055* mutants identified that these genes are differentially involved in flavonoids, JA, and SA signaling. In *anac019* mutants, genes involved in flavonoid biosynthesis and SA signaling are down-regulated, including *DFR* (dihydroflavonal reductase) and *F3H* (flavone 3-hydroxilase - Qi *et al*., 2011; Hickman *et al*., 2013; Li *et al*., 2014), whereas JA biosynthesis genes are up-regulated, including *LOX2* (lipoxygenase 2) and *PR4* (pathogenesis-related gene 4, Hickman *et al*., 2013). The opposite is observed in *anac055* mutants, suggesting that *ANAC019* enhances SA- and represses JA-signaling while *ANAC055* enhances JA- and represses SA-signaling, implying an antagonistic mechanism of these genes in pathogen-induced senescence (Qi *et al*., 2011; Hickman *et al*., 2013; Li *et al*., 2014; Podzimska-Sroka*et al*., 2015). The putative orthologous of *GmNAC085*, ANAC072, is implicated in the expression of chlorophyll catabolic and nutrients management genes, such as *CV* (chloroplast vesiculation) and *SWEET15*, an essential gene in chloroplast protein degradation and sugars transport in Arabidopsis, respectively (Li *et al*., 2016; Kamranfar *et al*., 2018).

We also detected GmNAC-SAGS in the NAM subfamily, represented by genes from groups 1 and 2. *ANAC016*, *ORS1*, and *ORE1* are well-characterized senescence promoting genes in Arabidopsis. ANAC016 is a positive regulator of *AtNAP* and *ORE1*, participating in the activation cascade of chlorophyll catabolic genes. *The anac016*mutant shows delayed senescence and down-regulation of several SAGs under salt and oxidative stresses (Kim *et al*., 2013). *ORE1* expression is controlled by *EIN2* during ethylene-induced senescence. It promotes senescence by binding the GLKs directly and inhibiting their transcriptional activities, affecting the chloroplasts maintenance and accelerating chlorophyll degradation through the activation of its catabolic genes, including *BFN1* (bifunctional nuclease 1) and *SWEET15* (Balazadeh *et al*., 2010; Rauf *et al*., 2013; Qiu *et al*., 2015). Similarly, *ORS1* integrates the *EIN2* GRN

and is responsive to severe salt- and oxidative-stress (Balazadeh *et al*., 2011; Kim *et al*., 2014).

Almost all NAC-SAGs are associated with the positive progression of leaf senescence. However, few NAC-SAG genes are involved in senescence delay and stress-protective mechanisms (Yang *et al*., 2011; Wu *et al*., 2012). The genes of groups 3 and 4 are phylogenetically divergent, and, naturally, may unroll different functions in senescence. The group 3 is represented by *ANAC042/JUB1*, a gene involved in the control of H_2O_2 levels. JUB1 overexpression results not exclusively in delayed senescence, but also in enhanced plant performance under several abiotic stresses (Wu *et al*., 2012). Additionally, *VNI2* (group 4) integrates ABA-dependent salvation pathways and directly activates COR and RD genes, already associated with plant longevity under stressful conditions (Yang *et al*., 2011; Wu *et al*., 2012). Surprisingly, VNI2 interacts with VND7, a PCD positive regulator, and its expression is regulated by ORE1 and AtNAP, also positive regulators of senescence (Yamaguchi *et al*., 2010; Kim *et al*., 2014). In soybean, GmNAC065 is up-regulated during senescence and by multiple stresses, including drought, ER-stress, and biotic stress. The GmNAC065 ectopic expression causes discrete symptoms of senescence (Melo *et al*., 2018) and, curiously, it interacts with GmNAC085, which is significantly up-regulated by drought and promotes senescence symptoms in transient expression in *N. benthamiana* (Melo *et al*., 2018).

The transcriptome-wide analysis demonstrated that many of *Gm*NAC-SAGs are differentially regulated by multiple stresses and hormones. They are also induced by age-triggered senescence. Thus, it is not surprising that NAC TFs integrate dPCD and ePCD signals in a fine-tuned hormone-mediated GRN (Jensen *et al*., 2014). Olvera-Carrillo *et al*. (2015) analyzed genes differentially expressed in Arabidopsis under multiple stress and during natural senescence, revealing a distinct set of genes involved in the control of ePCD and dPCD and suggesting independent pathways for age- and stress-triggered programmed cell death.

The soybean genes *GmNAC109*, *GmNAC011*, *GmNAC085*, *GmNAC043*, *GmNAC101*, and *GmNAC092* (groups 6 and 7 – SNAC-A and –B) are up-regulated by drought and oxidative stress. The increase on ROS production is a classical symptom shared by

different abiotic stresses and acts as a signal for the modulation ofePCD-related genes (Baena-Gonzalez *et al*., 2007; Miller *et al*., 2010; Jaspers and Kangasjarvi, 2010; Mittler and Blumwald, 2010; Atkinson and Urwin, 2012; Gechev *et al*., 2012). Interestingly, these genes were down-regulated during age-induced senescence, except for *GmNAC043* (a *GmNAC085* paralog), which was discretely up-regulated under this condition, suggesting that SNAC genes are strongly related with stress-responsiveness and environmental-triggered cell death. Genes phylogenetically related to negative regulators of senescence in Arabidopsis, such as *GmNAC065* and *GmNAC179* (group 4), are up-regulated by age-induced senescence and ethylene, and inductor of natural senescence, whereas *GmNAC154*, and *GmNAC106* (group 3) are exclusively regulated by age. These genes are not induced by stresses, substantiating the notion that different gene sets control dPCD and ePCD in soybean. Only the genes *GmNAC074*, *GmNAC0149*, *GmNAC010*, and *GmNAC003*, besides the non-classical SAGs *GmNAC081* (and the paralogous *GmNAC077*) and *GmNAC030*, are induced by drought and age-induced senescence.

Despite the divergent expression profile of *Gm*NAC-SAGs by multiple stresses and age-induced senescence, all genes were induced by bleomycin-treated soybean. Bleomycin acts as a genotoxic molecule and triggers DNA damage and PCD. As expected, the *Gm*NAC-SAGs respond differently to the treatment; NAM and SNAC-A and -B genes (groups 1, 2, 5, 6, and 7) are highly induced, including *GmNAC074*, *GmNAC023*, *GmNAC003*, *GmNAC109*, *GmNAC85*, and *GmNAC092*. Their putative paralogs also demonstrate a moderate induction in bleomycin-treated seedlings. In contrast,*GmNAC106* and *GmNAC065* from groups 3 and 4 are slightly induced by the bleomycin treatment. All pieces of evidence from the phylogenetic relationship of *Gm*NAC- and *At*NAC-SAGs, the structural and functional conservation of NAC subfamilies, the transcriptome analysis of NAC-SAGs in soybean, and their expression profile in response to bleomycin treatment suggest distinct groups of genes involved in dPCD and ePCD, as reported in Arabidopsis (Olvera-Carillo *et al*., 2015). Collectively, these observations make evident the contrasting roles of *GmNAC065* and *GmNAC085* in stress-responses and senescence in soybean.

The promoter analysis of *GmNAC065* and *GmNAC085* show overlapped elements and conserved blocks between soybean and Arabidopsis genes. However, their expression

profile in soybean under normal development and under different stresses link GmNAC065 and GmNAC085 to different functions. Both genes display recognition sites for NAC, MYB, AP2, and WRKY transcription factors, which are multiple-stress responsive genes that regulate senescence (Luoni *et al*., 2019). The W-box is the cognate element of WRKY, and the G-box is the cognate *cis*-element of bZIP, bHLH, and NAC proteins. These cis-elements are recognized by senescence and hormone-induced TFs, which act as nodes in the integration of ABA, cytokinins, brassinosteroids, auxin, gibberellins, and JA signals (Liu *et al*., 2016).

In soybean under normal development, *GmNAC065* and *GmNAC085* also have different expression patterns. In early developmental stages, *GmNAC065* is expressed in leaves and roots, but not in stems. In maize, Senu5 subfamily members, the same as *GmNAC065*, are abundantly expressed in many tissues during the vegetative stage, suggesting some conserved expression patterns of these genes in crops (Fan *et al*., 2014). GmNAC065 displays significantly higher expression in the reproductive stage, which indicates a function in developmental senescence (Guo and Gan, 2006; Fan *et al*., 2014; Melo *et al*., 2018). In contrast, G*mNAC085* displays lower expression in the vegetative stage and is only expressed during the reproductive stage, with lower expression levels than *GmNAC065*. Curiously, it displays an accentuated expression in stems and flowers, whose senescence and abscission are more evident during normal development, suggesting a weak relation with developmental programs.

During multiple stresses, *GmNAC065* and *GmNAC085* not only display different induction patterns with opposed kinetics. These genes are only co-expressed in drought treatments, and *GmNAC085* responds more effectively to the stress. In addition, *GmNAC065* displays an early-to-intermediate expression, whereas *GmNAC085* is stably expressed, with higher expression at the late stages of the stress. *GmNAC043*, a GmNAC085 paralog, shows the same expression profile in response to PEG, ABA, and air-dry treatments (Freitas *et al*., 2019). This pattern reinforces the role of *GmNAC085* in ePCD, triggered in advanced stages of stress-responses. *GmNAC065* and *GmNAC085* are co-related to a set of genes that indicates different cell environments. *GmNAC065* positively correlates to genes involved in plant maintenance and redox homeostasis. Late-embryogenesis abundant (LEA) proteins comprise a family of hydrophilic proteins well characterized as crucial regulators of plant desiccation tolerance in normal

development, mainly in seeds, and under different abiotic stresses (Dalal *et al., 2009). In soybean, LEA-extensins have been also implicated in*root maturation and elongation control (Ahn *et al*., 1998). *VNI2/ANAC083* (a *GmNAC065* orthologous) has been reported as a negative regulator of root development and xylem vessel formation (Yamaguchi *et al*., 2010), implicating *GmNAC065* as a presumable controller of the root developmental process. Furthermore, GmNAC065 shares a redox-balanced environment with enzymes involved in pigments metabolism; β-carotene hydroxylase 1 participates in the reaction that converts β-carotenoids to xanthophylls, which are pigments involved in redox balance in chloroplasts (Kim *et al*., 2009; Arango *et al*., 2014). Likewise, acyl-CoA oxidase is an enzyme of β-oxidation, and it is involved in several processes, such as energy suppliers in oilseeds, lipid turnover in senescence, and hormone production (JA and IAA – indol-acetic acid). In oxidative stress, this enzyme is also activated to increase the production of reducing intermediates, as a secondary product of its reaction (Arent, *et al*., 2008).

Differently, *GmNAC085* is expressed in drastic conditions, with ROS accumulation and depletion of biomolecules. ROS play an elementary role in cell death during the hypersensitive response (HR), a special pathogen-triggered PCD (Doke and Ohashi, 1988; Babbs *et al*., 1989). The oxidative burst triggers cell death and serves as secondary transducers, which diffuse the signals for induction of defense-related genes in neighboring cells (Levine *et al*., 1994). Many downstream processes are activated, such as the synthesis of lignins, phytoalexins, flavonoids, phenolic compounds, and other metabolites related to defense functions (Lamb *et al*., 1989; Cutt and Klessig, 1992; León *et al*., 1995). Moreover, during the HR,the cells undergo rapid lipid peroxidation and protein depletion, which, collectively, contributes to increasing the resistance of the host against the pathogen (Kato and Misawa, 1976; León *et al*., 1995). Several HR-related genes are co-expressed with *GmNAC085*, including enzymes of lignin biosynthesis, aromatic amino acids and many proteases, peroxidases and subunits of proteasome, suggesting a role of this gene in pathogen defense mechanisms.

Not surprisingly, *GmNAC065* and *GmNAC085* are negatively co-expressed with different genes that corroborate our previous observations. *GmNAC065* displays negative co-relation with gibberellins' metabolism genes and allene cyclase, an enzyme of JA bioavailability (Stenzel *et al*., 2012), indicating that it is not related to biotic

stress-mediated PCD. For *GmNAC085*, the gene is negatively co-related to enzymes involved in carotenoids and other antioxidant pigments and proteins biosynthesis (Zheng *et al*., 2015). Carotenoids play an important role in chloroplasts homeostasis during environmental stresses, as it exhibits photo-protective properties to the biotic and abiotic stresses-induced oxidative damages. GmNAC085 expression also diverges from the light-harvesting complexes (LHC), responsible for light-harvesting in normal photosynthesis andcatalyzing photo-protective reactions in oxidative stresses (Ballotari *et al*., 2012).

GmNAC065 and _GmNAC085_ expression in Arabidopsis impose different plant phenotypes under normal development and stress conditions.

The ectopic expression of GmNAC065 and GmNAC085 caused growth and development retardation, decreased number of leaves and rosette diameter, and reduced inflorescence length. Since the soybean genes are associated with different signaling pathways and cell environments, it is not clear why they cause similar phenotypes in Arabidopsis. One possible explanation would be that their function on senescence differentially affects growth-hormone pathways that converge to same phenotype. In Arabidopsis, *ANAC083/JUB1* negatively regulates brassinosteroid and gibberellin metabolism, leading to a plant dwarfism as observed in GmNAC065-OX plants (Shahnejat-Busheri *et al*., 2016). The same observation was reported in *ANAC046* and *ATAF-1* overexpressing lines, which exhibit imbalances in ABA-signaling, encompassing lower photosynthetic rate, consonant with the lower chlorophyll content of these plants (Wu *et al*., 2009; Garapati *et al*., 2015; Oda-Yamamizo *et al*., 2016)

Besides the reduced size, GmNAC065-OX plants exhibited a longer life cycle, with late flowering and delayed senescence. The reduced size of GmNAC065-OX plants might be due to their function on plant morpho-physiology control. The co-expression analysis of this gene in soybean indicates a negative co-expression of *GmNAC065* with gibberellins biosynthesis genes. Gibberellins are hormones related to inter-nodal, leaf, and shoot growth in plants (Brian, 1959), and these results suggest some repressive effect of the gene over the hormone-metabolism and plant development. In Arabidopsis, the expression of negative regulators of senescence leads to the same phenotype. *35S::VNI2* transgenic plants exhibited retarded growth in early stages of plant

development and enhanced leaf longevity as an effect of the positive regulation of COR/RD genes, whereas the mutant *vni2-1* displays the opposite phenotype (Yang *et al*., 2011). Additionally, the overexpression of *ANAC083/VNI2*, the putative paralogous of *GmNAC065*, also imposes plant growth delay, possibly because of its effect on vessel formation inhibition (Yamaguchi *et al*., 2010). As expected, the expression of *ANAC042/JUB1*, another negative regulator of senescence, negatively affects the synthesis of gibberellins and brassinosteroids, leading to a defective phenotype on growth, late flowering, and enhanced stress-tolerance, as observed to GmNAC065-OX plants (Shahnejat-Bushehri *et al*., 2016).

GmNAC085-OX plants displayed the same reduced phenotype, but, in contrast, exhibited accelerated life cycle and senescence. This phenotypic pattern is also observed in other SNAC-overexpressing plants; the expression of *OsNAC6/SNAC2* in rice causes developmental delay and yield losses (Nakashima *et* al., 2007), and the overexpression of *ATAF1* in Arabidopsis reduced lower growth ratio and accelerated senescence (Wu *et al*., 2009; Garapati *et al*., 2015). Not surprisingly, the expression of *ANAC072* (*RD26*), the *GmNAC085* paralog in Arabidopsis, leads to the activation of *the CV* gene, essential for chloroplast degradation, and *PES1*, involved in phytol degradation (Kamranfar *et al*., 2018). ANAC072 expression also promotes ABA-hypersensitivity, causing stunted growth, shorter inflorescences, and reduced flowers' number and seed yield, in addition to reduced chlorophyll content, precocious leaf yellowing, and anticipated senescence (Fujita *et al*., 2004).

At the molecular level, precedents in the literature have shown that senescence is associated with increases in ABA endogenous content and imbalances in enzymatic and non-enzymatic anti-oxidants for ROS-scavenging (Lee *et al*., 2011; Finkelstein, 2013; Garapati *et al*., 2015; Petrov *et al*., 2015; Zhu *et al*., 2016). Previous expression analyses of *GmNAC065* and *GmNAC085* in soybean established that *GmNAC085* rapidly responds to ABA external-stimuli in leaves and roots. Moreover, its ectopic expression accelerates senescence in *N. benthamiana* (Melo *et al*., 2018) and Arabidopsis (this work), strongly associating GmNAC085 with ABA-hypersensibility and ROS-mediated signaling.

To investigate further the *GmNAC085* and *GmNAC065* roles in senescence, we performed a robust characterization of enzymatic and non-enzymatic plant antioxidant systems in the transgenic lines overexpressing these genes. Our results demonstrated that GmNAC085-OX lines do not exhibit a robust anti-oxidative performance associated with lower transcription and activity of CAT, SOD, and APX, soluble sugars and carotenoids levels, and a remarkable decrease in chlorophyll content. The same phenotype is also observed in transgenic plants overexpressing other SNAC members, such as ATAF1 and ATAF2 (Garapati *et al.,* 2015; Nagahage *et al*., 2020). 35S::ATAF1 plants exhibit high levels of H_2O_2 and inhibited catalase activity, besides the up-regulation of genes involved in chlorophyll breakdown and ABA accumulation, as *ORE1* and *NCED3*, respectively. Overexpression of *ORE1* inhibits GLK, responsible for chloroplast maintenance, negatively affecting chlorophyll stability in transgenic plants (Garapati*et al*, 2015). Moreover, *ORE1* expression induces *SAG112*, accentuating the symptoms of senescence throughout GRN coordinated by ABA and ATAF1 (Mayta*et al*., 2019).

Along withthe enzymatic system inhibition, the non-enzymatic antioxidant system also responds weekly in the GmNAC085-OX lines. Carotenoids are poli-conjugated molecules that act as powerful anti-oxidizers in plants. The high content of carotenoids is generally associated with tolerant plants to stresses that cause ROS accumulation (Shah *et al*., 2017). Soluble sugars act in osmoregulation and protection, hydrating membranes, protecting the photosynthetic apparatus, and scavenging ROS (Tarkowski and Van den Ende, 2015). The content of carotenoids and soluble sugars in GmNAC085-OX plant are significantly lower than observed in wild type plants. The impaired enzymatic and non-enzymatic anti-oxidative systems of GmNAC085-OX lines result in the highest protein decay ratio in response to multiple stresses and the activation of ePCD mechanisms, observed as extensive cell damage in leaves and roots.

Only the anthocyanin content in GmNAC085-OX lines is not lower than those observed in GmNAC065-OX and Col-0 plants. Anthocyanins are commonly associated with tolerant plant-phenotypes to dehydration and high-light exposure (Chalker-Scott, 1999). Even with the hypersensitive phenotype of GmNAC085-OX plants to multiple stresses, the anthocyanin content remains higher than the other lines, suggesting a compensatory mechanism for oxidative stress tolerance once the ectopic expression of the soybean

gene leads to an impaired antioxidant system. Furthermore, *GmNAC085* responds to SA in soybean and, in Arabidopsis, triggers ROS production and accumulation. These features are classic responses against pathogens and might be associated with a SA-mediated activation of the phenylpropanoid pathway, as reported in grape and Arabidopsis (Obinata *et al*., 2003; Xu and Rothstein, 2018).

In contrast, GmNAC065-OX lines do not accumulate high ROS levels displaying lower MDA production, lower protein decay ratio, and less-extensive cell damage in leaves and roots as compared to Col-0 and GmNAC085-OX lines. These attenuated stress-induced cell death phenotypes may result from an improved antioxidant system, associated with a higher expression of CAT, SOD, and APX and higher sugar and carotenoid content. High concentrations of these metabolites reflect an efficient ROS-protective mechanism and reduce protein degradation under multiple stresses (Munné-Bosch and Alegre, 2000).

The contrasting phenotypes observed in GmNAC065-OX and GmNAC085-OX lines are not only explained by the differential expression profiles of these genes in soybean and their phylogenetic relatedness with different SAGs in Arabidopsis, but, mainly, by the differential regulation of age- and-stress integrated GRN. In GmNAC085-OX lines, the different stresses tested massively up-regulated the central regulators of ePCD, as *ATAF1* and *AtNAP*, besides other nodes in dPCD and ePCD, like *ORE1*. In **Figure 10,** we summarized the effect of environmental stimuli over the plant hormones and the GRNs integrated by AtSAGs in age and stress-induced PCD, extensively reviewed by Podzimska-Sroka *et al*., (2015) and Luoni *et al*., (2019), and the effect of GmNAC-SAGs expression in their regulation.

ORE1 integrates dPCD and ePCD by ethylene- and ABA-converging signals. Ethylene accumulation leads to the activation of the EIN TFs (ETHYLENE-INSENSITIVE - Kim et al., 2014; 2018), which activates a dPCD cascade that directly regulates chlorophyll catabolic genes (CCGs), such as*NYC1* and *PaO* (PHEOPHORBIDE A OXYGENASE) (Qiu *et al.*, 2015). The effect of ORE1 on chlorophyll degradation is due to its inhibitory activity on GLKs transcription, negatively affecting chloroplast maintenance and triggering leaf senescence (Rauf *et al*., 2013). Additionally, ORE1 disrupts cell integrity by activating genes involved in biomolecules degradation, as

BFN1, *Sweet15* (SUGARS WILL EVENTUALLY BE EXPORTER TRANSPORTERS 15), and *SINA1*(Matallana-Ramirez *et al.*, 2013).

The connection of ethylene and ABA-signaling throughout ORE1 is because ORE1 also controls the expression of *AtNAP*, whose expression increases in the presence of ABA and up-regulates *SAG113*, involved in stomatal opening/closure and water loss control in senescent leaves (Zhang *et al*., 2011). Most importantly, AtNAP inhibits AREB-1 (Garapati *et al*., 2015), consequently inhibiting the expression of RD genes and their positive effects in plant performance under stress (Melo *et al*., 2020). *AtNAP* also up-regulates the expression of ANAC016, which direct binding its promoter and the promoter of CCGs, accentuating senescence phenotype (Kim *et al*., 2013; Sakuraba *et al*., 2016).

The phenotypes resulting from the GmNAC085-mediated regulation of AtSAGs and their downstream targets reinforces the role of *GmNAC085* as a GmNAC-SAG by promoting ePCD coordinated by ABA and SA. GmNAC085-OX plants respond to different stresses and accumulate ROS, a classical feature of environmental stresses. We can also associate these features with the up-regulation of *ATAF1*, another important NAC-SAG which integrates ABA and ROS-signaling (Lu *et al*., 2007; Garapati *et al*., 2015). *ATAF1* accentuates senescence symptoms in three different manners: i. activating the expression of *ORE1* (Garapati *et al*., 2015); ii. blocking *GLK1* transcription (Garapati *et al*., 2015); iii. activating a feedforward regulation in ABA synthesis throughout the activation of NCED3, an essential enzyme in abscisic acid biosynthesis (Iuchi *et al*., 2001; Jensen *et al*., 2013), as observed in transgenic lines overexpressing *GmNAC085*.

Interestingly, the negative regulator of leaf senescence ANAC083 is also responsive to ABA (Yang *et al*., 2011), as the soybean orthologous GmNAC065, further demonstrating a complex plant regulatory pathway and the intricacy of how plant hormones can trigger survival or cell death pathways. In contrast to other ABA-induced positive senescence regulators, such as *ANAC019*, *ANAC055,* and *ANAC072* (Fujita *et al*., 2004; Hickman *et al*., 2013; Takasaki *et al*., 2015; Li *et al*., 2016), *ANAC083* improves plant longevity. Plants overexpressing the negative regulators of senescence *VNI2* and *JUB1* display an attenuated age- and stress-induced senescence (Yang *et al*.,

2011; Wu *et al*., 2012). *VNI2*-overexpressing plants, as well as *AREB-1*, exhibit higher transcriptional levels of *RD* (responsible for desiccation) genes, which integrate the AREB-1 pathway and enhance the enzymatic antioxidant system in plants (Yang *et al*., 2011; Melo *et al*., 2020). In *JUB1*-overexpressing plants, the same phenotype is observed. However, the stress attenuation mechanism involves the activation of DREB TF, which improves the anti-oxidative plant system via up-regulation of the glutathione S-transferase gene, and increases in proline and trehalose contents (Wu *et al*., 2012), similarly as observed in GmNAC065-OX plants.

Conclusion

Since the previous characterization of stress-responsive and senescence-associated genes in soybean, *GmNAC065* and *GmNAC085* have been associated with different functions in the control and integration of developmental- and environmental-triggered cell death programs. The results of the genome-wide analysis performed in this investigation allowed the establishment of a strong relationship between the soybean genes and the well-characterized AtNAC-SAGs. Interestingly, *GmNAC065* is a putative ortholog of *ANAC083/VNI2* and *GmNAC085* is a putative ortholog of *ANAC072*.These Arabidopsis genes belong to different SAGs groups and exhibit contrasting senescence functions, as suggested for the soybean genes. *GmNAC065* and *GmNAC085* are differentially induced by biotic and abiotic stresses, as well as by natural- and bleomycin-induced PCD in soybean. Additionally, they display different expression profiles in soybean tissues during reproductive and vegetative stages. The expression of *GmNAC085*is higher in advanced life-stages and tissues, in which the senescence process is more evident, such as leaves, stems, and flowers. Co-expression analysis in soybean revealed that *GmNAC065* is positively co-expressed with anti-oxidative-associated genes, whereas *GmNAC085* is positively co-expressed with genes involved in pigments and proteins breakdown, and hormone signaling. Finally, the characterization of transgenic Arabidopsis lines ectopically expressing *GmNAC065* and *GmNAC085* offered new insights into the function of these soybean genes in dPCD and ePCD. GmNAC065-OX lines harbor a robust enzymatic and non-enzymatic antioxidant system, with higher chlorophyll, carotenoid and soluble sugar contents, besides up-regulation and increased activity of anti-oxidant enzymes. Moreover, the expression of

positive-regulators of senescence in Arabidopsis is attenuated in these lines, conferring them a senescence-delayed phenotype under multiple stresses and normal development. In contrast, in the GmNAC085-OX lines, key regulators of ABA-, SA- and ROS-mediated programmed cell death are up-regulated, contributing to the accelerated senescence phenotype in the same conditions. Collectively, our data provide new insights into the integrated regulatory mechanisms of normal development, stress-responses, and programmed cell death, setting up GmNAC-SAGS, especially *GmNAC065* and *GmNAC085*, as suitable targets for biotechnology intervention and modern crop breeding.

References

Ahn JH, Choi Y, Kim S-G, Kwon YM, Choi YD, Lee JS. (1998). Expression of a soybean hydroxyproline-rich glycoprotein gene is correlated with maturation of roots. Plant Physiol. 116:671–679

Arango J, Jourdan M, Geoffriau E, Beyer P, Welsch R.(2014). Carotene Hydroxylase Activity Determines the Levels of Both α-Carotene and Total Carotenoids in Orange Carrots. Plant Cell, 26(5):2223-2233. doi: 10.1105/tpc.113.122127.

Arent S, Pye VE, Henriksen A. (2008). Structure and function of plant acyl-CoA oxidases. Plant PhysiolBiochem., 46(3):292-301. doi: 10.1016/j.plaphy.2007.12.014.

Atkinson N. J., Urwin P. E. (2012). The interaction of plant biotic and abiotic stresses: from genes to the field. J. Exp. Bot., 63, 3523–3543. doi:10.1093/jxb/ers100

Babbs CF, Pham JA, Coolbaugh RC. (1989) Lethal hydroxyl radical production in paraquat-treated plants. Plant Physiol90: 1267–1270.doi: 10.1104/pp.90.4.1267

Baena-Gonzalez E., Rolland F., Thevelein J. M., Sheen J. (2007). A central integrator of transcription networks in plant stress and energy signalling. Nature 448 938–942. doi:10.1038/nature06069

Balazadeh, S., Riaño-Pachón, D.M., Mueller-Roeber, B. (2008). Transcription factors regulating leaf senescence in Arabidopsis thaliana. Plant Biol., 10, 63–75. doi: 10.1111/j.1438-8677.2008.00088.x

Balazadeh, S., Siddiqui, H., Allu, A. D., Matallana-Ramirez, L. P., Caldana, C., Mehrnia, M., Zanor, M.-I., Köhler, B., and Mueller-Roeber, B. (2010). A gene regulatory network controlled by the NAC transcription factor ANAC092/AtNAC2/ORE1 during salt-promoted senescence: ANAC092 gene regulatory network. The Plant Journal 62:250–264.

Balazadeh, S., Kwasniewski, M., Caldana, C., Mehrnia, M., Zanor, M. I., Xue, G. P., & Mueller-Roeber, B. (2011). ORS1, an H_2 O_2 -responsive NAC transcription factor, controls senescence in Arabidopsis thaliana. Molecular plant, 4(2), 346–360. https://doi.org/10.1093/mp/ssq080

Ballottari M., Girardon J., Dall'osto L., Bassi R. (2012). Evolution and functional properties of photosystem II light harvesting complexes in eukaryotes. Biochim. Biophys. Acta, 1817(1):143-57. doi: 10.1016/j.bbabio.2011.06.005

Basu, S., and Roychoudhury, A. (2014). Expression Profiling of Abiotic Stress-Inducible Genes in response to Multiple Stresses in Rice (Oryza sativa L.) Varieties with Contrasting Level of Stress Tolerance. BioMed Research International 2014:1–12.

BengoaLuoni, S., Astigueta, F. H., Nicosia, S., Moschen, S., Fernandez, P., and Heinz, R. (2019). Transcription Factors Associated with Leaf Senescence in Crops. Plants 8:411.

Breeze, E., Harrison, E., McHattie, S., Hughes, L., Hickman, R., Hill, C., Kiddle, S., Kim, Y., Penfold, C. A., Jenkins, D., et al. (2011). High-Resolution Temporal Profiling of Transcripts during Arabidopsis Leaf Senescence Reveals a Distinct Chronology of Processes and Regulation. Plant Cell 23:873–894.

Buchanan-Wollaston, V. (2007). Senescence in Plants. In Encyclopedia of Life Sciences (ed. John Wiley & Sons, Ltd, p. a0020133. Chichester, UK: John Wiley & Sons, Ltd.

Buchanan-Wollaston, V., Earl, S., Harrison, E., Mathas, E., Navabpour, S., Page, T., and Pink, D. (2002). The molecular analysis of leaf senescence - a genomics approach: Molecular analysis of plant senescence. Plant Biotechnology Journal 1:3–22.

Buchanan-Wollaston, V., Page, T., Harrison, E., Breeze, E., Lim, P. O., Nam, H. G., Lin, J. F., Wu, S. H., Swidzinski, J. and Ishizaki, K. et al. (2005). Comparative transcriptome analysis reveals significant differences in gene expression and signalling pathways between developmental and dark/starvation-induced senescence in Arabidopsis. Plant J. 42, 567–585. doi:10.1111/j.1365-313X.2005.02399.x

Cao ZH, Zhang SZ, Wang RK, Zhang RF, Hao YJ. (2013). Genome wide analysis of the apple MYB transcription factor family allows the identification of MdoMYB121 gene confering abiotic stress tolerance in plants. PLoS One, 26;8(7):e69955. doi:10.1371/journal.pone.0069955

Cao, L., Yu, Y., Ding, X., Zhu, D., Yang, F., Liu, B., et al. (2017). The Glycine soja NAC transcription factor GsNAC019 mediates the regulation of plant alkaline tolerance and ABA sensitivity. Plant. Mol. Biol. 95, 253–268. doi: 10.1007/s11103-017-0643-3

Carrión, C. A., Costa, M. L., Martínez, D. E., Mohr, C., Humbeck, K., and Guiamet, J. J. (2013). In vivo inhibition of cysteine proteases provides evidence for the involvement of ‘senescence-associated vacuoles’ in chloroplast protein degradation during dark-induced senescence of tobacco leaves. Journalof Experimental Botany 64:4967–4980.

Carvalho, H. H., Brustolini, O. J., Pimenta, M. R., Mendes, G. C., Gouveia, B. C., Silva, P. A., et al. (2014a). The molecular chaperone binding protein BiP prevents leaf

dehydration-induced cellular homeostasis disruption. PLoS ONE 9:e86661. doi: 10.1371/journal.pone.0086661

Chalker- Scott L. (1999). Environmental significance of anthocyanins in plant stress responses. Photochemistry and Photobiology70: 1– 9. doi:10.1111/j.1751-1097.1999.tb01944.x

Chen, X., Wang, Y., Lv, B., Li, J., Luo, L., Lu, S., Zhang, X., Ma, H., and Ming, F. (2014). The NAC Family Transcription Factor OsNAP Confers Abiotic Stress Response Through the ABA Pathway. Plant and Cell Physiology 55:604–619.

Cheng MC, Liao PM, Kuo WW, Lin TP (2013) The Arabidopsis ETHYLENE RESPONSE FACTOR1 regulates abiotic stress-responsive gene expression by binding to different cis-acting elements in response to different stress signals. Plant Physiol162: 1566–1582. doi:10.1104%2Fpp.113.221911

Christiansen, M. W., and Gregersen, P. L. (2014). Members of the barley NAC transcription factor gene family show differential co-regulation with senescence-associated genes during senescence of flag leaves. Journal of Experimental Botany 65:4009–4022.

Christiansen, M. W., Matthewman, C., Podzimska-Sroka, D., O'Shea, C., Lindemose, S., Møllegaard, N. E., Holme, I. B., Hebelstrup, K., Skriver, K., and Gregersen, P. L. (2016). Barley plants over-expressing the NAC transcription factor gene HvNAC005 show stunting and delay in development combined with early senescence. EXBOTJ 67:5259–5273.

Christiansen, M.W.; Holm, P.B.; Gregersen, P.L. (2011). Characterization of barley (Hordeum vulgare L.) NAC transcription factors suggests conserved functions

compared to both monocots and dicots. BMC Res. Notes, 4, 1–13. doi: 10.1186/1756-0500-4-302

Chung, P.J.; Jung, H.; Choi, Y.D.; Kim, J.-K. (2018) Genome-wide analyses of direct target genes of four rice NAC-domain transcription factors involved in drought tolerance. BMC Genom., 19, 40. doi: 10.1186/s12864-017-4367-1

Costa MDL, Reis PAB, Valente MAS, Irsigler AST, Carvalho CM, Loureiro ME, Aragão FJL, Boston RS, Fietto LG, Fontes EPB. (2008). A new branch of endoplasmic reticulum stress signaling and the osmotic signal converge on plant-specific asparagine-rich proteins to promote cell death. J Biol Chem 283: 20209–2021. doi:10.1104/pp.111.179697

Cutt, J.R. and D.F. Klessig. (1992). Salicylic acid in plants: A changing perspective. Pharmaceut. Technol., 16: 26-34

Dalal, M., Tayal, D., Chinnusamy, V. & Bansal, K. C. (2009). Abiotic stress and ABA-inducible group 4 LEA from Brassica napus plays a key role in salt and trought tolerance. J. Biotechnol. 139, 137–145

Davison PA, Hunter CN, Horton P (2002) Overexpression of β-carotene hydroxylase enhances stress tolerance in Arabidopsis. Nature, 418:203–206. doi: 10.1038/nature00861

de Camargos, L.F., Fraga, O.T., Oliveira, C.C. et al.(2019). Development and cell death domain-containing asparagine-rich protein (DCD/NRP): an essential protein in plant development and stress responses. Theor. Exp. PlantPhysiol.31, 59–70. doi:10.1007/s40626-018-0128-z

de Melo, B. P., Lourenço-Tessutti, I. T., Paixão, J. F. R., Noriega, D. D., Silva, M. C. M., de Almeida-Engler, J., Fontes, E. P. B., and Grossi-de-Sa, M. F. (2020). Transcriptional modulation of AREB-1 by CRISPRa improves plant physiological performance under severe water deficit. Sci Rep 10:16231.

Doke, N., Ohashi, Y. (1988). Involvement of an O_2^- generating system in the induction of necrotic lesions on tobacco-leaves infected with tobacco mosaic virus. Physiol Mol Plant Pathol., 32:163–175. doi:10.1016/S0885-5765(88)80013-4

Du, H., Yang, S., Liang, Z. et al. Genome-wide analysis of the MYB transcription factor superfamily in soybean. BMC Plant Biol12, 106 (2012). doi:10.1186/1471-2229-12-106

El Mannai, Y., Akabane, K., Hiratsu, K., Satoh-Nagasawa, N., and Wabiko, H. (2017). The NAC Transcription Factor Gene OsY37 (ONAC011) Promotes Leaf Senescence and Accelerates Heading Time in Rice. IJMS 18:2165.

Even-Chen Z., Itai C. (2015). The role of abscisic acid in senescence of detached tobacco leaves. Physiol. Plant., 34:97–100. doi: 10.1111/j.1399-3054.1975.tb03799.x

Fan K, Wang M, Miao Y, et al. (2014). Molecular evolution and expansion analysis of the NAC transcription factor in Zea mays. PLoSOne, 9(11):e111837. doi:10.1371/journal.pone.0111837

Faria JAQA, Reis PAB, Reis MTR, Rosado GL, Pinheiro GL, Mendes GC, Fontes EPB. (2011). The NAC domain-containing protein, GmNAC6, is a downstream component of the ER stress- and osmotic stress-induced NRP-mediated cell-death signaling pathway. BMC Plant Biol 11: 129. doi: 10.1186/1471-2229-11-129

Finkelstein R. (2013). Abscisic Acid synthesis and response. Arabidopsis Book., 11:e0166. doi:10.1199/tab.0166

Freitas EO, Melo BP, Lourenço-Tessutti IT, et al. Identification and characterization of the GmRD26 soybean promoter in response to abiotic stresses: potential tool for biotechnological application. BMC Biotechnol. 2019;19(1):79. Published 2019 Nov 20. doi:10.1186/s12896-019-0561-3

Fujita, M., Fujita, Y., Maruyama, K., Seki, M., Hiratsu, K., Ohme-Takagi, M., et al. (2004). A dehydration-induced NAC protein, RD26, is involved in a novel ABA-dependent stress-signaling pathway. Plant J. 39, 863–876. doi: 10.1111/j.1365-313X.2004.02171.x

Garapati, P., Xue, G. P., Munné-Bosch, S., and Balazadeh, S. (2015). Transcription factor ATAF1 in Arabidopsis promotes senescence by direct regulation of key chloroplast maintenance and senescence transcriptional cascades. Plant Physiol. 168, 1122–1139. doi: 10.1104/pp.15.00567

Gates, D.J., Strickler, S.R., Mueller, L.A. et al. (2016). Diversification of R2R3-MYB Transcription Factors in the Tomato Family Solanaceae. J Mol Evol83, 26–37. doi:10.1007/s00239-016-9750-z

Gechev T. S., Dinakar C., Benina M., Toneva V., Bartels D. (2012). Molecular mechanisms of desiccation tolerance in resurrection plants. Cell Mol. Life Sci., 69, 3175–3186. doi:10.1007/s00018-012-1088-0

Gechev T. S., Hille J. (2005). Hydrogen peroxide as a signal controlling plant programmed cell death.*J. Cell Biol.*168 17–20. doi:10.1083/jcb.200409170

Gepstein S., Thimann K.V. (1980). Changes in the abscisic acid content of oat leaves during senescence. Proc. Natl. Acad. Sci. USA., 77:2050–2053. doi: 10.1073/pnas.77.4.2050.

Guo H, Ecker JR. (2004) The ethylene signaling pathway: new insights. CurrOpin Plant Biol., 7(1):40-9. doi: 10.1016/j.pbi.2003.11.011

Guo, M., Liu, J.-H., Ma, X., Luo, D.-X., Gong, Z.-H., and Lu, M.-H. (2016). The Plant Heat Stress Transcription Factors (HSFs): Structure, Regulation, and Function in Response to Abiotic Stresses. Front. Plant Sci. 7.

Guo, Y., and Gan, S. (2006). AtNAP, a NAC family transcription factor, has an important role in leaf senescence. Plant J. 46, 601–612. doi: 10.1111/j.1365-313X.2006.02723.x

Guo, Y., Cai, Z., and Gan, S. (2004). Transcriptome of Arabidopsis leaf senescence. Plant Cell Environ 27:521–549.

Guo, Y.; Gan, S. (2006). AtNAP, a NAC family transcription factor, has an important role in leaf senescence. Plant J., 46, 601–612. doi: 10.1111/j.1365-313X.2006.02723.x

H.J., Hong, S.H., Kim, Y.W., Lee, I.H., Jun, J.H.,Phee, B.K.,Rupak, T.,Jeong, H., Lee, Y.,Hara-Nishimura, I., Hatsugai, N., Nakaune, S., Kuroyanagi, M., and Nishimura, M. (2005). Vacuolar processing enzyme: an executor of plant cell death. Current Opinion in Plant Biology 8:404–408.

He P., Osaki M., Takebe M., Shinano T., Wasaki, J. (2005). Endogenous hormones and expression of senescence-related genes in different senescent types of maize. J. Exp. Bot.,56: 1117–1128

He, Q., Jones, D., Li, W. et al. (2016) Genome-Wide Identification of R2R3-MYB Genes and Expression Analyses During Abiotic Stress in Gossypium raimondii. Sci Rep6, 22980. doi:10.1038/srep22980

Hickman, R., Hill, C., Penfold, C. A., Breeze, E., Bowden, L., Moore, J. D., Zhang, P., Jackson, A., Cooke, E., Bewicke-Copley, F., et al. (2013). A local regulatory network around three NAC transcription factors in stress responses and senescence in Arabidopsis leaves. Plant J 75:26–39.

Hong, B.S.; et al. (2014). Gene regulatory cascade of senescence-associated NAC transcription factors activated by ETHYLENE-INSENSITIVE2-mediated leaf senescence signalling in Arabidopsis. J. Exp. Bot. 65, 4023–4036. doi: 10.1093/jxb/eru112

Irsigler, A. S., Costa, M. D., Zhang, P., Reis, P. A., Dewey, R. E., Boston, R. S., and Fontes, E. P. (2007). Expression profiling on soybean leaves reveals integration of ER- and osmotic-stress pathways. BMC Genomics 8:431.

Iuchi,S., Kobayashi, M., Taji, T., Naramoto, M., Seki, M., Kato,T., Tabata, S., Kakubari, Y., Yamaguchi-Shinozaki, K., Shinozaki, K. (2001). Regulation of drought tolerance by gene manipulation of 9-cis-epoxycarotenoid dioxygenase, a key enzyme in abscisic acid biosynthesis in Arabidopsis. Plant J., 27, 325-333. doi: 10.1046/j.1365-313x.2001.01096.x

Jaspers P, Kangasjärvi J. (2010) Reactive oxygen species in abiotic stress signaling. Physiol Plant., 138(4):405-13. doi: 10.1111/j.1399-3054.2009.01321.x.

Jensen MK, Skriver K. (2014). NAC transcription factor gene regulatory and protein-protein interaction networks in plant stress responses and senescence. IUBMB Life, 66(3):156-166. doi: 10.1002/iub.1256

Jensen, M.K., Kjaersgaard,T., Nielsen,M.M., Galberg, P., Petersen,K., O'Shea, C., Skriver, K. (2010). The *Arabidopsis thaliana* NAC transcription factor family: structure–function relationships and determinants of ANAC019 stress signalling. *Biochem, J*., 426 (2): 183–196. 0.1042/BJ20091234

Kamranfar, I., Xue, G.-P., Tohge, T., Sedaghatmehr, M., Fernie, A. R., Balazadeh, S., and Mueller-Roeber, B. (2018). Transcription factor RD26 is a key regulator of metabolic reprogramming during dark-induced senescence. New Phytol 218:1543–1557.

Kato, S., Misawa, T. (1976). Lipid peroxidation during the appearance of hypersensitive reaction in cowpea leaves infected with cucumber mosaic virus. Annu. Phytopathol. Soc. lp n. 42:472-80

Kim JH, Woo HR, Kim J, Lim PO, Lee IC, Choi SH, Hwang D, Nam HG. (2009). Trifurcate feed-forward regulation of age-dependent cell death involving miR164 in Arabidopsis. Science, 323(5917):1053-7. doi: 10.1126/science.1166386.

Kim, H. J., Nam, H. G., and Lim, P. O. (2016). Regulatory network of NAC transcription factors in leaf senescence. Current Opinion in Plant Biology 33:48–56.

Kim, H. J., Park, J.-H., Kim, J., Kim, J. J., Hong, S., Kim, J., Kim, J. H., Woo, H. R., Hyeon, C., Lim, P. O., et al. (2018). Time-evolving genetic networks reveal a NAC troika that negatively regulates leaf senescence in Arabidopsis. Proc Natl Acad Sci USA 115:E4930–E4939.

Kim, H.J., Hong, S.H., Kim, Y.W., Lee, I.H., Jun, J.H.,Phee, B.K., Rupak, T., Jeong, H., Lee, Y., Kim, Y.S.,Sakuraba, Y., Han, S.H.,Yoo, S.C.,Paek, N.C. (2013). Mutation of the Arabidopsis NAC016 Transcription Factor Delays Leaf Senescence. Plant Cell Physiol., 54, 1660–1672. doi: 10.1093/pcp/pct113

Lam, E. (2004). Controlled cell death, plant survival and development. Nat Rev Mol Cell Biol 5:305–315.

Lamb, C.J., Lawton, M.A., Dron, M., Dixon, R.A. (1989). Signals and transduction mechanisms for activation of plant defenses against microbial attack. Cell, 56(2):215-24. doi: 10.1016/0092-8674(89)90894-5.

Lee I. C., Hong S. W., Whang S. S., Lim P. O., Nam H. G., Koo J. C. (2011). Age-dependent action of an ABA-inducible receptor kinase, RPK1, as a positive regulator of senescence in Arabidopsis leaves.*Plant Cell Physiol.*52 651–662. doi:10.1093/pcp/pcr026

Lees, D. H.; Francis, F. J. Standardization of pigment analyses in cranberries. Hortscience, Alexandria 7, 1, p. 83-84, 1972

Leon J., Lawton, M.A., Raskin, I. (1995). Hydrogen peroxide stimulates salicylic acid biosynthesis in tobacco. Plant Physiol108**:** 1673–1678. doi:10.1104%2Fpp.108.4.1673

Leshem, Y. (1988). Plant senescence processes and free radicals. Free Radical Biology and Medicine 5:39–49.

Levine A, Tenhaken R, Dixon R, Lamb C. (1994). H_2O_2 from the oxidative burst orchestrates the plant hypersensitive disease resistance response. Cell, 18;79(4):583-93. doi: 10.1016/0092-8674(94)90544-4

Li S. (2014). Transcriptional control of flavonoid biosynthesis: fine-tuning of the MYB-bHLH-WD40 (MBW) complex. Plant Signal Behav., 9(1):e27522. doi: 10.4161/psb.27522

Li, X.; Li, M.; Yan, Y.; Liu, X.; Li, L. (2016). Dual Function of NAC072 in Gene Regulation in Arabidopsis. Front. Plant Sci.,7, 1075. doi:10.3389%2Ffpls.2016.01075

Liang, C., Wang, Y., Zhu, Y., Tang, J., Hu, B., Liu, L., Ou, S., Wu, H., Sun, X., Chu, J., et al. (2014). OsNAP connects abscisic acid and leaf senescence by fine-tuning abscisic acid biosynthesis and directly targeting senescence-associated genes in rice. Proc Natl Acad Sci USA 111:10013–10018.

Lim, P. O., Kim, H. J., and Gil Nam, H. (2007). Leaf Senescence. Annu. Rev. Plant Biol. 58:115–136.

Lindemose, S., Jensen, M. K., de Velde, J. V., O'Shea, C., Heyndrickx, K. S., Workman, C. T., Vandepoele, K., Skriver, K., and Masi, F. D. (2014). A DNA-binding-site landscape and regulatory network analysis for NAC transcription factors in Arabidopsis thaliana. Nucleic Acids Res 42:7681–7693.

Liu J, Chen X, Liang X, Zhou X, Yang F, Liu J, et al. (2016). Alternative splicing of rice WRKY62 and WRKY76 transcription factor genes in pathogen defense. Plant Physiol., 171:1427–42.doi: 10.1104/pp.15.01921

Llorca, C. M., Potschin, M., and Zentgraf, U. (2014). bZIPs and WRKYs: two large transcription factor families executing two different functional strategies. Front. Plant Sci. 5.

Lu, C.- A., Ho, T.- h.D., Ho, S.- L. and Yu, S.- M. (2002) Three novel MYB proteins with one DNA binding repeat mediate sugar and hormone regulation of α- amylase gene expression. Plant Cell, 14, 1963– 1980. doi:10.1105/tpc.001735

Lu, P. L., Chen, N. Z., An, R., Su, Z., Qi, B. S., Ren, F., et al. (2007). A novel drought-inducible gene, ATAF1, encodes a NAC family protein that negatively regulates the expression of stress-responsive genes in Arabidopsis. Plant Mol. Biol. 63, 289–305 doi: 10.1007/s11103-006-9089-8

Magwanga RO, Lu P, Kirungu JN, Lu H, Wang X, Cai X, Zhou Z, Zhang Z, Salih H, Wang K, Liu F. (2018). Characterization of the late embryogenesis abundant (LEA) proteins family and their role in drought stress tolerance in upland cotton. BMC Genet., 15;19(1):6. doi: 10.1186/s12863-017-0596-1

Martínez, D.E., Costa, M.L., Gomez, F.M., Otegui, M.S., Guiamet, J.J. (2008). Senescence-associated vacuoles are involved in the degradation of chloroplast proteins in tobacco leaves. Plant J., 56, 196–206. doi: 10.1111/j.1365-313X.2008.03585.x

Matallana-Ramirez, L.P., Rauf, M., Farage-Barhom, S., Dortay, H., Xue G.P., Dröge-Laser W., Lers, A., Balazadeh, S., Mueller-Roeber, B. (2013). NAC transcription factor ORE1 and senescence-induced BIFUNCTIONAL NUCLEASE1 (BFN1) constitute a regulatory cascade in Arabidopsis. Mol. Plant., 6(5):1438-52. doi: 10.1093/mp/sst012

Mayta M.L., Hajirezaei, M.R., Carrillo, N., Lodeyro, A.F. (2019). Leaf Senescence: The Chloroplast Connection Comes of Age. Plants, 8(11):495. doi:10.3390/plants8110495.

Melo, B. P., Fraga, O. T., Silva, J. C. F., Ferreira, D. O., Brustolini, O. J. B., Carpinetti, P. A., Machado, J. P. B., Reis, P. A. B., and Fontes, E. P. B. (2018). Revisiting the Soybean GmNAC Superfamily. Frontiers in Plant Science 9:1864.

Mendes, G. C., Reis, P. A. B., Calil, I. P., Carvalho, H. H., Aragao, F. J. L., and Fontes, E. P. B. (2013). GmNAC30 and GmNAC81 integrate the endoplasmic reticulum stress- and osmotic stress-induced cell death responses through a vacuolar processing enzyme. Proceedings of the National Academy of Sciences 110:19627–19632.

Miller G., Suzuki N., Ciftci-Yilmaz S., Mittler R. (2010). Reactive oxygen species homeostasis and signalling during drought and salinity stresses. Plant Cell Environ. 33 453–467. doi:10.1111/j.1365-3040.2009.02041.x

Mittler R., Blumwald E. (2010). Genetic engineering for modern agriculture: challenges and perspectives. Annu. Rev. Plant Biol. 61, 443–462. doi:10.1146/annurev-arplant-042809-112116

Munné-Bosch S. and Alegre L. (2003). Drought-induced changes in the redox state of alpha-tocopherol, ascorbate, and the diterpene carnosic acid in chloroplasts of Labiatae species differing in carnosic acid contents. Plant Physiol., 131(4):1816-1825. doi:10.1104/pp.102.019265

Nagahage I.S.P., Sakamoto S., Nagano M., Ishikawa T., Mitsuda N., Kawai-Yamada M., Yamaguchi M. (2020). An Arabidopsis NAC domain transcription factor, ATAF2, promotes age-dependent and dark-induced leaf senescence. Physiol Plant., 170(2):299-308. doi: 10.1111/ppl.13156

Nakashima, K., Takasaki, H., Mizoi, J., Shinozaki, K., and Yamaguchi-Shinozaki, K. (2012). NAC transcription factors in plant abiotic stress responses. Biochimica et Biophysica Acta (BBA) - Gene Regulatory Mechanisms 1819:97–103.

Nakashima, K., Tran, L. S., Van Nguyen, D., Fujita, M., Maruyama, K., and Todaka, D. (2007). Functional analysis of a NAC- type transcription factor OsNAC6 involved in

abiotic and biotic stress- responsive gene expression in rice. Plant J. 51, 617–630. doi: 10.1111/j.1365-313X.2007.03168.x

Obinata, N., Yamakawat, T., Takamiya, M., Tanaka, N., Ishimaru, K., Kodama, T. (2003). Effects of Salicylic Acid on the Production of Procyanidin and Anthocyanin in Cultured Grape Cell. Plant Biotechnol., 20, 105–111. doi:10.5511/plantbiotechnology.20.105

Oda-Yamamizo, C., Mitsuda, N., Sakamoto, S. et al. (2016). The NAC transcription factor ANAC046 is a positive regulator of chlorophyll degradation and senescence in Arabidopsis leaves. Sci. Rep.,6, 23609. doi:10.1038/srep23609

Oh, S. A., Park, J. H., Lee, G. I., Paek, K. H., Park, S. K. and Nam, H. G. (1997). Identification of three genetic loci controlling leaf senescence in Arabidopsis thaliana. Plant J. 12, 527–535. doi:10.1046/j.1365-313X.1997.00527.x

Olsen A.N., Ernst H.A., Leggio L.L., Skriver K. (2005). NAC transcription factors: Structurally distinct, functionally diverse. Trends Plant Sci., 10:79–87. doi:10.1016/j.tplants.2004.12.010.

Olvera-Carrillo, Y., Van Bel, M., Van Hautegem, T., Fendrych, M., Van Durme, M., Huysmans, M., Šimášková, M., Buscaill, P., Rivas, S., Coll, N. S., et al. (2015). A conserved core of PCD indicator genes discriminates developmentally and environmentally induced programmed cell death in plants. Plant Physiol. Advance Access published October 5, 2015, doi:10.1104/pp.15.00769.

Park, S.-Y., Yu, J.-W., Park, J.-S., Li, J., Yoo, S.-C., Lee, N.-Y., Lee, S.-K., Jeong, S.-W., Seo, H. S., Koh, H.-J., et al. (2007). The Senescence-Induced Staygreen Protein Regulates Chlorophyll Degradation. Plant Cell 19:1649–1664.

Paz, M. M., Martinez, J. C., Kalvig, A. B., Fonger, T. M., and Wang, K. (2006). Improved cotyledonary node method using an alternative explant derived from mature seed for efficient Agrobacterium-mediated soybean transformation. Plant Cell Rep 25:206–213.

Penfold, C. A., and Buchanan-Wollaston, V. (2014). Modelling transcriptional networks in leaf senescence. Journal of Experimental Botany 65:3859–3873.

Petrov V. D., Van Breusegem F. (2012). Hydrogen peroxide-a central hub for information flow in plant cells.*AoB Plants* 14. doi: 10.1093/aobpla/pls014

Petrov, V., Hille, J., Mueller-Roeber, B., and Gechev, T. S. (2015). ROS-mediated abiotic stress-induced programmed cell death in plants. Front Plant Sci 6:69–69.

Philosoph-Hadas S., Hadas E., Aharoni N. (1993). Characterization and use in ELISA of new monoclonal antibody for quantitation of abscisic acid in senescing rice leaves. Plant Growth Regul., 12:71–78. doi: 10.1007/BF00144585.

Pimenta, M. R., Silva, P. A., Mendes, G. C., Alves, J. R., Caetano, H. D. N., Machado, J. P. B., et al. (2016). The stress-induced soybean NAC transcription factor GmNAC81 plays a positive role in developmentally programmed leaf senescence. Plant Cell Physiol. 57, 1098–1114. doi: 10.1093/pcp/pcw059

Podzimska-Sroka, D., O'Shea, C., Gregersen, P., and Skriver, K. (2015). NAC Transcription Factors in Senescence: From Molecular Structure to Function in Crops. Plants 4:412–448.

Pruneda-Paz, J. L., Breton, G., Nagel, D. H., Kang, S. E., Bonaldi, K., Doherty, C. J., Ravelo, S., Galli, M., Ecker, J. R., and Kay, S. A. (2014). A Genome-Scale Resource for the Functional Characterization of Arabidopsis Transcription Factors. Cell Reports 8:622–632.

Puniran-Hartley N., Hartley J., Shabala L., Shabala S. (2014). Salinity-induced accumulation of organic osmolytes in barley and wheat leaves correlates with increased oxidative stress tolerance: in planta evidence for cross-tolerance. Plant Physiology and Biochemistry, 83:32-39. doi:10.1016/j.plaphy.2014.07.005.

Puranik, S., Sahu, P. P., Srivastava, P. S., and Prasad, M. (2012). NAC proteins: regulation and role in stress tolerance. Trends in Plant Science 17:369–381.

Qi T, Song S, Ren Q, Wu D, Huang H, Chen Y, Fan M, Peng W, Ren C, Xie D. (2011). The Jasmonate-ZIM-domain proteins interact with the WD-repeat/bHLH/MYB complexes to regulate jasmonate-mediated anthocyanin accumulation and trichome initiation in *Arabidopsis thaliana*. The Plant Cell23, 1795–1814. doi: 10.1105/tpc.111.083261

Qiu, K.; Li, Z.; Yang, Z.; Chen, J.; Wu, S.; Zhu, X.; Gao, S.; Gao, J.; Ren, G.; Kuai, B.; et al. (2013). EIN3 and ORE1 Accelerate Degreening during Ethylene-Mediated Leaf Senescence by Directly Activating Chlorophyll Catabolic Genes in Arabidopsis. PLoS Genet., 11, e1005399. doi: 10.1371/journal.pgen.1005399

Quirino B.F., Noh Y.S., Himelblau E., Amasino R.M. (2000) Molecular aspects of leaf senescence. Trends Plant Sci., 5:278–282. doi: 10.1016/S1360-1385(00)01655-1.

Rauf, M., Arif, M., Dortay, H., Matallana-Ramírez, L.P., Waters, M.T., Gil Nam, H., Lim, P.O., Mueller-Roeber, B., Balazadeh, S. (2013) ORE1 balances leaf senescence

against maintenance by antagonizing G2-like-mediated transcription. EMBO Rep., 14, 382–388. doi:10.1038%2Fembor.2013.24

Rauf, M., Arif, M., Fisahn, J., Xue, G.-P., Balazadeh, S., and Mueller-Roeber, B. (2013). NAC Transcription Factor SPEEDY HYPONASTIC GROWTH Regulates Flooding-Induced Leaf Movement in Arabidopsis. PlantCell 25:4941–4955.

Reis, P. A. B., Rosado, G, L., Silva, L.A.C., Oliveira, L.C., Oliveira, L.B., Costa, M.D.L., Alvim, F. C., Fontes, E.P.B. (2011). PlantPhysiology, 157 (4) 1853-1865. doi: 10.1104/pp.111.179697

Reis, P. A., Carpinetti, P. A., Freitas, P. P., Santos, E. G., Camargos, L. F., Oliveira, I. H., et al. (2016). Functional and regulatory conservation of the soybean ER stress-induced DCD/NRP mediated cell death signaling in plants. BMC Plant Biol. 16:156. doi: 10.1186/s12870-016-0843-z

Ricachenevsky, F. K., Menguer, P. K., and Sperotto, R. A. (2013). kNACking on heaven's door: how important are NAC transcription factors for leaf senescence and Fe/Zn remobilization to seeds? Front. Plant Sci. 4.

Saha B, Borovskii G, Panda SK. (2016). Alternative oxidase and plant stress tolerance. Plant Signal Behav., 11(12):e1256530. doi:10.1080/15592324.2016.1256530

Sakuraba, Y., Han, S.H., Lee, S.H., Hörtensteiner, S., Paek, N.C. (2016). Arabidopsis NAC016 promotes chlorophyll breakdown by directly upregulating STAYGREEN1 transcription. Plant Cell Rep., 35(1):155-66. doi: 10.1007/s00299-015-1876-8

Sakuraba, Y., Kim, Y.-S., Han, S.-H., Lee, B.-D., and Paek, N.-C. (2015). The Arabidopsis Transcription Factor NAC016 Promotes Drought Stress Responses by

Repressing AREB1 Transcription through a Trifurcate Feed-Forward Regulatory Loop Involving NAP. Plant Cell 27:1771–1787.

Shah, S.H., Houborg, R., McCabe, M.F. (2017). Response of Chlorophyll, Carotenoid and SPAD-502 Measurement to Salinity and Nutrient Stress in Wheat (*Triticum aestivum* L.). *Agronomy, 7*, 61. doi:3390/agronomy7030061

Shahnejat-Bushehri S., Tarkowska D., Sakuraba Y., Balazadeh S. (2016). Arabidopsis NAC transcription factor JUB1 regulates GA/BR metabolism and signalling. Nat Plants, 29;2:16013. doi: 10.1038/nplants.2016.13.

Sheshadri SA, Nishanth MJ, Simon B. (2016). Stress-Mediated cis-Element Transcription Factor Interactions Interconnecting Primary and Specialized Metabolism in planta. Front Plant Sci., 7:1725. doi:10.3389/fpls.2016.01725

Shi H, Wang B, Yang P, Li Y, Miao F. (2016). Differences in Sugar Accumulation and Mobilization between Sequential and Non-Sequential Senescence Wheat Cultivars under Natural and Drought Conditions. PLoS One, 4;11(11). doi: 10.1371/journal.pone.0166155

Sims, D.A. and Gamon, J.A. (2002) Relationships Between Leaf Pigment Content and Spectral Reflectance across a Wide Range of Species, Leaf Structures and Developmental Stages. Remote Sensing of Environment, 81, 337-354. doi: 10.1016/S0034-4257(02)00010-X

Stenzel I., Otto M., Delker C., et al. (2012). ALLENE OXIDE CYCLASE (AOC) gene family members of Arabidopsis thaliana: tissue- and organ-specific promoter activities and in vivo heteromerization. J Exp Bot., 63(17):6125-6138. doi:10.1093/jxb/ers261zhe

Stenzel, I., Hause, B., Miersch, O. et al. (2003). Jasmonate biosynthesis and the allene oxide cyclase family of Arabidopsis thaliana .Plant Mol Biol51, 895–911. doi:10.1023/A:1023049319723

Stracke R, Ishihara H, Huep G, et al. (2007). Differential regulation of closely related R2R3-MYB transcription factors controls flavonol accumulation in different parts of the Arabidopsis thaliana seedling. Plant J., 50(4):660-677. doi:10.1111/j.1365-313X.2007.03078.x

Takasaki, H., Maruyama, K., Takahashi, F., Fujita, M., Yoshida, T., Nakashima, K., Myouga, F., Toyooka, K., Yamaguchi-Shinozaki, K., Shinozaki, K. (2015). SNAC-As, stress-responsive NAC transcription factors, mediate ABA-inducible leaf senescence. Plant J., 84(6):1114-23. doi: 10.1111/tpj.13067

Takasaki, H., Maruyama, K., Takahashi, F., Fujita, M., Yoshida, T., Nakashima, K., et al. (2015). SNAC-As, stress-responsive NAC transcription factors, mediate ABA-inducible leaf senescence. Plant J. 84, 1114–1123. doi: 10.1111/tpj.13067

Tarkowski,Ł. P., and Van den Ende, W. (2015). Cold tolerance triggered by soluble sugars: a multifaceted countermeasure. Front. Plant Sci., 6:203. doi: 10.3389/fpls.2015.00203

Thomas, H., Huang, L., Young, M., and Ougham, H. (2009). Evolution of plant senescence. BMC Evol Biol 9:163.

Thompson, B. G., and Lake, B. H. (1987). The effect of radiation on the long term productivity of a plant based CELSS. Advances in Space Research 7:133–140.

Torres MA, Jones JD, Dangl JL. (2006). Reactive oxygen species signaling in response to pathogens. Plant Physiol., 141(2):373-8. doi: 10.1104/pp.106.079467.

Tran, L. S., Nakashima, K., Sakuma, Y., Simpson, S. D., Fujita, Y., Maruyama, K., et al. (2004). Isolation and functional analysis of Arabidopsis stress-inducible NAC transcription factors that bind to a drought-responsive cis-element in the early responsive to dehydration stress 1 promoter. Plant Cell 16, 2481–2498. doi: 10.1105/tpc.104.022699

Wei K., Chen J., Wang Y., Chen Y., Chen S., Lin Y., et al. (2012). Genome-wide analysis of bZIP-encoding genes in maize.*DNA Res.*, 19 463–476. doi:10.1093/dnares/dss026

Woo, H. R., Kim, H. J., Nam, H.G., Lim, O.P. (2013). Plant leaf senescence and death – regulation by multiple layers of control and implications for aging in general. Journal of Cell Science, 126: 4823-4833. doi: 10.1242/jcs.109116

Woo, H. R., Chung, K. M., Park, J. H., Oh, S. A., Ahn, T., Hong, S. H., Jang, S. K. and Nam, H. G. (2001). ORE9, an F-box protein that regulates leaf senescence in Arabidopsis. Plant Cell 13, 1779–1790. doi: 10.1105/tpc.010061

Woo, H. R., Kim, H. J., Lim, P. O., and Nam, H. G. (2019). Leaf Senescence: Systems and Dynamics Aspects. Annu. Rev. Plant Biol. 70:347–376.

Woo, H. R., Kim, J. H., Kim, J., Kim, J., Lee, U., Song, I.-J., Kim, J.-H., Lee, H.-Y., Nam, H. G., and Lim, P. O. (2010). The RAV1 transcription factor positively regulates leaf senescence in Arabidopsis. Journal of Experimental Botany 61:3947–3957.

Woo, H. R., Kim, J. H., Nam, H. G., and Lim, P. O. (2004). The Delayed Leaf Senescence Mutants of Arabidopsis, ore1, ore3, and ore9 are Tolerant to Oxidative Stress. Plant and Cell Physiology 45:923–932.

Wu, A., Allu, A. D., Garapati, P., Siddiqui, H., Dortay, H., Zanor, M.-I., Asensi-Fabado, M. A., Munné-Bosch, S., Antonio, C., Tohge, T., et al. (2012). JUNGBRUNNEN1 , a Reactive Oxygen Species–Responsive NAC Transcription Factor, Regulates Longevity in Arabidopsis. Plant Cell 24:482–506.

Wu, Y., Deng, Z., Lai, J. et al. (2009). Dual function of Arabidopsis ATAF1 in abiotic and biotic stress responses. Cell Res19, 1279–1290. doi: 10.1038/cr.2009.108

Wu, Y., Deng, Z., Lai, J. et al. (2009). Dual function of Arabidopsis ATAF1 in abiotic and biotic stress responses. Cell Res19, 1279–1290. doi:10.1038/cr.2009.108

Xu Z. and Rothstein S.J. (2018). ROS-Induced anthocyanin production provides feedback protection by scavenging ROS and maintaining photosynthetic capacity in Arabidopsis. Plant Signal Behav., 13:e1451708. doi:10.1080/2F15592324.2018.1451708

Yamaguchi S.(2008). Gibberellin metabolism and its regulation. Annu Rev Plant Biol., 59:225-51. doi: 10.1146/annurev.arplant.59.032607.092804.

Yamaguchi, M., Mitsuda, N., Ohtani, M., Ohme-Takagi, M., Kato, K., and Demura, T. (2011). VASCULAR-RELATED NAC-DOMAIN7 directly regulates the expression of a broad range of genes for xylem vessel formation. Plant J. 66, 579–590. doi: 10.1111/j.1365-313X.2011.04514.x

Yamaguchi, M., Ohtani, M., Mitsuda, N., Kubo, M., Ohme-Takagi, M., Fukuda, H., et al. (2010). VND-INTERACTING2, a NAC domain transcription factor, negatively regulates xylem vessel formation in Arabidopsis. Plant Cell 22, 249–263. doi: 10.1105/tpc.108.064048

Yang, S.-D., Seo, P. J., Yoon, H.-K., and Park, C.-M. (2011). The Arabidopsis NAC Transcription Factor VNI2 Integrates Abscisic Acid Signals into Leaf Senescence via the COR / RD Genes. Plant Cell 23:2155–2168.

Yang, Z. T., Lu, S. J., Wang, M. J., Bi, D. L., Sun, L., Zhou, S. F., et al. (2014). A plasma membrane-tethered transcription factor, NAC062/ANAC062/NTL6, mediates the unfolded protein response in Arabidopsis. Plant J. 79, 1033–1043. doi: 10.1111/tpj.12604

Zeng J., Wang C., Chen X., et al. (2015). The lycopene β-cyclase plays a significant role in provitamin A biosynthesis in wheat endosperm. BMC Plant Biol., 15:112. doi:10.1186/s12870-015-0514-5

Zhang, L.; Zhao, G.; Jia, J.; Liu, X.; Kong, X. (2012). Molecular characterization of 60 isolated wheat MYB genes and analysis of their expression during abiotic stress. J. Exp. Bot., 63, 203–214. doi:10.1093%2Fjxb%2Ferr264

Zhao J., Guo R., Guo C., Hou H., Wang X., Gao H. (2016). Evolutionary and expression analyses of the apple basic leucine zipper transcription factor family. Front. Plant Sci.7:376. 10.3389/fpls.2016.00376

Zheng, X., Spivey, N. W., Zeng, W., Liu, P.-P., Fu, Z. Q., Klessig, D. F., He, S. Y., and Dong, X. (2012). Coronatine Promotes Pseudomonas syringae Virulence in Plants by Activating a Signaling Cascade that Inhibits Salicylic Acid Accumulation. Cell Host & Microbe 11:587–596.

Zhou, W., Lozano-Torres, J. L., Blilou, I., Zhang, X., Zhai, Q., Smant, G., Li, C., and Scheres, B. (2019). A Jasmonate Signaling Network Activates Root Stem Cells and Promotes Regeneration. Cell 177:942-956.e14.

Zhou, Y.; Huang, W.; Liu, L.; Chen, T.; Zhou, F.; Lin, Y. (2013). Identification and functional characterization of a rice NAC gene involved in the regulation of leaf senescence. BMC Plant Biol., 13, 132. doi: 10.1186/1471-2229-13-132

Zhu, J.K. (2016). Abiotic stress signaling and responses in plants. Cell, 167:313–324. doi: 10.1016/j.cell.2016.08.029

Figures

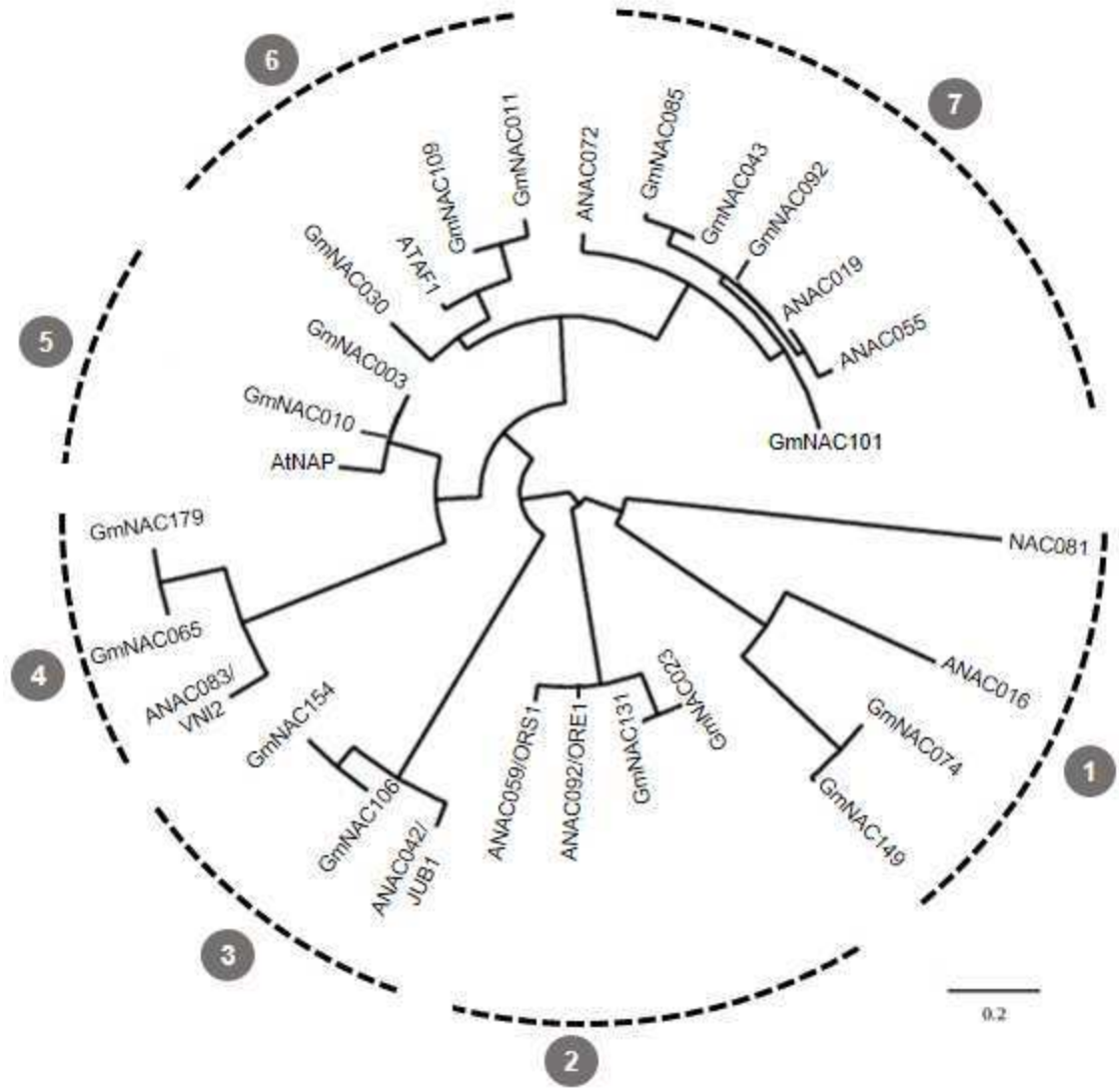

Figure 1. Phylogenetic reconstruction of *Arabidopsis thaliana* and soybean (*Glycine max*) NAC-SAGs.The deduced amino acid sequences of previously described NAC-SAGs of Arabidopsis were interrogated against soybean genome and their putative orthologous genes (GmNAC-SAGs) recovered. The phylogenetic reconstruction resulted in seven distinct groups with stable branch collapse. Phylogenetic relationships were established by neighbor-joining statistical method with 10,000 bootstraps and tree was rendered MABL interface.

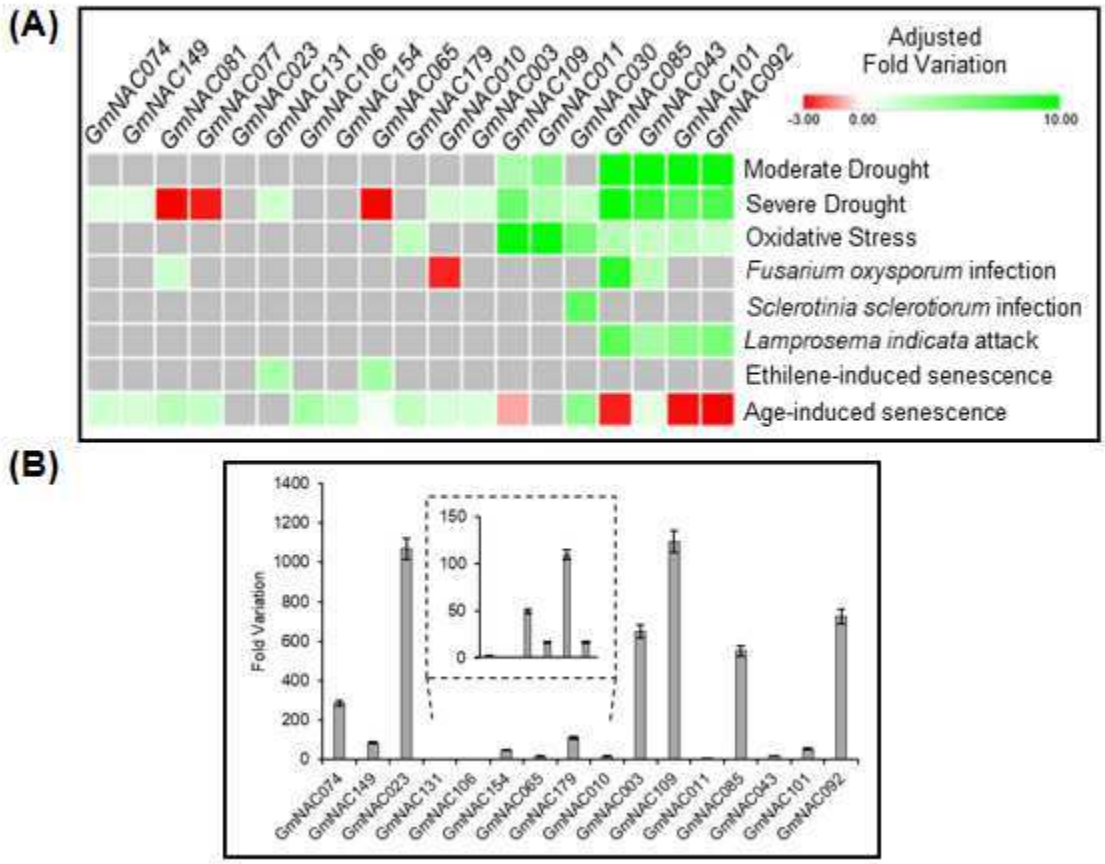

Figure 2. Expression pattern of GmNAC-SAGs in different stresses and bleomycin-induced cell death in soybean. (A) Heatmap of GmNAC-SAGs expression in soybean submitted to different stresses. Transcriptome-wide data from publically accessed RNAseq repository on NCBI was accessed and the expression of GmNAC-SAGs investigated in drought (moderate and severe), oxidative stress, biotic stresses (fungi and insect attack) and senescence (ethylene-induced and age-induced). Fold variation values from DEGs were recovered and converted into the heatmap. **(B)** Expression profile of GmNAC-SAGs in soybean seedlings submitted to bleomycin-treatment (420 mM) for 24h. Total RNA was isolated from V3/V4 soybean leaves and the transcript accumulation of genes was measured by qRT-PCR. *ELF2A*was used as the normalizer, endogenous control gene. Relative gene expression was quantified using the comparative $2^{-\Delta\Delta Ct}$ method.

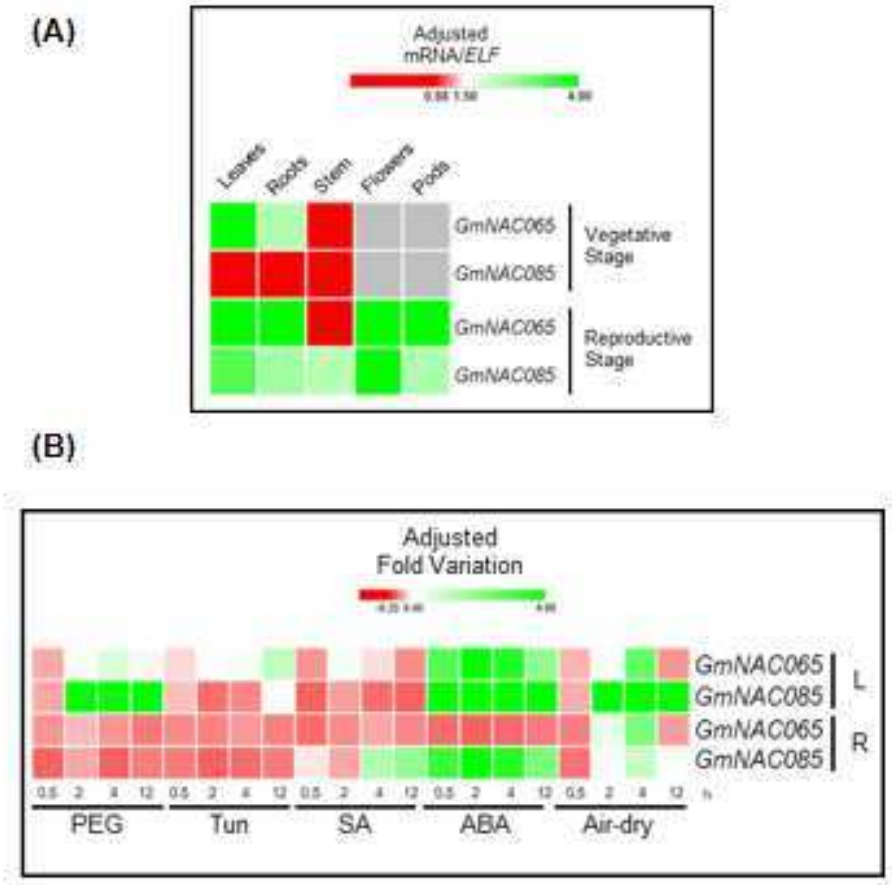

Figure 3. Tissue-specific expression of *GmNAC065* and *GmNAC085* in Williams82 soybean seedlings under normal development and multiple stresses. (A) Expression pattern of *GmNAC065* and *GmNAC085* in soybean vegetative and reproductive stages. **(B)** Expressionpattern of*GmNAC065* and *GmNAC085* in soybean seedlings submitted to simulated drought (PEG 8,000 – 10% w/v; air-dry and ABA – 150 mM), ER-stress (Tun – 5 µg/mL) and biotic stress (SA – 75 µM). Plants were previously acclimated on Hoagland hydroponic solution and gene expression level analyzed after 2h, 4h and 12h in leaves and roots. All treatments were performed with biological triplicates, consisting of three pools of three plants.*ELF1A*was used as the normalizer control gene. Relative gene expression was determined by the comparative $2^{-\Delta\Delta Ct}$ method.

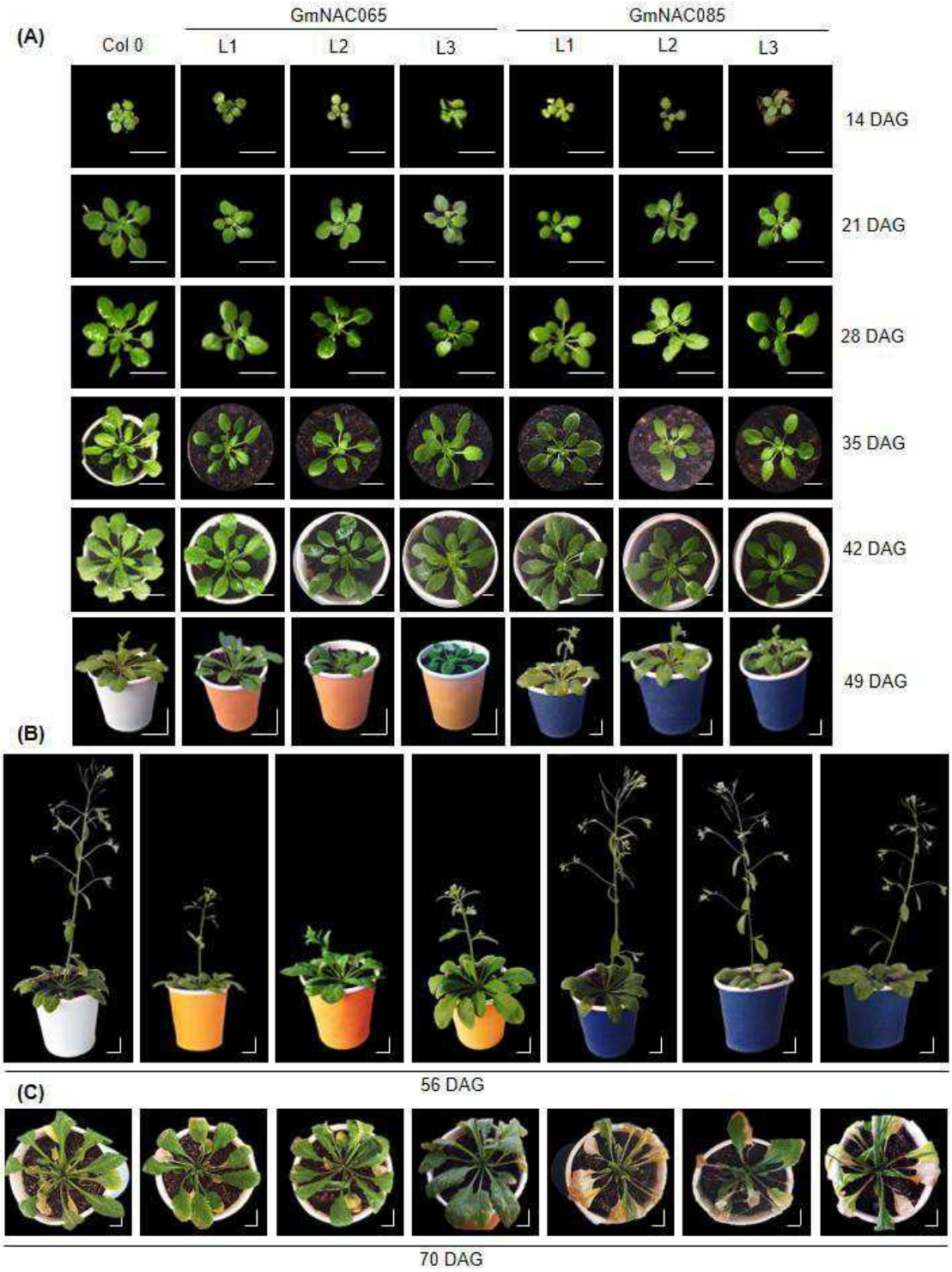

Figure 4. Phenotypical characterization of three homozygous independent lines of Arabidopsis overexpressing *GmNAC065* and *GmNAC085*. (A) Phenotypical characterization of GmNAC065-OX and GmNAC085-OX lines (L1, L2 and L3) during the vegetative stage and the onset of reproductive stage. Plants were analyzed up to 42 DAG in the vegetative stage and up to 56 DAG in reproductive stage, considering 49 DAG as the onset of reproductive stage, hallmarked by the emergence of inflorescence.

(B) Phenotypical characterization of GmNAC065-OX and GmNAC085-OX lines in reproductive stage. **(C)** Phenotypical characterization of transgenic Arabidopsis lines during senescence. All experiments were performed in plants under normal development, cultivated in growth chamber with standard settings (12 h of photoperiod, 21 °C and 70% of relative humidity). Scale bars = 0.5 cm.

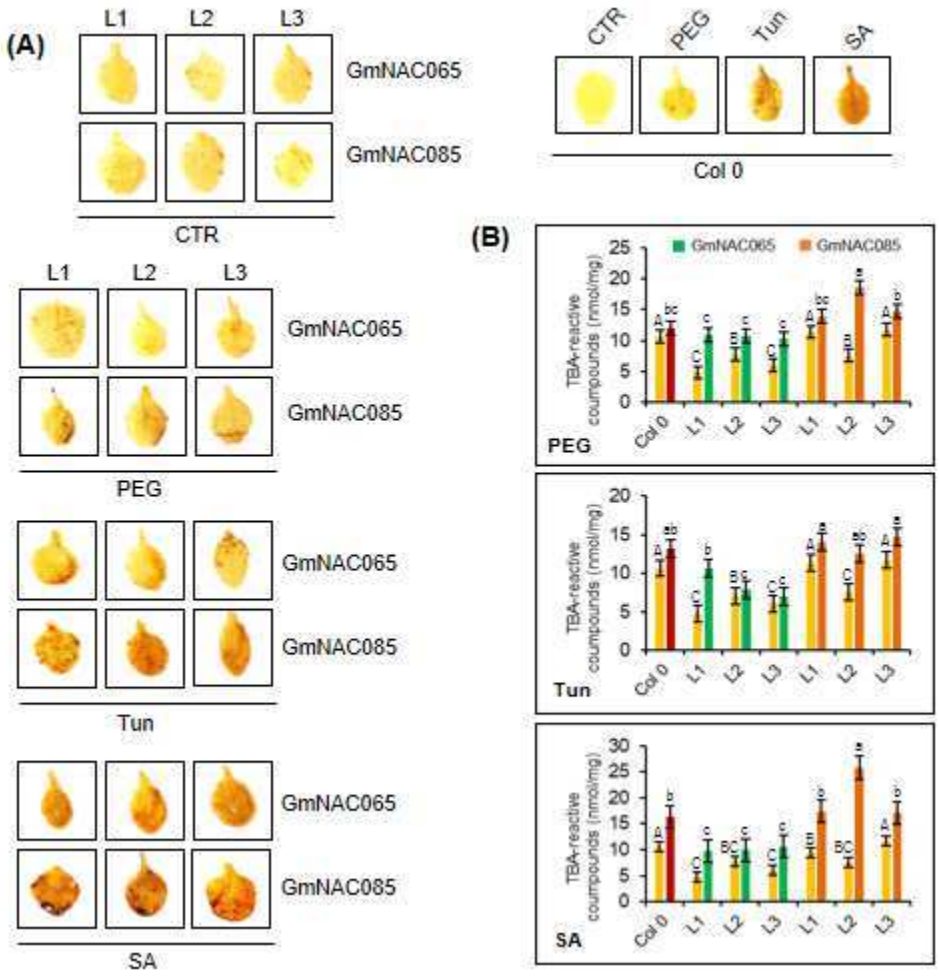

Figure 5. Expression of *GmNAC065* and *GmNAC085* lead to H_2O_2 accumulation and lipid peroxidation. (A) DAB-leaf staining to detect H_2O_2 accumulation in Arabidopsis leaves submitted to different stresses for 24h. Plants were previously acclimated in MS solution and after transferred to stressor-solution. Leaves were collected, stained for 8h in DAB and distained in ethanol (100%) until total chlorophyll removing. **(B)** TBA-reactive compounds quantification in GmNAC065-OX and GmNAC085-OX lines under multiple stresses. Yellow bars represent untreated-control plants and colored bars the respective treatments in Col 0, GmNAC076-OX and GmNAC085-OX lines. Upper bars indicate standard-error (95% of confidence). Uppercase letters indicate significant differences in control samples and lowercase indicate significant differences in treated-samples by Tukey test ($p < 0.05$, n=3).

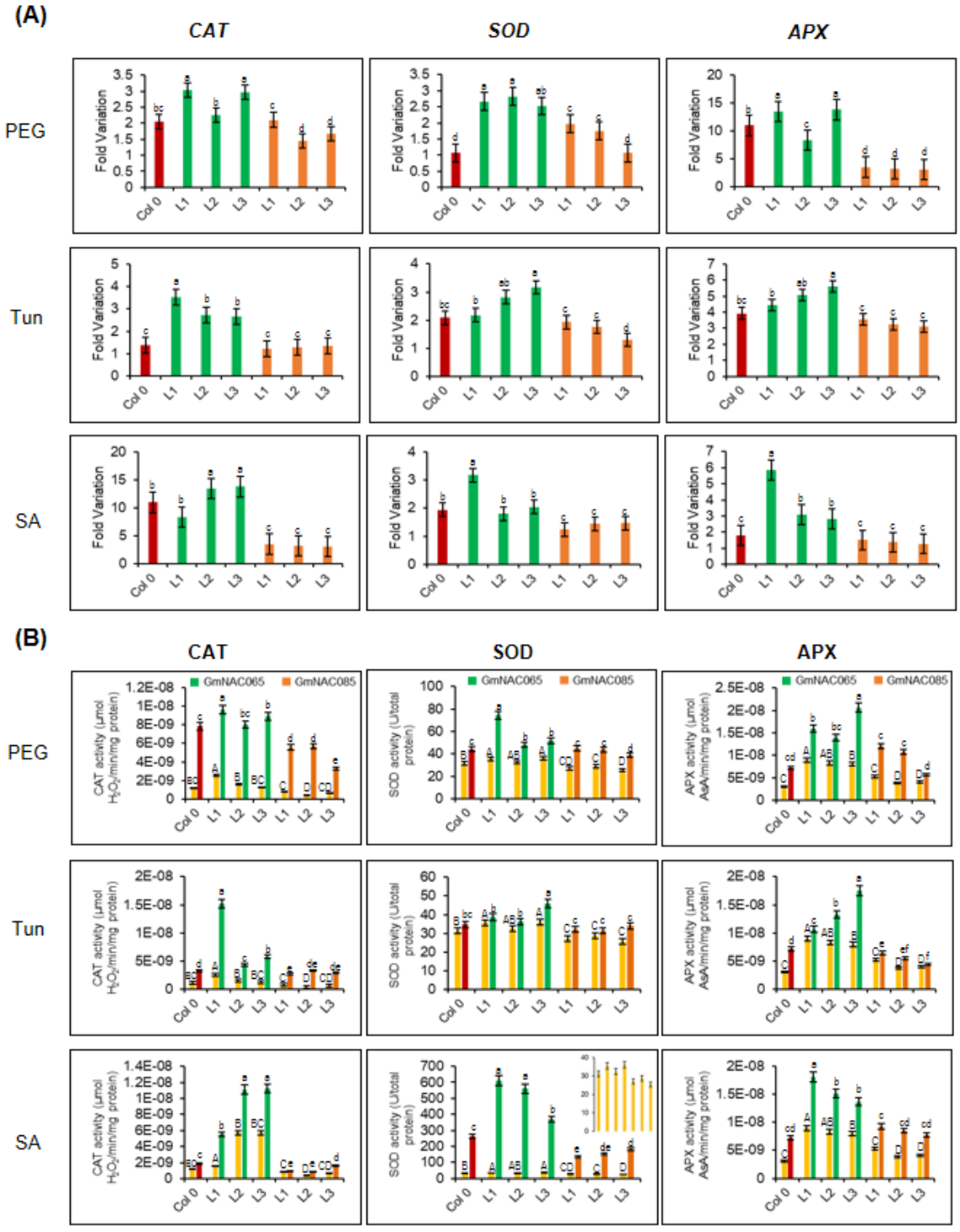

Figure 6. Expression profile and activity of antioxidative enzymes catalase (CAT), superoxide-dismutase (SOD) and ascorbate-peroxidase (APX) in GmNAC065-OX and GmNAC085-OX lines under multiple stresses. (A) Expression profile of CAT, SOD and APX in transgenic Arabidopsis lines submitted to 24h of multiple stresses. Fold variation data was normalized according to the expression levels in the control

samples (FV = 1.0) and expressed in a relative way. **(B)** Enzymatic activity of CAT, SOD and APX in GmNAC065-OX and GmNAC085-OX plants under multiple stresses. Yellow bars represent untreated-control plants and colored bars the respective treatments in Col 0, GmNAC076-OX and GmNAC085-OX lines. Upper bars indicate standard-error (95% of confidence). Uppercase letters indicate significant differences in control samples and lowercase indicate significant differences in treated-samples by Tukey test ($p < 0.05$, n=3).

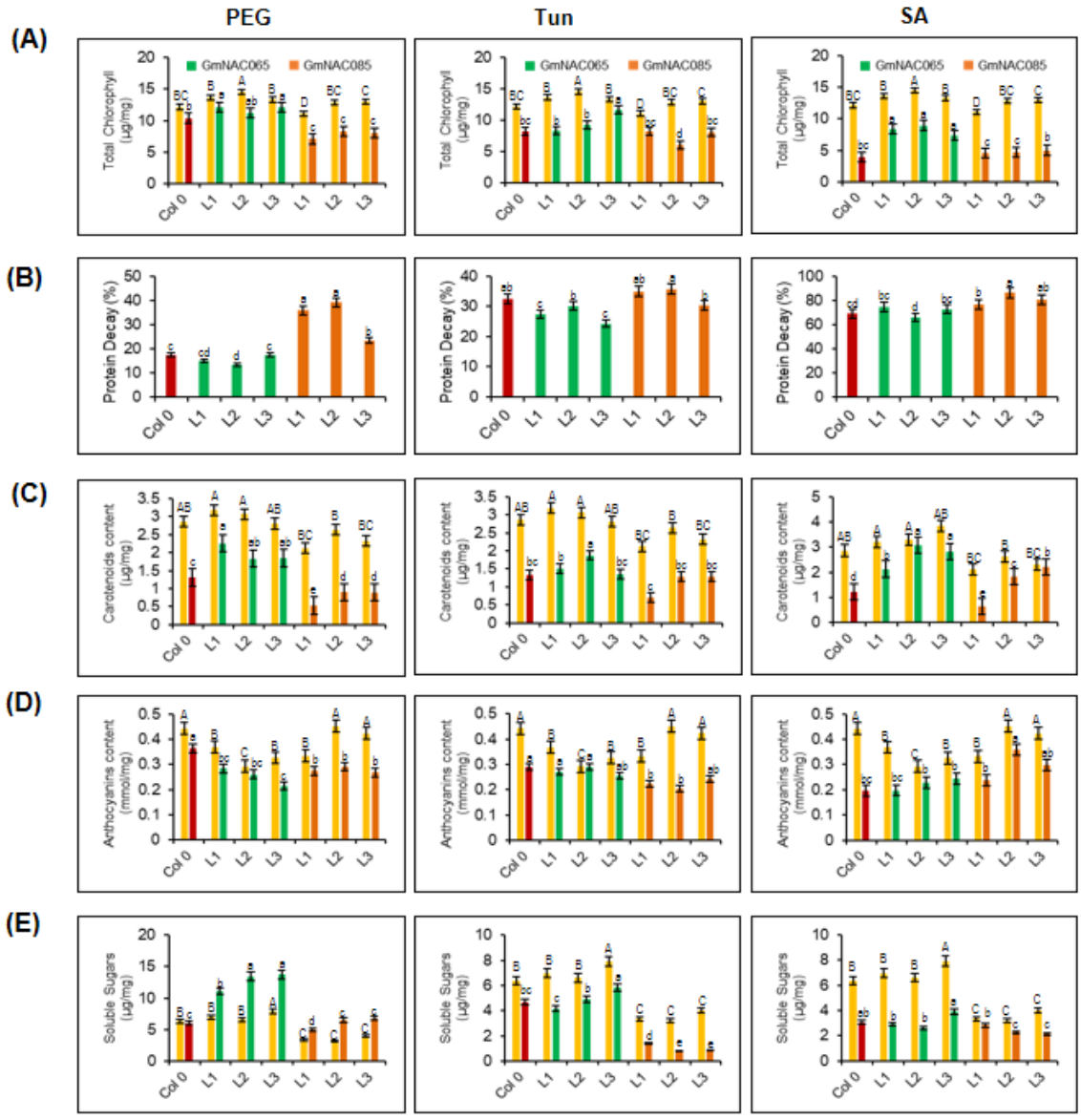

Figure 7. Metabolites content in transgenic Arabidopsis lines overexpressing *GmNAC065* and *GmNAC085* in multiple stresses. (A) Chlorophyll content. The chlorophyll content was accessed spectrophotometrically in ethanolic plant-extracts submitted to 645 nm and 663 nm reading. **(B)** Protein decay ratio. The protein decay rate after stress was calculated according to the total protein content, determined by Bradford method. The protein content of untreated plants was considered 100% and degradation ratio expressed as the percentage of protein in relation to the control. **(C)** Carotenoids content. The carotenoids content was determined spectrophotometrically in ethanolic plant-extracts submitted to 480 nm reading. **(D)** Anthocyanins content. Anthocyanins content was determined spectrophotometrically and samples were

analyzed at 529 nm and 650 nm. **(E)** Soluble sugars content was determined by DNS-reducing method. Samples were submitted to DNS-reaction and sugars concentration determined based on a glucose standard-curve. Yellow bars represent untreated-control plants and colored bars the respective treatments in Col 0, GmNAC076-OX and GmNAC085-OX lines. Upper bars indicate standard-error (95% of confidence). Uppercase letters indicate significant differences in control samples and lowercase indicate significant differences in treated-samples by Tukey test ($p < 0.05$, n=3).

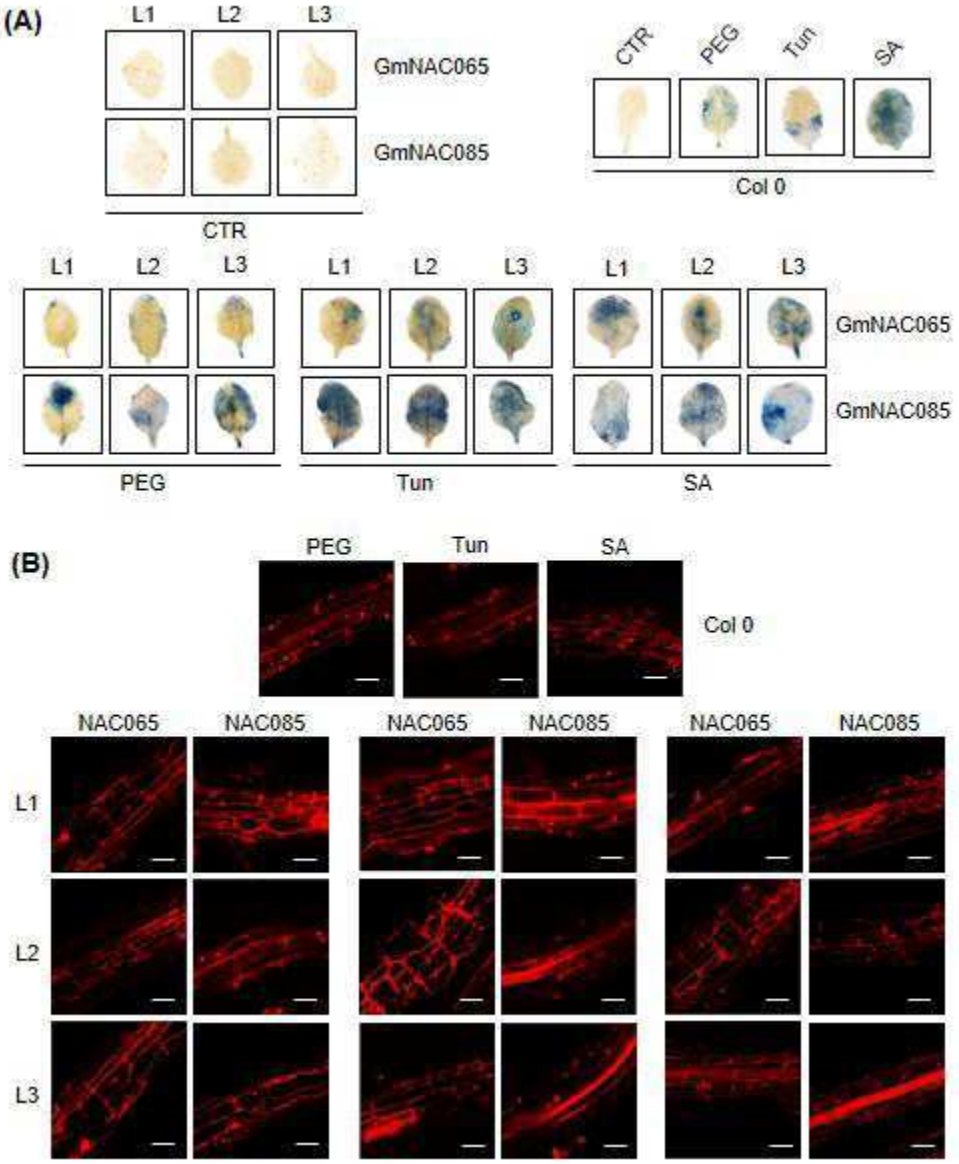

Figure 8. Cell death extent in leaves and roots of GmNAC065-OX and GmNAC085-OX plants. (A) Evans blue leaf-staining of GmNAC065-OX and GmNAC085-OX lines under different stresses. 24h-stressed and non-stressed leaves were submitted to Evans dye staining-solution (0.5% w/v) for 8h and distained in absolute ethanol for 24h. Intense blue color indicates the extent of cell death. **(B)** Propidium-iodide (PI) root-staining in transgenic plants ectopically expressing *GmNAC065* and *GmNAC085*. Stressed and non-stressed roots were submitted to PI-staining solution (0.6 µg/mL) for 24 hours until confocal microscopy scanning. Scale bars = 20 µm.

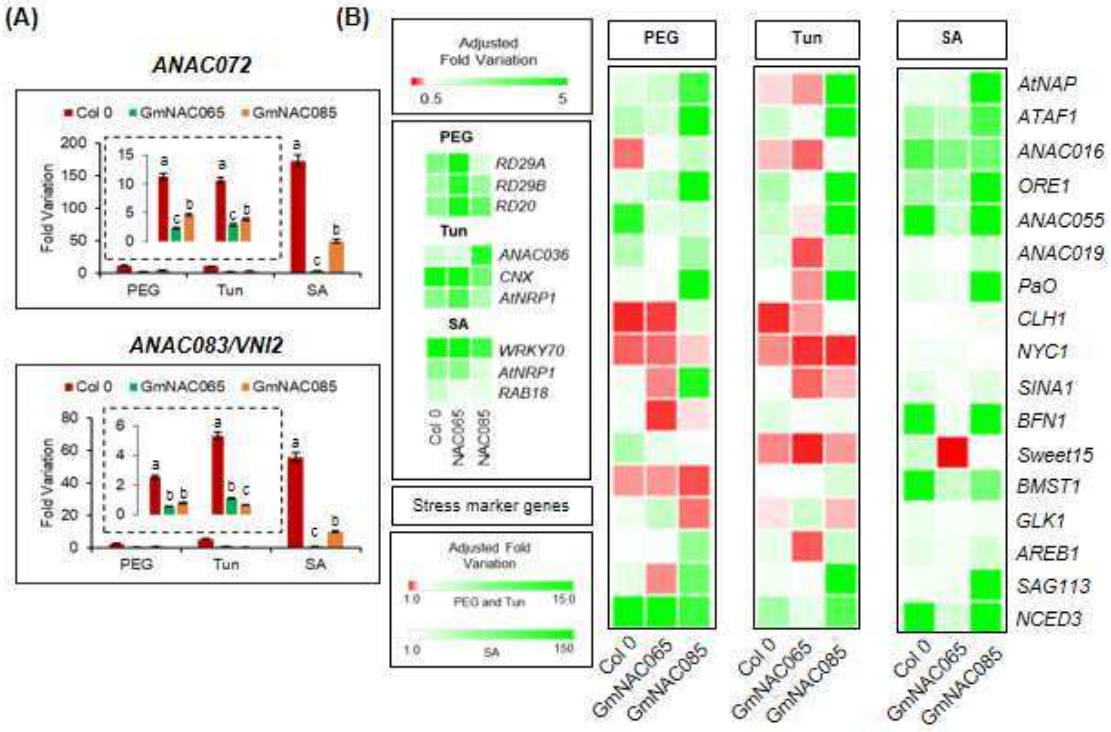

Figure 9. AtSAGs expression in GmNAC065-OX and GmNAC085-OX plants in multiple stresses. (A) Expression levels of *ANAC083/VNI2* and *ANAC072*, a negative and positive regulators of senescence in Arabidopsis and the putative orthologous of *GmNAC065* and *GmNAC085*, respectively. **(B)** Expression levels of stress marker genes and AtSAGs in transgenic lines ectopically expressing *GmNAC065* and *GmNAC085*. Total RNA was isolated from 4-week-old plants and the transcript accumulation of the indicated genes was measured by qRT-PCR. *ACT2* was used as the endogenous control gene. Relative gene expression was quantified using the comparative $2^{-\Delta\Delta Ct}$ method. Upper bars indicate standard-error (95% of confidence) and the letters indicate significant differences between the lines by Tukey test ($p < 0.05$, n=3).

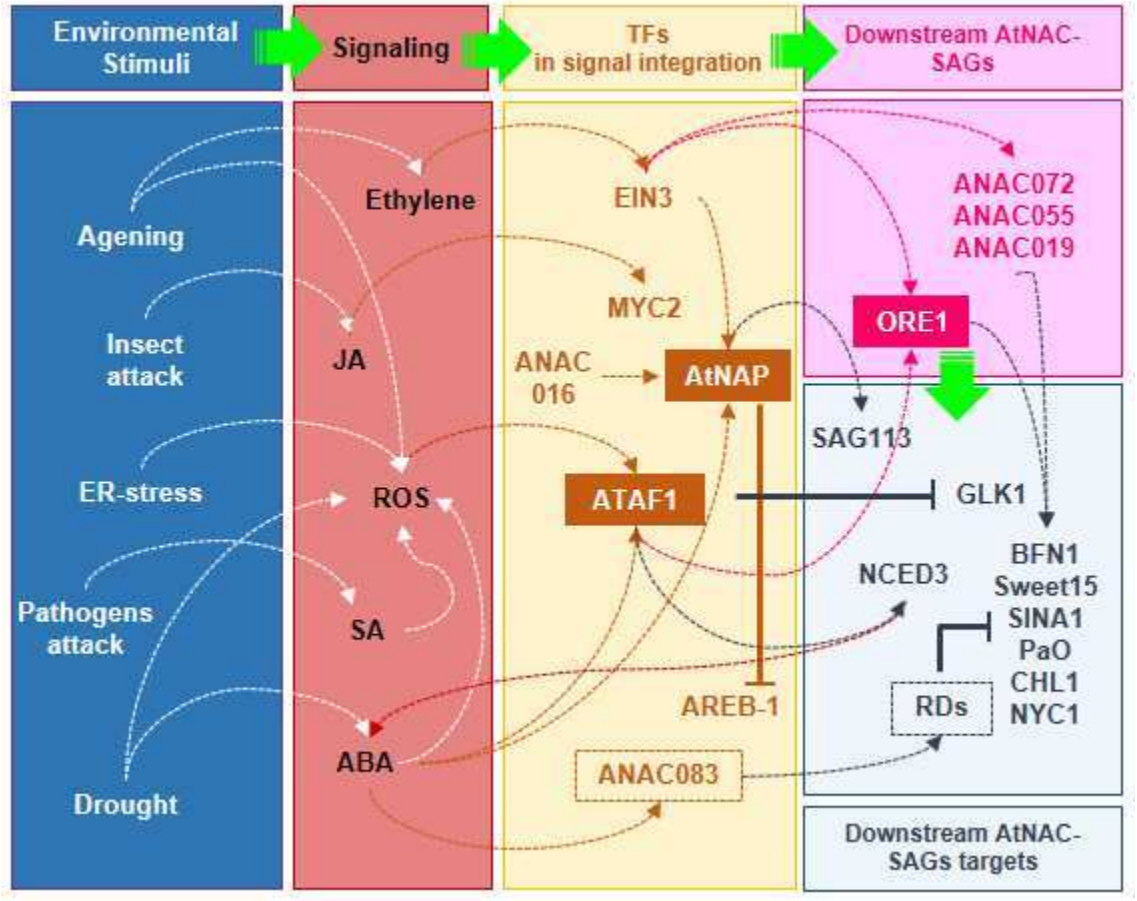

Figure 10. Schematic representation of gene regulatory network coordinated by environmental stimuli, plant hormones and AtNAC-SAGs. The different environment stimuli culminate on plant hormone signaling, which activates several SAGs in response to multiple stresses. Consequently, the expression of these SAGs triggers an age- or –environment cell death. The expression of *GmNAC085* up-regulates *ATAF1*, *ORE1* and *AtNAP*, involved in the integration of ABA, age and ROS-signals. Increased expression of these genes results in the activation of several downstream SAGs genes, involved in chlorophyll and other molecules catabolism that confers accentuated senescence phenotype. Contrastingly, the expression of these genes is attenuated in *GmNAC065* leading to a best plant performance under multiple stresses and a delayed senescence phenotype. Figure modified from Luoni *et al*. (2019).

Supplementary Figures

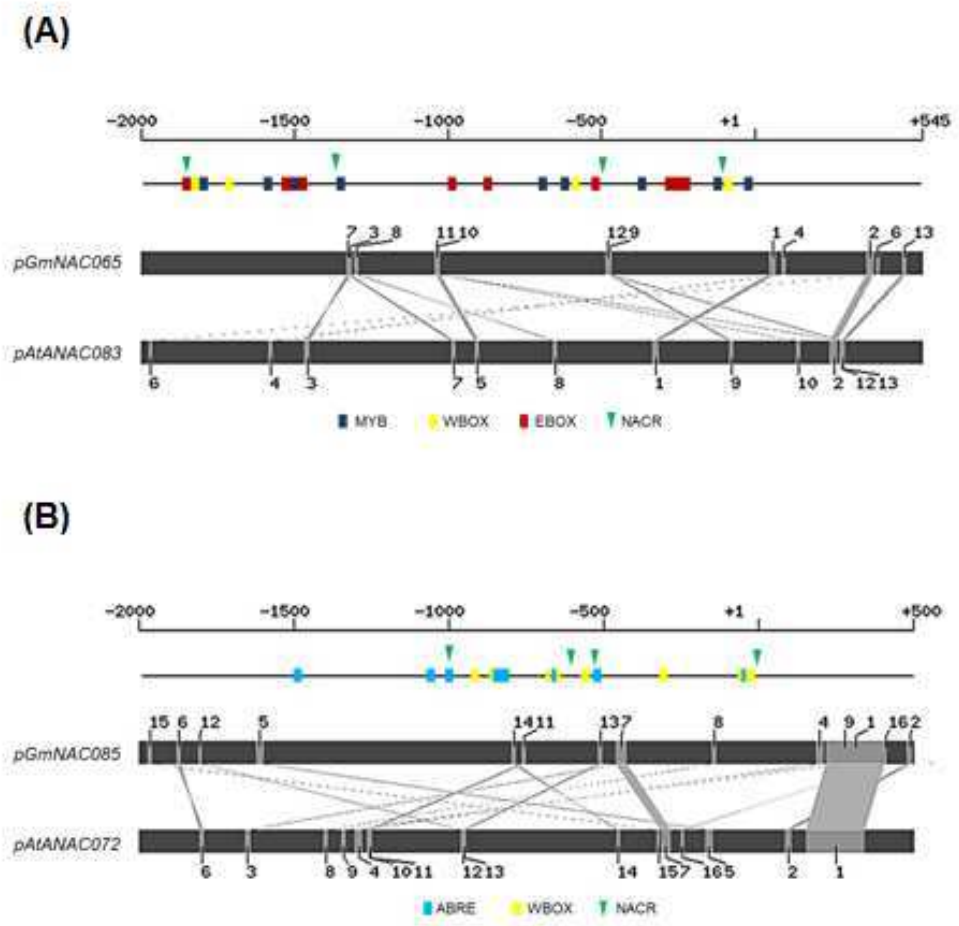

Supplemental Figure 1. Schematic distribution of canonical *cis*-acting elements in **(A)** *pGmNAC065* and **(B)***pGmNAC085* and the conserved blocks in Arabidopsis orthologs genes *ANAC083/VNI2* and *ANAC072*, respectively.

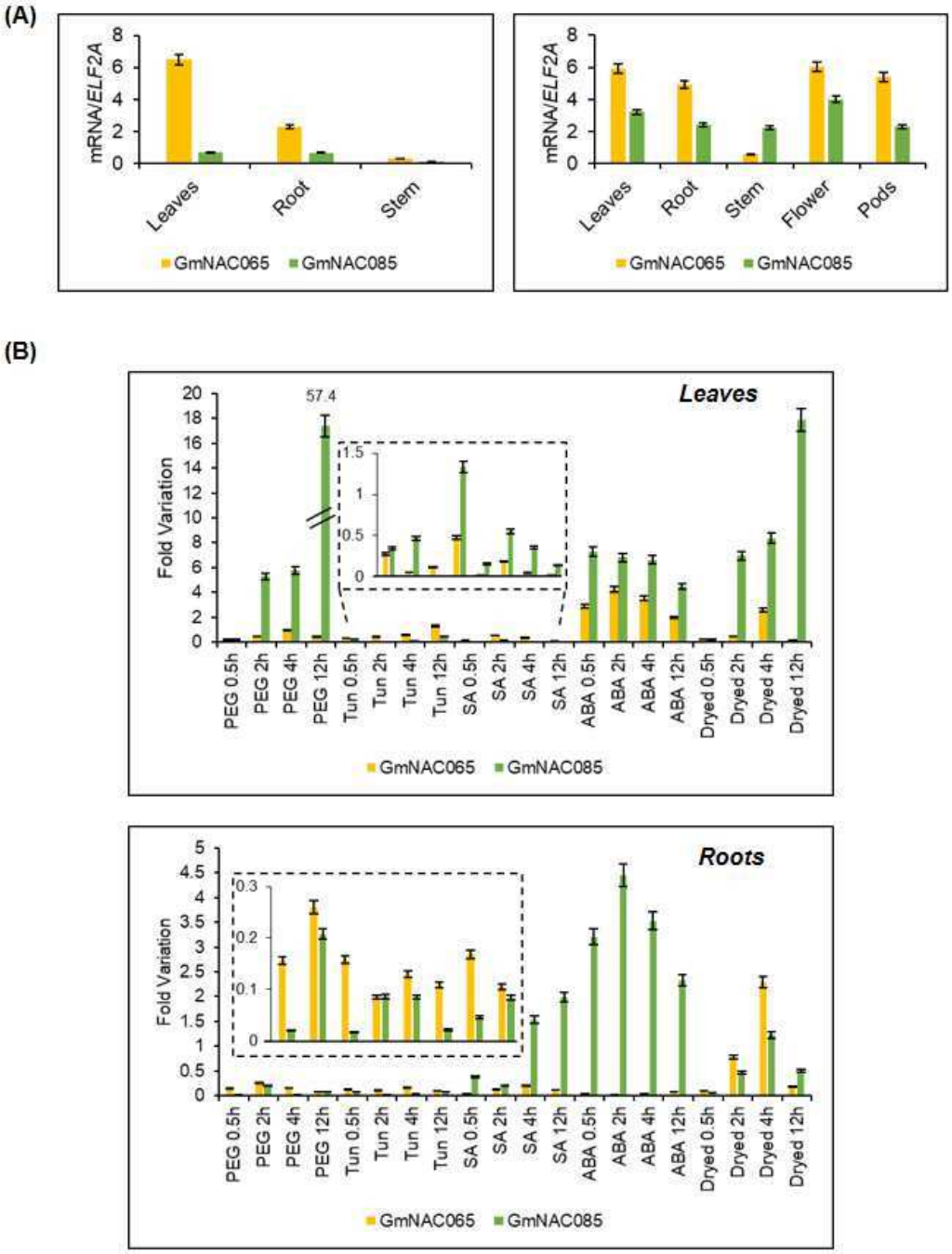

Supplemental Figure 2. (A) Expression levels of *GmNAC065* and *GmNAC085* in different soybean Williams82 tissues in vegetative and reproductive stages. **(B)** Expression levels of soybean *GmNAC065* and *GmNAC085* in roots and leaves submitted to different stresses. Transcript accumulation of the indicated genes was measured by qRT-PCR. *ELF1A*was used as the normalizer, endogenous control gene. Relative gene expression was quantified using the comparative $2^{-\Delta\Delta Ct}$ method.

(A)

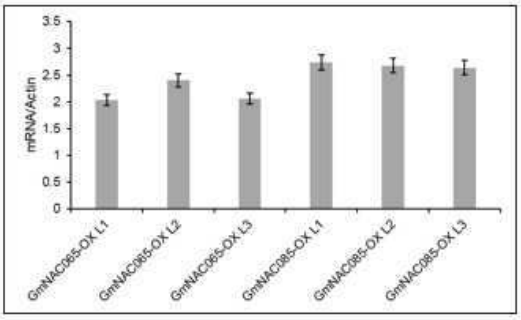

(B)

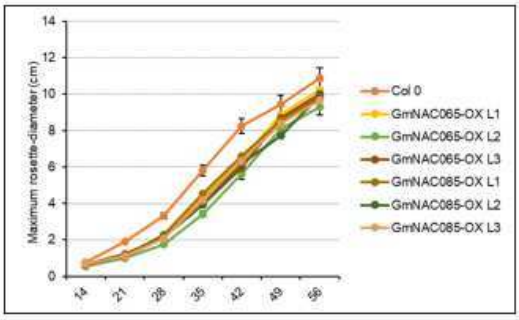

(C)

Average of number of leaves in GmNAC065 and GmNAC085 overexpressing-lines during vegetative developmental stage

DAG	Leaves						
	Col 0	GmNAC065-OX			GmNAC085-OX		
		L1	L2	L3	L1	L2	L3
14	9.1 ± 1.44	7.4 ± 0.54	6.4 ± 0.55	8.0 ± 0.11	7.2 ± 0.83	6.6 ± 1.14	6.8 ±1.09
21	12.33 ± 1.00	10.8 ± 0.44	9.2 ± 0.83	9.8 ± 0.83	10.8 ± 1.78	9.8 ± 1.48	10.2 ± 1.48
28	16.44 ± 1.01	13.0 ± 1.41	10.8 ± 1.09	11.8 ± 1.09	13 ± 1.98	11.4 ± 1.34	11.6 ± 0.89
35	18.44 ± 1.66	15.8 ± 0.44	14 ± 0.11	15.6 ± 0.89	15.2 ± 1.78	14.4 ± 0.89	15.2 ± 1.09
42	≥ 25[1]	19.6 ± 0.89	18.0 ± 0.11	19.6 ± 1.67	22.4 ± 2.19	21.2 ± 1.09	22.0 ± 3.46

[1] After 42 DAG, Col 0 plants displayed more than 25 leaves/plant and this time was considered maximum for full vegetative-stage development. For GmNAC065-OX and GmNAC085-OX lines, more than 25 leaves/plant were observed after 49 DAG and Col 0 plants displayed more than 30 leaves/plant at the same time-point.

(D)

Average of shoot length of GmNAC065 and GmNAC085 overexpressing-lines during reproductive stage

DAG	Shoot Length (cm)						
	Col 0	GmNAC065-OX			GmNAC085-OX		
		L1	L2	L3	L1	L2	L3
49	2.61 ± 1.70	0.58 ± 0.29[1]	-*	-*	1.98 ± 2.12	0.96 ± 0.44	0.98 ± 1.39
56	15.0 ± 3.12	9.84 ± 3.08	4.64 ± 2.65	3.46 ± 1.82	12.7 ± 3.90	9.32 ± 3.08	10.5 ± 3.86
63	21 ± 4.37	16.53 ± 1.54	8.16 ± 2.08	7.79 ± 4.45	19.27 ± 4.67	14.31 ± 2.61	14.28 ± 2.35

(*) GmNAC065-OX: plants of L2 and L3 lines did not display shoot elongation up to 49 DAG and only one of five plants of L1 line displayed shoot elongation at the same time-point.

Supplemental Figure 3. Phenotypical and molecular characterization of GmNAC065-OX and GmNAC085-OX lines (L1, L2 and L3).**(A)**Transcript accumulation of the transgene *GmNAC065* and *GmNAC085* in transgenic Arabidopsis lines. Total RNA was isolated from 14 DAG T2-homozygous lines and transcript accumulation determined as the relative expression of soybean gene and *ACT2* endogenous control, calculates by $2^{-\Delta Ct}$ method. **(B)** Rosette diameter of transgenic lines during the vegetative stage and the onset of reproductive stages. **(C)** Number of leaves data accessed in GmNAC065 and GmNAC085-OX lines. **(D)** Rosette diameter data accessed in GmNAC065 and GmNAC085-OX lines.

Supplementary Table 1. Raw datasets available in GEO – NCBI used for the putative GmSAGs expression analysis in soybean under multiple stresses and senescence.

Stress	Treatment/Time	NCBI-access number	Reference
Moderate Drought	Water withdraw – 7 days	PRJNA324522	Chen *et al*., 2016
Severe Drought	Water withdraw – 25 days	GSE50408	Carvalho *et al*., 2014
Oxidative Stress	Plant intermittent-flooding – 7 days	PRJNA324522	Chen *et al*., 2016
*Fusarium oxysporum*infection	1.10^{16} conidial aspersion - 72 hours	GSE66861	Lanubile*et al*., 2015
Sclerotinia sclerotiorum infection	Simulated infection by oxalic acid (5.0 mM) vacuum-infiltration – 2 hours	GSE15369	Calla *et al*., 2014
Lamprosema indicate attack	Insect artificial attack	SRA549	Zeng *et al*., 2017
Ethylene-induced senescence	Leaves-explants under 25 µM of ethylene pressure – 12 hours	SRP050050	Kim *et al*., 2018
Age-induced senescence	Late R7 developmental stage leaves	GSE122915	Melo *et al*., 2018

REFERENCES

Calla, B., Blahut-Beatty, L., Koziol, L., Simmonds, D. H., and Clough, S. J. (2014). Transcriptome analyses suggest a disturbance of iron homeostasis in soybean leaves during white mould disease establishment. *Mol. PlantPathol.* 15, 576–588. doi:10.1111/mpp.12113.

Carvalho, H. H., Brustolini, O. J. B., Pimenta, M. R., Mendes, G. C., Gouveia, B. C., Silva, P. A., Silva, J. C. F., Mota, C. S., Soares-Ramos, J. R. L., and Fontes, E. P. B. (2014). The molecular chaperone binding protein BiP prevents leaf dehydration-induced cellular homeostasis disruption. *PLoS ONE* 9, e86661. doi:10.1371/journal.pone.0086661.

Chen, W., Yao, Q., Patil, G. B., Agarwal, G., Deshmukh, R. K., Lin, L., Wang, B., Wang, Y., Prince, S. J., Song, L., et al. (2016). Identification and Comparative Analysis of Differential Gene Expression in Soybean Leaf Tissue under Drought and Flooding Stress Revealed by RNA-Seq. *Front. PlantSci.* 7, 1044. doi:10.3389/fpls.2016.01044.

Kim, J., Yang, J., Yang, R., Sicher, R. C., Chang, C., and Tucker, M. L. (2016). Transcriptome analysis of soybean leaf abscission identifies transcriptional regulators of organ polarity and cell fate. *Front. Plant Sci.* 7, 125. doi:10.3389/fpls.2016.00125.

Lanubile, A., Muppirala, U. K., Severin, A. J., Marocco, A., and Munkvold, G. P. (2015). Transcriptome profiling of soybean (Glycine max) roots challenged with pathogenic and non-pathogenic isolates of Fusariumoxysporum. *BMC Genomics* 16, 1089. doi:10.1186/s12864-015-2318-2.

Melo, B. P., Fraga, O. T., Silva, J. C. F., Ferreira, D. O., Brustolini, O. J. B., Carpinetti, P. A., Machado, J. P. B., Reis, P. A. B., and Fontes, E. P. B. (2018). Revisiting the soybean gmnac superfamily. *Front. Plant Sci.* 9, 1864. doi:10.3389/fpls.2018.01864.

Zeng, W., Sun, Z., Cai, Z., Chen, H., Lai, Z., Yang, S., and Tang, X. (2017). Comparative transcriptome analysis of soybean response to bean pyralid larvae. *BMC Genomics* 18, 871. doi:10.1186/s12864-017-4256-7.

Supplementary Table 2. qRT-PCR primers used to determine the expression of *GmNAC065* and *GmNAC085*in soybean tissues and multiple stresses and the expression of GmNAC-SAGs in bleomycin-treated soybean

Endogenous Control	
qRT_ELF1A_fwd	GACCTTCTTCGTTTCTCGCA
qRT_ELF1A_revs	CGAACCTCTCAATCACACGC
Target Genes	
qRT_GmNAC065_fwd	TGGGATTTGCCAGGTGATTT
qRT_GmNAC065_revs	GAGCGATTTCCGTTGGGATA
qRT_GmNAC085_fwd	GCAATGGGTCATCACCTTCT
qRT_GmNAC085_revs	GACCCAAATTCGGAAACTGA
GmNAC-SAGs	
qRT_GmNAC074_fwd	TCCTAGTGGTGAGCGGACTGA
qRT_GmNAC074_revs	TAACACCCAGGCATCTCTTAAGC
qRT_GmNAC081_fwd	GGAGCAAAGGGCAGCACTAG
qRT_GmNAC081_revs	TGTCCGTGGAGGAAGGAGAA
qRT_GmNAC023_fwd	CGAGCACCCAAAGGAGAGAA
qRT_GmNAC023_revs	CGAGCACCCAAAGGAGAGAA
qRT_GmNAC131_fwd	CTGCCACCTCTCTCGGATTC
qRT_GmNAC131_revs	GAGAAGCAGGGCACGTAAGC
qRT_GmNAC106_fwd	GTGTGGACGCTATGCCGAAT
qRT_GmNAC106_revs	GGTGCTGCCGAGTCTTTCAA
qRT_GmNAC010_fwd	AGTCCACGAGAGAGGAAGTATCCA
qRT_GmNAC010_revs	GTGCCAGTGGCCTTCCAATA
qRT_GmNAC109_fwd	CAACATATCGCGGTTCCCATA
qRT_GmNAC109_revs	TACAAAGCCATTCCTGGAAGGT
qRT_GmNAC030_fwd	GATTCCACCCCACTGACGAT
qRT_GmNAC030_revs	GATGGGAACAGCAATGGTTTG
qRT_GmNAC101_fwd	TCAGCCCCAGAGACAGGAAAT
qRT_GmNAC101_revs	TCCGGTGGCTTTCCAATAAC

qRT_GmNAC092_fwd CGATGCCACGTGTCAACAC

qRT_GmNAC092_revs TAACCCCCCTTCACCCAAGT

qRT_GmNAC149_fwd CGGGAGATAGGCAATGGTTCT

qRT_GmNAC149_revs TCTGGTTGCTCGGTTAGACCTT

qRT_GmNAC077_fwd GGAGCAAAGGGCAGCACTAG

qRT_GmNAC077_revs TGGAGGAAGGAGGAGAAGCA

qRT_GmNAC154_fwd TCTGACAACGGCAAGCCATA

qRT_GmNAC154_revs GCCGGTTTCCTTTCATTTTG

qRT_GmNAC179_fwd TGGGATTTGCCAGGTGATTT

qRT_GmNAC179_revs GAGCGATTTCCGTTGGGATA

qRT_GmNAC003_fwd TGTACTCCCACCTGGCTTCAG

qRT_GmNAC003_revs TTGATGAGGCTTGGTTGCAA

qRT_GmNAC011_fwd TACCCCCTGGATTCCGATTC

qRT_GmNAC011_revs TTCTTGCGAAGCGCATTTG

qRT_GmNAC043_fwd GGATCGTTGCCGGAGATAAA

qRT_GmNAC043_revs TCATCCTGCTGGTGCATTGT

Supplementary Table 3. qRT-PCR primers used to determine the expression of antioxidant enzymes, stress marker genes and AtNAC-SAGs in *Arabidopsis thaliana*

Endogenous Control	
ACT2-F	GATCTCCAAGGCCGAGTATGAT
ACT2-R	CCCATTCATAAAACCCCAGC
Anti-oxidant enzymes CAT, SOD and APX	
APX-F	CCTCCGGAGGGTATCGTTATCTA
APX-R	ACAGCCAGAAACATTGTCCAAAAGG
CAT1-F	TGGGATTCAGACAGGCAAGAACG
CAT1-R	GTTTGGCCTCACGTTAAGACGAGT
CSD1-F	TGAACTCAGCCTGGCTACTGG
CSD1-R	AGCCACACACCAGAAGATACACAC
Stress marker genes	
Drought	
RD29A-F	GATTTCTTCTGATCGACAAAACCTA
RD29A-R	AGCAAACCCAACTTATTACATTACG
RD29B-F	GCAAGCAGAAGAACCAATCA
RD29B-R	CTTTGGATGCTCCCTTCTCA
RD20-F	TTAGCTCCGGTCACCAGTCA
RD20-R	CATGTATGGTTTTGGTAATGTTTCC
ER-stress	
ANAC036 – F	GCTCAAGAAGACGCTTGTGTT
ANAC036 - R	CTCGTTCATCACCCAATCAG
CNX fwd	TGATGGGGAGGAGAAGAAAAAGGC
CNX rvs	CGGTGTAGACATGGGAAAGC
Biotic Stress	
NPR1 – F	CTGCAGACTCATACACTCTGG
NPR1 – R	ATCCGAGTCTCACTGACTTTC
RAB18-F	GGCTTGGGAGGAATGCTT
RAB18-R	TTGATCTTTTGTGTTATTCCCTTCT

AtNAC-SAGs	
ANAC072- F	GCACGAGTATCGCTTAATAGAACA
ANAC072 - R	CGACACAACACCCAATCATC
ANAC083 – F	TTTGCAGAGCTGATCCTTGG
ANAC083 – R	CGGTTCCCATTTGGGTATTT
ANAC019 - F	AACTGTGGCTACCTGAAGACG
ANAC019 - R	CCGAGTTATTAAACCCGTGACT
AtNAP - F	GAAACCAGACCATGTCTAAACCA
AtNAP - R	TTTCTCCAAACTCTGTTTTCTCG
ANAC016 - F	ATTCACTTCACAGTCAACAGGTG
ANAC016 - R	GCTGATGAGAACTGGCTCCT
ANAC055 - F	TTCTCGAGTCGTTGCATGAG
ANAC055 - R	CTATGAGGCAGCGCGTTT
ORE1 - F	GTGGGTATGAAGAAAACTTTGG
ORE1 - R	TTCGTTCTTAGCTGTTTGGGG
ATAF1 – F	AGGCTGGATGATTGGGTTCTCTG
ATAF1 – R	GATTTCGTCGCCGTAAACAACCG
SAG113 - F	AGGAAAACTCAACATCCTCGTC
SAG113 - R	GCTGACTCGAGATTTGTAGCC
GLK1 – F	GCTACGAGATTTAGAGCACCG
GLK1 – R	TTGACGGATGTAAGTCTACCG
SINA1 - F	TCCTGCGAAATGGAACCTCGAATC
SINA1 – R	TTCGATGTGGTCGTTGGGACACTC
BFN1 – F	TTGAAGAGAAGAGTGTGGCTTGG
BFN1 – R	AGAAGAGCCGCTTGGTCGTATG
NCED3 – F	ACTCATGCTATT CTACGCCAGAG
NCED3 – R	ACCAACGGTTT TTAAATCTCCAT
Sweet15 – F	CAATGACATATGCATAGCGATTCCAA
Sweet15 – R	GGACTCATCACGACAATACTCTTAAG
NYC1- F	GCAGAGAACAGGACGAGGTT
NYC1 - R	CGCAAACAACAGAAAGAGAGAA
PaO - F	CCCAGGCAGACCGTTTTGT
PaO - R	TGACTCTTACCATGCCGTCTGA
CLH1 - F	CCCGTCGTTTTATTCTTCCA

CLH 1- R	AGCATCGTCCACTTCCACTT
BSMT1 – F	CATTCAACATGCCGTTTTATG
BMST1 – R	CATTGGTTCACTAACAGCTC

Supplementary Table 4. Canonical *cis*-regulatory elements and their TFs in *pGmNAC065* and *pGmNAC085*

Cis-element	Positions in *pGmNAC065*	Positions in *pGmNAC085*	Consensus Sequence	TF-binding group
ABRECORE	444; 551; 828	65; 243; 532; 657; 687; 795; 828; 1013; 1480; 1485	ACGT/ MACGYGB	ERD, AREB, bZIP
AMYBOX1	779; 1009; 1241; 1602	1657	TAACARA	MYB
EBOXBNNAPA/ MYCCONSENSUSAT	230; 522; 815; 991; 1468; 1540; 1886	243; 657; 687; 1531	CANNTG	bLHL and MYB
DRECORE	1295; 1301	-	CCGAC	DREB, ERF/AP2
EIN/EIL	206; 306; 699; 1550	1017	TGCA/ATAC	EIN3
MYB1AT	17; 668; 731; 1810; 1816; 1822; 1828	862; 1644	WAACCA	MYB
MYBCORE	121; 186; 1599; 779; 1488	789	GTTAGTT	
MYBCOREATCYCB1	1347	266; 789; 1416; 1563	AACGG	
MYBGAHV	1104	1449; 1657	TAACAAA	
MYBPZM	1368	60; 428; 1337	CCWACC	
MYBST1	221; 1115; 1546; 1978	1298	GGATA	
NAC-R	87; 501; 1331; 1886	48; 576; 631; 1084	TTGAC/TACG	NAC
NAPINMOTIFBN	231	-	TACACAT	MYB, bZIP, bHLH
RAV1AAT	430; 589; 1404	48; 945; 966; 1016	CAACA	AP2/ERF
WBOX	80; 395; 620; 1562; 1686; 1851	51; 57; 68; 311; 578; 663; 702; 793; 957; 1086; 1120	TTTGACY	WRKY
G-BOX	-	64	CACGTC	bZIP

Note: K=G/T; R=G/A; W=A/T; N=A/C/G/T; Y =T C

CHAPTER IV

SOYBEAN EMBRYONIC AXIS TRANSFORMATION: COMBINING BIOLISTIC AND *AGROBACTERIUM*-MEDIATED PROTOCOLS TO OVERCOME TYPICAL COMPLICATIONS OF IN VITRO PLANT REGENERATION

Published article

Bruno Paes de Melo, Isabela Tristan Lourenço-Tessutti, Carolina Vianna Morgante, Naiara Cordeiro Santos, Luanna Bezerra Pinheiro, Camila Barrozo de Jesus Lins, Maria Cristina Matar Silva, Leonardo Lima Pepino Macedo, Elizabeth Pacheco Batista Fontes and Maria Fatima Grossi-de-Sá

Pages 172 to 185

RESUMO

A primeira tentativa bem-sucedida de gerar plantas geneticamente modificadas que expressam um transgene foi realizada por meio de transferência de genes baseada em T-DNA, empregando a transformação genética mediada por *Agrobacterium tumefaciens*. As limitações sobre a infectividade e a cultura de tecidos *in vitro* levaram ao desenvolvimento de outros sistemas de transfecção de DNAs exógenos, como o método biolístico. Este trabalho apresenta um fluxograma completo de novo protocolo de etapa única para a transformação e recuperação de plantas de soja transgênicas, combinando dois métodos de transformação diferentes. O protocolo consiste das seguintes etapas: preparação da agrobactéria, esterilização de sementes, excisão de embriões de sementes de soja, lesão de células da parte aérea por bombardeamento de micropartículas de tungstênio, transformação mediada por *A. tumefaciens*, co-cultivo de embriões *in vitro* e seleção de plantas transgênicas. O tempo total de execução do protocolo é de aproximadamente 30–40 semanas para a recuperação de linhagens férteis. A eficiência média de transformação foi de 9,84%, semelhante a outros protocolos descritos anteriormente. Porém, introduzimos uma metodologia de recuperação de plantas transgênicas mais econômica, direta e curta, que permite o co-cultivo e a regeneração da planta em uma única etapa, diminuindo as chances de contaminação e facilitando a manipulação. Finalmente, como marca registrada, nosso protocolo não gera quimeras de plantas, em contraste com os protocolos tradicionais de regeneração de plantas aplicados em outros métodos de transformação mediados por *Agrobacterium*. Portanto, esta nova abordagem de transformação de plantas é aplicável para estudos de função gênica e produção de cultivares transgênicas com diferentes características para programas de melhoramento genético.

frontiers in Plant Science

METHODS
published: 12 August 2020
doi: 10.3389/fpls.2020.01228

Soybean Embryonic Axis Transformation: Combining Biolistic and *Agrobacterium*-Mediated Protocols to Overcome Typical Complications of *In Vitro* Plant Regeneration

Bruno Paes de Melo[1,2,3,4†], *Isabela Tristan Lourenço-Tessutti*[2,4†], *Carolina Vianna Morgante*[2,4], *Naiara Cordeiro Santos*[2,4], *Luanna Bezerra Pinheiro*[2,4,5], *Camila Barrozo de Jesus Lins*[2,4], *Maria Cristina Matar Silva*[2,4], *Leonardo Lima Pepino Macedo*[2,4], *Elizabeth Pacheco Batista Fontes*[1,3] and *Maria Fatima Grossi-de-Sa*[2,4,5*]

[1] Biochemistry and Molecular Biology Department, Universidade Federal de Viçosa (UFV), Viçosa, Brazil, [2] Embrapa Genetic Resources and Biotechnology, Brasilia, Brazil, [3] National Institute of Science and Technology in Plant-Pest Interactions (INCTIPP), BIOAGRO, Viçosa, Brazil, [4] National Institute of Science and Technology, INCT PlantStress Biotech, EMBRAPA, Brasilia, Brazil, [5] Genomic Sciences and Biotechnology PPG, Universidade Católica de Brasília (UCB), Brasilia, Brazil

The first successful attempt to generate genetically modified plants expressing a transgene was preformed via T-DNA-based gene transfer employing *Agrobacterium tumefaciens*-mediated genetic transformation. Limitations over infectivity and *in vitro* tissue culture led to the development of other DNA delivery systems, such as the biolistic method. Herein, we developed a new one-step protocol for transgenic soybean recovery by combining the two different transformation methods. This protocol comprises the following steps: agrobacterial preparation, seed sterilization, soybean embryo excision, shoot-cell injury by tungsten-microparticle bombardment, *A. tumefaciens*-mediated transformation, embryo co-cultivation *in vitro*, and selection of transgenic plants. This protocol can be completed in approximately 30–40 weeks. The average efficiency of producing transgenic soybean germlines using this protocol was 9.84%, similar to other previously described protocols. However, we introduced a more cost-effective, more straightforward and shorter methodology for transgenic plant recovery, which allows co-cultivation and plant regeneration in a single step, decreasing the chances of contamination and making the manipulation easier. Finally, as a hallmark, our protocol does not generate plant chimeras, in contrast to traditional plant regeneration protocols applied in other *Agrobacterium*-mediated transformation methods. Therefore,

OPEN ACCESS

Edited by:
Yule Liu,
Tsinghua University, China

Reviewed by:
Kan Wang,
Iowa State University, United States
Aihua Sha,
Yangtze University, China

***Correspondence:**
Maria Fatima Grossi-de-Sa
fatima.grossi@embrapa.br

[†]*These authors have contributed equally to this work*

Specialty section:
This article was submitted to Technical Advances in Plant Science, a section of the journal Frontiers in Plant Science

Received: *09 May 2020*
Accepted: *27 July 2020*
Published: *12 August 2020*

Citation:
Paes de Melo B, Lourenço-Tessutti IT, Morgante CV, Santos NC, Pinheiro LB, de Jesus Lins CB, Silva MCM, Macedo LLP, Fontes EPB and Grossi-de-Sa MF (2020) Soybean Embryonic Axis Transformation: Combining Biolistic and Agrobacterium-Mediated Protocols to Overcome Typical Complications of In Vitro Plant Regeneration. Front. Plant Sci. 11:1228. doi: 10.3389/fpls.2020.01228

this new approach of plant transformation is applicable for studies of gene function and the production of transgenic cultivars carrying different traits for precision-breeding programs.

Keywords: *Glycine max*, genetic transformation, *Agrobacterium*-mediated transformation, particle bombardment high-efficiency plant transformation, embryonic axis

INTRODUCTION

Genetic transformation is an essential key technique of genetic engineering tool kits. Modification of the genome allows us to discover the functions of genes and, consequently, the cellular processes under their control, raising many possibilities for biotechnological intervention and bioengineering. In plant science, genetic transformation has become a basic tool for precision genetic breeding, which allows specific characteristics to be directly encoded in the plant genome by foreign DNA delivery insertion or genome editing techniques.

Plant genetic transformation workflows are not trivial and their success depends not only on exogenous DNA insertion into the host genome but also on the regeneration of a whole-new functional and reproductive plant. Therefore, several studies have been conducted to enhance plant transformation and regeneration capacities and to develop easier protocols for execution, avoiding ordinary problems associated with *in vitro* tissue culture, the main limiting factor for precision genetic engineering in plant breeding (Rech et al., 2008).

There are two main methods of plant transformation according to the DNA-delivery system: a) particle bombardment, also called biolistic delivery (McCabe et al., 1988), and b) *Agrobacterium*-mediated transformation (Hinchee et al., 1988; Lee et al., 2009). The *Agrobacterium*-mediated method is still the most commonly used. *Agrobacterium ssp.* are plant-pathogenic bacteria that infiltrate plant cells by wounds and are capable of transferring and integrating T-DNA in plant-host genomes (Gelvin, 2000). Currently, optimized *Agrobacterium*-mediated protocols are successfully applied to generate transgenic plants; almost 85% of all species of transgenic plants have been generated by this method (Wu and Zhao, 2017). Perhaps it is suitable only for a few plant species, and the success of T-DNA transfer depends on several variable factors, such as bacterial virulence or the type of explant, which, combined with plant-explant recalcitrance and plant regeneration capacity, directly affect the success of plant transformation protocols.

The *Agrobacterium*-mediated method is highly reproducible, simple to operate, inexpensive and, mainly, allows one or a few insertions of exogenous DNA fragments in the host genome, which are its main advantages over the biolistic method (McCabe et al., 1988; Rech et al., 2008; Li et al., 2017). In general, several plant tissues can be used as explants for this transformation workflow, such as leaf nodes, epicotyls, hypocotyls, immature embryo axillary buds and cotyledonary nodes (Li et al., 2017), and the elementary steps of plant transformation are shared by many protocols. However, the steps of tissue cultivation and plant regeneration change completely according to the characteristics of each explant, and the choice of the explant type to be used should consider its regeneration capacity.

In soybean, cotyledonary nodes are often selected as the main explant type. They display a simple and efficient regeneration process (Kim et al., 1990; Sato et al., 1993; Li et al., 2017), and the transformation workflow is performed as follow: isolation of sterile explants, infection, cocultivation, shoot induction, root induction and, finally, seedling acclimation (Li et al., 2017). Normally, to ensure plant regeneration, phytohormones are applied in different combinations into plant culture media (co-cultivation medium (CCM), shoot elongation medium (SEM) and rooting medium (RM)) to promote shoot elongation followed by rooting. The most useful phytohormones are auxins, cytokinins, and gibberellins (Li et al., 2017), as they affect cell growth, tissue development, and plant regeneration. Auxin promotes cell elongation and plant growth, and cytokinins trigger cell division (Skoog and Miller, 1957; Normanly, 1997). When combined, they can induce callus formation or promote shoot elongation. On the other hand, a combination of auxin and gibberellin can stimulate root development (Nishijima, 2003; Thomas and Sun, 2004; Yamauchi et al., 2007; Gao et al., 2017).

The main source of troubles in plant transformation is the tissue culture step. In *Agrobacterium*-mediated protocols, the co-cultivation of bacteria and plant explants triggers defensive pathways in plants, culminating in the production of reactive oxygen species (ROS). ROS accumulation leads to tissue browning and necrosis, which limit the regenerative process (Li et al., 2017). To reduce tissue browning and enhance regeneration, CCM is often supplemented with antioxidants such as dithiothreitol (DTT), L-cysteine and PVPP (polyvinylpolypyrrolidone; Dutta Gupta, 2010; Li et al., 2017). Furthermore, the continuous manipulation and medium exchanges required during the process of plant regeneration are the sources of contamination with fungi and bacteria, decreasing the efficiency of the process.

These *Agrobacterium* transformation-derived troubles are partially overcome by biolistic protocols, in which exogenous DNA is directly bombarded against plant tissue and delivered to plant cells (Liu and Godwin, 2012). However, the biolistic method requires all the steps of tissue culture, and DNA bombardment frequently leads to undesirable multiple insertions. Additionally, it does not allow the transference of large DNA fragments and displays lower transformation efficiency than *Agrobacterium*-mediated methods (Li et al., 2017).

Rech et al. (2008) described a DNA bombardment-derived method for soybean, cotton and common bean transformation in which the embryonic axis is isolated from mature seeds and used as explants. The protocol avoids excessive tissue manipulation

and explores the enhanced regenerative capacity of shoot meristematic cells. The limitation of this protocol is mainly in the selection of putative transgenic plants. Normally, selectable marker genes are widely used to ensure the regeneration of only transformed cells in a selective culture medium supplied with antibiotics or herbicides. Using embryonic axis as explants, the shoot meristematic cells are not in contact with the selective agent once just the embryo radicle is immersed into the selective culture medium. The embryos are nourished by the radicle-shoot axis and molecules that are systemically translocated and capable of accumulating on shoot cells are suitable for use as selective agents. To date, only the Imazapyr herbicide can be used for this purpose. Imazapyr is an imidazolinone-based herbicide that inhibits the activity of acetohydroxyacid synthase, which disrupts the biosynthesis of the amino acids leucine, isoleucine, and valine (Shaner et al., 1984). Plants carrying the mutated *Arabidopsis thaliana ahas* gene display specific imidazolinone resistance and are suitable for selection with imazapyr during the transformation workflow.

Herein, we provide a complete protocol for soybean embryonic axis transformation mediated by *A. tumefaciens*. It has already been described a combination of particle-bombardment and *A. tumefaciens*-mediated protocols using embriogenic callus from half-seeds as plant-explant (Droste et al., 2000). Despite presenting a new method for soybean transformation, the work reported low-efficiency compared with other methods. In addition, the choice of callus as plant explant does not eliminate ordinary complications arising from tissue culture steps. Recently, Pareddy et al. (2020) described a method of *Agrobacterium*-mediated transformation with approximately 19% of transformation efficiency, superior to other already described. The new methodology takes as explant the half-imbibed seeds and explores the competence of shoot cells in the embryonic axis for genetic transformation and regeneration by *in vitro* organogenesis. Mechanical removal of radicle system enhances the *Agrobacteria* infectivity and contributes to high reported efficiency. However, the plant regeneration demands *in vitro* organogenesis and the plant recovery workflow is superior to 15 weeks. For shoot induction, elongation and rooting steps, continuous media-changes and supplementation with several phytohormones and growth regulators, such as BAP, timentin, IAA, zeatin, and GA_3, are required. In spite of the high efficiency of transgene-integration, these protocol's features make it long, expensive and do not overcome ordinary complications of *in vitro* plant regeneration, which comprises the limiting step on soybean transformation workflow.

Our protocol explores the main advantages of each soybean transformation system to overcome typical issues on plant regeneration, making it easily reproductive into obtaining transgenic fertile-lines in a direct and time- and cost-optimized way, with reasonable transformation efficiency. These advantages include i) the particle acceleration by biolistic systems for explant wounding, which is required for *Agrobacterium*-mediated plant infection; ii) the capacity of *A. tumefaciens* to transfer exogenous large foreign DNA as single or few copies in the host genome; and iii) the use of the embryonic axis as a plant explant. The shoot cells of the embryonic axis display high transformability and regeneration capacity and can be submitted to a one-step transformation, co-cultivation, and regeneration workflow, avoiding excessive manipulation of explants, comprising the main advantage over other organogenesis-based methods. These combined features reduce the challenges in soybean transformation and enhance the efficiency of the process, making it more suitable for studying gene function and generating new engineered cultivars.

MATERIALS AND EQUIPMENT

General Reagents, Equipment, and Materials

- Sterile distilled and deionized water
- Absolute ethanol
- Isopropanol
- Tweezers
- Glass sterile Petri dishes (135 mm diameter)
- Scalpel (n.10)

Bacterial Culture

- Luria-Bertani (LB) medium
- Bacteriological agar
- Gentamicin
- Rifampicin
- Kanamycin

Biological Material

- Mature seeds of soybean Williams 82
- *tumefaciens* GV3101 with the desired construct

Embryo Transformation and Plant Tissue Culture

- Sodium hypochlorite (2.5% v/v)
- Sterile Whatman paper
- Glycerol
- B5 basal plant medium (Gamborg)
- MES buffer (2-N-morpholinoethanosulfonic acid)
- Sucrose
- DTT (dithiothreitol)
- BAP (6-benzylaminopurine)
- Acetosyringone (4′-hydroxy-3′,5′-dimethoxyacetophenone)
- GA_3 (gibberellin analog)
- L-cysteine
- Sodium thiosulfate
- MS (Murashige and Skoog) plant medium
- Activated charcoal
- Imazapyr (2-(4,5-dihydro-4-methylethyl)-5-oxo-1H-imidazol-2-yl)-3-pyridinecarboxylic acid)

- Tungsten microparticles
- Carrier membrane (50 μm thickness and 24 mm diameter)
- Rupture disks (250 μm thickness and 13.2 mm diameter)
- Petri dishes (5 cm diameter)
- Magenta plant tissue culture boxes

Equipment

- Biological laminar flow chamber
- Autoclave
- Shaker incubator
- Centrifuge
- (Bio)spectrophotometer
- Helium pressure-driven microparticle acceleration system
- Ultrasonic bath
- Standard plant tissue culture room and greenhouse

Reagent Set-Up

Acetosyringone Stock Solution: Dissolve 1.96 g of acetosyringone (3,5- dimethoxy-4-hydroxy-acetophenone) in 100 ml of ethanol (100%) to obtain a final concentration of 100 mM and store in a refrigerator at 4°C.

BAP Stock Solution: Dissolve 50 mg of 6-BAP in 1 N NaOH, complete the volume to 10 ml with distilled water, sterilize by autoclaving along with the culture medium. Store at -20°C for up to 6 months.

GA_3 Stock Solution: Add 100 mg of gibberellic acid 3 to 100 ml of distilled water and stir until dissolved to make a solution with a final concentration of 1 mg/ml (1000 ppm). It is best to use this solution fresh. However, a stock solution can be stored in the dark at -20°C for up to 6 months. Sterilize the solution by filtration (0.22 μm)

Imazapyr Stock Solution: Prepare a stock solution to a 1 mM final concentration. Dissolve 13.17 mg of imazapyr in 50 ml of distilled and deionized sterile water. Using a microfilter (0.22 μm), sterilize the solution and stock 1 ml aliquots in aluminum-protected tubes at -20°C for up to 1 month.

Tungsten Particle Pre-Preparation: Separate 60 mg of tungsten particles in a sterile tube and add 1 ml of 70% ethanol (v/v). Homogenize the suspension by vortexing for 15 min. Centrifuge at 3,000 g—5 min. Remove the ethanol with a pipette without disrupting the pellet. Add 1 ml of sterile distilled and deionized water, mix very well by vortexing, centrifuge as described and repeat the cleaning steps 3 times. At the last washing, remove the water and resuspend the microparticles with 1 ml of sterile 50% glycerol (v/v). Store the particles at -20°C.

METHODS

The following procedures introduce a one-step method for soybean embryonic axis transformation by *A. tumefaciens*. The workflow describes the process of embryo isolation, explant infection, plant-bacteria co-cultivation and putative transgenic plant regeneration and selection (**Figure 1**) to overcome issues and, consequently, low efficiency. All described steps were adjusted for transformation of 150 embryo axes.

Day 1 ‖ Bacterial Preparation • Time: 30 min + 16 h

1. To prepare an *Agrobacterium* culture, pick up a single colony of *A. tumefaciens* GV3101 that had been previously transformed with the vector of interest to inoculate 5 ml of LB medium supplemented with 50 mg/L gentamicin, 100 mg/L rifampicin and 100 mg/L kanamycin (or a corresponding dosage of a plasmid-selective agent).
2. Incubate in shaker under agitation—180 rpm—28°C—overnight (ON).
3. After bacterial growth, dilute 100 μl of preinoculum into 100 ml of LB medium with the same concentrations of the selective agents. Incubate under the same conditions until the OD_{600} = 0.6 (~ 16 h). ▲**CRITICAL** The OD_{600} accuracy at this point is very important to guarantee bacterial virulence. At this OD, the bacterium culture is in the log phase, and its metabolism is completely active. The culture can be stored in the refrigerator (4°C) until embryo incubation.

Day 1 ‖ Plant Culture Medium • Time: 180 min

Initial notes:

- 100 ml of liquid CCM for each round of transformation/plasmid.
- 20 ml of solid CCM for each bombardment plate containing 30 embryos

P.S. 300 embryos (distributed on 10 plates) are normally bombarded at one round of transformation.

CCM contains 0.3 g/L B5 basal medium (Gamborg), 3.9 g/L MES (2-N-morpholinoethanosulfonic acid), 30 g/L sucrose and 154.2 mg/L DTT (dithiothreitol).

1. Separately dissolve all the components of CCM in distilled and deionized water.
2. After medium preparation, adjust the pH to 5.4.
3. Sterilize by autoclaving.
4. The liquid medium can be stored at 4°C for 1 week.

To prepare solid CCM, follow the protocol for preparation of liquid medium.

1. Supplement the liquid medium with 400 mg/L L-cysteine and 158 mg of sodium thiosulfate.
2. After pH adjustment, add 5 g/L bacteriological agar.
3. Sterilize by autoclaving.
4. Supplement the sterile medium with 835 μg/L BAP (6-benzylaminopurine), 40 mg/L acetosyringone and 0.25 mg/L GA_3 (gibberellin analog), all filter-sterilized, and immediately distribute it in 5 cm (ϕ) plastic Petri dishes

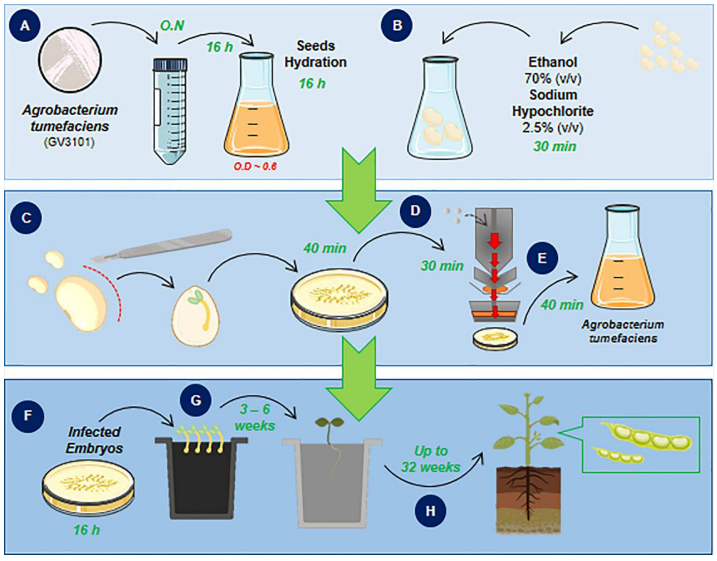

FIGURE 1 | Biolistic and *Agrobacterium*-mediated soybean embryonic axis transformation workflow. The workflow of the proposed protocol in this study consists of a one-step soybean embryo infection followed by plant regeneration to obtain transgenic soybean plants. The workflow is divided into three main parts that are followed day-by-day until the plant regeneration step, which requires up to 6 weeks until seedling acclimation. The protocol starts with isolation and bacterial culture **(A)** in parallel with seed sterilization and hydration **(B)**. The next step achieves the isolation of embryonic axis **(C)**, bombardment of shoot cells that will be transformed and regenerated into a reproductive plant, **(D)** and, finally, *A. tumefaciens* (GV3101 strain) infection **(E)**. After embryo infection, cocultivation occurs **(F)** and is immediately followed by plant regeneration **(G)** until the acclimation step and plant recovery **(H)**.

(approximately 20 ml medium/plate), forming a layer of 0.6–0.7 mm. ▲**CRITICAL** Do not add the sterile hormones to hot medium. The ideal temperature for adding hormones to a culture medium is 55°C, preferably measured by an infrared thermometer. Add the acetosyringone only when resuspending the bacterial culture.

The development and root medium (DRM) contained 4.3 g/L MS (Murashige and Skoog) medium, 30 g/L sucrose, 1.0 mg/L BAP, and 1.0 g/L activated charcoal.

1. Take all the components of the DRM except the charcoal and dissolve them in distilled and deionized water.
2. Adjust the pH to 5.7.
3. After the pH adjustment, add 5.0 g/L bacteriological agar and activated charcoal. ▲**CRITICAL** Do not shake the flask to mix the components. The charcoal is not soluble in water and mixing it by shaking spreads the particles; hence, they will stay heterogeneously distributed in the final medium.
4. Supplement DRM with a selective agent (herbicide) according to the literature-recommended dosage. ▲**CRITICAL** If the selective marker gene is *bar*, which confers resistance to ammonium glufosinate-derived herbicides, the DRM should not be supplemented with ammonium glufosinate. Ammonium glufosinate is not a systemic herbicide and requires the contact between transformed cells and culture medium. During plant regeneration, apical meristem cells are not in contact with the culture medium; hence, non-transformed radicle cells will not be in contact with the herbicide (Zhang et al., 1999; Li et al., 2017). The selection of putatively transformed plants is performed after complete plant regeneration by herbicide pulverization in a greenhouse. However, if the selective marker gene is *ahas*, which confers imidazolinone resistance, the DRM should be supplemented with 600 nM imazapyr. Imazapyr is sensitive to light and heat. Keep aliquots in an amber flask until utilization and add them to cold medium (55°C).

Day 1 ‖ Seed Sterilization • Time: 30 min + 16 h

(!) CAUTION All the following steps should be performed in a laminar flow chamber previously cleaned with sodium hypochlorite (2.5% v/v) and ethanol (70% v/v) and exposed to UV radiation for 20 min.

1. As only 50% of the embryonic axis is recovered for transformation during the isolation process, it is recommended to sterilize double the number of seeds. For

example, if you start with 600 seeds, you will have approximately 300 embryonic axes viable for transformation. Distribute the seeds in two sterile 350 ml Erlenmeyer flasks. Immerse the seeds in 75% (v/v) ethanol for 2 min. The following steps are adjusted for embryonic axis isolation from 300 seeds and transformation of 150 embryo axes.

2. Remove the ethanol and immerse the seeds in commercial sodium hypochlorite (2,5% v/v) for 20 min, gently mixing every 5 min.
3. Remove the sodium hypochlorite and rinse the seeds 3 times with sterile water.
4. Immerse the seeds with sterile water leaving a 3 cm layer above them; seal the Erlenmeyer and store under dark for 24 h until embryo isolation. ▲**CRITICAL:** Floating seeds should be discarded.

Day 2 ‖ Preparation of Tungsten Microparticle-Carrying Membranes • Time: 30 min

The microparticle accelerator system demands two types of membranes: the carrier membrane (24 mm diameter, **Figure 2A**), where tungsten is deposited to be accelerated against plant tissue, and the rupture disk (13.2 mm diameter, **Figure 2B**), for sealing the helium at the high-pressure chamber in the particle accelerator.

The setup of this transformation requires a 1200 p.s.i. rupture pressure. If necessary, use more than one rupture disk to achieve the desired pressure, *e.g.*, 4 x 300-p.s.i. rupture disks.

The carrier membranes are attached to a metallic ring that should be stored in ethanol and flame-sterilized before use (**Figure 2C**).

Particle preparation:

- 1 carrier membrane for each round of bombardment. P.S. 150 embryo axes divided into 7–8 bombardment plates may be available at this step.
- 4 rupture (300 p.s.i.) disks for each round of bombardment.

1. Vortex the pre-prepared aliquot of tungsten microparticles 1 min and homogenize it very well.
2. Separate an aliquot of 100 µl in a sterile microtube.
3. Add 100 µl of sterile distilled and deionized water and homogenize gently.
4. Centrifuge at 3,000 g—30 s.
5. Carefully remove the supernatant with the help of a micropipette. Take care to not aspirate the particles at the bottom of the tube.
6. Add 300 µl of absolute ethanol and homogenize gently.
7. Centrifuge 30 s at 3,000 g.
8. Repeat steps 6 and 7 twice.
9. Carefully remove the supernatant and add 48 µl of absolute ethanol to the particles.
10. Sonicate the particles for 30 s at maximum intensity to assure that the tungsten particles are well separated, which provides a better distribution at the carrier membrane surface.
11. Attach the ethanol-humidified carrier membrane to the metallic ring. ▲**CRITICAL** The membrane should be very

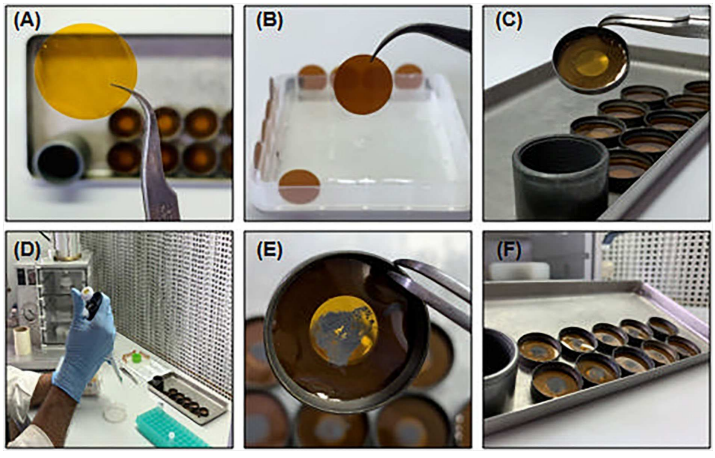

FIGURE 2 | Tungsten-coated carrier membrane preparation. **(A)** Carrier membrane (24 mm diameter); **(B)** Rupture disk (13.2 mm diameter); **(C)** Metallic ring support of carrier membrane; **(D, E)** Distribution of prepared tungsten microparticles at carrier membrane surface; **(F)** Prepared tungsten-coated carrier membranes under hood to drying. All manipulation in tungsten-coated membranes' preparing may be performed under pre-cleaned and UV-sterile hood.

well attached to the metallic ring, avoiding roughness and irregularities at the surface of the membrane. This step is important for the correct acceleration of tungsten particles and their homogeneous distribution at the embryo axis shoot meristem.

12. Using a micropipette, homogenize the particles and distribute 8 µl at the center of ethanol-humidified membranes (**Figures 2D, E**). ▲**CRITICAL** Do not distribute the particles on dry membranes. The ethanol at the surface of the carrier membrane ensures the homogeneous distribution of tungsten particles.
13. Distribute the metallic-coated membranes on a sterile petri dish and let them dry under a hood (**Figure 2F**). The membranes are kept under a sterile atmosphere until utilization.

Day 2 ‖ Embryonic Axis Excision and Shoot Exposure • Time: 180 min

(!) CAUTION All the following steps should be performed in a hood previously cleaned with sodium hypochlorite (2.5% v/v) and ethanol (70% v/v) and exposed to UV radiation for 20 min.

1. Spread the hydrated seeds in a plate dish filled with fresh sterile water.
2. Pick up each seed individually with a flame-sterilized tweezers and make a longitudinal section opposite to the hilo (**Figure 3A**) with the help of a new and flame-sterilized scalpel (n. 10). ▲**CRITICAL** To avoid embryo damage, do not insert the scalpel very deep.
3. Separate the half-cotyledon attached to the embryo and discard the other part. Turn the half-cotyledon with the abaxial surface in contact with the plate. With the help of the scalpel and tweezers, press the opposite side of the embryo until embryo detachment (**Figures 3B, C**).
4. Remove the primordia to expose the shoot meristem cells (**Figure 3D**).
5. With the tip of a scalpel, repeatedly move the tip of the embryo with friction to ensure the exposure of the shooting area.
6. Transfer the isolated embryo to a petri dish with sterile distilled and deionized water.

Day 2 ‖ Preparation of Embryos for Bombardment • Time: 40 min

1. Organize the embryos at the CCM solid (petri dish 5 cm ϕ) for bombardment. Make a bisected circle with 15 overlapped embryos in each line (**Figure 3E**). ▲**CRITICAL** The embryonic axis should be positioned with the shoot meristem directed upward and lightly angled to enhance the penetration of tungsten particles at the particle distribution radius. It is also important to avoid the distribution of embryos into the "death zone", where the incidence of microparticles is higher and the shock of tungsten particles to shoot cells is more intense. It can generate damage to the tissue, making it unviable for genetic transformation.
2. Close the Petri dishes, seal them with parafilm and keep the embryos in a sterile environment until bombardment. ▲**CRITICAL** Avoid water-film formation after embryo axis preparation. The water accumulated at the surface of shooting cells acts as a block for microparticle penetration,

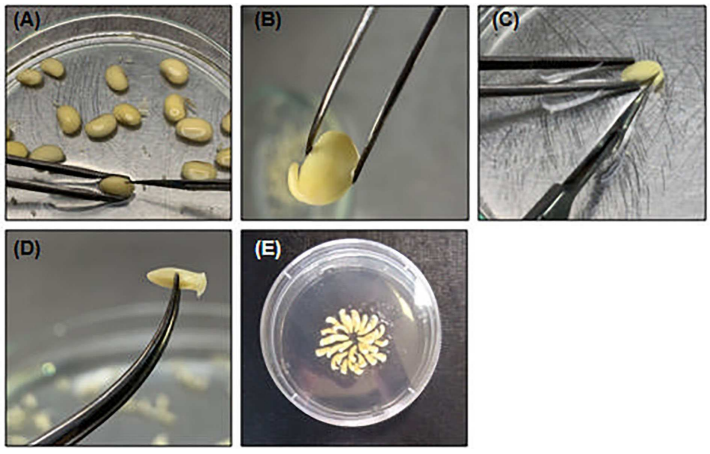

FIGURE 3 | Embryonic axis excision and shoot exposing. **(A)** Pick one hydrated soybean seed and with help of a tweezes and a scalpel make a small section in the opposite of hilo; **(B)** Discard the embryo non-associated cotyledon and **(C)** carefully detach the embryo axis with scalpel. **(D)** Remove the primary leaves to expose shoot cells; **(E)** Organized embryo in CCM to bombardment.

thereby reducing the wounding ratio and the frequency of transformation.

Day 2 ‖ Agrobacterium Preparation • Time: 50 min

1. Under the pre-cleaned hood, transfer the *A. tumefaciens* culture to sterile 50 ml tubes.
2. Centrifuge at 5,000 g—10 min.
3. Discard the supernatant, gently resuspend the pellet in 50 ml of CCM supplemented with acetosyringone, and transfer it to a sterile 100 ml Erlenmeyer flask.
4. Incubate the CCM-resuspended *Agrobacterium* in shaker under agitation—180 rpm—28°C—30 min. ▲**CRITICAL** The incubation of CCM-resuspended bacteria is an important step to enhance bacterial virulence. The acetosyringone in CCM will activate virulence genes, which are required for T-DNA transfer during the embryo infection step.

Day 2 ‖ Soybean Embryo Axis Bombardment • Time: 30 min

Follow straightly the manufacturer instructions to use the helium pressure-driven microparticle acceleration system. This protocol utilizes the following settings: the pressure of helium entering the high-pressure chamber—1,200 p.s.i; vacuum pressure under the bombardment chamber—25 mmHg.

1. Attach four isopropanol-soaked rupture disks at the tip of the helium trigger (**Figure 4A**). ▲**CRITICAL** Avoid air bubbles between the membranes to reach the correct pressurization of the helium chamber. Isopropanol promotes better adhesion of membranes and chamber sealing.
2. Place the metallic net protection at the support of the carrier membrane (**Figure 4B**). The protective net avoids plastic particle spreading, which results from membrane rupture, under the soybean embryo axis.
3. Attach the tungsten-coated carrier membrane at the support and close it tightly (**Figures 4C, D**).
4. Put the opened petri dish with the soybean embryo axis at the center of the bombardment chamber (**Figure 4E**) and close the hermetic door.
5. Activate the vacuum pump to set the pressure at 25 mmHg in the bombardment chamber. Close the airflow valve and open the helium flow until the helium high-pressure chamber is filled. ▲**CRITICAL** The time it takes for the high-pressure chamber to fill is 3–5 s. Excessive helium pressure disrupts the protective disks and triggers the energized needle, liberating the helium pressure under the embryo axis prematurely.
6. Trigger the energized needle. The helium pressure will trigger the needle towards the carrier membranes, and the mechanical shock between gas and microparticles will spread them over the shoot meristems at high speed, generating micro-wounds, which are required for *Agrobacterium* infiltration.
7. Release the pressure under the bombardment chamber and helium chamber, subsequently. Remove the embryo axis of the bombardment chamber and close the petri dish with parafilm until *Agrobacterium* incubation.

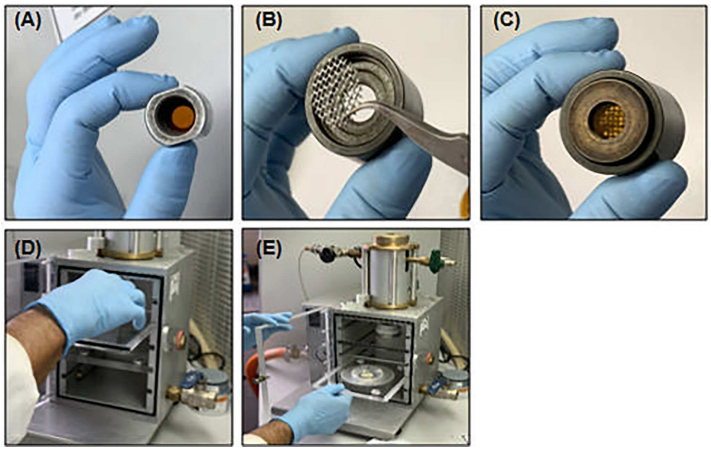

FIGURE 4 | Soybean embryo axis bombardment. **(A)** Isopropanol-soaked rupture disks attached to the tip of helium pressure chamber; **(B)** Protective metallic net at the support of carrier membrane; **(C, D)** Carrier membrane attached to ring support at holder in bombardment chamber; **(E)** Embryonic axis at CCM plate into bombardment chamber.

Day 2 ‖ *Agrobacterium Tumefaciens*-Mediated Transformation and Embryo Cocultivation • Time: 60 min + 16 h

1. Carefully remove the bombarded embryo axis from the CCM plate with the help of a flame-sterilized tweezers. To avoid embryo damage, do not squeeze tweezers tightly.
2. Immerse the embryos on CCM-resuspended bacteria (**Figure 5A**) and incubate the co-culture under shaking—120 rpm—28°C—40 min.
3. Remove the bacterial culture and wash the embryos with sterile distilled and deionized water 3 times.
4. Pour off the water and transfer the embryo axis to sterile Whatman filter paper to remove excess water (**Figure 5A**).
5. Arrange the embryo axis in the CCM petri dish with the radicle completely immersed in the medium (**Figure 5B**). The hormones and metabolites present in the medium will stimulate the development of shoot and root meristem and *Agrobacterium* infection.
6. Seal the plates with parafilm. Keep the infected embryos under darkness for 16 h until transference to DRM.

Day 3 ‖ In Vitro Culture of Soybean Embryonic Axis • Time: 60 min + 3–6 weeks

1. Transfer the embryo axes to the DRM. ▲**CRITICAL** The positioning of the embryo axes at the DRM should be well organized. Each magenta box containing the DRM has 12 embryo axes (4 × 3) distributed equidistantly (**Figure 5C**).
2. Transfer the magenta boxes with infected embryos to an *in vitro* culture room—28°C—16 h photoperiod—50 $\mu mol.m^{-2}.s^{-1}$. After 3–6 weeks in the DRM, the putatively transformed shoot meristem cells develop into elongated shoots, and the radicles develop into roots (**Figures 5D, E**).

(!) **CAUTION** The protocol of soybean embryonic axis transformation mediated by *A. tumefaciens* is a co-cultivation, shoot and root elongation one-step protocol. Therefore, the bacteria from the embryo axis are not removed or eliminated by antibiotics or any other chemical treatment. During the *in vitro* culture period, embryos should be surveyed daily. Excessive bacterial growth can be controlled by treating the embryo axes with cefotaxime solution (150 mg/L) after co-cultivation. Fungal and/or bacterial contamination sources can affect seedling development and decrease the efficiency of transformation, leading to a very low success ratio. During 3–6 weeks of shoot and root elongation, healthy embryos were transferred to another DRM magenta box if contamination spots appeared and contaminated embryos were eliminated.

Up to 6 weeks ‖ *Greenhouse Plant Development* • Time: 24–32 weeks

1. Transfer the shoot- and root-developed plants to individual 1 dm^3 (1.0 L) pots filled ¾ with fertilized soil:vermiculite (2:1).

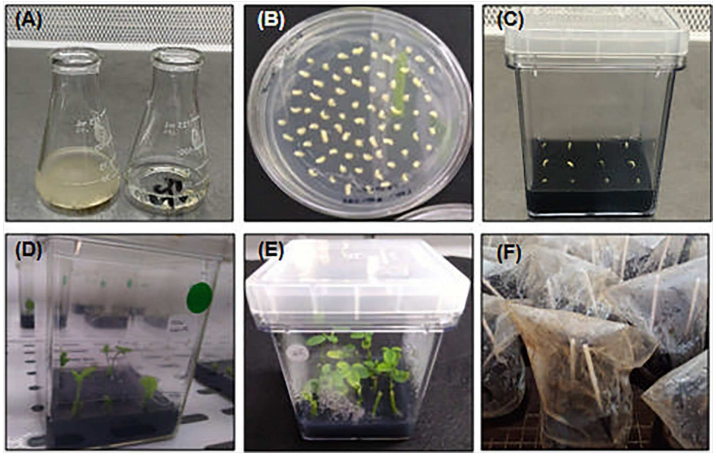

FIGURE 5 | *Agrobacterium tumefaciens* infection, co-cultivation and plant regeneration. **(A)** Bombarded embryos in *Agrobacterium* suspension (left) and after washing (right), performed after 40 min of infection; **(B)** Infected embryos at CCM. The duration of co-cultivation step at CCM is 16 h; **(C)** Infected embryos at DRM after co-cultivation in CCM. The plant-regenerative process starts as from the transference of infected embryos to DRM. The *A. tumefaciens* is not inactivated by chemical treatment and the infection continues along with plant regeneration. At this point, plant surveying is essential to avoid contamination, which should be eliminated by transferring the plant to a new medium or by chemical treatment, if necessary; **(D, E)** Shoot- and root-regenerated seedlings after 3–6 weeks in DRM. **(F)** After complete seedlings' regeneration, the plants can be acclimated in standard greenhouse protected with a plastic bag for 1 week and follow normal cycle of development until seeds recovery. All steps of plant characterization can be performed at this point.

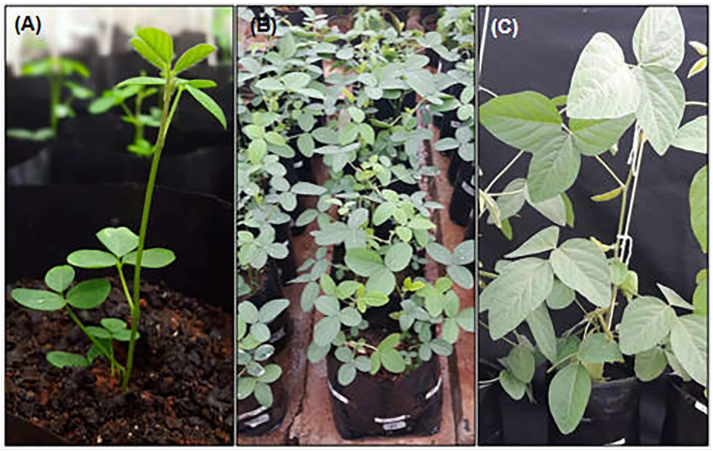

FIGURE 6 | Regenerated plants under full development in greenhouse. **(A)** *In vitro* recovered seedling after DRM-regeneration and 1-week of plant acclimation. **(B)** Putative transgenic T0-matrixes in vegetative stage. **(C)** T1-recovered plants in reproductive stage.

2. Cover the plants with a transparent plastic bag supported on side straws and seal with a rubber band (**Figure 5F**).
3. Keep the plants in a greenhouse under normal development —27—30°C—14 h photoperiod and 75% relative humidity. ▲**CRITICAL** The soil humidity should be checked daily. Take care with the water drops generated at the surface of the plastic bag during the evapotranspiration of seedlings returning to the soil.
4. After 1 week, remove the plastic bag and perform a careful watering of seedlings, avoiding soil erosion and root exposure by strong water flow (**Figure 6A**).

The acclimatized plants still under normal development in the same pot until seed recovery, normally complete at 30 weeks after acclimation (**Figures 6B, C**). During this period, standard procedures of plant care may be adopted to keep plants healthy and productive. The selection of putative transformants should be performed during this period. For ammonium glufosinate-mediated selection, prepare a 125 mg/L solution and, with the help of a swab, spread the solution in half of some leaves. Resistant plants can be adopted as putative transgenic plants.

The final diagnosis of transgenic plants can be performed by PCR or other analytical methods to detect the presence of the foreign gene and/or by methods to detect the protein. In our protocol, we performed an analysis of melting temperature (Tm) by qPCR. We compared the Tm of amplicons generated by a reaction performed with 50 ng of standard plasmid DNA (used to transform *A. tumefaciens*) and 50 ng of plant DNA as follows: 94°C for 3 min; 40 cycles of 94°C for 5 s and 56°C for 40 s, followed by a melting step with a resolution of 0.5°C.

ANTICIPATED RESULTS

The newly described protocol was validated with five different series of soybean embryo axis transformations that employed distinct cassettes for transformation harboring different vector backbones and selective marker genes. In the presence of a selective agent in DRM, the regeneration ratio (rounds 1, 2, and 5—**Table 1**) was 31.16%. In its absence, the regeneration rate reached almost 86% (rounds 3 and 4—**Table 1**). Concerning the average transformation efficiency (percentage of PCR-positive plants relative to the number of bombarded embryos), our protocol resulted in approximately 9.84% (± 2.49) efficiency rate, as described in **Table 1**. To guarantee a similar transformation efficiency as determined by the preliminary screening of T0 matrixes, we also analyzed the heritability of the transgene in T1-segregating plants. The average of heritability in T1 plants was 52.89% (± 11.23), demonstrating a similarly high ratio of T1 plants carrying out the transformation cassette as previously described for other soybean transformation methods (**Table 2**, Pareddy et al., 2020). In addition, as expected from an *Agrobacterium*-mediated transformation method, the positively recovered T1 plants harbor only a single copy or two copies of the transgene (**Table 3**). The copy number was estimated by qPCR analysis, according to Yi and Hong (2019). A standard DNA curve ($1–10^{-5}$ ng) was obtained using a binary plasmid carrying an endogenous reference gene and a transgene against the linear cycle threshold (Ct) values. The absolute amount of the endogenous gene and the transgene was calculated based on the standard curve, as follows: $A_{gene} = S_{gene} \times Ct + I_{gene}$, in which A = absolute amount; S = curve slope; I = intersection curve. The relative copy number was

TABLE 1 | Regeneration efficiency (number of recovered seedlings/number of bombarded embryos x 100) and transformation efficiency (number of PCR-positive T0 plants/number of bombarded embryos x 100).

Series	Bombarded Embryos	Recovered Seedlings	Selective Marker Gene in Vector Backbone	Selective Agent	Regeneration (%)	PCR (+) Plants	Efficiency (%)
1	150	48	*ahas*	Imazapyr	32	21	14
2	150	40	*ahas*	Imazapyr	26.7	14	9.3
3	300	282	*bar*	-*	94	22	7.3
4	300	232	*bar*	-*	77.3	29	9.6
5	300	99	*ahas*	Imazapyr	33	27	9

These data resulted from five independent series of soybean embryo axis transformations.
(*) Ammonium glufosinate or any other topic herbicide, which does not accumulate into shoot apex cells, cannot be used in selective DRM to avoid radicle necrosis.

TABLE 2 | Gene-insertion heritability in T1 transformed plants.

Series of selected T0-matrixes	Number of T0-selected matrixes	Assayed T1 plants	PCR (+) T1 Plants	Heritability*
1 and 2	7	37	20	54.05%
3 and 4	15	107	44	41.12%
5	10	75	47	63.51%

(*) The heritability rate (number of PCR-positive T1 plants x 100/number of assayed T1 plants) was calculated according to the number of PCR-positive T1 plants obtained from the putative T0-matrix selected on the first screening of transformed plants.

TABLE 3 | Transgene copy number in T1 plants estimated by qPCR.

PCR (+) T1 assayed plants	Estimated transgene copy number	Number of Plants	(%)
24	1	18	75
	2	6	25
	3	0	–

estimated by dividing the absolute amount of the transgene by the absolute amount of endogenous reference gene. Troubleshooting and limiting steps are described in **Table 4**.

DISCUSSION

Soybean is one of the most important nutritional crops around the world and is considered the main source of oil and protein for animal and human food and feed (Han et al., 2016; Li et al., 2017). For this reason, soybean has become the largest commercial crop planted worldwide, and genetic breeding programs have been extensively developed to generate new soybean varieties adapted to different climates and other agribusiness demands. Soybean has attracted attention between the main targets of modern molecular breeding programs and was one of the earliest genetically modified crops to be introduced for commercial cultivation (Wang et al., 2006; Krishna et al., 2010; Yamada et al., 2012). However, the genetic transformation of soybean is not trivial, and the described protocols display very low efficiency. It is expected that one superior cultivar of soybean with reasonable value and agricultural importance is a result of thousands of transformation events (Wang et al., 2006). Fundamental science would also benefit tremendously from the development of a simple and efficient transformation method because many genes in the soybean genome are still annotated as unknown functional genes (Schmutz et al., 2010; Li et al., 2017).

Despite the availability of well-established methods to deliver a foreign gene to plant cells, from the choice of explant to the DNA-delivery method, there are intrinsic factors that limit the efficiency of soybean transformation protocols. These factors are related to *A. tumefaciens* virulence, multiple-copy integration, the limiting size of integrative cassettes in the biolistics method and, mainly, the multiple steps of explant *in vitro* cultivation with subsequent plant regeneration. To overcome these problematic steps, our protocol combined the main advantages of each pre-established system of soybean transformation, and we developed a new method with higher plant regeneration and efficiency ratios.

Agrobacterium-mediated transformation is widely employed to generate transgenic plants. The main limitations of this DNA-delivery method are associated with the effectiveness of infection and explant regeneration, resulting in long and inefficient protocols. The growth stage of the *Agrobacterium* culture, culture concentration, infection time, medium composition and the regeneration capacity of explants directly affect the transformation efficiency (Zhou et al., 1983; Hinchee et al., 1988; Bailey et al., 1993; Donaldson and Simmonds, 2000; Paz et al., 2006).

The infectivity of plant cells by *Agrobacterium* ssp. is dependent on chemotaxis. Throughout cell wounding, metabolite exudates are released by plant cells and perceived by bacteria that trigger the process of colonization and T-DNA delivery. During the logarithmic growth stage, the bacteria display increased metabolic effectiveness, resulting in enhanced infectivity (Zhou et al., 1983; Paz et al., 2006). For soybean cotyledonary nodes, Li et al. (2017) described 96% efficiency of infection, which was monitored and reported by the highest GUS activity after the co-cultivation step of embryos and with a bacterial culture displaying an OD_{650} = 0.6. At this OD, the concentration of bacteria during the infection step is not too low to decrease its infection capacity and not too high to hamper its removal from explants before *in vitro* cultivation.

Many protocols of soybean transformation employ cotyledonary nodes isolated from germinated seeds as explants. After isolation, they are mechanically wounded, and submitted to the infection step. Reproductive plants are regenerated from the pluripotent cells present in this part of the embryo through multiple steps of *in vitro* cultivation, including shoot induction and elongation followed by rooting. The choice of cotyledonary

TABLE 4 | Troubleshooting and limiting steps of *Agrobacterium*-mediated soybean embryonic axis transformation.

Step	Problem	Expected Consequence	Possible Solution
Medium Preparation *(Day 1)*	pH checking	The wrong pH can modify the ionic state of chemical components in culture media, interfering with their bioavailability during plant development.	Check the pH during medium preparation using a calibrated and accurate pH meter. Adjust the pH precisely.
	Hormones and other chemical supply	The absence or the inactivity of hormones in culture media does not allow the shoot and root induction during plant regeneration.	Do not forget to supply the medium with all hormones and other chemicals during its preparation. Follow the reagents setup and storage recommendations exactly. Check the medium temperature before the supplementation with hormones.
	Selective agent—ammonium glufosinate	The presence of ammonium glufosinate in DRM may rot the embryonic axes during the regenerative process.	If the selective marker gene confers resistance to ammonium glufosinate, prepare DRM without a selective agent, and after seedling regeneration, follow the recommendations to select putative transgenic plants.
Tungsten-coated membrane preparation *(Day 1)*	Dried membrane	Depositing tungsten at the dried membrane surface does not allow its adhesion and correct spread, decreasing the number of particles bombarded against the shoot meristem and the wounding ratio for the bacterial infection.	Be aware of the membrane storage in ethanol and prepare the tungsten particles before removing it. Quickly apply the particles at the membrane surface.
Embryonic axis excision and shoot exposing*(Day 2)*	Damaged/broken embryos	Damaged shooting cells may not regenerate into an apical system, resulting in low regeneration frequency.	Remove the embryo axis carefully with the help of suitable tweezers and scalpel. Check the integrity of the shoot apex using a stereoscope. If embryo removal displays any resistance, make sure that the seeds were well hydrated. It is possible to hydrate them for more time.
Bombardment preparation*(Day 2)*	Embryo position	Shooting damage at the death zone or low frequency of particle bombardment, resulting in low transformation efficiency.	Avoid the positioning of the embryo axis at the death zone, where the incidence of microparticles is high during the bombardment. Make sure that the embryos are oriented vertically and completely dried to guarantee maximum exposure of the shoot cells.
Embryo axis *in vitro* cultivation *(Up to 3 weeks)*	Bacterial and fungal contamination	The availability of nutrients in culture medium enhances the chance of bacterium and fungus development during plant regeneration, culminating in unviable embryos that can result from many factors, including pathogen-mediated embryo oxidation. Biological contamination represents the most limiting factor, leading to low regeneration frequency and transformation efficiency.	Verify the quality of seeds. Sterilization must be well executed in a laminar flow chamber. During the regenerative process, be aware of any contamination, taking care to eliminate it by removal or suitable antibiotic treatment.

nodes facilitates the generation of explants, as they can be easily isolated from germinated seeds. However, their efficiency of regeneration is very low, and shoot induction is considered the limiting step of this protocol, whose efficiency fluctuates between 2.5% and 4.0% (Paz et al., 2006; Song et al., 2013).

The problem of explant regeneration is partially overcome by medium supplementation with plant hormones (Gonbad et al., 2014; Li et al., 2017). The supplementation of SIM (shoot induction medium), SEM and RM with auxin, cytokines, and gibberellin analogs improves plant regeneration, raising the elongation efficiency to 26%–34%, although multiple steps of tissue culture are still necessary (Li et al., 2017). However, the demand for successive medium changes leads to yield losses by contamination caused by excessive explant manipulation, which makes the protocol long and expensive and eliminates the effects of improved regeneration protocols on plant transformation efficiency.

In our *Agrobacterium*-mediated transformation protocol, we overcame problems of both plant regeneration and excessive manipulation by changing the explant type. We developed a method that takes advantage of *Agrobacterium* ssp. T-DNA insertion and explored the high regenerative capacity of shoot cells in the embryonic axis, also derived from mature seeds, already reported by biolistic protocols (Rech et al., 2008). In our protocol, the embryo axis displayed 27% to 94% regenerative capacity in one-step *in vitro* tissue culture after co-cultivation. In the presence of the selective agent imazapyr, the average plant regeneration was 30.56 (± 2.76%). Other protocols reported regeneration rates between approximately 11% and 34%, reached by medium supplementation with a diverse combination of growth hormones and antioxidants (Li et al., 2017; Pareddy et al., 2020), against DRM only supplemented with BAP. In the absence of a selective agent, the maximum regeneration rate was 77% to 94%. This rate was already expected because all bombarded shoot cells in the embryo axis display full capacity to develop into a new plant, reinforcing the high regenerative capacity of the soybean embryo axis that supported our explant choice.

Complete plant regeneration was performed only in the DRM, which was composed of basic nutrients of plant media and only supplemented with the cytokinin BAP and charcoal. BAP is necessary to activate shoot elongation after its induction in CCM, also supplemented with GA_3 and charcoal, which stimulates natural geotropic mechanisms of rooting. The use of the embryonic axis offers an enormous advantage to the plant regenerative process and explant manipulation. The one-step regeneration in DRM comprises the main advantage of our protocol: it dismisses the continuous media-changes supplemented with several phytohormones and growth regulators

demanded by *in vitro* tissue culture and introduce an efficient alternative to the long steps of tissue culture reported by other protocols with close-related or higher efficiency (Paz et al., 2006; Li et al., 2017; Pareddy et al., 2020).

Our results demonstrate high reproducibility regarding both regeneration and transformation efficiency, reaching an average of 9.84%. This value is close to those reported by other *Agrobacterium*-mediated soybean transformation protocols, which fluctuate between 2% and 10%, depending on the soybean genotype (Meurer et al., 1998; Olhoft and Somers, 2001; Liu et al., 2004; Li et al., 2017). It is also close to the frequency of transformation obtained by biolistic protocols (Rech et al., 2008). In addition, our protocol offers a stable genetic transformation workflow, with a heritability of almost 50% in T1-segregating plants, reinforcing its usability and efficiency. As desirable by opting for the *Agrobacterium*-mediated method of plant transformation, the transgenic events harbor few T-DNA insertions, as 75% of the recovered germlines harbor a single transgene insertion and 25%, double insertions. Finally, the described protocol, which combines biolistic delivery and *Agrobacterium*-mediated transformation, provides a feasible, highly reproductive and efficient soybean transformation method.

DATA AVAILABILITY STATEMENT

All datasets presented in this study are included in the article/supplementary material.

AUTHOR CONTRIBUTIONS

BM, IL-T, and CM designed the study, performed protocol adjustment and supervised all the experiments. BM, IL-T, NS, LP, and CJ performed plant transformation series. MG-D-S was the leading researcher for all the work and provided intellectual input and financial support. MS and LM provided material and technicians resources. EF provided intellectual input and critically read and corrected the manuscript. BM, IL-T, and CM wrote and amended the manuscript.

ACKNOWLEDGMENTS

This work was supported by fellowships from INCT Plant Stress Biotech, EMBRAPA, UCB, CNPq, CAPES, and FAPDF. We are grateful to Gilanna Falcão Ferreira for the pictures of soybean transformation workflow.

REFERENCES

Bailey, M. A., Boerma, H. R., and Parrott, W. A. (1993). Genotype effects on proliferative embryogenesis and plant regeneration of soybean. *Vitro Cell Dev. Biol. Plant* 29, 102–108. doi: 10.1007/BF02632279

Donaldson, P. A., and Simmonds, D. H. (2000). Susceptibility to *Agrobacterium tumefaciens* and cotyledonary node transformation in short-season soybean. *Plant Cell Rep.* 19, 478–484. doi: 10.1007/s002990050759

Droste, A., Pasquali, G., and Bodanese-Zanettini, M. H. (2000). Integrated bombardment and Agrobacterium transformation system: An alternative method for soybean transformation. *Plant Mol. Biol. Rep.* 18, 51–59. doi: 10.1007/BF02825294

Dutta Gupta, S. (2010). "Role of free radicals and antioxidants in in vitro morphogenesis," in *Reactive Oxygen Species and Antioxidants in Higher Plants*, (USA: CRC Press and Sci. Pub.) 229–247.

Gao, X., Zhang, Y., He, Z., and Fu, X. (2017). "Gibberellins," in *Hormone Metabolism and Signaling in Plants* (Cambrigde, USA: Elsevier), 107–160. doi: 10.1016/B978-0-12-811562-6.00004-9

Gelvin, S. B. (2000). *Agrobacterium* and plant genes involved in T-DNA transfer and integration. *Annu. Rev. Plant Physiol. Plant Mol. Biol.* 51, 223–256. doi: 10.1146/annurev.arplant.51.1.223

Gonbad, R. A., Sinniah, U. R., Abdul Aziz, M., and Mohamad, R. (2014). Influence of Cytokinins in Combination with GA $_3$ on Shoot Multiplication and Elongation of Tea Clone Iran 100 (*Camellia sinensis* (L.) O. Kuntze). *Sci. World J.* 2014, 1–9. doi: 10.1155/2014/943054

Han, Y., Zhao, X., Liu, D., Li, Y., Lightfoot, D. A., Yang, Z., et al. (2016). Domestication footprints anchor genomic regions of agronomic importance in soybeans. *New Phytol.* 209, 871–884. doi: 10.1111/nph.13626

Hinchee, M. A. W., Connor-Ward, D. V., Newell, C. A., McDonnell, R. E., Sato, S. J., Gasser, C. S., et al. (1988). Production of Transgenic Soybean Plants Using Agrobacterium-Mediated DNA Transfer. *Nat. Biotechnol.* 6, 915–922. doi: 10.1038/nbt0888-915

Kim, J., LaMotte, C. E., and Hack, E. (1990). Plant Regeneration In Vitro from Primary Leaf Nodes of Soybean (*Glycine max*) Seedlings. *J. Plant Physiol.* 136, 664–669. doi: 10.1016/S0176-1617(11)81341-6

Krishna, G., Palicherla, S., Ramteke, P., and Bhattacharya, P. (2010). Progress of tissue culture and genetic transformation research in pigeon pea [*Cajanus cajan* (L.) Millsp.]. *Plant Cell Rep.* 29, 1079–1095. doi: 10.1007/s00299-010-0899-4

Lee, C.-W., Efetova, M., Engelmann, J. C., Kramell, R., Wasternack, C., Ludwig-Müller, J., et al. (2009). *Agrobacterium tumefaciens* Promotes Tumor Induction by Modulating Pathogen Defense in *Arabidopsis thaliana*. *Plant Cell* 21, 2948–2962. doi: 10.1105/tpc.108.064576

Li, S., Cong, Y., Liu, Y., Wang, T., Shuai, Q., Chen, N., et al. (2017). Optimization of Agrobacterium-Mediated Transformation in Soybean. *Front. Plant Sci.* 8, 246. doi: 10.3389/fpls.2017.00246

Liu, G., and Godwin, I. D. (2012). Highly efficient sorghum transformation. *Plant Cell Rep.* 31, 999–1007. doi: 10.1007/s00299-011-1218-4

Liu, H.-K., Yang, C., and Wei, Z.-M. (2004). Efficient *Agrobacterium tumefaciens*-mediated transformation of soybeans using an embryonic tip regeneration system. *Planta* 219, 1042–1049. doi: 10.1007/s00425-004-1310-x

McCabe, D. E., Swain, W. F., Martinell, B. J., and Christou, P. (1988). Stable transformation of soybean (*Glycine max*) by particle acceleration. *Nat. Biotechnol.* 6, 923–926. doi: 10.1038/nbt0888-923

Meurer, C. A., Dinkins, R. D., and Collins, G. B. (1998). Factors affecting soybean cotyledonary node transformation. *Plant Cell Rep.* 18, 180–186. doi: 10.1007/s002990050553

Nishijima, T. (2003). Effect of Gibberellin Biosynthesis Inhibitor on Prevention of Precocious Bolting and Flowering in Japanese Radish (*Raphanus sativus* L.). *JARQ* 37, 175–181. doi: 10.6090/jarq.37.175

Normanly, J. (1997). Auxin metabolism. *Physiol. Plant* 100, 431–442. doi: 10.1111/j.1399-3054.1997.tb03047.x

Olhoft, P., and Somers, D. (2001). L-Cysteine increases Agrobacterium-mediated T-DNA delivery into soybean cotyledonary-node cells. *Plant Cell Rep.* 20, 706–711. doi: 10.1007/s002990100379

Pareddy, D., Chennareddy, S., Anthony, G., Sardesai, N., Mall, T., Minnicks, T., et al. (2020). Improved soybean transformation for efficient and high throughput transgenic production. *Transgenic Res.* 29, 267–281. doi: 10.1007/s11248-020-00198-8

Paz, M. M., Martinez, J. C., Kalvig, A. B., Fonger, T. M., and Wang, K. (2006). Improved cotyledonary node method using an alternative explant derived from mature seed for efficient Agrobacterium-mediated soybean transformation. *Plant Cell Rep.* 25, 206–213. doi: 10.1007/s00299-005-0048-7

Rech, E. L., Vianna, G. R., and Aragão, F. J. L. (2008). High-efficiency transformation by biolistics of soybean, common bean and cotton transgenic plants. *Nat. Protoc.* 3, 410–418. doi: 10.1038/nprot.2008.9

Sato, S., Newell, C., Kolacz, K., Tredo, L., Finer, J., and Hinchee, M. (1993). Stable transformation via particle bombardment in two different soybean

regeneration systems. *Plant Cell Rep.*, 12, 408–413. doi: 10.1007/BF00234702

Schmutz, J., Cannon, S. B., Schlueter, J., Ma, J., Mitros, T., Nelson, W., et al. (2010). Genome sequence of the palaeopolyploid soybean. *Nature* 463, 178–183. doi: 10.1038/nature08670

Shaner, D. L., Anderson, P. C., and Stidham, M. A. (1984). Imidazolinones: Potent Inhibitors of Acetohydroxyacid Synthase. *Plant Physiol.* 76, 545–546. doi: 10.1104/pp.76.2.545

Skooh, F., and Miller, W. (1957). Chemical regulation of growth and organ formation in plant tissues cultured in vitro. *Symp. Soc. Exp. Biol.* 11, 118–130.

Song, Z., Tian, J., Fu, W., Li, L., Lu, L., Zhou, L., et al. (2013). Screening Chinese soybean genotypes for Agrobacterium-mediated genetic transformation suitability. *J. Zhejiang Univ. Sci. B.* 14, 289–298. doi: 10.1631/jzus.B1200278

Thomas, S. G., and Sun, T. (2004). Update on Gibberellin Signaling. A Tale of the Tall and the Short. *Plant Physiol.* 135, 668–676. doi: 10.1104/pp.104.040279

Wang, L., Guan, Y., Guan, R., Li, Y., Ma, Y., Dong, Z., et al. (2006). Establishment of Chinese soybean *Glycine max* core collections with agronomic traits and SSR markers. *Euphytica* 151, 215–223. doi: 10.1007/s10681-006-9142-3

Wu, E., and Zhao, Z.-Y. (2017). "Agrobacterium-Mediated Sorghum Transformation," in *Plant Germline Development Methods in Molecular Biology*. Ed. A. Schmidt (New York, NY: Springer New York), 355–364. doi: 10.1007/978-1-4939-7286-9_26

Yamada, T., Takagi, K., and Ishimoto, M. (2012). Recent advances in soybean transformation and their application to molecular breeding and genomic analysis. *Breed. Sci.* 61, 480–494. doi: 10.1270/jsbbs.61.480

Yamauchi, Y., Takeda-Kamiya, N., Hanada, A., Ogawa, M., Kuwahara, A., Seo, M., et al. (2007). Contribution of Gibberellin Deactivation by AtGA2ox2 to the Suppression of Germination of Dark-Imbibed *Arabidopsis thaliana* Seeds. *Plant Cell Physiol.* 48, 555–561. doi: 10.1093/pcp/pcm023

Yi, C., and Hong, Y. (2019). Estimating the Copy Number of Transgenes in Transformed Cotton by Real-Time Quantitative PCR. *Methods Mol. Biol.* 1902, 137–157. doi: 10.1007/978-1-4939-8952-2_11

Zhang, J., Nguyen, H. T., and Blum, A. (1999). Genetic analysis of osmotic adjustment in crop plants. *J. Exp. Bot.* 50, 291–302. doi: 10.1093/jxb/50.332.291

Zhou, G., Weng, J., Zeng, Y., Huang, J., Qian, S., and Liu, G. (1983). "[29] Introduction of exogenous DNA into cotton embryos," in *Methods in Enzymology* (Elsevier) (Cambrigde, USA: Academic Press), 433–481. doi: 10.1016/0076-6879(83)01032-0

Conflict of Interest: The authors declare that the research was conducted in the absence of any commercial or financial relationships that could be construed as a potential conflict of interest.

GENERAL CONCLUSION

The results of this investigation highlight the importance of transcription factors in plant adaption to environmental stresses and programmed cell death control. It is estimated that the world's population will reach 9 billion people in 2050, and hence the necessity of new strategies for plant productivity is urgent, not only for food supply but also for energy generation. Understanding how plants respond to multiple stresses and developing new tools to manipulate these stress responses comprise the most essential biotechnological approach to generate new and superior crops.

Our study demonstrated that the overexpression of AREB-1 mediated by the CRISPRa strategy resulted in highly improved drought stress responses in plants exposed to long-term dehydration, close to the field conditions. The sgRNA-driven transcriptional activators encompass a new powerful biotechnology tool for genetic engineering, comprising a strategy for enhancing transcriptional activity without the pleiotropic effects associated with the use of constitutive promoters controlling gene expression in transgenic plants. The positive regulation of AREB-1 led to lower biomass loss and higher relative water content along water deprivation, enhancing the antioxidant enzyme activity and osmoregulation by higher levels of soluble sugars. Consequently, ROS accumulation is lower in transgenic plants, promoting effective chlorophyll maintenance and plant survival.

Despite the extensive characterization of NAC transcription factors in Arabidopsis, they remain poorly understood in crops, such as maize and soybean. With numerous members responsible for controlling plant morph-physiology, stress responses, and senescence, studying NAC TFs provides valuable information about molecular mechanisms of plant development and physiological adaption in plants. In summary, the investigation of the NAC superfamily in soybean represents an update of the NAC inventory. Thirty-two novel members were identified, and their expression profiles were monitored in response to multiple stresses, validating the genome annotation and reinforcing the plasticity of biological functions played by GmNACs. Our genome-revisiting studies clustered the soybean GmNACsinto 15 subfamilies, which display a consistent relationship between structure, expression, and function with Arabidopsis orthologous genes. Additionally, the characterization of GmNAC065 and GmNAC085 indicates that the large number of proteins encoded by this family and their

great diversity allow plants to elaborate complex responses, with gradual levels of hormonal, temporal, and spatial regulation with the high plasticity of responses.

GmNAC065 and *GmNAC085* belong to senescence-associated genes in soybean and their phylogenetic relatedness with ANAC083/VNI2 and ANAC072/ORE1, a negative and positive regulator of senescence in Arabidopsis, respectively, suggested different roles of these genes in the control of stress responses and senescence. The expression of *GmNAC085* is drastically enhanced by bleomycin-treatment in soybean, whereas the expression of *GmNAC*065 is weakly affected, suggesting a different role of these genes in the environmental-induced PCD.

The contrasting roles of *GmNAC065* and *GmNAC085* are reinforced by analyzing the ectopic expression of GmNAC065 and GmNAC085 in plants. When transiently expressed in *Nicotianabenthamiana* leaves, GmNAC085 promotes accentuated hallmarks of senescence, while GmNAC065 expression triggers these symptoms very discreetly. Not surprisingly, in transgenic Arabidopsis lines overexpressing these TFs, GmNAC065-OX lines display effective mechanisms of ROS-avoidance, with delayed senescence phenotype and enhanced oxidative performance under multiple stresses. In contrast, GmNAC085-OX lines display accentuated senescence, leading to the up-regulation of several downstream SAGs in Arabidopsis, affecting photosystem stability, chlorophyll degradation, and anti-oxidative plant system.

Finally, we developed an *Agrobacterium*-mediated soybean transformation protocol for the translational research from model-plant systems to crops. This protocol takes advantage of *Agrobacterium ssp*. T-DNA insertion and explores the high regenerative capacity of shoot cells in the embryonic axis. Apart from the natural regenerative capacity of the explant, co-cultivation, shoot elongation and root development are conducted in a one-step way, representing the primary advantage of this protocol. Our results demonstrated high reproducibility and transformation efficiency reaches an average of 9.84%. More importantly, the protocol confers a stable heritability, with almost 50% of T1-segregating plants carrying the transgene, with 75% of positive plants introgressed with a single copy.

In the last decades, significant progress has been made towards the characterization of transcription factors and the effects of their overexpression or suppression in plant stress responses. However, most of these studies have been conducted in model-plants, and there are limiting steps into transferring them to field-

crops. Throughout modern approaches of transcriptome-wide analysis and genome editing, our results offer new insights into the function of transcription factors. The proposed protocol for soybean transformation validates new methodologies to overcome the barriers in modern plant-breeding.

APÊNDICE

LISTA DE PUBLICAÇÕES

As publicações listadas abaixo correspondem à produção científica do estudante Bruno Paes de Melo durante o período em que desenvolveu seu doutorado pelo Programa de Pós-Graduação em Bioquímica Aplicada da Universidade Federal de Viçosa em parceria com as intuições receptoras durante sua mobilidade interinstitucional para a Embrapa Recursos Genéticos e Biotecnologia - Brasília, DF e *Institute Nacional de la Recherche Agronomique* - INRAe, Sophia-Antipolis, França.

Arraes, F. B. M., Martins-de-Sa, D., Noriega Vasquez, D. D., **Melo, B. P**., Faheem, M., de Macedo, L. L. P., Morgante, C. V., Barbosa, J. A. R. G., Togawa, R. C., Moreira, V. J. V., Danchin, E. G. J., & Grossi-de-Sa, M. F. (2020). Dissecting protein domain variability in the core rna interference machinery of five insect orders. *RNA Biology*, 1–29. https://doi.org/10.1080/15476286.2020.1861816

de Melo, Bruno Paes, Lourenço-Tessutti, I. T., Paixão, J. F. R., Noriega, D. D., Silva, M. C. M., de Almeida-Engler, J., Fontes, E. P. B., & Grossi-de-Sa, M. F. (2020). Transcriptional modulation of AREB-1 by CRISPRa improves plant physiological performance under severe water deficit. *Scientific Reports*, *10*(1), 16231. https://doi.org/10.1038/s41598-020-72464-y

Freitas, E. O., **Melo, B. P**., Lourenço-Tessutti, I. T., Arraes, F. B. M., Amorim, R. M., Lisei-de-Sá, M. E., Costa, J. A., Leite, A. G. B., Faheem, M., Ferreira, M. A., Morgante, C. V., Fontes, E. P. B., & Grossi-de-Sa, M. F. (2019). Identification and characterization of the GmRD26 soybean promoter in response to abiotic stresses: potential tool for biotechnological application. *BMC Biotechnology*, *19*(1), 79. https://doi.org/10.1186/s12896-019-0561-3

Li, B., Ferreira, M. A., Huang, M., Camargos, L. F., Yu, X., Teixeira, R. M., Carpinetti, P. A., Mendes, G. C., Gouveia-Mageste, B. C., Liu, C., Pontes, C. S. L., Brustolini, O. J. B., Martins, L. G. C., **Melo, B. P**., Duarte, C. E. M., Shan, L., He, P., & Fontes, E. P. B. (2019). The receptor-like kinase NIK1 targets FLS2/BAK1 immune complex and inversely modulates antiviral and antibacterial immunity. *Nature Communications*, *10*(1), 4996. https://doi.org/10.1038/s41467-019-12847-6

Melo, Bruno P, Fraga, O. T., Silva, J. C. F., Ferreira, D. O., Brustolini, O. J. B., Carpinetti, P. A., Machado, J. P. B., Reis, P. A. B., & Fontes, E. P. B. (2018). Revisiting the soybean gmnac superfamily. *Frontiers in Plant Science*, *9*, 1864. https://doi.org/10.3389/fpls.2018.01864

Morgante, C. V., Arraes, F. B. M., Pinto, C. M., **Melo, B. P**., Sa, M. F. G. (2020). Modulação da expressão gênica em plantas via tecnologia CRISPR/dCas9. In Molinari, H., Vieira, L., Silva, N., Souza Prado, G., & Hernandes-Lopes, J. (2020). *Tecnologia CRISPR na edição genômica de plantas: biotecnologia aplicada à agricultura*.

Mota, A. P. Z., Fernandez, D., Arraes, F. B. M., Petitot, A.-S., de **Melo, B. P**., de Sa, M. E. L., Grynberg, P., Saraiva, M. A. P., Guimaraes, P. M., Brasileiro, A. C. M., Albuquerque, E. V. S., Danchin, E. G. J., & Grossi-de-Sa, M. F. (2020). Evolutionarily conserved plant genes responsive to root-knot nematodes identified by comparative genomics. *Molecular Genetics and Genomics*, *295*(4), 1063–1078. https://doi.org/10.1007/s00438-020-01677-7

Paes de Melo, B., Lourenço-Tessutti, I. T., Morgante, C. V., Santos, N. C., Pinheiro, L. B., de Jesus Lins, C. B., Silva, M. C. M., Macedo, L. L. P., Fontes, E. P. B., & Grossi-de-Sa, M. F. (2020). Soybean Embryonic Axis Transformation: Combining Biolistic and Agrobacterium-Mediated Protocols to Overcome Typical Complications of In Vitro Plant Regeneration. *Frontiers in Plant Science*, *11*, 1228. https://doi.org/10.3389/fpls.2020.01228

Roca Paixão, J. F., Gillet, F.-X., Ribeiro, T. P., Bournaud, C., Lourenço-Tessutti, I. T., Noriega, D. D., **Melo, B. P. de**, de Almeida-Engler, J., & Grossi-de-Sa, M. F. (2019). Improved drought stress tolerance in Arabidopsis by CRISPR/dCas9 fusion with a Histone AcetylTransferase. *Scientific Reports*, *9*(1), 8080. https://doi.org/10.1038/s41598-019-44571-y

Teixeira Fraga, O., **Paes de Melo, B**., Fernando de Camargos, L., Pellanda Fagundes, D., Cabral Oliveira, C., Bassi Simoni, E., Augusto Braga dos Reis, P., & Pacheco Batista Fontes, E. (2020). A Regulatory Circuit Integrating Stress-Induced with Natural

Leaf Senescence. In A. Gonzalez, M. Rodriguez, & N. Gören Sağlam (Eds.), *Plant Science - Structure, Anatomy and Physiology in Plants Cultured in Vivo and in Vitro*. IntechOpen. https://doi.org/10.5772/intechopen.89498